ISSN1794-6190

Earth Sciences Research Journal

UNIVERSIDAD NACIONAL DE COLOMBIA
SEDE BOGOTÁ

Volume 16 – Special Issue

April 2012

Evaluating total Yet-to-Find hydrocarbon volume in Colombia

Carlos A. Vargas J.

UNIVERSIDAD NACIONAL DE COLOMBIA

UNIVERSIDAD NACIONAL DE COLOMBIA
FACULTAD DE CIENCIAS
DEPARTAMENTO DE GEOCIENCIAS
Research Group in Geophysics

PRESIDENT OF THE REPUBLIC OF COLOMBIA

Dr. JUAN MANUEL SANTOS CALDERON

MINISTER OF MINES AND ENERGY

Dr. MAURICIO CARDENAS SANTAMARIA

PRESIDENT NATIONAL AGENCY OF HYDROCARBONS

Dr. ORLANDO CABRALES SEGOVIA

TECHNICAL DIRECTOR

Dr. JUAN FERNANDO MARTINEZ

AUTOR AND EDITOR

CARLOS ALBERTO VARGAS JIMENEZ.
Associated Professor, Department of Geosciences
UNIVERSIDAD NACIONAL DE COLOMBIA

TECHNICAL TEAM

ALEJANDRA J. ANGULO
JOHN H. ARENAS
MAURICIO MORENO M.
JOSE ARAUJO
UNIVERSIDAD NACIONAL DE COLOMBIA

EDILSA AGUILAR GOMEZ
GERMAN OROZCO
AGENCIA NACIONAL DE HIDROCARBUROS

Cite this work as:

Vargas, C. A. Evaluating total Yet-to-Find hydrocarbon volume in Colombia. Earth Sci. Res. J., Vol. 16, Special Issue (April, 2012): 1-246.

Content

AGENCIA NACIONAL DE HIDROCARBUROS

1 INTRODUCTION

The present work combines estimations of conventional and non-conventional yet-to-find recoverable hydrocarbons in Colombia's 23 sedimentary basins. The work adopts a probabilistic approach using the Monte Carlo statistical method aimed at defining available and trapped resources and comparing such simulation with in situ resources regarding their conventional and non-conventional expression.

A series of considerations and hypotheses support the work's conceptual and procedural framework regarding all the estimations so made. Such hypotheses were statistically based by compiling a series of events tracing a determined pattern which may not always correspond to the geographical reality posed by the hypotheses. The foregoing means that some of the hypotheses could be reconsidered in future estimates; this is why the Excel sheets underlying fresh calculations have been attached so that they can be evaluated in new scenarios.

As well as the resource being produced, the first chapters (2 to 4) present volumetric estimates and expectations regarding news reserves related to conventional potential, i.e. oil, gas and associated gas. These three chapters also try to differentiate between the following concepts: generated resource, original in situ resource and yet-to-find (YTF) resources.

Chapter 5 gives an outline of a systematic exercise orientated towards estimating gas hydrates in Colombia. The estimates were based on information from 28 wells and more than 40,000 km of seismic 2D. The resources did not include the deep basins and Los Cayos basin due to gaps in the information or the poor quality of some available data.

Chapter 6 gives estimates of coalbed methane, supported by figures drawn from cartographic information from carbon occurrences in Colombia, and data regarding gas production in mines in Colombia, as well as Alberta (Canada).

Potential resources associated with tar sands are calculated in Chapter 7. Information of differing nature, age and sources was compiled for this exercise. Estimating potential was based on a map of tar sand occurrences produced from an inventory of areas having manifestations of the resource obtained from available information.

Chapters 8 and 9 deal with results concerning oil and gas in shale; two different but complementary approaches led to establishing this resource's great potential in Colombia. The lack of certain geochemical data and in-depth distribution data impeded using conventional techniques for analysing shale oil, oil shale and shale gas. However, the approach was valuable as the working hypotheses were coherent. A conventional analysis of shale gas and shale oil based on well and seismic data led to extending concepts to other basins.

An approach based on well information and data regarding area from other basins around the world led to estimating tight sands (Chapter 10), a resource which is becoming marginal compared to other resources.

One chapter has been devoted to heavy crudes (Chapter 11) for estimating this resource in five sedimentary basins having more occurrences and/or effective production. Well and seismic information as well as approximations of areas were fundamental for such estimate.

Chapter 12 gives a forecast concerning hydrocarbon production in Colombia. Given that the numerical exercise was based on the cointegral time series concept, the lack of historical production data regarding non-conventional resources limited the exercise to conventional gas and oil. The advantage of an approach using cointegral variables was based on analysing production evolution along with other macroeconomic variables maintaining long-term ratio and seasonality.

All the chapters have digital appendixes relating the databases used, the electronic spreadsheets with data fitted for running simulations and/or the results found. Other information such as seismic and well data duly integrated into projects using Kingdom Suite software is attached to the present document.

2 HYDROCARBONS PRODUCED IN COLOMBIAN SEDIMENTARY BASINS

2.1 General comments

The history of petroleum (oil) in Colombia began in 1537 when Gonzalo Jiménez de Quesada and his followers saw, "a source of bitumen or boiling pool," producing a viscous black liquid when close to what today is Barrancabermeja in the Magdalena Valley. What they saw was oozing, such as that which can still be found in different parts of the country. It was almost 400 years later (1905) when two concessionaries, De Mares and Barco, were allowed to explore and exploit petroleum; this then marked the start of the modern period in Colombian oil history. De Mares began geological studies in 1915, perforation in 1916 and the first oil was produced in 1918 (Griess, 1946).

The Colombian government created the Colombian Petroleum Company (Empresa Colombiana del Petróleo - ECOPETROL) in 1951 which has administered exploration and production in Colombian sedimentary basins for more than 50 years. Ecopetrol became a public corporation in 2003 and was released from its petroleum management functions, giving place to the newly created Colombian Hydrocarbon Agency (Agencia Nacional de Hidrocarburos - ANH).

Colombian territory has been divided into 23 sedimentary basins during ANH's administration period (Pardo et al., 2007): Amagá, Caguán - Putumayo, Catatumbo, Cauca - Patía, Cesar-Ranchería, Chocó, Chocó offshore, Colombia, Deep Pacific area, the Eastern Cordillera, the Eastern Llanos, the Guajira, Guajira offshore, Los Cayos, San Jacinto in Sinú, Sinú offshore, Tumaco, Tumaco offshore, Urabá, Vaupés - Amazonas, the Upper Magdalena Valley, the Middle Magdalena Valley and the Lower Magdalena Valley (Figure 1-1).

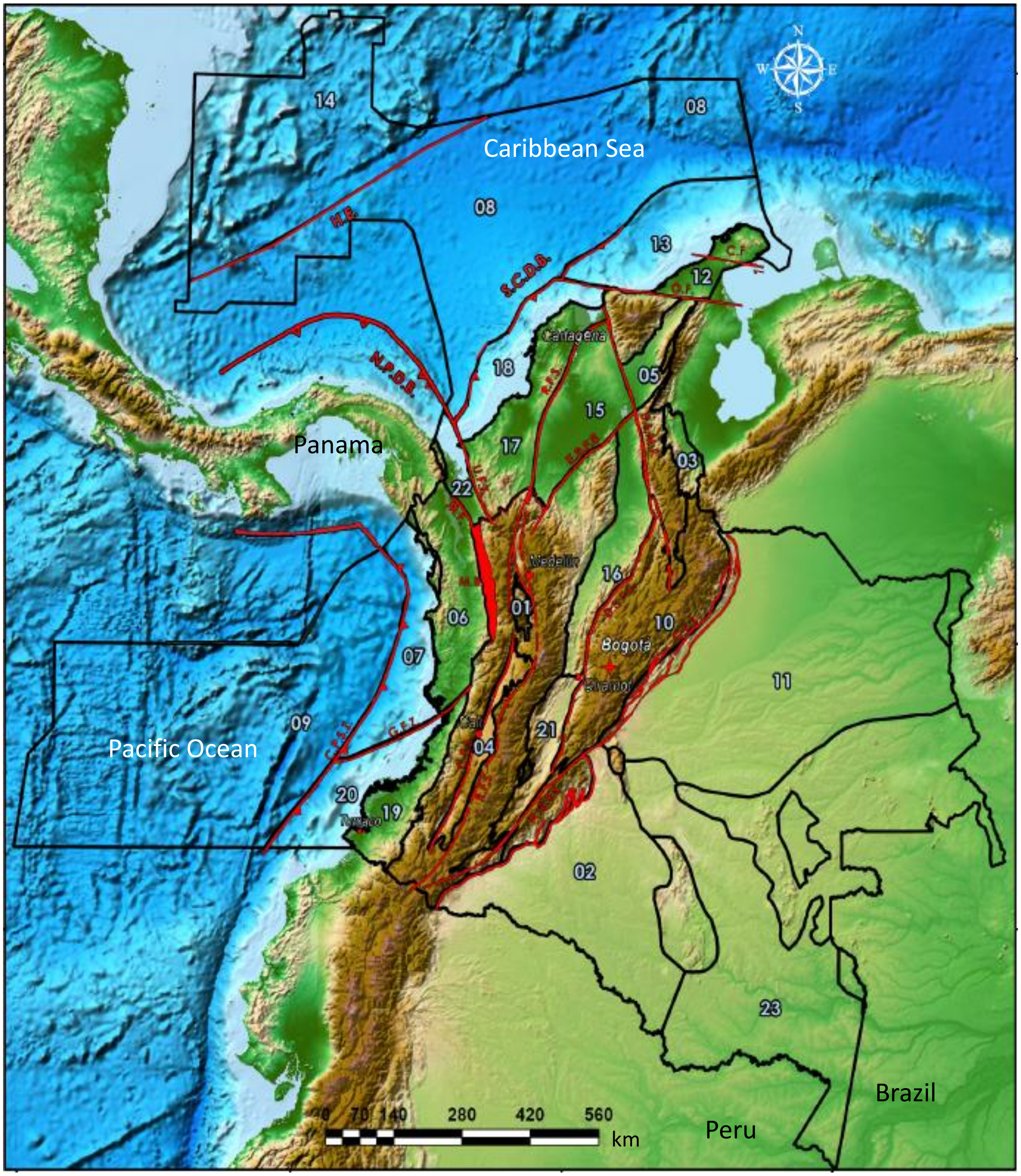

Figure 2-1 Map of Colombian basins, modified from Colombian Hydrocarbon Agency (2007). 01. Amaga; 02. Caguan-Putumayo; 03. Catatumbo; 04. Cauca-Patía; 05. Cesar-Ranchería; 06. Choco; 07. Choco Offshore; 08. Colombia; 09. Deep Pacific; 10. Eastern Cordillera; 11. Eastern Llanos; 12. Guajira; 13. Guajira Offshore; 14. Los Cayos; 15. Lower Magdalena Valley; 16. Middle Magdalena Valley; 17. Sinu-San Jacinto; 18. Sinu Offshore; 19. Tumaco; 20. Tumaco Offshore; 21. Upper Magdalena Valley; 22. Uraba; 23. Vaupes-Amazonas. Main Structures: CF – Cuiza Fault; CFS – Cauca Fault System; CPSZ – Colombian Pacific Subduction Zone; ESFS – Espiritu – Santo Fault System; HE – Hess Escarpment; MF – Murindo Fault; NPDB – North Panama Deformed Belt; OF – Oca Fault; RFS- Romeral Fault System; SCDN – South Caribbean Deformed Belt; UFS – Uramita Fault System.

Several estimations have been made for measuring Colombian yet-to-find hydrocarbon volume in its sedimentary basins. The large differences in results regarding studies carried out during the last 15 years has been due to the nature of the methodologies and data used; the most outstanding studies are mentioned below.

Ortiz (1997) estimated 15,800 MBOE resources using a fractal geometry model and field production and distribution data. The US geological service (USGS) estimated 1.3 to 10.9 BBOE yet-to-find hydrocarbons for Colombia (Ahlbrandt, 2000). D'Little (2008) estimated a yet-to-find figure of 10,000 MBOE using a fractal approach and by surveying experts. The Universidad Industrial de Santander (2009) used mass balance methodology regarding 11 Colombian sedimentary, suggesting 37,000 to 296,000 MBOE resources. Vargas (2009) estimated P_{10} and P_{90} resources ranging from 82,177 and 34,141 MBOE based on a ratio referring to production being proportional to basin size and homogenous recovery conditions (20%) and geological risk (30%).

As the current work is aimed at estimating conventional and non-conventional yet-to-find hydrocarbon resources, a start was made by evaluating the resource available in Colombian basins to provide a reference framework and compare available resources. The hydrocarbons generated in Colombian basins were calculated by using the mass balance method proposed by Schmoker (1994). Such method uses the percentage of total organic carbon (TOC) present in rock and current and original hydrogen indices as entry data. Once the hydrogen produced by the generating rocks has been calculated, then an evaluation is made of how much of this volume will become accumulated and how much can be extracted. Figure 2-2 shows the general scheme for such procedure.

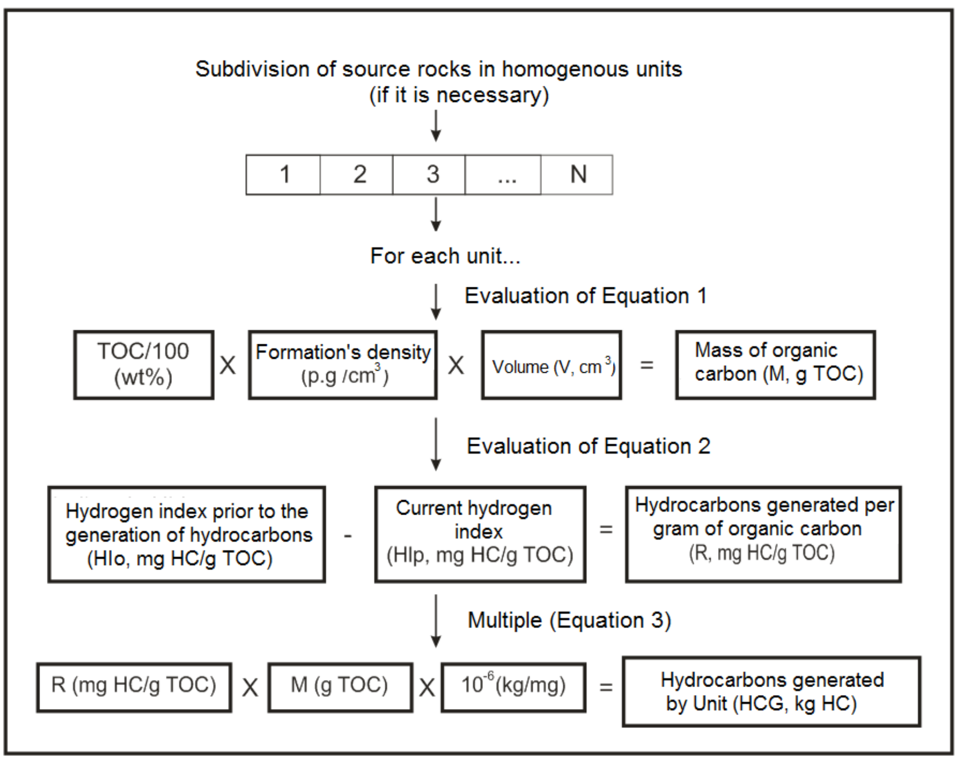

Figure 2-2 . General scheme of the procedure proposed by Schmoker (1994). Modified from Universidad Industrial de Santander (2009).

The procedure was carried out for the 12 basins having basic data available for reproducing the methodology (Catatumbo, Cesar - Ranchería, the Eastern Cordillera, the Eastern Llanos, Sinú offshore, Sinú - San Jacinto, Tumaco, the Lower Magdalena Valley, the Middle Magdalena Valley, the Upper Magdalena Valley, Caguán - Putumayo and Guajira offshore). Calculations were made for the rest of the basins for which there was little or no data available, based on a hypothesis of linearity regarding hydrocarbon available for production being directly related to basin area (e.g. Vargas, 2009).

A brief description is given below of the basins for establishing a referent to the petroleum (oil) system; the resource which could be produced is then estimated and the uncertainty of the figures so found is analysed.

2.2 Colombia's sedimentary basins

The following paragraphs summarise the most notable aspects regarding Colombia's 23 sedimentary basins. A more detailed description concerning the elements defining them or the most relevant referents regarding their oil systems can be found in ANH's book about the sedimentary basins of Colombia (ANH, 2007).

2.2.1 The Amagá basin

The Amagá basin is a rear arc basin, associated with later ocean-continent collision and convergence. It is located to the west of the Romeral fault system (Figure 2-3). It covers an area located to the southeast of the Antioquia department and the northern part of the Caldas department. This basin is bounded to the west and east by Cretaceous sedimentary and igneous rocks from the western and central cordilleras, respectively.

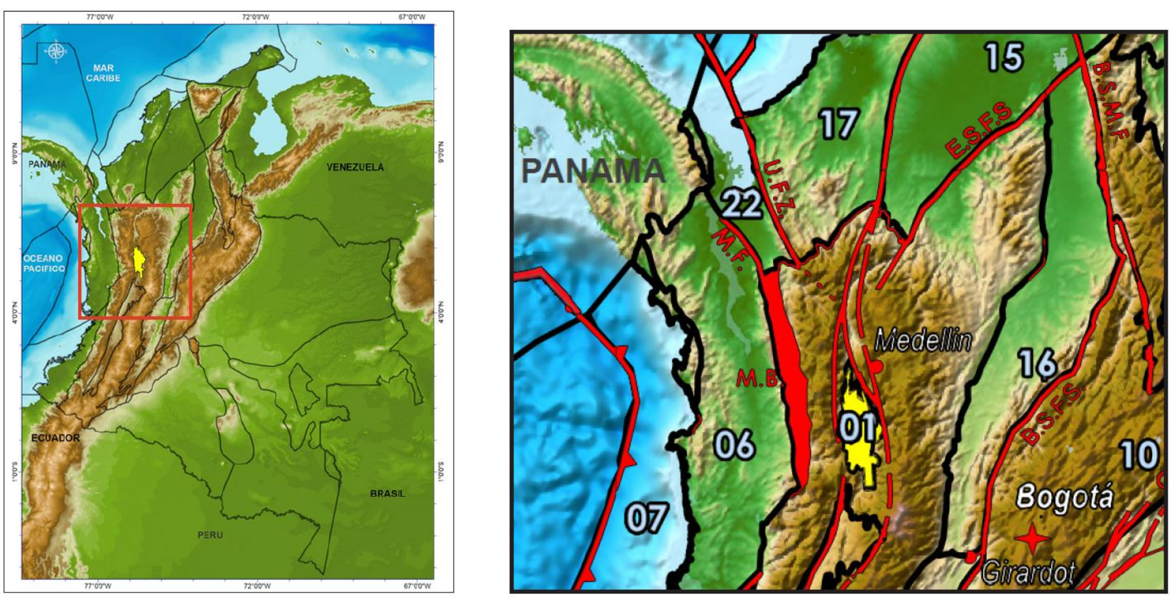

Figure 2-3 Location and borders of the Amagá basin.
01. Amagá basin; R.F.S. – Romeral fault system C.F.S. – Cauca fault system.

The basin consists of fluvial deposits having important coal layers covered by Neogene volcanic clasts, mudstones and lava flows. Figure 2-4 gives a schematic model of the basin.

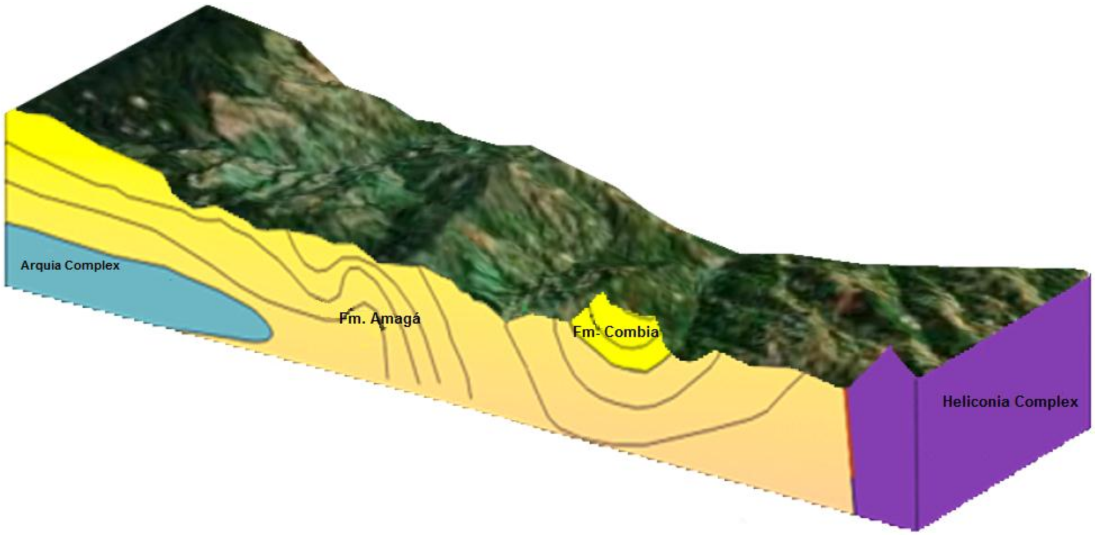

Figure 2-4. Schematic section of the Amagá basin.

2.2.2 The Caguán – Putumayo basin

The Caguán - Putumayo basin, shares its geological history with the eastern basin in Ecuador, being part of a foreland basin. The basin is bounded to the northeast by the Macarena mountain range, the international border with Ecuador and Peru to the south, the Chiribiquete Mountain range to the east and the Eastern Cordillera's piedmont fault system to the northwest (Figure 2-5).

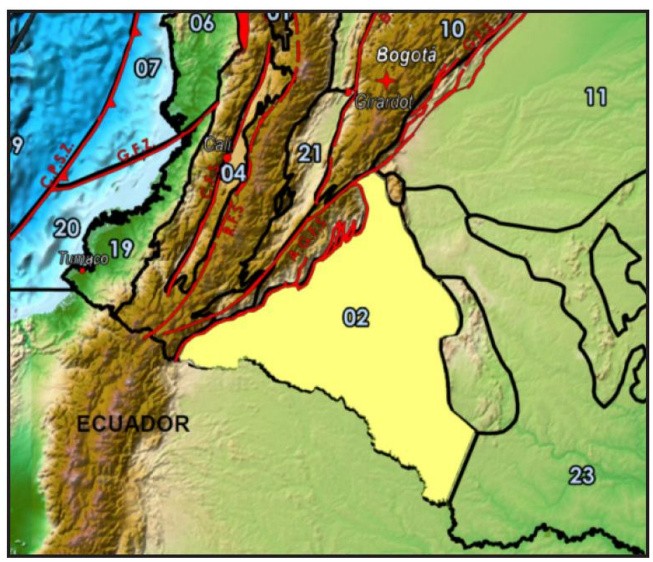

Figure 2-5. Location and borders of the Caguán – Putumayo basin. 02 – Caguán - Putumayo basin; R.F.S. – Romeral fault system; SCH – Chiribiquete mountain range; S.M. – Macarena mountain range.

The Caguán – Putumayo basin covers a 110,304 km^2 region. The Villeta formation's Cretaceous limestone and shale represent the basin's reservoir rock. Shale from the Caballos formation forms a secondary hydrocarbon source and the reservoir rock consists of sand from the Caballos formation (Figure 2-6).

ANH AGENCIA NACIONAL DE HIDROCARBUROS

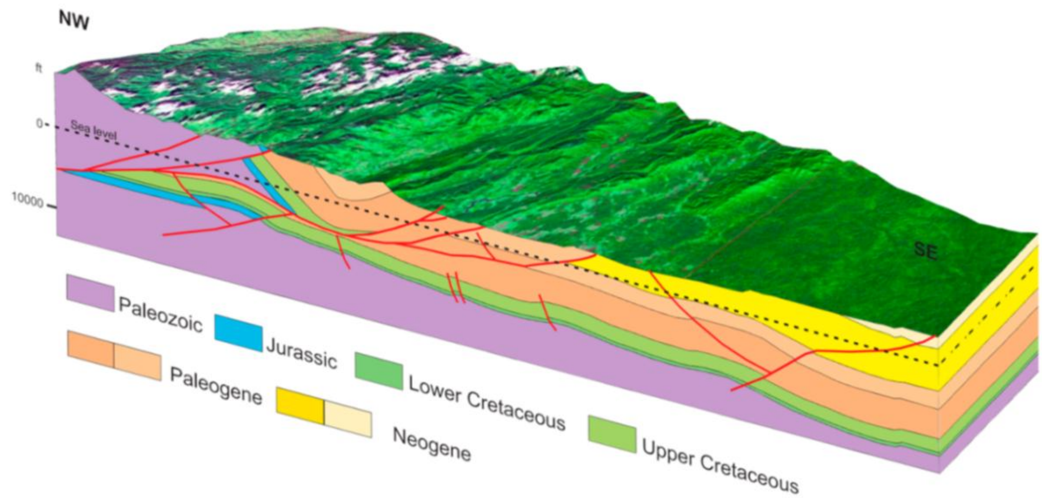

Figure 2-1. Schematic section of the Caguán – Putumayo basin.

2.2.3 The Catatumbo basin

The Catatumbo basin is the Colombian portion of the Maracaibo basin in Venezuela. It has geographical borders with Venezuela in the north and east; it is bounded by Cretaceous rocks from the Eastern Cordillera to the south and igneous and metamorphic rocks from the Santander massif to the west (Figure2-7).

Figure 2-7. Location and borders of the Catatumbo basin. 03 – Cuenca Catatumbo; B.S.M.F. – Bucaramanga-Santa Marta Fault System.

La Luna formation is the basin's main generating unit, having a thickness of around 200 feet. Pelitic rocks from the Cretaceous age (La Luna, Capacho, Tibú and Mercedes formations) are present throughout the Catatumbo basin (Figure 2-8).

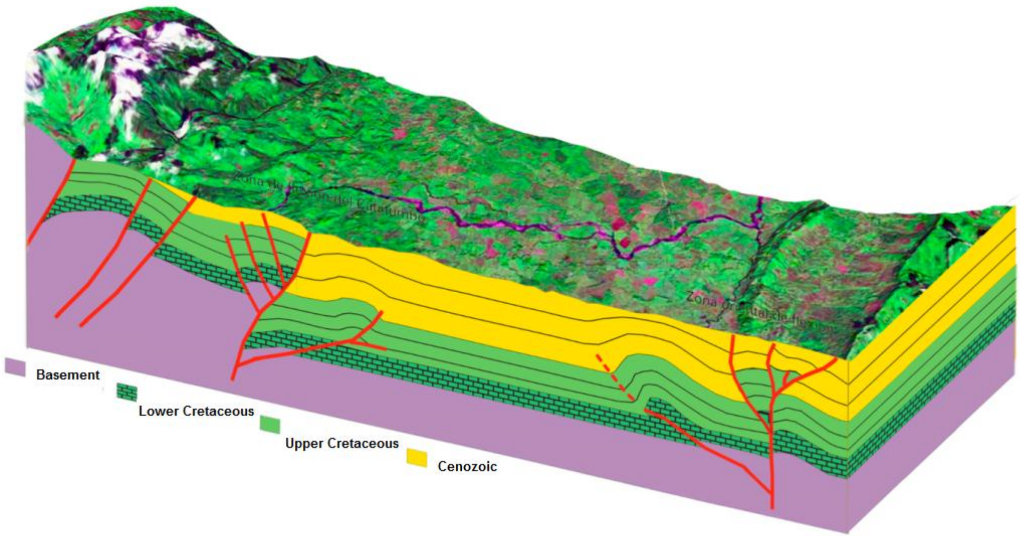

Figure 2-8. Schematic section of the Catatumbo basin.

2.2.4 The Cauca - Patía basin

The Cauca-Patía basin is an active margin basin associated with a back-arc, being genetically related to the Amagá basin. It is bounded to the north and south by basic igneous rocks from the Cretaceous age, to the west by the Cauca system fault and sedimentary and volcanic rocks from the Western Cordillera and to the east by the Romeral fault system and the Central Cordillera (Fig. 2-9).

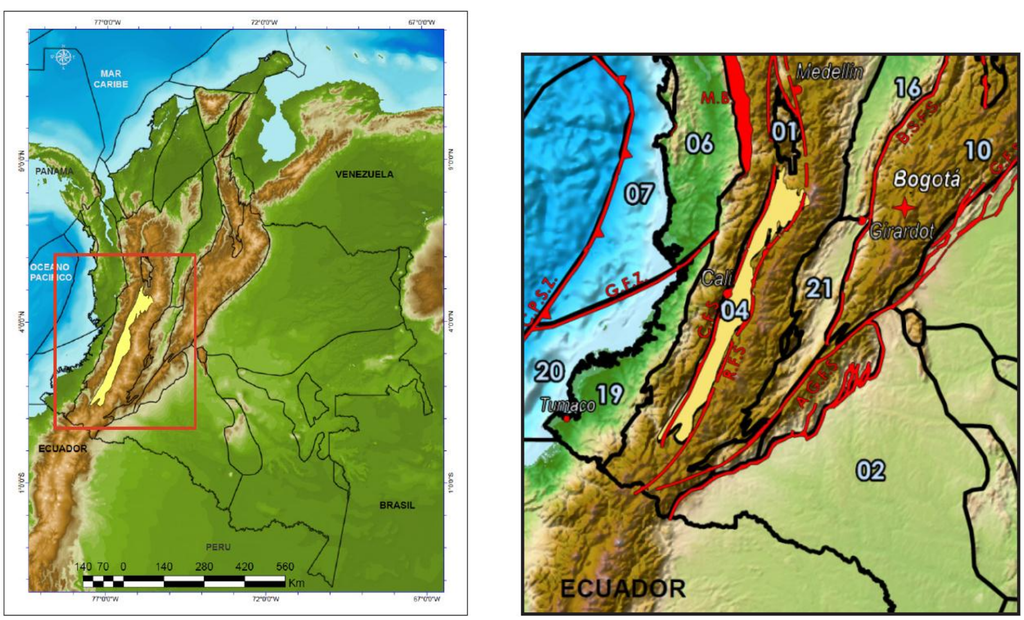

Figure 2-9. Location and borders of the Cauca-Patía basin. 04 – Cauca-Patía basin; R.F.S. – Romeral Fault System; C.F.S. – Cauca fault system; G.F.Z. – Garrapatas Fault System.

This basin has an oil-bearing system characterised by large anticlines and structural traps associated with faults in the Patía region (Figure 2-10).

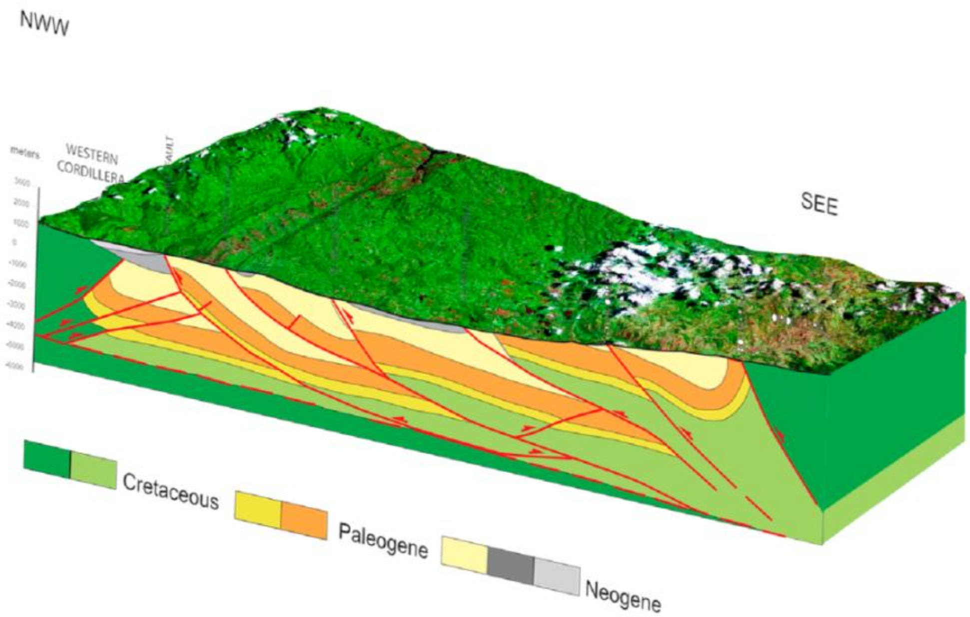

Figure 2-10. Schematic section of the Cauca-Patía basin.

2.2.5 The Cesar-Ranchería basin

The Cesar-Ranchería basin is bounded to the southeast by the Bucaramanga-Santa Marta fault, to the east-southeast by Cretaceous rocks from the Perijá mountain range and by the border between Colombia and Venezuela, to the northeast by the Oca fault and to the northwest by pre-Cretaceous rocks from the Sierra Nevada de Santa Marta (Figure 2-11).

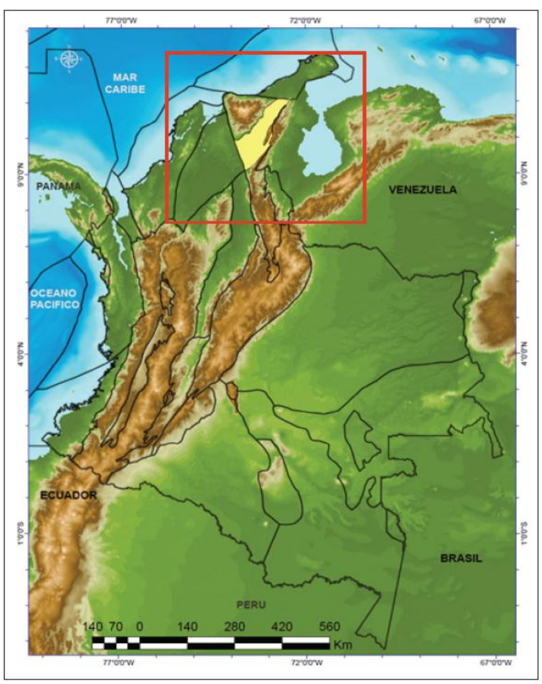

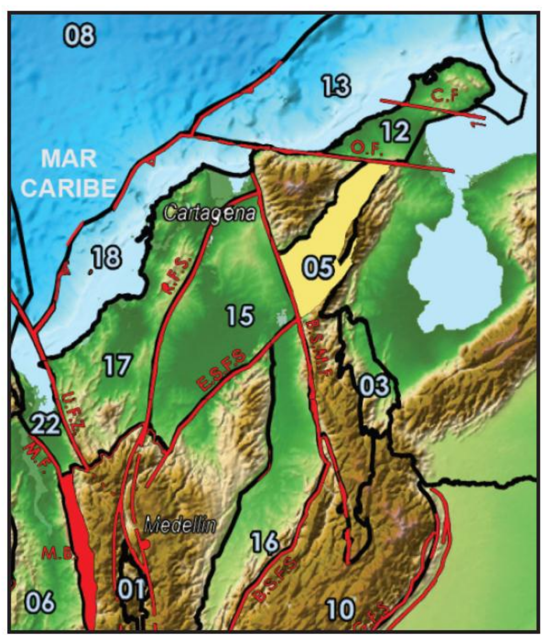

Figure 2-11. Location and borders of the Cesar-Ranchería basin. 05 – Cesar - Ranchería basin; B.S.M.F. – Bucaramanga-Santa Marta fault system; O.F. – Oca fault.

The rocks of the Molino, La Luna and Aguas Blancas formations (Figure 2-12) have excellent hydrocarbon generating potential due to their high kerogen type 2 and 3 content.

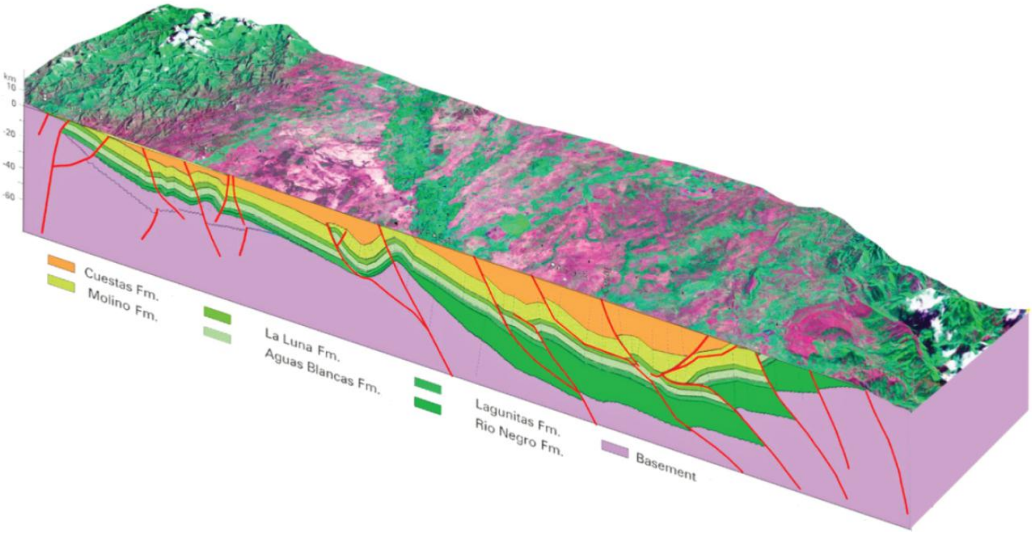

Figure 2-12. Schematic section of the Cesar-Ranchería basin.

2.2.6 The Choco basin

The Chocó basin is bounded to the northwest by the geographical border with Panamá and the Baudó mountain range, to the south by the Garrapatas fault area, to the southeast by the Pacific coastline and to the east by quartz diorites from the Mande batholith, the Cretaceous rocks from the Western Cordillera and partially by the Murindó fault (Figure 2-13).

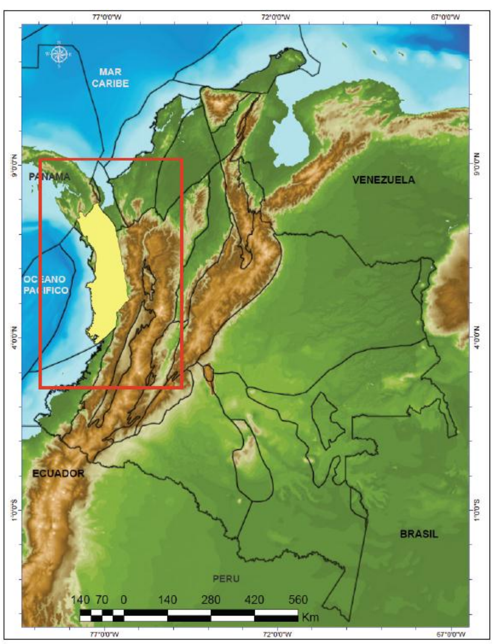

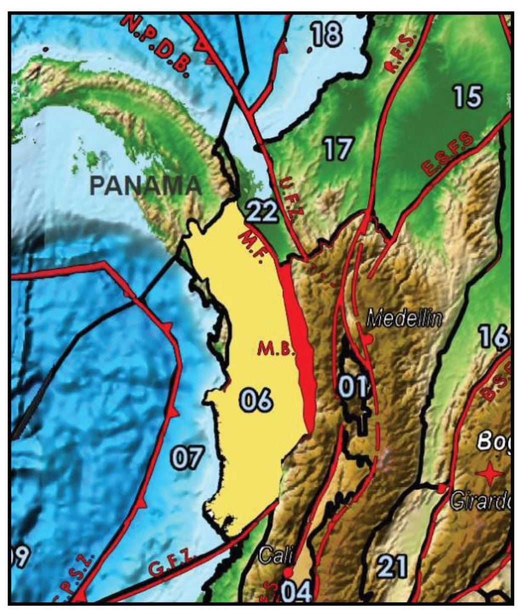

Figure 2-13. Location and borders of the Chocó basin. 06 – Chocó basin; G.F.Z. – Garrapatas fault system; S.B. – Baudó mountain range; M.B. – Mande quartz diorites; M.F. – Murindó fault; WC – Western Cordillera.

All the hydrocarbon samples found in the Chocó basin are believed to have mainly been produced in the Iró formation (Figure 2-14). This formation's thickness is not known with certainty, but it has been estimated from seismic data that it could vary from 650 to 1,200 m. It is divided into three segments: lower, intermediate and upper.

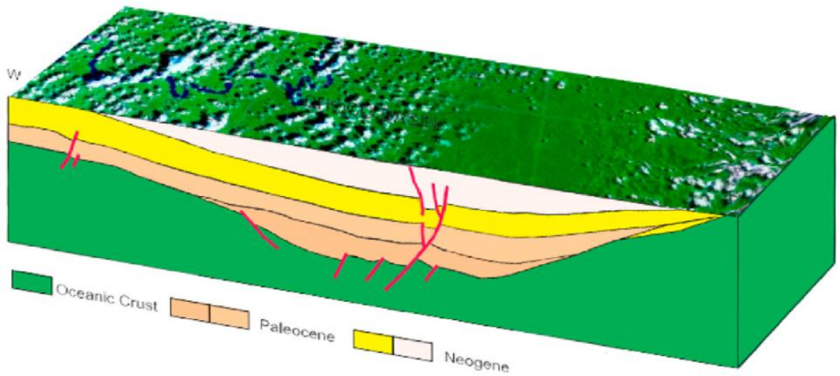

Figure 2-14. Schematic section of the Chocó basin

2.2.7 The Chocó offshore basin

The Chocó offshore basin is located in north-western Colombia; it lies beneath the water of the Pacific Ocean and its western border is shared with the Chocó department's coastline. It is bordered to the north by waters of Panamá. This offshore basin extends to the trench of the present subduction area. It is bounded to the south by the Garrapatas fault area (Figure 2-15). Figure 2-16 gives a schematic model of the basin.

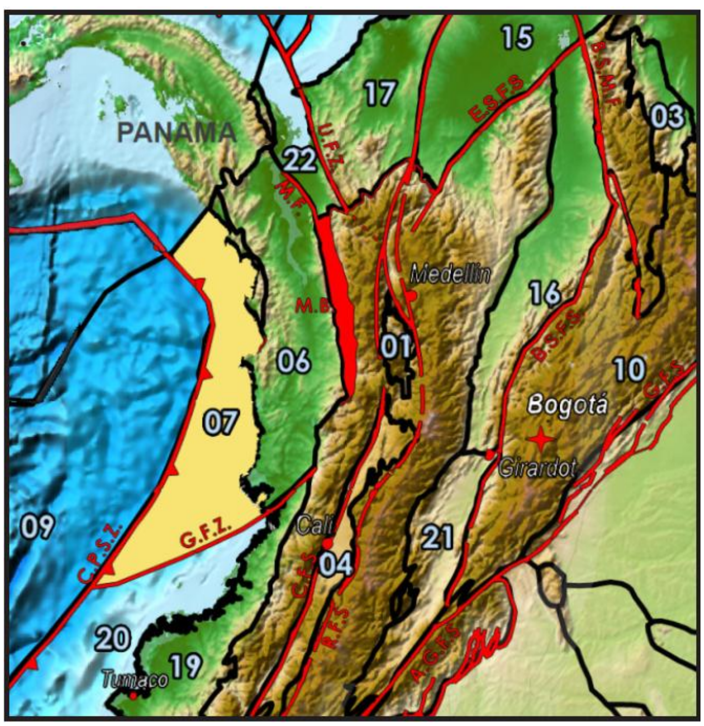

Figure 2-15. Location and borders of the Chocó offshore basin. 07– Chocó offshore basin; G.F.Z. – Garrapatas fault zone; S.Z. – Subduction zone.

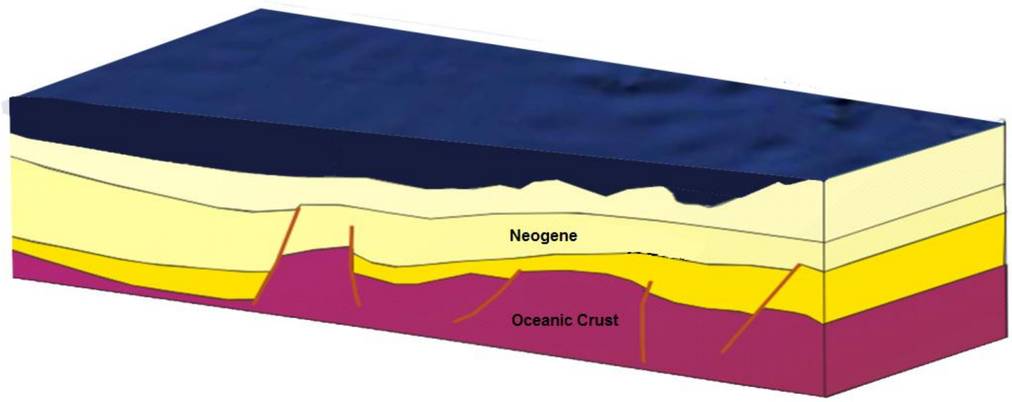

Figure 2-16. Schematic section of the Chocó offshore basin.

2.2.8 The Colombia basin

The Colombia basin is is a deep water basin located in the Caribbean Sea. It is bounded to the northwest by the Hess Escarpment, to the southeast by marine borders with Costa Rica and Panamá, to the southeast by the front of the South Caribbean deformed belt, to the east by the Colombian-Venezuelan marine frontier and to the north by maritime borders with Jamaica, Haiti and the Dominican Republic (Figure 2-17).

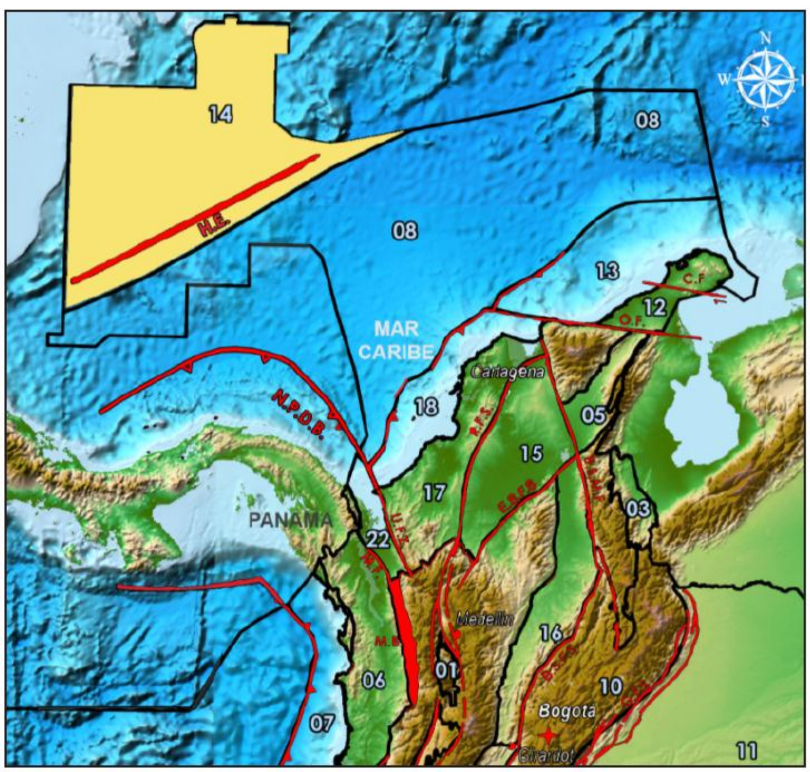

Figure 2-17. Location and borders of the Colombia basin. 08 – Colombia basin; 14 – Los Cayos basin; 18 – Sinú offshore basin; H.E. – Hess Escarpment; N.P.D.B. – North Panamá deformed belt; S.C.D.B. – South Caribbean deformed belt.

2.2.9 The Colombian Deep Pacific basin

The Colombian Deep Pacific basin is mainly composed of oceanic volcanic rocks and deep marine sediments. It is bounded to the north by the maritime border between Colombia and Panamá, to the west by the maritime border between Colombia and Costa Rica, to the south by maritime border between Colombia and Ecuador and to the east by Colombian Pacific subduction area (Fig. 2-18).

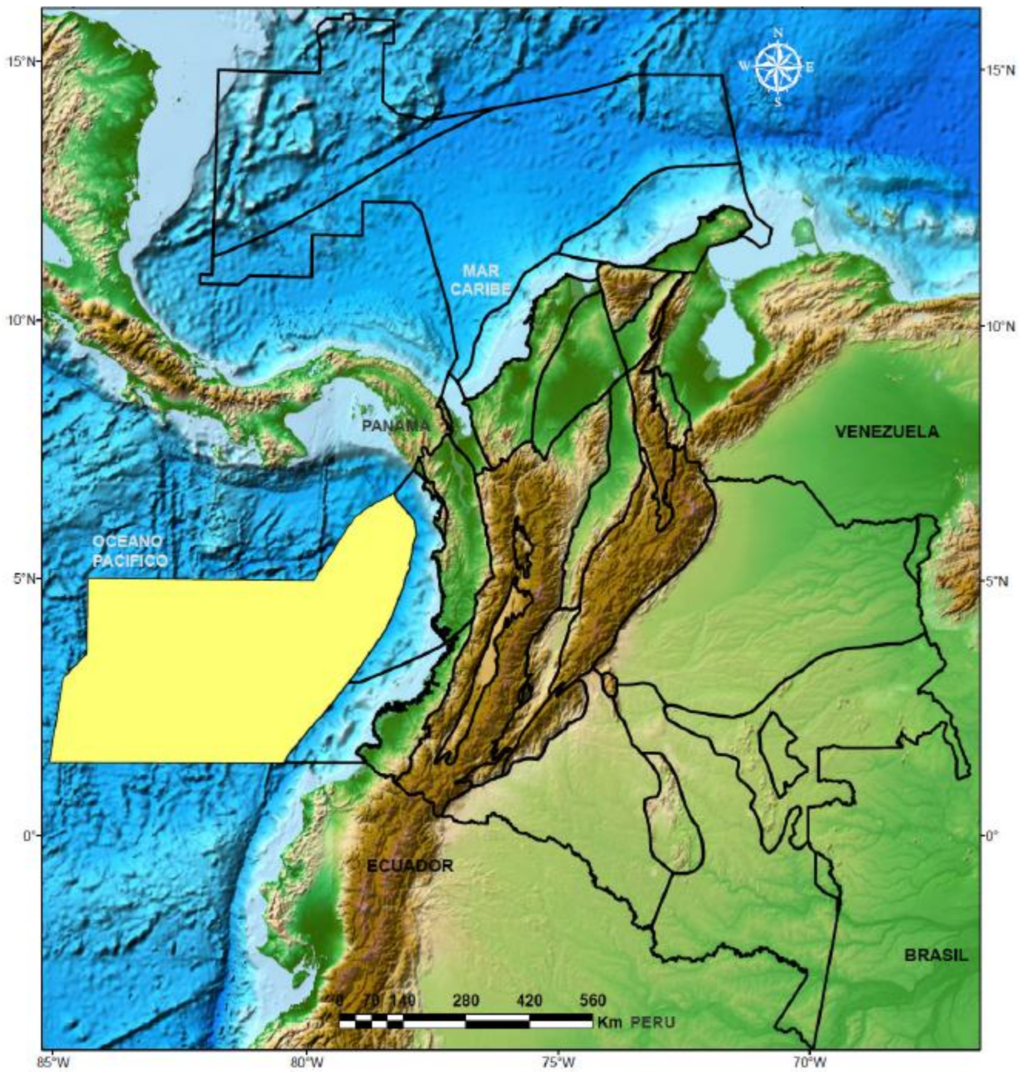

Figure 2-18. Location and borders of the Colombian Deep Pacific basin.

2.2.10 The Eastern Cordillera basin

The Eastern Cordillera basin consists of rocks formed in a Late Triassic rupture system resulting from the breakup of Pangaea and was filled by marine sediment from the Mesozoic age and continental sediment from the Cenozoic age. As a consequence of its origin and structural developments, the basin's current boundaries are very irregular and difficult to describe. The basin is bounded to the north by igneous and metamorphic rocks from the Santander massif, to the south by the Algeciras-Garzón fault system, to the west by the Bituima and Salina fault systems and to the east by the Eastern Cordillera's frontal overlapping system (Figure 2-19).

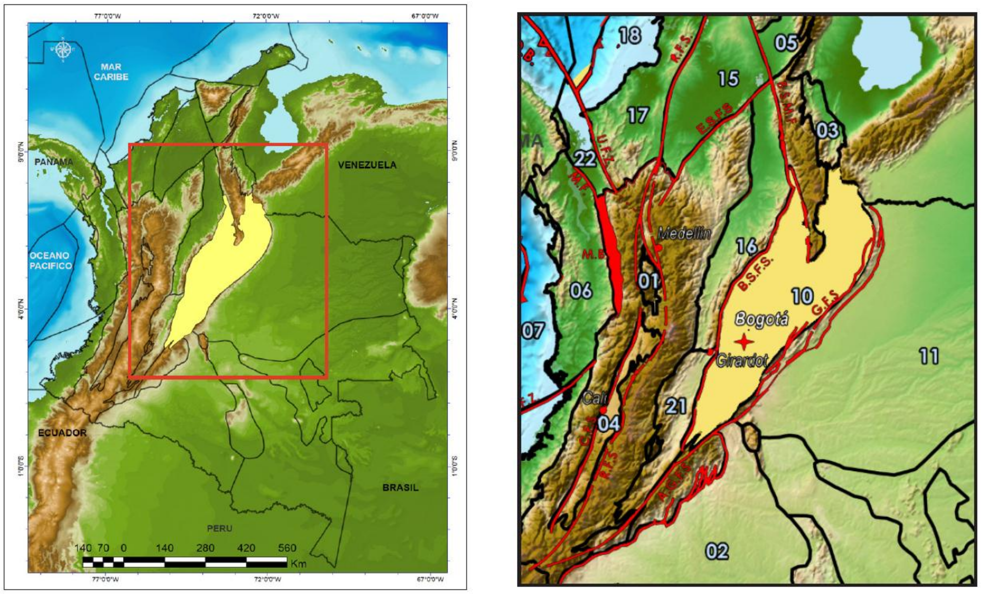

Figure 2-19. Location and borders of the Eastern Cordillera basin. 10 – Eastern Cordillera basin; B.S.F.S. – Bituima and La Salina fault system; S.M. – Santander massif; A.G.F.S. – Algeciras-Garzón fault system.

Two middle Albian and Turonian age condensed sections deposited during worldwide anoxic events are considered the main rock source, including the Simití and La Luna formations (Figure 2-20).

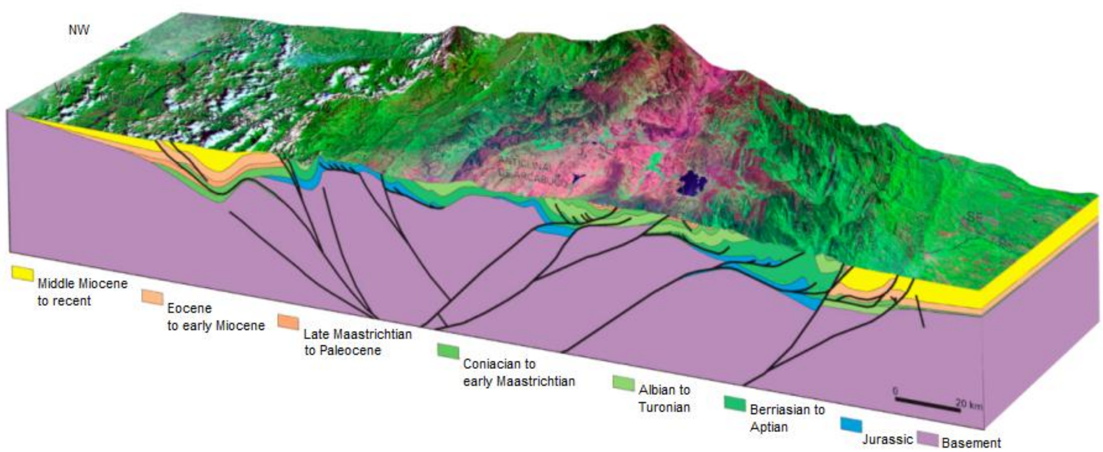

Figure 2-20. Schematic section of the Eastern Cordillera basin.

2.2.11 The Eastern Llanos basin

The Eastern Llanos basin is the most prolific hydrocarbon basin on the continental part of Colombia. This basin's northern limit is the border between Colombia and Venezuela; the basin extends to the south to the Macarena range, the Vaupés Arch and the pre-Cambrian metamorphic rocks outcropping to the south of the Guaviare River. It is bounded to the east by the outcropping of pre-Cambrian plutonic rocks from the Guyana shield and to the west by the Eastern Cordillera's overlapping system (Figure 2-21).

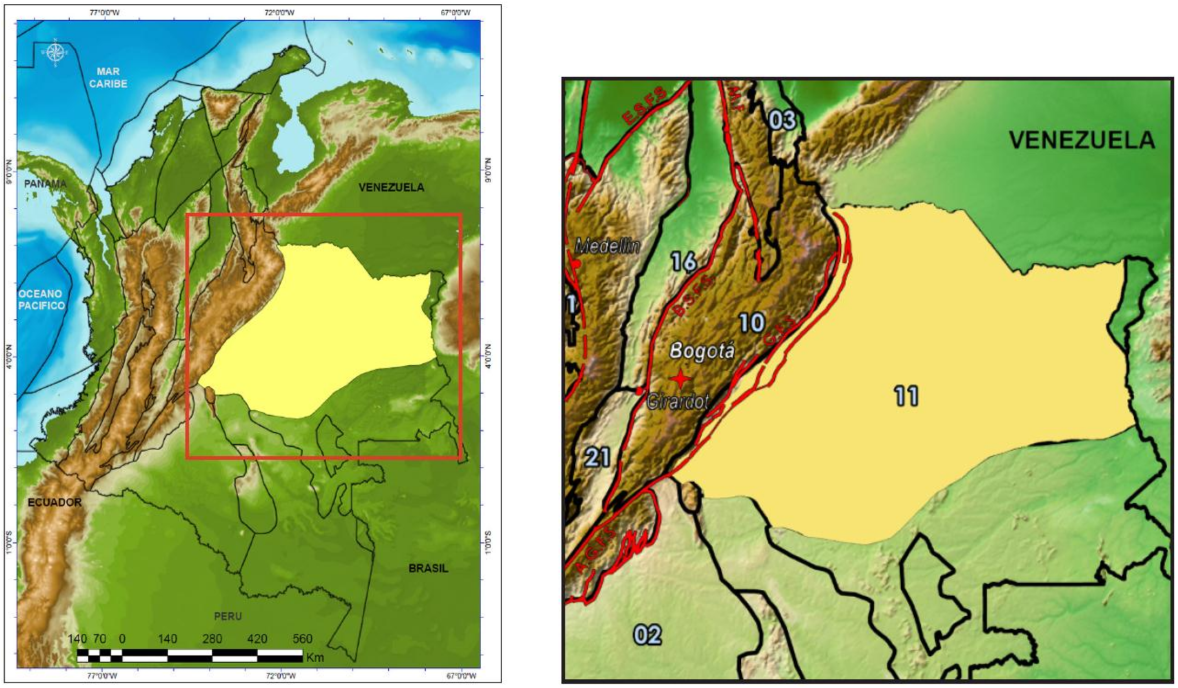

Figure 2-21. Location and borders of the Eastern Llanos basin.

The Carbonera and Mirador formations' sands form reservoir rocks. The León formation forms the basin's regional seal (Figure 2-22).

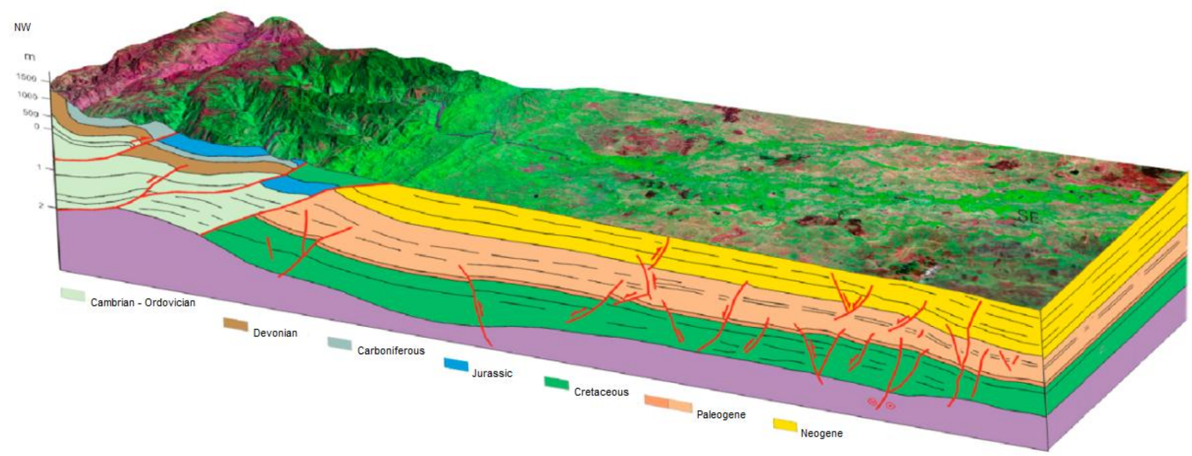

Figure 2-22. Schematic section of the Eastern Llanos basin.

2.2.12 The Guajira basin

The Guajira basin is located in the most northerly region of Colombia. The basin is bounded to the north, north-west and north-east by the actual Colombian Caribbean coastline, to the southeast by its geographical border with Venezuela and to the south by the Oca fault. The basin has been divided by the Cuiza fault trace in the Guajira upper and lower sub-basins (Figure 2-23).

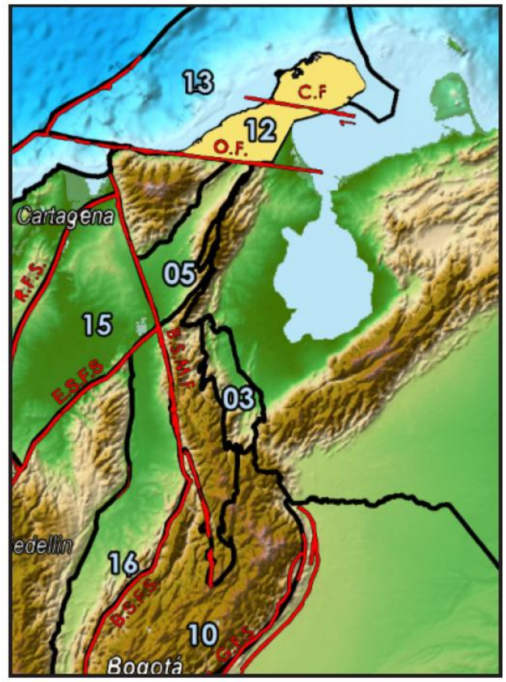

Figure 2-23. Location and borders of the Guajira basin. 12 – Guajira basin; O.F. – Oca fault; C.F. – Cuiza fault.

La Luna formation's shale, calcareous limolite and limestone have been identified as hydrocarbon-generating rocks; limestone and sandstone from the Macarao and Siamaná formations form reservoir rocks and the seals come from the Siamaná formation's lodolite (Figure 2-24).

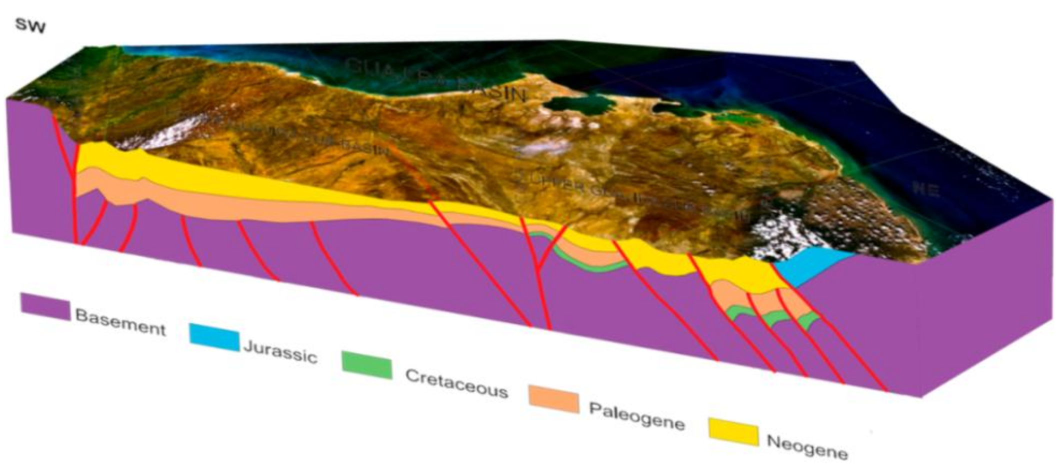

Figure 2-24. Schematic section of the Guajira basin

2.2.13 The Guajira offshore basin

The Guajira offshore basin is bordered to the north and northwest by the front of the south Caribbean deformed belt originated by the interaction between the South American and Caribbean plates, to the east by the geographical line defining the border between Colombia and Venezuela and to the southeast from the part off the coast near the Oca fault to the continental Guajira coastline (Figure 2-25). Figure 2-26 gives a schematic model of the basin.

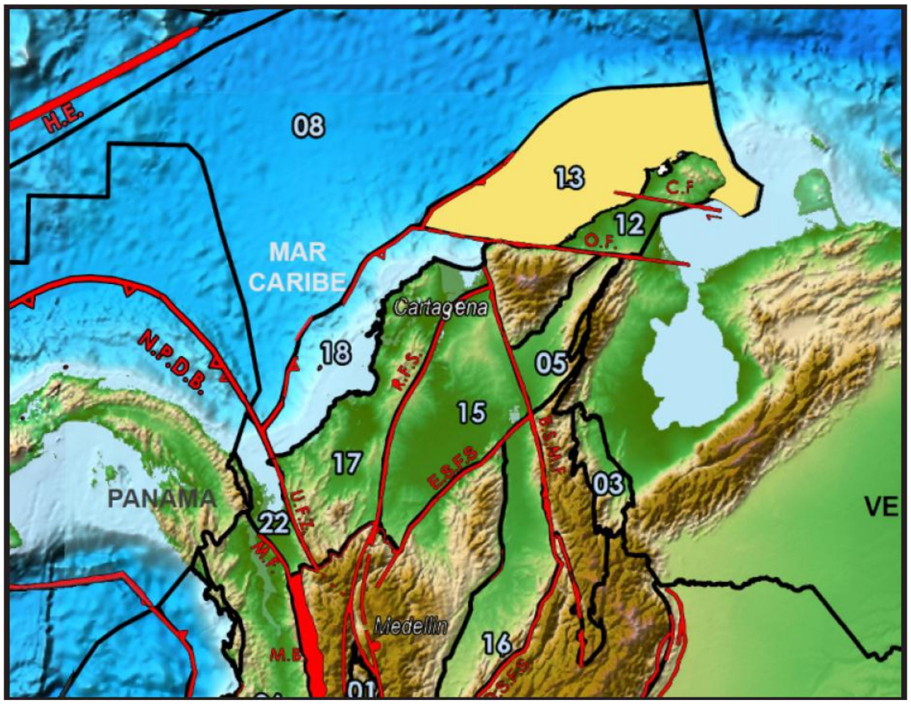

Figure 2-25. Location and borders of the Guajira offshore basin. 13 – Guajira offshore basin; O.F. – Oca fault; C.F. – Cuiza fault; S.C.D.B. – South Caribbean deformed belt.

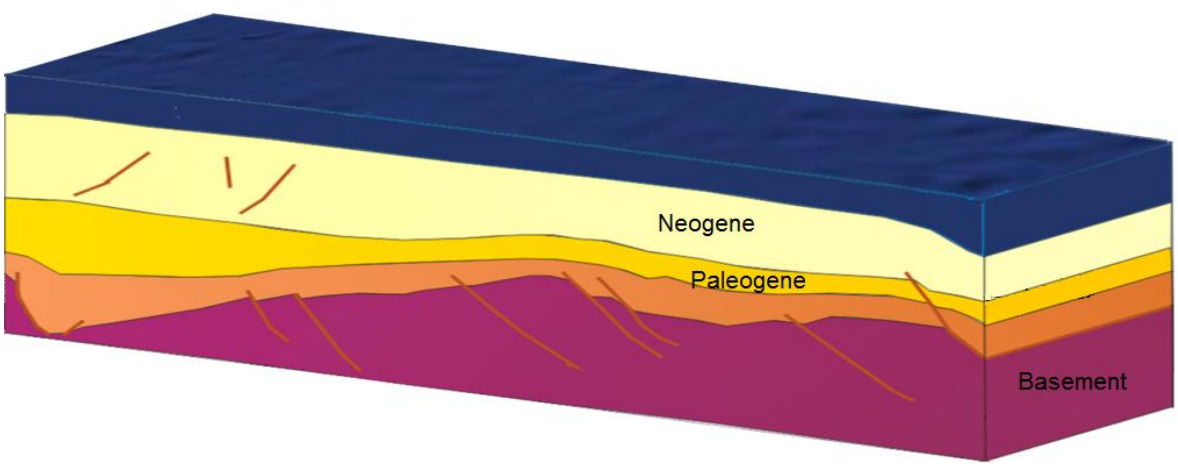

Figure 2-26. Schematic section of the Guajira basin.

2.2.14 Los Cayos basin

Los Cayos basin is an oceanic basin in the Caribbean Sea region. This basin is bounded to the north, east and west by international borders and to the south-southeast it borders the Hess escarpment (Figure 2-27).

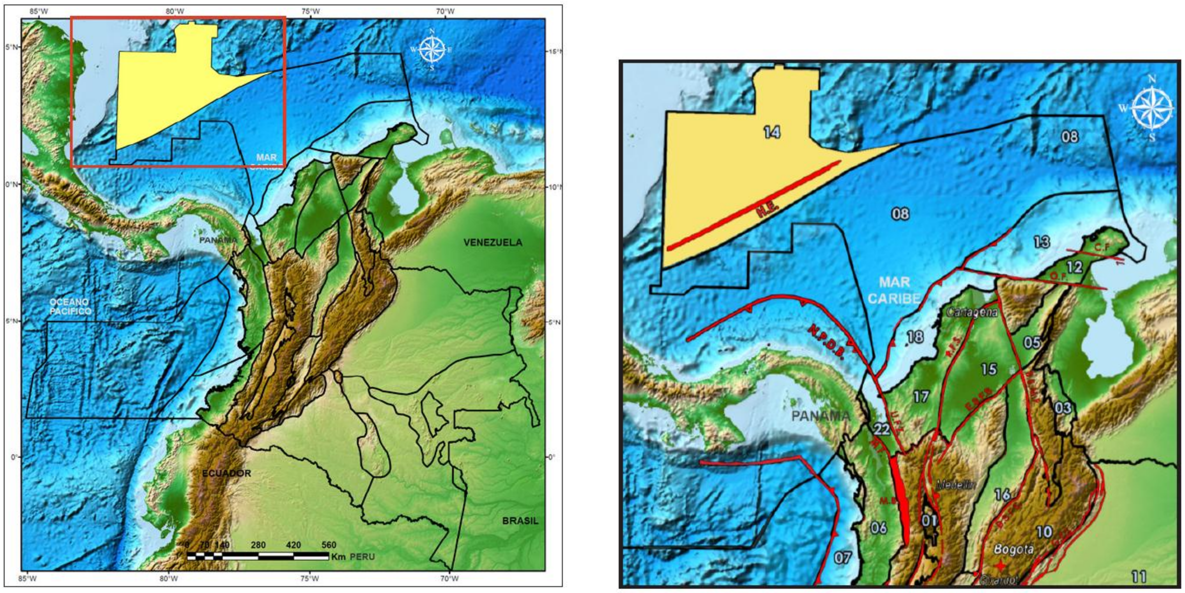

Figure 2-27. Location and borders of Los Cayos basin. 14 – Los Cayos basin; 08 – Colombia basin; H.E. – Hess Escarpment.

The basin's fill consist of Palaeogene carbonate-siliciclastic sequences followed by Neogene siliciclasts. Figure 2-28 gives a schematic model of the basin.

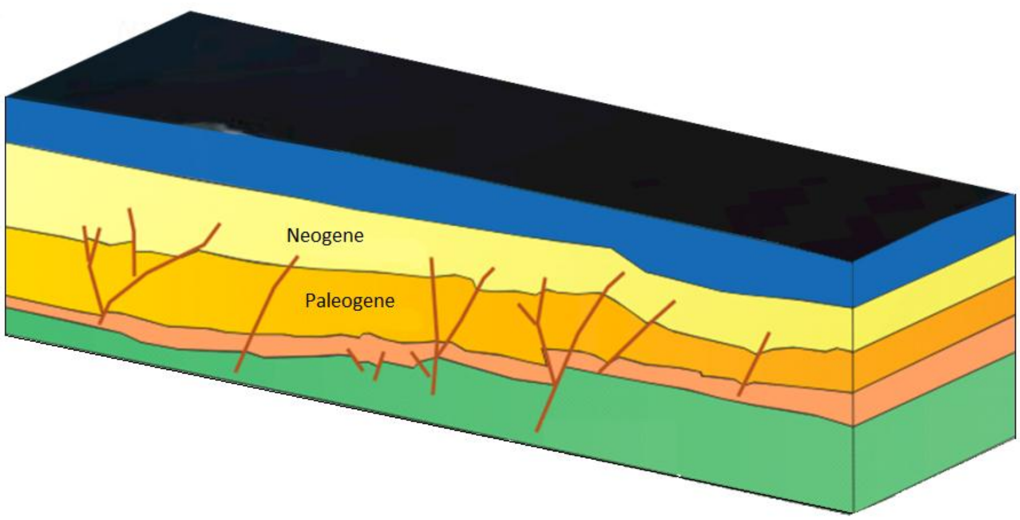

Figure 2-28. Schematic section of Los Cayos basin.

2.2.15 Lower Magdalena Valley basin

The Lower Magdalena Valley basin is a triangular transtensional basin bounded to the west and north by the Romeral fault system and to the south and southeast by the igneous and metamorphic complex of the Central Cordillera and the San Lucas mountain range. The basin is bounded to the east by the northern portion of the Bucaramanga-Santa Marta fault system (Figure 2-29). A plinth-type range divides the basin into the Plato sub-basin to the north and the San Jorge sub-basin to the south.

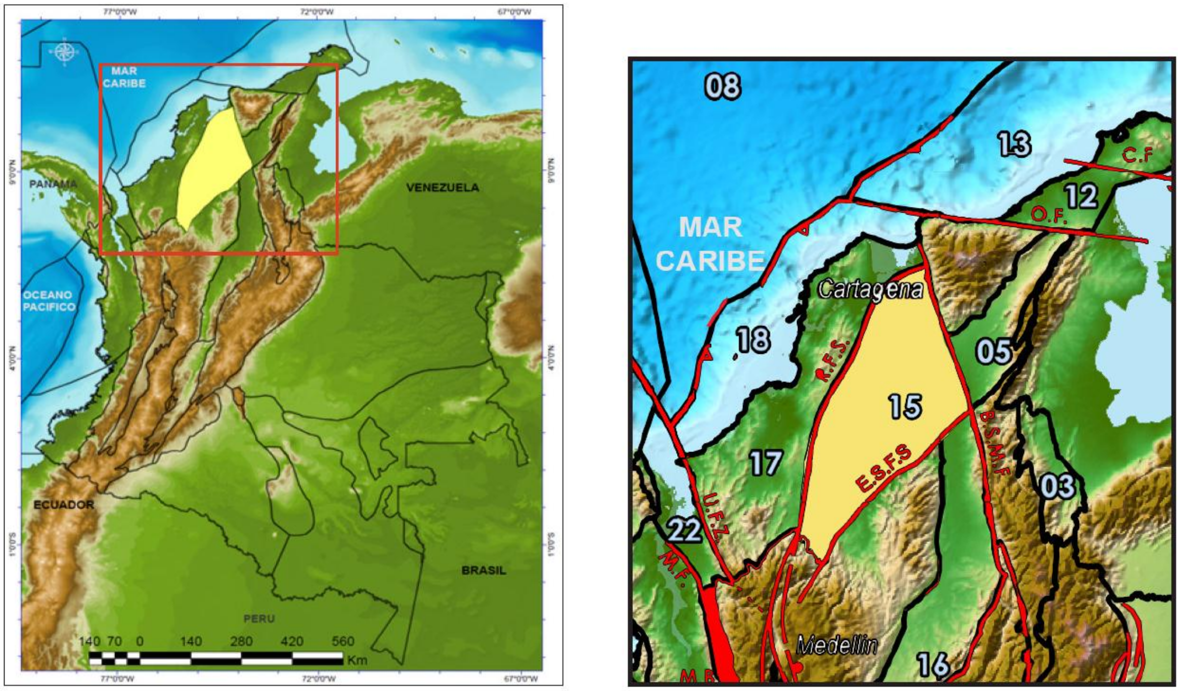

Figure 2-29. Location and borders of the Lower Magdalena Valley basin. 15 – Lower Magdalena valley basin; B.S.M.F. – Bucaramanga-Santa Marta fault system; R.F.S. – Romeral fault system; C.C.– Central Cordillera; S.L. – San Lucas mountain range.

The Ciénaga de Oro (literally, the golden swamp) formation's different levels act as generating rock, reservoir and seal (Figure 2-30).

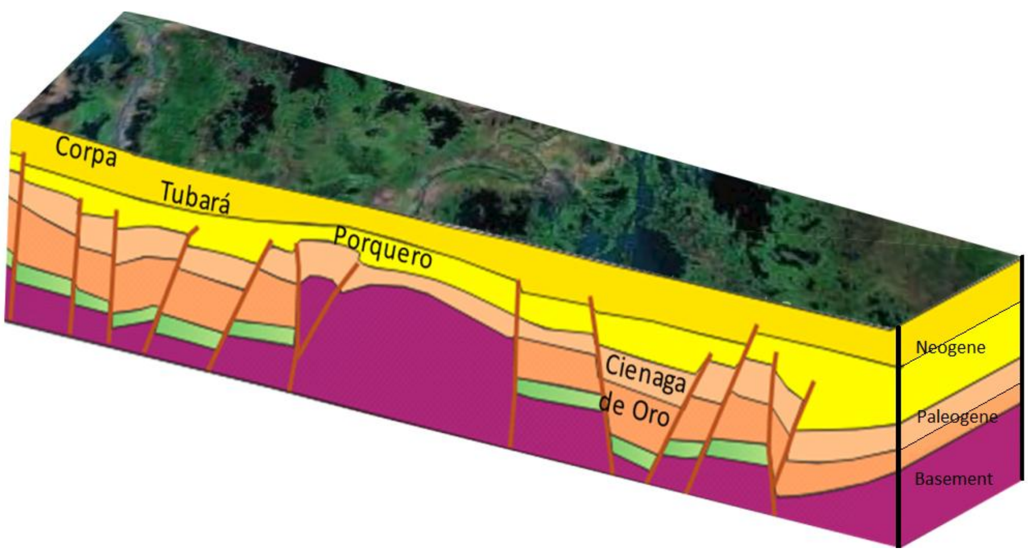

Figure 2-30. Schematic section of the Lower Magdalena Valley basin.

2.2.16 Middle Magdalena Valley basin

The Middle Magdalena Valley basin consists of a so-called poly-historic basin. Its structural Development took place during different stages linked to tectonic events regarding the north-western corner of South America which occurred during the Late Triassic, Middle Cretaceous, Early

Palaeocene and Middle Neogene ages. The basin is bounded to the southeast by the Bituima and Salina fault systems, to the north by the Espiritú Santo fault system, to the west by the Neogene sediments onlap over the San Lucas mountain range and the Central Cordillera's plinth, to the south by the Girardot fold belt and to the northeast by the Bucaramanga-Santa Marta fault system (Figure 2-31).

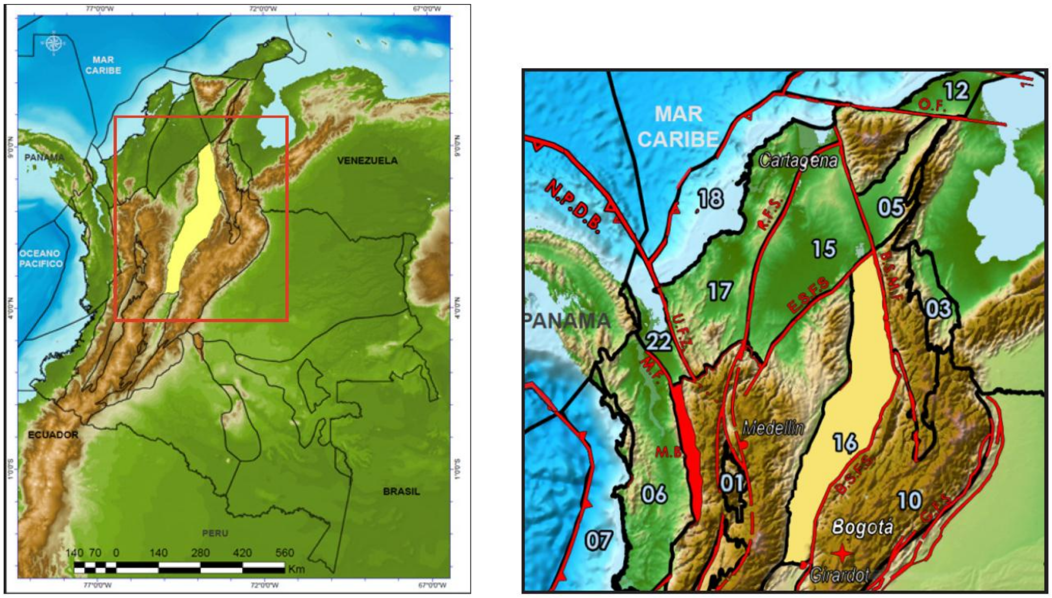

Figure 2-31. Location and borders of the Middle Magdalena Valley basin. 16 – Middle Magdalena Valley basin; B.S.M.F. – Bucaramanga - Santa Marta fault system; B.S.F.S. – Bitumina and La Salina fault system; E.S.F.S. – Espiritú Santo fault system; S.L. – San Lucas mountain range; G.F.B. – Girardot fold belt; C.C. – Central Cordillera.

Limestone and lutite from La Luna, Simití and Tablezo formations are the main source rocks; the reservoir rocks present in the basin are from the Lisama, Esmeralda, La Paz, Colorado and Mugrosa formations (Figure 1-32).

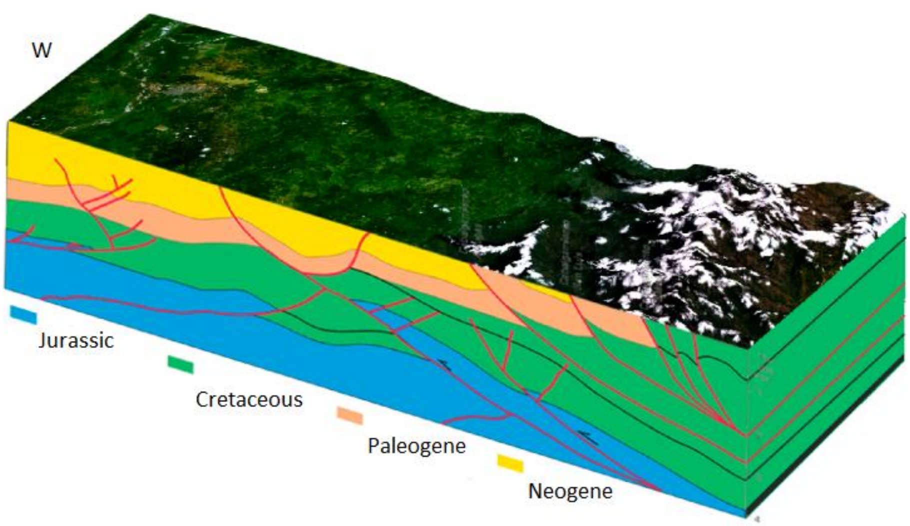

Figure 1-32. Schematic section of the Middle Magdalena Valley basin.

2.2.17 Upper Magdalena Valley basin

The basin is bounded to the north by the Girardot fold belt; to the southeast it is partially bounded by the Algeciras-Garzón fault system, to the northeast by the Bituima-Salina fault system and to the west by pre-Cretaceous rocks from the Central Cordillera (Figure 2-33).

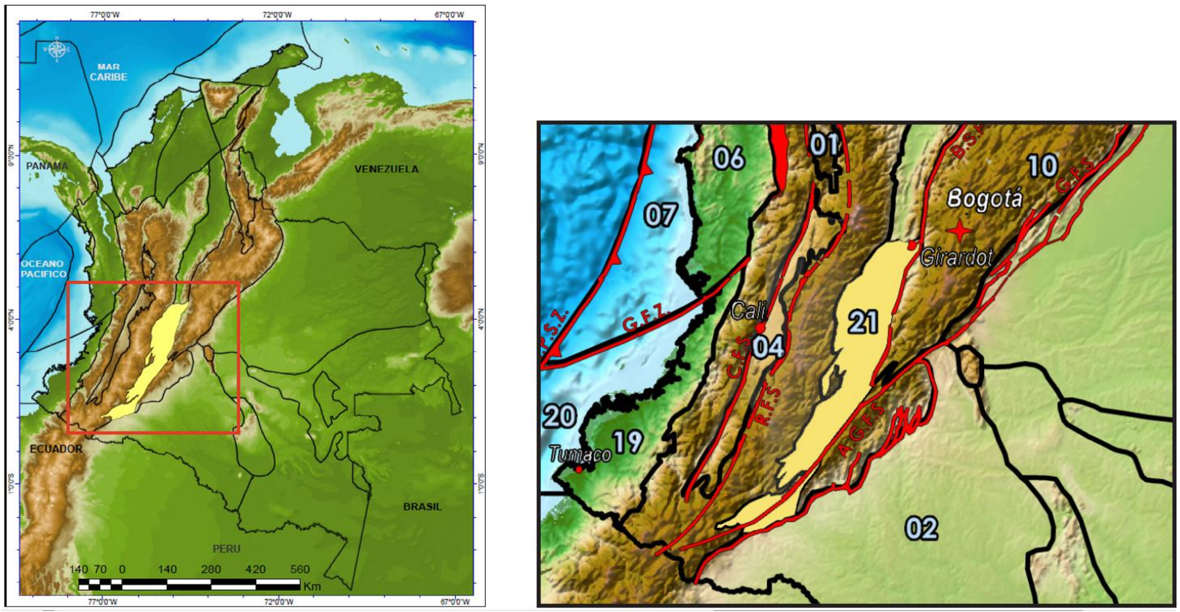

Figure 2-33. Location and borders of the Upper Magdalena Valley basin. 21 – Upper Magdalena Valley basin; B.S.F.S. – Bitumina and La Salina fault system; A.G.F.S. – Algeciras-Garzón fault system; G.F.B. – Girardot fold belt; C.C. – Central Cordillera.

The basin has been actively explored for hydrocarbons during the last two decades. However, it is thought that important petroleum reserves still lie trapped in stratigraphic plays. The basin's generating rocks are lutite and limestone from the Tetuán, Bambucá and La Luna formations; reservoir rock is present in the Caballos, Monserrate and Honda formations and the rock seal is represented by arcillolite from the Bambucá formation (Figure 2-34).

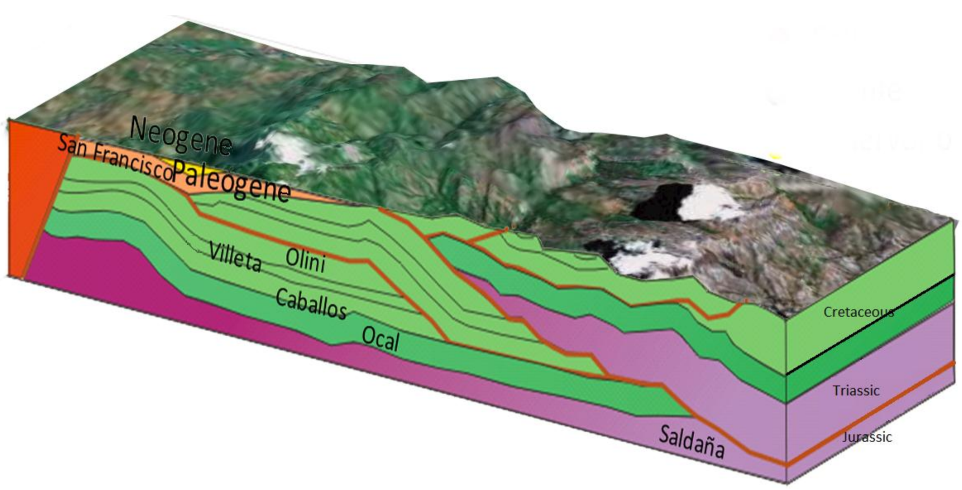

Figure 2-34. Schematic section of the Upper Magdalena Valley basin.

2.2.18 Sinu- San Jacinto basin

The Sinu-San Jacinto basin is located in the north of Colombia and is the most prolific area in terms of oil seeps (ooze) and gas throughout Colombia. This basin is bounded to the east by the Romeral fault system, to the north-northwest by the Caribbean coast, to the west by the Uramita fault system and to the south by cretaceous sedimentary and volcanic rocks from the Western Cordillera (Figure 2-35). The basin's structural development is linked to the transpressional deformation produced by the Caribbean plate's displacement. Figure 1-36 gives a schematic model of the basin.

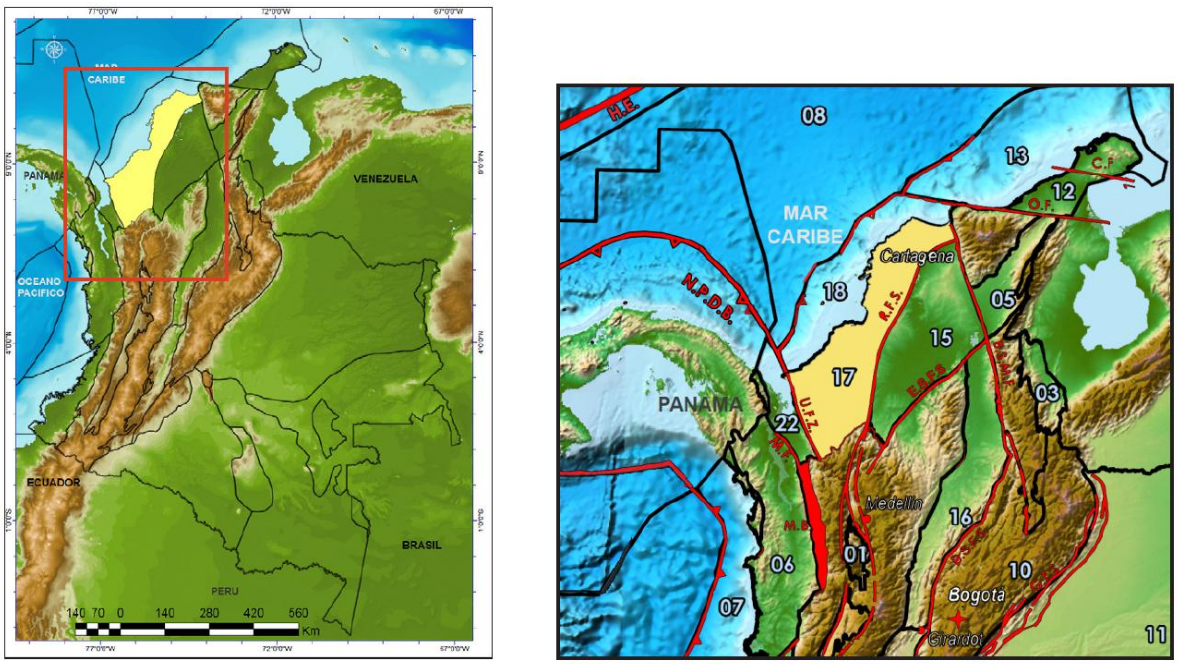

Figure 2-35. Location and borders of the Sinu - San Jacinto basin. 17 – Sinu - San Jacinto basin; U.F.S. – Uramita fault system; W.C. – Western Cordillera: R.F.S. – Romeral fault system.

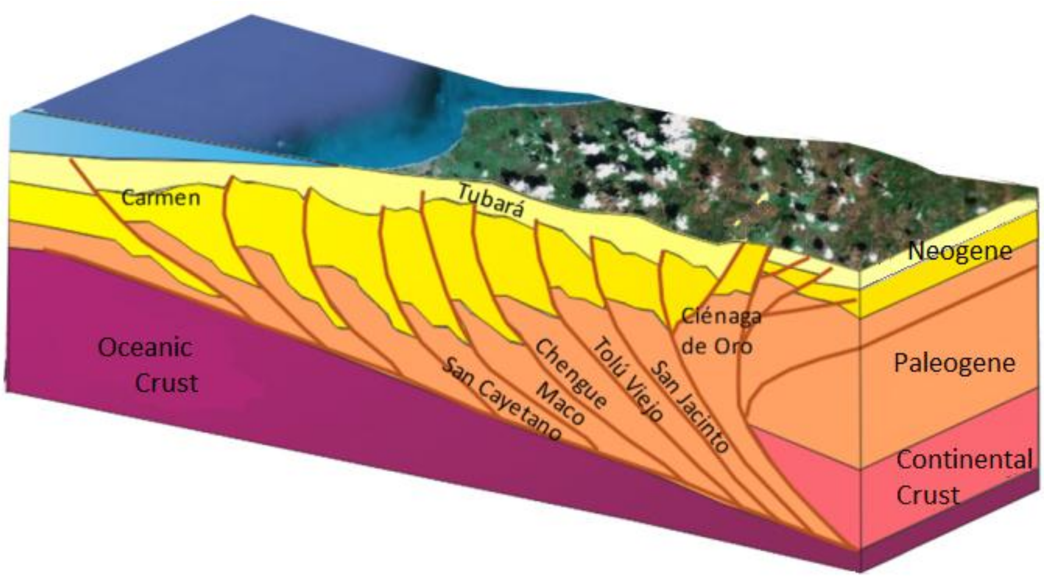

Figure 2-36. Schematic section of the Sinu-San Jacinto basin.

ANH AGENCIA NACIONAL DE HIDROCARBUROS

2.2.19 Sinú offshore basin

This basin lies entirely below the waters of the Caribbean Sea and is bounded to the northeast by the Oca fault, to the southeast by the coastline, to the northwest by the front of the South Caribbean deformed belt and to the southeast by the Uramita fault system (Figure 2-37). Figure 2-38 gives a schematic model of the basin.

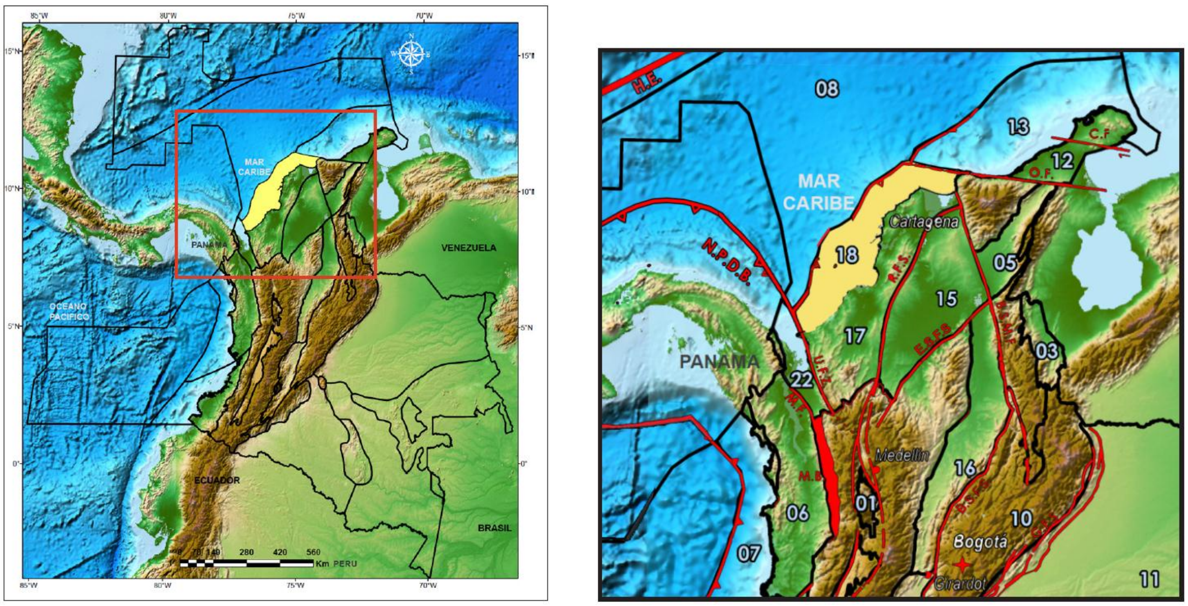

Figure 2-37. Location and borders of the Sinú offshore basin. 18 – Sinú offshore basin; O.F.– Oca fault; U.F.S. – Uramita fault system; S.C.D.B. – South Caribbean deformed belt.

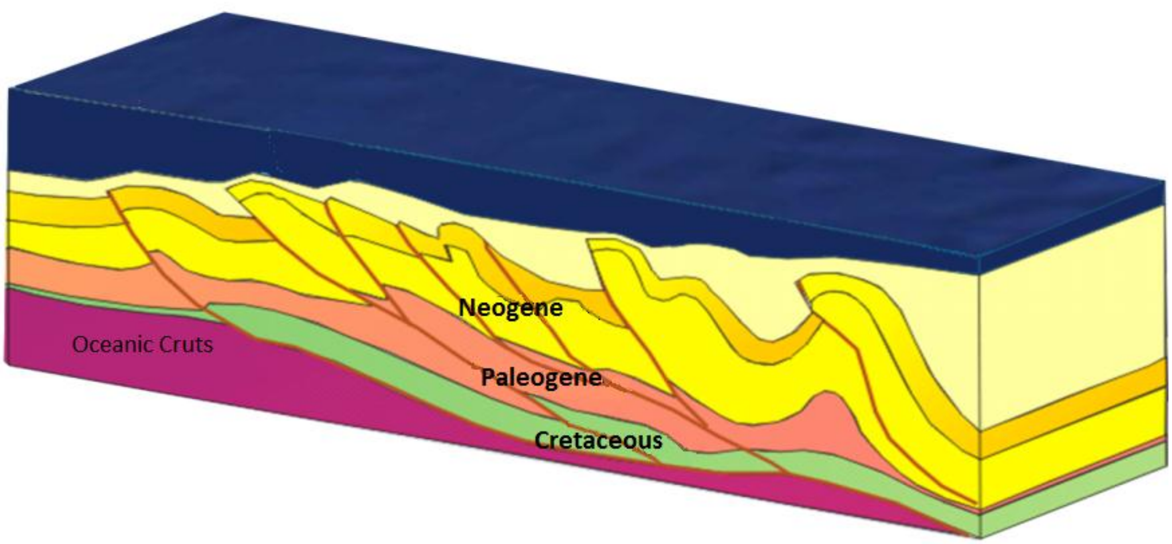

Figure 2-38. Schematic section of the Sinú offshore basin.

2.2.20 Tumaco basin

The Tumaco basin is located in the south-western region of Colombia. The basin is bounded to the north by the Garrapatas fault system; it extends to the south down to the border between Ecuador and Colombia, to the east as far as the Western Cordillera's Cretaceous rocks and to the west as far as the Pacific Ocean coastline (Figure 2-39). Figure 2-40 gives a schematic model of the basin.

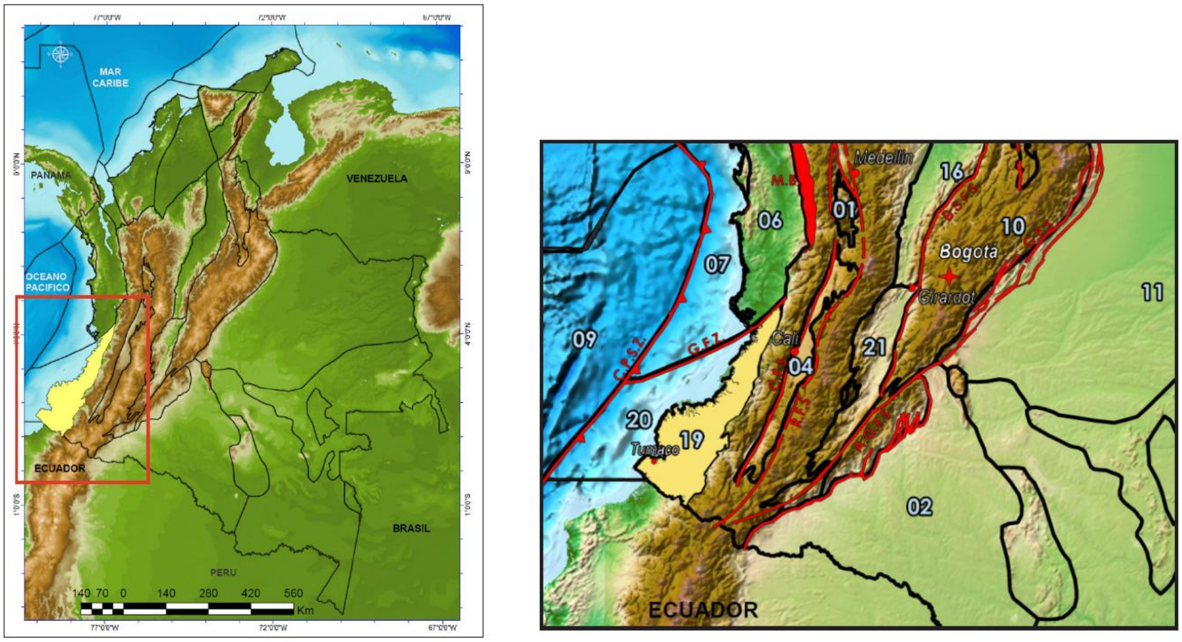

Figure 2-39. Location and borders of the Tumaco basin. 19 – Tumaco basin; G.F.Z. – Garrapata fault zone; W.C. – Western Cordillera.

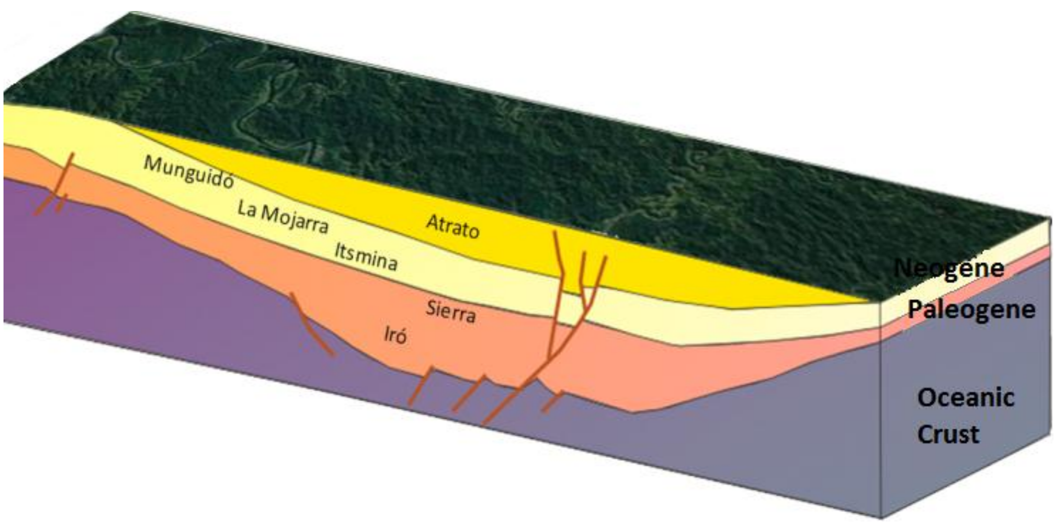

Figure 2-40. Schematic section of the Tumaco basin.

2.2.21 Tumaco offshore basin

The Tumaco offshore basin is located in the marine region in the southeast of Colombia, below the waters of the Pacific Ocean. This basin is bounded to the north by the Garrapatas fault system, to the south by the frontier with Ecuador, to the east by the coastline and to the west by the Colombian Pacific subduction area trench (Figure 2-41). Figure 2-42 gives a schematic model of the basin.

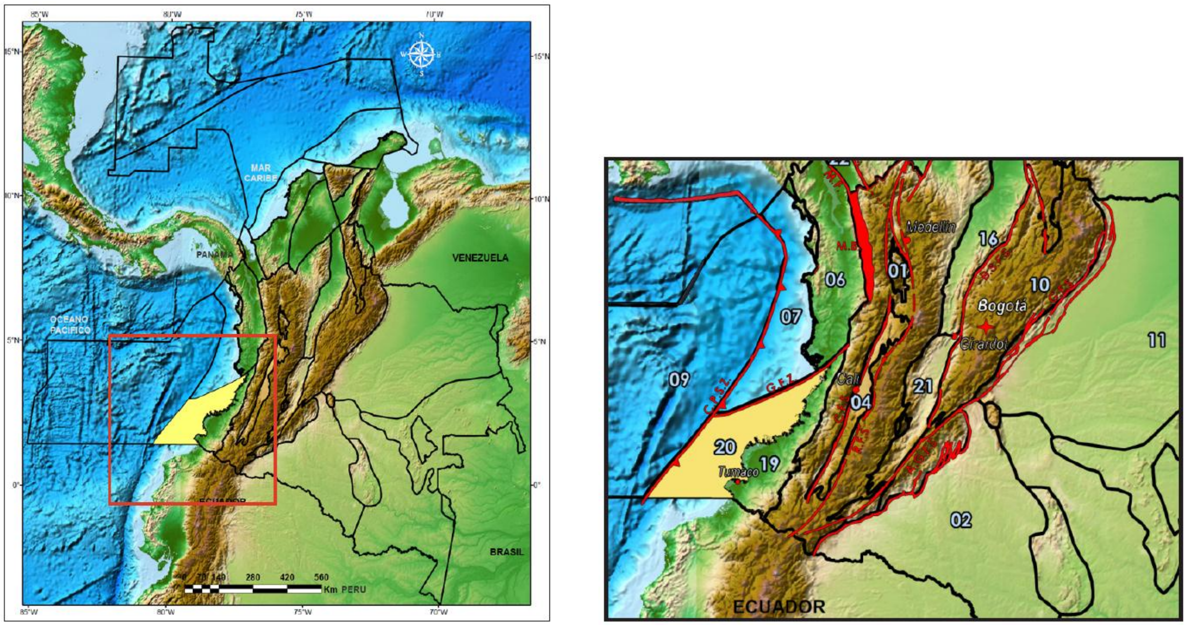

Figure 2-41. Location and borders of the Tumaco offshore basin. 20 – Tumaco offshore basin; G.F.Z. – Garrapata fault zone; C.P.S.Z. – Colombian Pacific subduction zone.

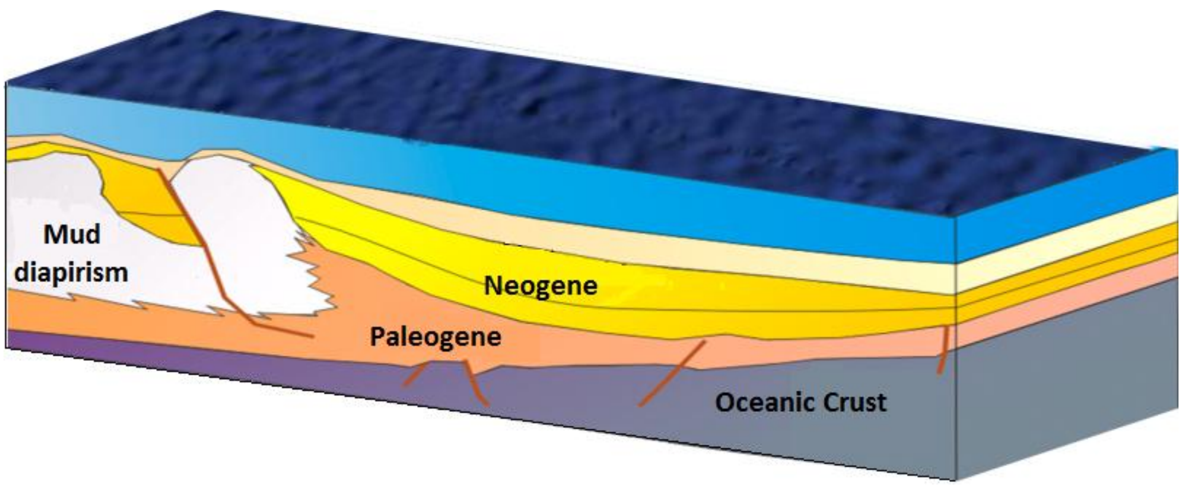

Figure 2-42. Schematic section of the Tumaco offshore basin.

2.2.22 Urabá basin

The Urubá basin is bounded to the north-northwest by the border between Colombia and Panamá, to the southeast by the Mandé batholith and the Murindó fault, to the east by the Uramita fault system, to the west by the Darien mountain range and to the south by Cretaceous rocks from the Western Cordillera (Figure 2-43). Figure 2-44 gives a schematic model of the basin.

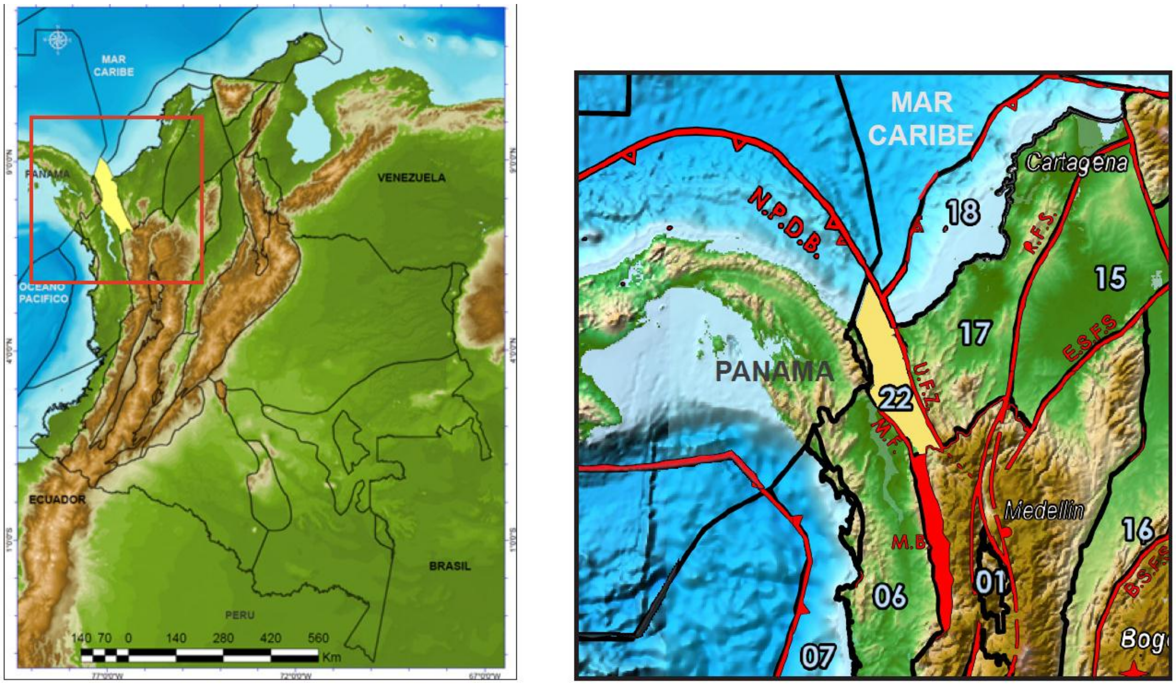

Figure 2-43. Location and borders of the Urabá basin. 22 - Urabá basin; U.F.S. – Uramita fault system; M.B. – Mandé batholith; M.F. – Murindó fault; S.D. – Darien mountain range; W.C. – Western Cordillera.

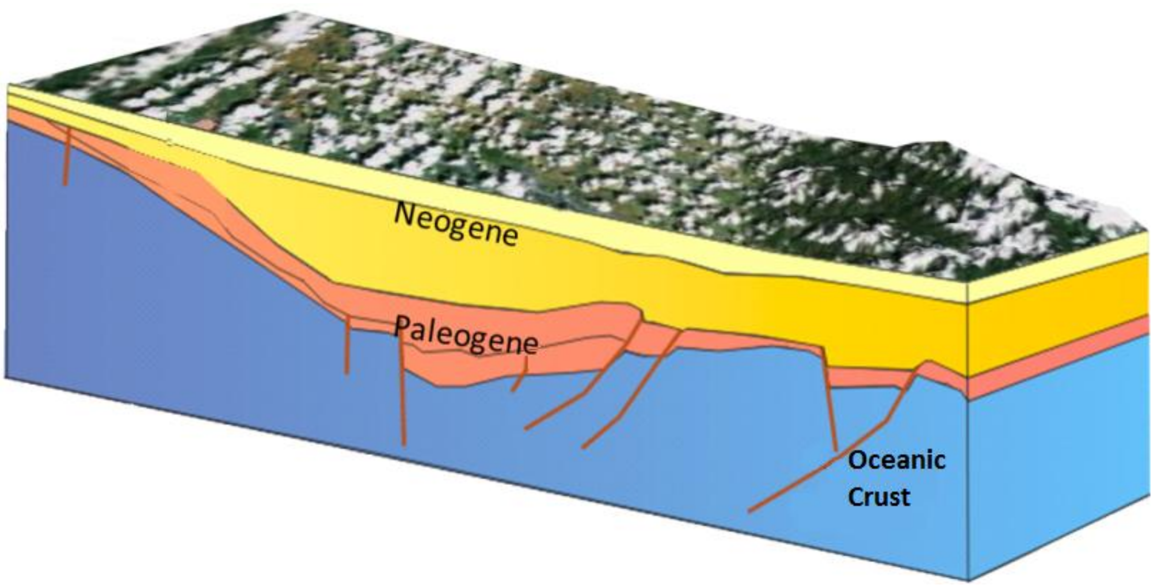

Figure 2-44. Schematic section of the Urabá basin.

2.2.23 Vaupés – Amazonas basin

The Vaupés-Amazonas basin is bounded to the north by the Vaupés Arch, to the south-southeast by the frontiers with Brazil and Peru, to the west by the Chiribiquete mountain range and to the east by the Trampa-Carurú mountain range (Figure 2-45). Figure 2-46 gives a schematic model of the basin.

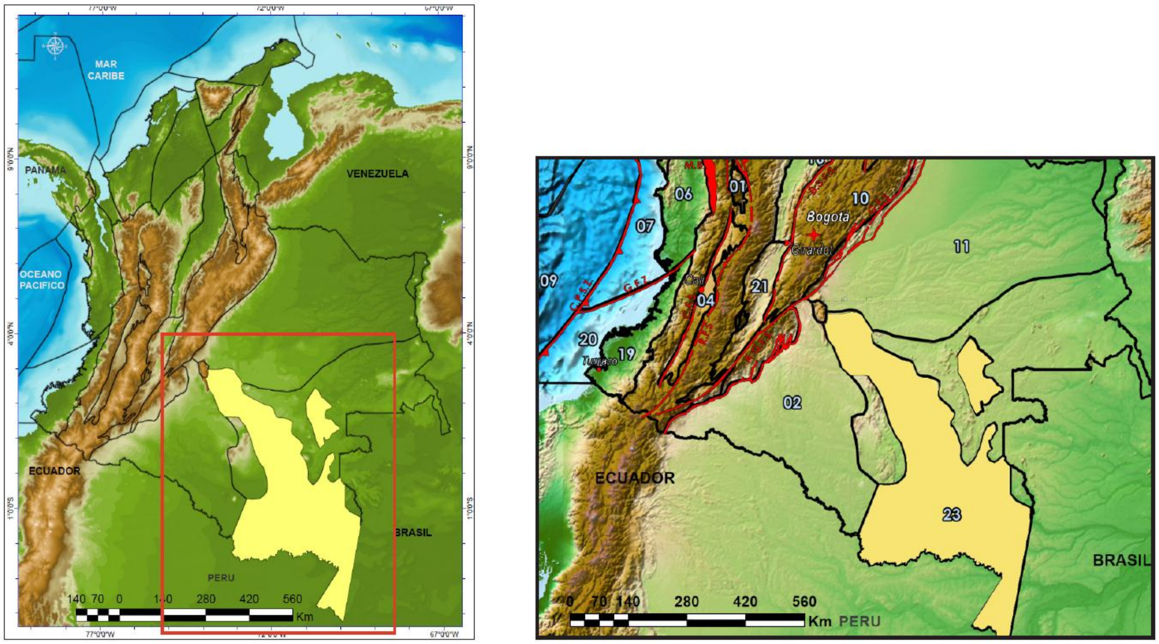

Figure 2-45. Location and borders of the Vaupés basin, Amazonas. 23 – Vaupés – Amazonas basin; V.A. – Vaupés arch; S.C. – Chiribiquete mountain range; T.C. – La Trampa – Carurú mountain range.

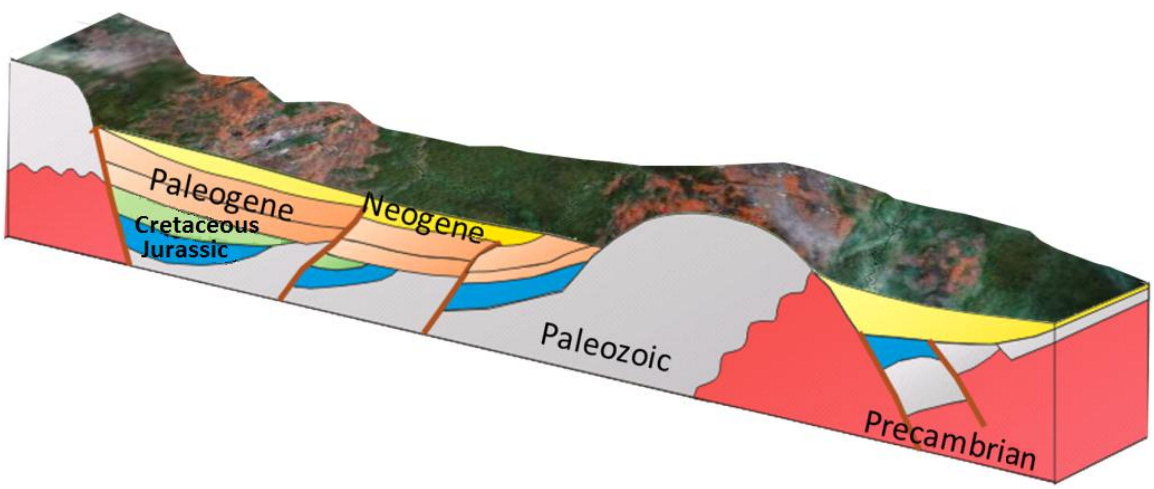

Figure 2-46. Schematic section of the Vaupés – Amazonas basin.

2.3 Environmental considerations

Colombia has 56 natural areas forming the National Parks' system, occupying 9.98% of Colombia's terrestrial territory and 1.30% of its marine territory, giving a total area of 12,602,321 hectares (11,390,995 terrestrial hectares and 1,211,326 marine hectares).

The 56 natural areas were taken into account in the present study when making estimates so as not to count them when calculating the different resources. Table 2-1 shows the percentages for national park and conservation areas for each sedimentary basin in Colombia. Figure 2-47 gives the areas related to the Colombian Park system.

Basin	Natural reserve area (km²)	Percentage of basin (%)
Amagá	0.0	0.0
Caguán - Putumayo	8,550.0	7.8
Guajira offshore	75.1	0.1
Sinú offshore	1,579.4	5.3
Catatumbo	444.7	5.8
Cauca-Patía	4.8	0.0
Los Cayos	10.0	0.0
Cesar-Ranchería	0.0	0.0
Chocó	811.3	2.1
Colombia	0.0	0.0
Colombian Deep Pacific	9,571.8	3.6
The Eastern Cordillera	7,807.3	10.9
The Guajira	317.8	2.3
The Eastern Llanos	5,189.1	2.3
Chocó offshore	592.9	1.6
Tumaco offshore	1,080.6	3.1
Sinú - San Jacinto	4,071.1	10.3
Tumaco	588.9	2.5
Urabá	289.4	3.1
Lower Magdalena Valley	0.0	0.0
Middle Magdalena Valley	0.0	0.0
Upper Magdalena Valley	1,540.3	7.2
Vaupés - Amazonas	33,486.0	21.6
Non-prospective areas	50,220.1	13.3

Table 2-1. Percentage of area associated with the Colombian park system regarding total basin area.

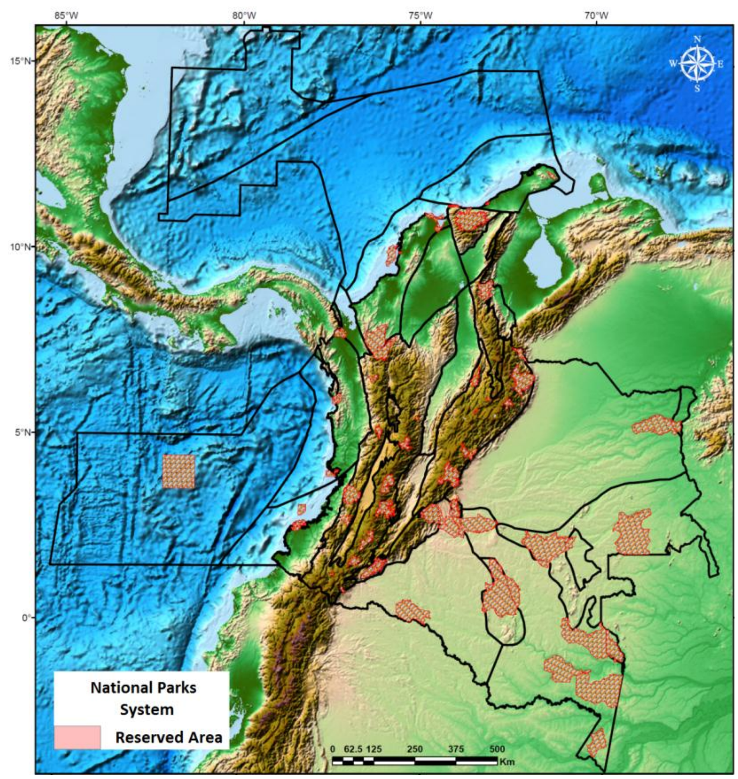

Figure 2-47. Distribution of conservation areas in Colombia. The red hatching indicates the coverage of such conservation areas.

2.4 Data and hypotheses

The resources generated and accumulated were estimated for the 12 sedimentary basins in Colombia, taking into account the information necessary for applying the procedure proposed by Schmoker (1994) and Hunt's proposed considerations (1995), i.e. Catatumbo, Cesar - Ranchería, The Eastern Cordillera, The Eastern Llanos, San Jacinto in Sinú, Sinú offshore, Tumaco, the Lower Magdalena Valley, the Middle Magdalena Valley, the Upper Magdalena Valley, Caguán in Putumayo and the Guajira offshore basins.

2.4.1 Data

Some of the data used was taken from the Colombian Geochemical Atlas (ANH, 2010), and forms part of a compilation analysis, showing wells and outcrops, obtained during regional recognition (Appendix 2-1). Other data were consulted from the Universidad Nacional de Colombia's bibliographic sources dealing with geological field studies for multiple basins and different generated units (Appendix 2-2).

2.4.2 Hypotheses

Hydrocarbons generated and trapped in Colombia's sedimentary basins were estimated in line with the following hypotheses:

2.4.2.1 Hypothesis 1

Following the mass balance method (Schmoker, 1994), the amount of hydrocarbons generated in Colombia is fixed according to the rock's total organic carbon mass and original and actual hydrogen indexes.

2.4.2.2 Hypothesis 2

The geological risk factors proposed by Hunt (1995) lead to estimating the volume of hydrocarbon generated (i.e. which was preserved and trapped).

2.4.2.3 Hypothesis 3

The ratio between hydrocarbon generated per basin and basin area leads to estimating the resource being produced in areas lacking information.

2.4.3 Methodology

The following equation was used for estimating the hydrocarbon generated in Colombia:

$$HC_v = 6.29 \cdot 10^{-3} * A * h * \rho_{roca} * \left[\frac{TOC}{100}\right] * \frac{(HI_o - HI_p)}{\rho_{HC}} \quad \textbf{(2-1)}$$

HC_v : volume de hydrocarbon generated (MBOE)

A : formation area (km²)

h : formation thickness (m)

ρ_{roca} : average formation density (g/cm³)

$\boldsymbol{TOC}$: percentage total organic carbon present in rock (% gTOC / groca)

$\boldsymbol{HI_o}$: original hydrogen index before hydrocarbon generation (mgHC/gTOC)

$\boldsymbol{HI_p}$: current hydrogen index (mgHC/gTOC)

$\boldsymbol{\rho_{HC}}$: average hydrocarbon density (g/cm^3).

The foregoing equation was obtained by substituting equations extracted from the scheme shown in Figure 2-2 into equation 1 and then transforming the mass of hydrocarbons generated to volume:

$$\boldsymbol{HC_m = 1 \cdot 10^{-6} * R * M} \qquad \textbf{(2-2)}$$

with,

$$\boldsymbol{M = \left[\frac{TOC}{100}\right] * \rho_{roca} * V} \qquad \textbf{(2-3)}$$

and

$$\boldsymbol{R = HI_o - HI_p} \qquad \textbf{(2-4)}$$

$\boldsymbol{HC_m}$: total mass of hydrocarbon generated in each unit of source rock (Kg)

$\boldsymbol{R}$: mass of hydrocarbon per gram of TOC (mgHC/gTOC)

$\boldsymbol{M}$: organic carbon mass (gTOC)

$\boldsymbol{V}$: formation volume (cm^3)

Applying equation 2-1 to each basin required a probabilistic method-based approach. Monte Carlo-based statistical distributions of probability were thus determined for representing thickness, TOC fraction and difference in hydrogen indexes. Area was the only parameter established as being constant in such calculations when using the Monte Carlo method, since this was determined in basins for which geological information was available. This approach considered the following stages:

- The area of rocks formed by cooking was approximated from the extension of generating rocks, whether derived from geological cartography or well information (e.g. Schmoker, 1994; UIS, 2009);
- A single distribution function was calculated from the thickness data obtained from the Universidad Nacional de Colombia's bibliographic sources (Appendix 2-1);
- An average 2.4 g/cm^3 rock density was taken;
- TOC and S2 data was taken from the Geochemical Atlas of Colombia (ANH, 2010);
- Statistical distributions were obtained for TOC/100 fraction per basin;
- Initial and actual hydrogen indices were determined per basin;
- Distribution functions were fitted to R in equation 2-4;

- An average 0.9 g/cm^3 hydrocarbon density was considered;
- Monte Carlo simulations were run;
- Once hydrocarbon generated per basin had been calculated for basins having the necessary information for applying the Monte Carlo method, a ratio was established between estimated generated hydrocarbons and basin area, thereby obtaining a line of tendency leading to establishing a ratio between such variables, which was used for projecting these results for those basins lacking the necessary information;
- The hydrocarbon generated for basins lacking the necessary data was estimated from their areas, using the ratio between hydrocarbon generated in a basin and its area (as obtained in the previous step); and
- Once total hydrocarbon generated value had been calculated, accumulated or trapped volume was evaluated considering Hunt's observations (1995).

2.4.4 Results

Most variables included in equation 2-1 were statistically analysed, leading to ascertaining their sensitivity. Such analysis consists of goodness-of-fit tests and leads to identifying the distribution of probability best fitting the data. This gives a value (test statistic) reflecting the deviation between the data and a distribution having determined parameters. Goodness-of-fit tests indicate whether it is valid to suppose that the information has a pattern corresponding to such distribution (null hypothesis).

The goodness-of-fit tests also allow ascertaining the degree of certainty in such calculations (probability), i.e. whether there could be greater deviation. Some of the test used gave intervals in which they were valid, according to supposed distribution pattern parameters (confidence intervals).

Different distributions were tried for random variables. Pattern parameters were first studied with the data according to each distribution and then goodness-of-fit tests were made for identifying the least deviation. This report only shows the results for the best fits and estimates.

2.4.4.1 Area of source rocks

Table 1-2 gives the values for the area being considered. These values represent total extensions of source rocks along several basins based on cartographic information or compilation on geophysical data (e.g. Universidad Industrial de Santander, 2009).

Basin	Area (km^2)
Catatumbo	7,715.0
Cesar - Ranchería	11,668.7
The Eastern Cordillera	71,766.2
The Eastern Llanos	225,603.3
Sinú offshore	29,576.5
Sinú - San Jacinto	39,644.6
Tumaco	23,732.4
Lower Magdalena Valley	38,017.4
Middle Magdalena Valley	32,949.4
Upper Magdalena Valley	21,512.8
Caguán - Putumayo	52,860.8
Guajira offshore	110,304.1

Table 2-2. Area of the 12 basins having information for applying Schmoker's methodology (1994).

2.4.5 Thickness of source rock

The thickness reported by the Universidad Nacional de Colombia's bibliographic sources (Appendix 2-1) for several basins was used for estimating distribution parameters for a set of functions. Lognormal gave the best fit for the 178 elements of data. Table 2-3 gives the results of such fit.

Estimated parameters						Goodness-of-fit test			
$\hat{x}$	Confidence interval		$\hat{y}$	Confidence interval		Null hypothesis	P	Statistical value	G.L
5.74	5.58	5.91	1.12	1.01	1.25	Was not rejected	0.13	2.25	1

Table 2-3. Goodness-of-fit parameters and results for the goodness-of-fit test applied to the thickness data for determining the distribution used in estimating the hydrocarbon generated. Estimated parameters $\hat{x}$ and $\hat{y}$ were lognormal distribution mean and standard deviation, respectively. Column P gives the value of probability of accepting or rejecting the null hypothesis. G.L means the degrees of freedom.

2.4.6 Mass of hydrocarbon generated per gram of TOC

Actual hydrogen index values were determined for calculating R (hydrocarbon mass per gram of TOC) distribution, taking TOC and S_2 data from the Colombian Geochemical Atlas (Atlas Geoquímico Orgánico de Colombia, 2010) and using the equation proposed by Barker (1974):

$$HI_p = 100 * \frac{S_2}{TOC} \tag{2-5}$$

S_2: hydrocarbons generated by kerogen distillation (mg_{HC}/g_{roca}).

Maximum value per basin was selected as initial hydrogen index once values had been calculated using equation 2-5. The distribution functions regarding best fit were then determined for the 12 basins (Table 2-4).

2.4.7 TOC fraction

Table 2-5 gives the results of the statistical analysis of TOC fraction data for basins having information.

Basin	Distribution	Estimated parameters						Goodness-of-fit test			
		$\hat{x}$	Confidence interval		$\hat{y}$	Confidence interval		Null hypothesis	P	Statistical value	G.L
CAG-PUT	Extreme min	513.8	509.8	517.8	83.89	80.65	87.28	Was not rejected	M.B	295.2	0
CAT	Extreme min	261.5	258.9	264.1	40.59	38.60	42.69	Was not rejected	M.B	79.41	0
CES-RAN	Triangular	88.90	0	139.2	N/A	N/A	N/A	N/A	N/A	N/A	N/A
COR	Extreme min	507.7	502.5	512.9	80.41	76.26	84.78	Was not rejected	M.B	188.79	6
GUA-OS	Triangular	135.8	0	208.0	N/A	N/A	N/A	N/A	N/A	N/A	N/A
LLA	Extreme min	402.2	398.1	406.4	68.9	65.7	72.3	Was not rejected	M.B	148.8	0
SIN-OS	Extreme min	150.3	146.9	153.6	22.39	19.77	25.36	Was not rejected	M.B	16.06	0
SIN-SJA	Extreme min	106.2	103.4	109.0	20.99	18.81	23.43	Was not rejected	M.B	39.10	0
TUM	Extreme min	68.70	65.62	71.78	13.15	10.94	15.82	Was not rejected	0.28	3.85	3
VIM	Extreme min	211.9	209.5	214.3	31.07	29.14	33.14	Was not rejected	M.B	160.3	0
VMM	Extreme min	348.9	342.2	355.6	62.8	57.2	69.0	Was not rejected	M.B	221.0	0
VSM	Weibull	413.9	405.7	422.3	2.06	1.99	2.13	Was not rejected	M.B	341.0	0

Table 2-4. Goodness-of-fit distributions, parameters and test results applied to the mass of hydrocarbon generated per gram of TOC data. CAG-PUT, CAT, COR, GUA-OS, LLA, SIN-OS, SIN-SJA, TUM, VIM, VMM and VSM refer to the Caguán - Putumayo, Catatumbo, Eastern Cordillera, Guajira offshore, Eastern Llanos, Sinú offshore, Sinú San - Jacinto, Tumaco, Lower Magdalena Valley, Middle Magdalena Valley and Upper Magdalena Valley basins. Estimated parameters $\hat{x}$ and $\hat{y}$ are extreme value distribution regarding location and scale, and to "a" and "b" for Weibull distribution, respectively. Estimated parameter $\hat{x}$ for triangular distribution was the most probable value and its confidence interval gave minimum and maximum values as extremes. N/A refers to the parameters which did not apply for the type of distribution considered. M.B refers to very low probability of the null hypothesis being accepted or rejected.

ANH AGENCIA NACIONAL DE HIDROCARBUROS

Basin	Distribution	Estimated parameters						Goodness-of-fit test			
		$\hat{x}$	Confidence interval		$\hat{y}$	Confidence interval		Null hypothesis	P	Statistical value	G.L
CAG-PUT	Gamma	0.65	0.61	0.68	0.02	0.02	0.03	Was not rejected	M.B	21.26	1
CAT	Lognormal	-4.72	-4.78	-4.66	0.80	0.76	0.85	Was not rejected	M.B	44.0	0
CES-RAN	Lognormal	-4.81	-4.91	-4.69	0.78	0.71	0.87	Was not rejected	M.B	2.39	0
COR	Lognormal	-4.63	-4.67	-4.59	0.66	0.63	0.69	Was not rejected	M.B	48.73	1
GUA-OS	Lognormal	-4.69	-4.75	-4.65	0.53	0.50	0.56	Was not rejected	M.B	2.01	0
LLA	Lognormal	-5.02	-5.07	-4.97	0.98	0.94	1.01	Was not rejected	M.B	16.40	0
SIN-OS	Extreme max	0.02	0.01	0.02	0.03	0.03	0.03	Was not rejected	M.B	96.7	2
SIN-SJA	Lognormal	-4.63	-4.70	-4.55	0.66	0.61	0.72	Was not rejected	M.B	0.04	0
TUM	Lognormal	-4.47	-4.61	-4.33	0.67	0.58	0.78	Was not rejected	M.B	4.25	0
VIM	Lognormal	-4.78	-4.82	-4.73	0.68	0.65	0.72	Was not rejected	M.B	12.02	0
VMM	Lognormal	-4.21	-4.28	-4.12	0.74	0.69	0.79	Was not rejected	M.B	17.81	0
VSM	Lognormal	-4.26	-4.31	-4.22	1.08	1.05	1.11	Was not rejected	M.B	144.9	0

Table 2-5. Goodness-of-fit parameters, test results and distributions applied to the TOC fraction data. Estimated parameters $\hat{x}$ and $\hat{y}$ are gamma distribution regarding form and scale, and for Weibull distribution regarding parameters "a" and "b", respectively.

2.4.8 Ratio between basin area and hydrocarbon generated

The Monte Carlo method was used for estimating hydrocarbon generated once the different distribution functions had been determined (using a million iterations). The results led to correlating hydrocarbon generated values and the different basins' area (Figure 2-48).

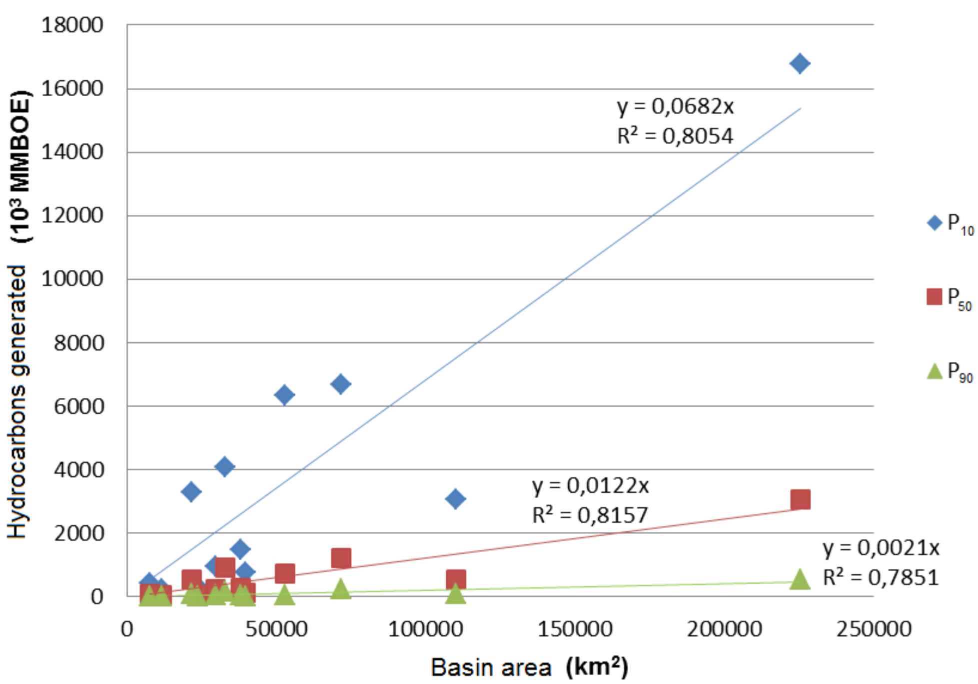

Figure 2-48. Basin area compared to hydrocarbon generated for P_{10}, P_{50} and P_{90}.

Figure 2-48 shows the high coefficients of correlation for each percentile plotted, thereby sustaining the fact that hypothesis 3 (the greater the basin area, the greater the resources), based on statistical occurrences, could be applied to Colombian basins and establish a ratio between a basin's area and the hydrocarbons generated in it. The ratios so obtained led to estimating hydrocarbon generated in P_{10}, P_{50} and P_{90} for the basins lacking information. Table 2-6 gives the areas of such basins.

Basin	Area (km²)
Amagá	2,824.9
Cauca-Patía	12,823.3
Los Cayos	144,755.0
Chocó	38,582.0
Colombia	256,995.3
Deep Pacific	272,426.6
Guajira	13,778.9
Chocó offshore	37,773.3
Tumaco offshore	34,552.7
Urabá	9,448.9
Vaupés-Amazonas	154,867.3

Table 2-6. Area of basins lacking information.

2.4.9 Volume of hydrocarbon generated

Table 2-7 gives the results (in P_{10}, P_{50} and P_{90}) for hydrocarbon generated for each of Colombia's 23 sedimentary basins.

Basin	P_{10}	P_{50}	P_{90}
Total OFFSHORE (10³MBOE)	54,666	9,574	1,613
Cayos	9,987	1,737	289
Chocó Offshore	2,565	446	74
Colombia	17,733	3,084	514
Guajira Offshore	3,061	530	87
Pacífico Profundo	18,125	3,152	525
Sinú Offshore	885	224	55
Tumaco Offshore	2,309	402	67
Total ONSHORE (10³MBOE)	51,937	9,054	1,504
Amagá	195	34	6
Caguán-Putumayo	5,836	666	31
Catatumbo	388	72	14
Cauca Patía	884	154	26
Cesar-Ranchería	217	38	6
Chocó	2,606	453	76
Eastern Cordillera	5,939	1,082	195
Guajira	929	161	27
Eastern Llanos	16,377	2,980	536
Sinú - San Jacinto	673	121	21
Tumaco	286	51	9
Urabá	632	110	18
Lower Magdalena Valley	1,477	271	49
Middle Magdalena Valley	4,061	897	174
Upper Magdalena Valley	3,059	505	75
Vaupés - Amazonas	8,377	1,457	243
TOTAL GENERATED (10³MBOE)	106,603	18,628	3,116

Table 2-7. Hydrocarbon generated in Colombia.

Figures 2-49, 2-50 and 2-51 give a graphic representation of values shown in Table 2-7.

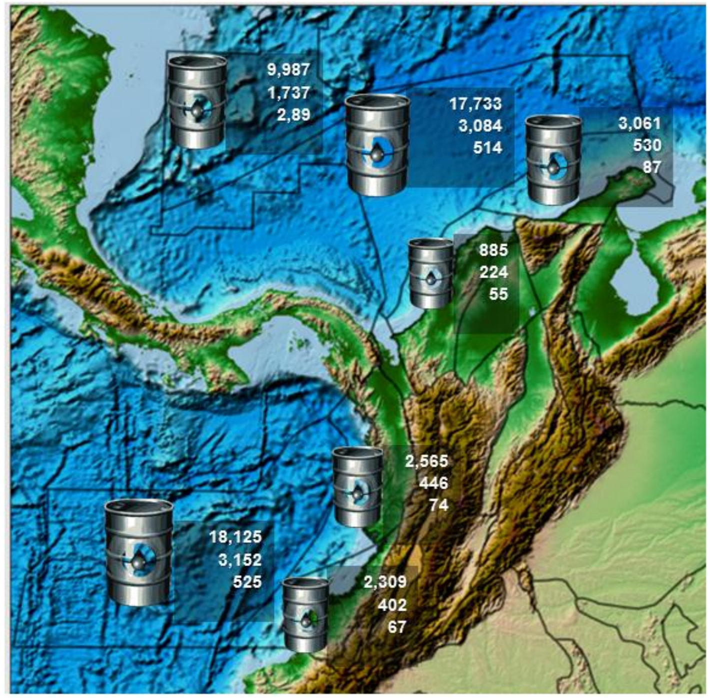

Figure 2-49. Hydrocarbon generated per Colombian offshore basin.

Figure 2-50. Hydrocarbon generated per Colombian onshore basin.

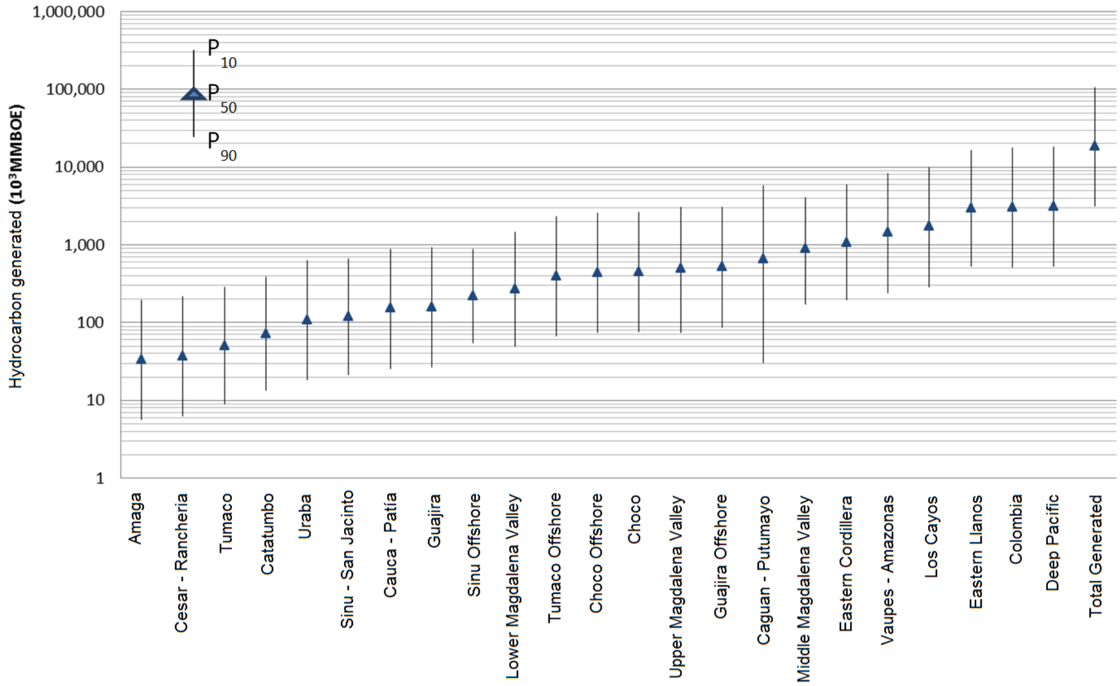

Figure 1-51. Hydrocarbon generated per basin.

2.4.10 Trapped hydrocarbons

Once hydrocarbon generated for Colombia had been ascertained, then total accumulated or trapped hydrocarbon was calculated using Hunt's observation (1995). Accordingly, only ~ 2.2% of hydrocarbon generated is accumulated (crude accounts for ~ 1.8 % of this and the remaining ~ 0.4 % is gas).

Tables 2-8, 2-9 and 2-10 show the values estimated for the resource for Colombia, discriminating between oil and gas. A 5,800 ft3/BOE factor was used for converting barrel of oil equivalent to cubic feet.

P_{10}	**2,345,000 MBOE**
P_{50}	409,000 MBOE
P_{90}	68,000 MBOE

Table 2-8. Total accumulated hydrocarbon.

P_{10}	**1,918,000 MMbbl**
P_{50}	335,000 MMbbl
P_{90}	56,000 MMbbl

Table 2-9. Total accumulated crude.

P_{10}	**2,477 Tcf**
P_{50}	429 Tcf
P_{90}	70 Tcf

Table 2-10. Total accumulated gas; a 5,800 cf/bbl conversion factor has been used.

2.4.11 Sensitivity analysis

A sensitivity analysis was carried out for establishing the degree of random variables' influence on the results of equation 2-1. This led to visualising the weighting of on the result when generating numbers according to the statistical distribution of a particular variable. Table 2-11 shows such sensitivity. Figure 2-52 shows average sensitivity.

Basin	Thickness (%)	R (%)	TOC/100 (%)
Caguán - Putumayo	25.9	1.5	72.6
Catatumbo	59.5	0.0	40.5
Cesar - Ranchería	59.4	0.0	40.6
The Eastern Cordillera	57.7	3.1	39.2
Guajira offshore	53.9	9.8	36.4
The Eastern Llanos	57.4	3.6	39.0
Sinú offshore	88.0	3.9	8.1
Sinú - San Jacinto	56.5	5.2	38.3
Tumaco	56.7	4.8	38.5
Lower Magdalena Valley	57.9	2.6	39.5
Middle Magdalena Valley	72.2	12.5	15.3
Upper Magdalena Valley	49.9	16.1	33.9
Average	57.9	5.3	36.8

Table 2-11. Sensitivity analysis regarding calculations made for hydrocarbon generated per basin.

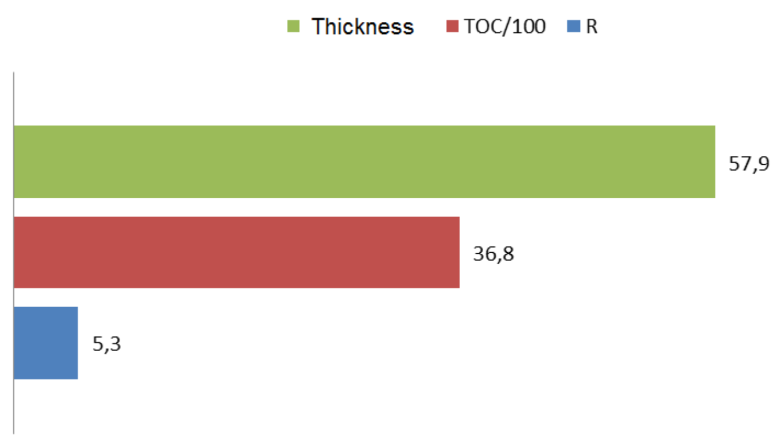

Figure 2-52. Average sensitivity regarding estimates of hydrocarbon generated in Colombia.

2.5 Conclusions

- The hydrocarbons generated for Colombia's 23 basins was estimated, thereby obtaining resources for P10 and P90 I the 2,345,000 and 68,000 MBOE range;
- A range of 1,918,000 to 56,000 MMbbl was obtained in P10 and P90 for oil and the remaining 2,477 to 70 Tcf for gas;
- Sensitivity analysis showed that thickness and the TOC/100 fraction were the variables having the greatest degree of uncertainty in the calculations;
- A series of data was used in the calculations which should be improved and complemented in the future (i.e. thickness values) through a detailed study leading to reducing its range of variability; and

- Regarding the percentage proposed by Hunt (1995), this could vary from basin to basin since each basin has a different history of generation, migration and loss. However, for the purpose of this research and considering the amount of data and information available, this represented a good approach.

2.6 Bibliography

Agencia Nacional de Hydrocarbons - ANH (2007). Colombian sedimentary basins: nomenclature, boundaries and petroleum geology, a new proposal. Bogota: B & M Exploration Ltda.

Agencia Nacional de Hydrocarbons. (2010). Atlas Geoquímico de Colombia. (U. N. Colombia, Ed.) Bogota.

Ahlbrandt , T. S. (2000). The USGS world oil and gas assessment. Search and Discovery (10006).

Barker, C. (1974). Pyrolysis techniques for source rock evaluation. The American Association of Petroleum Geologists Bulletin, 58(11), 2349-2361.

D. Little, A. (2008). Evaluation of potential of unconventional energy resources in Colombia. Agencia Nacional de Hydrocarbons. Houston: Arthur D. Little Inc.

Griess, P. R. (1946). Colombia's Petroleum Resources. Economic Geography, 22(4), 245-254.

Hunt, J. M. (1995). Petroleum Geochemistry and Geology (second edition). W.H. Freeman.

Ortiz, J. (1997). Oportunidades de desarrollo del sector hidrocarburos y su aporte a la economía del país. Cambio y Globalización: Oportunidades y retos para la industria Colombiana de los hidrocarburos. Pontificia Universidad Javeriana.

Schmoker, J. M. (1994). Volumetric calculations of hydrocarbons generated. The petroleum system from source to trap. American Association of Petroleum Geologist Memoirs, 60, 323-326.

Universidad Industrial de Santander. (2009). Evaluación del potencial hidrocarburo de las cuencas Colombianas. ANH-FONADE.

Vargas, C. A. (2009). Nuevos aportes a la estimacion del potencial de hidrocarburos en Colombia. Revista de la Academia Colombiana de Ciencias, XXXIII (126).

2.7 Appendices

2.7.1 Appendix 2-1

Digital file in the ANH'S Document Center:

- ✓ "Balance de Masas.xlsx"

2.7.2 Appendix 2-2

Author	Thesis title	Year
Cardozo P., E.	Estratigrafía, ambiente y paleogeografía de la Fm. Rosablanca en el área de Moniquirá-Villa de Leiva	1982
Moreno V., E.	Characteristics estratigráficas de la formación Villeta en el sector NW de la cuenca del Putumayo	1989
Gil V., A.	Análisis microfacial del grupo cogollo and formación de la Luna cuenca Cesar Cesar - Ranchería and Guajira, Colombia	1990
Sánchez Q., C.	Petrografía e interpretación environmental de la formación Tibú, grupo uribante (Aptiano) en el campo río de oro, cuenca del Catatumbo, con base en núcleos de perforación	1991
Mayorga M., M.	Caracterización geoquímica y facial de las rocas potencialmente generadoras de hidrocarburos en las formaciones del cretácico y terciario inferior de la Cordillera Oriental	1995
Mora B., J.	Estudio estratigraph del Cretácico y Terciario Inferior en el extreme Norte de la cuenca del Putumayo, alrededores de Belén de los Andaquies y Morella, Caquetá	1998
Mera P., R.	Correlación estratigráfica de las rocas del intervalo Paleoceno-Oligoceno subcuenca de San Juan, Chocó	2000
Caycedo G., H.	Propiedades de escalamiento para las poblaciones de fallas de formación Caballos en el sector sur del campo Orito: cuenca Putumayo, Colombia: moldeamiento de las sistemas de fallas por debajo del límite de la resolución seismic	2001
Malagón R., F.	Evaluación del potencial generador de hidrocarburos de las formaciones: Rosablanca, Paja y Tablezo, cuenca medio del Magdalena, Colombia	2001
Ramírez-J., R.	Sedimentología de la arenisca del Oso y su significado estratigraph, en el Cinturón de San Jacinto Norte, Valle Magdalena Inferior	2002
Gamba R., N.	Estratigrafía física, petrográfica y análisis del ambiente de depósito de la formación tetuán en el anticlinal de Chicuambe y la quebrada Bambucá, Valle Magdalena Superior	2002
Mayorga N., E.	Evaluación del potencial hidrocarburífero de la Formación Chipaque (unidad operacional K1 medio and superior) en el bosque Apiay-Ariari, cuenca de los Llanos Orientales	2005
Guzmán A., E.	Evaluación petrofísica de la formación Tetuan en el campo Balcón, Valle Magdalena Superior	2007

Table 2-12. Sources consulted for thickness data. Universidad Nacional de Colombia theses.

3 RECOVERABLE ORIGINAL RESOURCES

3.1 General comments

This section deals with estimating original in situ oil and gas initially in place for oil, conventional gas and associated gas from a volumetric approach. The calculated results were affected by geological and recovery risk factors for final estimate of recoverable resources by type of fluid.

3.1.1 Volumetric estimation

Volumetric estimation is a tool which allows evaluating in situ hydrocarbon in restricted conditions regarding information about production and deposits. Recoverable quantified resources affecting estimation have a recovery factor obtained from analogous deposits' yield and/or simulation studies (Dean, 2007).

The necessary data for making a volumetric estimation would be: deposit areas, deposit thickness, porosity, water saturation, volumetric factors, gas–oil ratio (GOR) and accumulated production per field.

3.2 Data and hypotheses

3.2.1 Data

Information reported to the Agencia Nacional de Hidrocarburos in reserves and resources' reports, technical reports and exploration and production reports by December 31st 2010 led to evaluating original resource in situ for a limited number of sedimentary basins in Colombia: 5 for oil and associated gas and 7 for gas.

The methodology proposed by Vargas (2009) was applied for deducing certain variables in basins where the information supplied by ANH was insufficient.

3.2.2 Hypothesis

Original resources in situ were estimated in line with the following hypothesis:

3.2.2.1 Hypothesis 1

There is a relationship between production area / MMbbl produced ratio and the production area / basin area ratio leading to inferring the maximum production area possible in sedimentary basins (Figure 3-1).

3.3 Methodology

The following equations were used for estimating in situ resources in Colombia:

$$\boldsymbol{OOIP = \frac{7758 * A * h * \varphi * (1 - S_w)}{B_o}} \quad \textbf{(3-1)}$$

$$GIIP = \frac{43560 * A * h * \varphi * (1 - S_w)}{B_g} \quad \textbf{(3-2)}$$

$\boldsymbol{OOIP}$: Original in situ oil (bbl)

$\boldsymbol{GIIP}$: Initial in situ gas (bbl)

$\boldsymbol{A}$: area of production (acres)

$\boldsymbol{h}$: total deposit thickness (ft)

$\boldsymbol{\varphi}$: deposit porosity (v/v)

$\boldsymbol{S_w}$: water saturation (v/v)

$\boldsymbol{B_o}$: oil volumetric factor (BblY / BblN)

$\boldsymbol{B_g}$: gas volumetric factor (ft^3Y/ft^3N)

Constants 7758 and 43560 were used for obtaining results in barrels (bbl and cubic feet - cf, respectively).

The Monte Carlo probabilistic method was used for the estimates in equations 3-1 and 3-2. The random variables were gas and oil thickness, porosity, water saturation and volumetric factor. Even though the volumetric factor could be marginal when estimating resources, its variability was taken into account due to the broad range of observations. Production area was taken as being constant. Such estimate included the following steps.

- Data regarding formations, units, areas, thickness, porosity, water saturation, API gravity, gas-oil ratio (GOR), volumetric factors and accumulated production per field in each basin was compiled, discriminating the type of fluid produced (gas or oil);
- Statistical analysis determined the distributions best fitting information regarding thickness, porosity, water saturation, volumetric factor and GOR:
    - Regarding oil, functions were obtained for each variable in five basins; Caguán - Putumayo, Catatumbo, the Eastern Llanos, Middle Magdalena Valley and Upper Magdalena Valley (Figure 3-1);
    - Regarding initial in situ gas, the amount of data was insufficient, meaning that only a single distribution was found per variable, incorporating all basins;
    - For the remaining basins lacking information about oil and gas, a common distribution function was associated for each variable (oil and gas), and constructed from information regarding all basins;
- Areas in production were added to the accumulated production of the different fields per basin, discriminating the type of fluid;
- Vargas' methodology (2009) was applied for basins lacking production areas:
    - The production area / basin area and production area / MMbbl ratios were calculated from total oil production, producing areas and each basin's areas;

- Production area / basin area and production area / MMbbl produced pairs were projected on a log-log graph's abscissa and ordinate;
- The equation for the curve best fitting the points was identified;
- The function so obtained was projected until cutting the axis of the abscissa at a defined value for the "1-8 Ha/MMbbl" ordinate. This value gives an upper "reasonable" limit which has been detected in the production series;
- Assuming basin areas having efficiency of up to 1-8 Ha for each MMbbl, then the maximum fraction of a basin could be inferred which could achieve such production efficiency conditions;
- Such fraction affected the area for the rest of the basins lacking information regarding oil and gas production areas;

- The production areas estimated per basin and type of fluid, thickness, porosity, water saturation, GOR and volumetric factor distributions were used for running Monte Carlo simulations for the estimating original in situ oil and initial in situ gas; and
- The results so obtained were affected by geological risk factors, recovery (oil or gas) and fraction of area associated with natural reserves.

3.4 Results

3.4.1 Production area

Table 3-1 gives production areas and the production area / accumulated production and production area / basin area ratios for the five basins having information used in estimating the original oil in place (OOIP).

Basin	Production área (ha)	Production area / MBOE (ha/MMbbl)	Production area / basin area (%)
Caguán - Putumayo	29,834.06	94.25	0.27
Catatumbo	18,359.82	41.94	2.38
The Eastern Llanos	102,248.95	36.26	0.45
The Middle Magdalena Valley	46,695.06	35.09	1.42
The Upper Magdalena Valley	15,539.54	23.57	0.72

Table 3-1. Production areas per basin and relationships for applying Vargas' approach (2009) used in OOIP calculations.

Figure 3-1 shows the semi-log regression values in Table 3-1; regarding OOIP, it was found that 6.97% was the fraction of the area of a basin which could be expected to produce 1 MMbbl per hectare based on these values. The foregoing is an optimistic scenario; however, a more conservative one giving an expectation of 1 MMbbl in 8 hectares would mean that the percentage of the area in production of such basin would fall to 3.44%. The lack of information for determining production areas for initial gas in place (IGIP) prevented calculating the percentage of the area in production; that calculated for OOIP was thus taken instead.

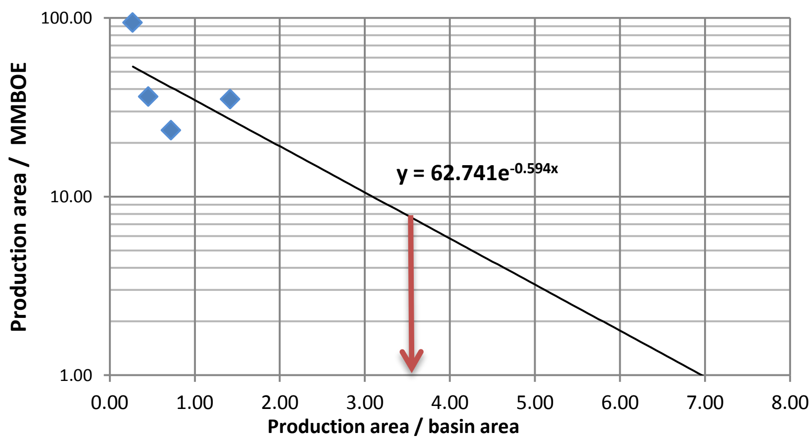

Figure 3-1. Estimated percentage area in production for estimating OOIP. The point corresponding to the Catatumbo basin was not considered for this fit as it went outside the tendency given for the remaining basins, since it has high production (MMbbl) for the extension of area (ha) found in production regarding the rest of the basins. The red arrow indicates the percentage of the basin area which would produce in line with an expectation of 1 MMbbl for each 8 Ha; 3.44% (a more conservative scenario).

Table 3-2 gives the areas calculated in the different basins by applying the percentages so obtained.

Basin	Area (ha)
OFFSHORE	
Los Cayos	1,010,422.06
Chocó offshore	263,665.98
Colombia	1,793,883.99
Guajira offshore	368,980.45
Deep Pacific	1,901,598.01
Sinú offshore	206,450.36
Tumaco offshore	241,185.41
ONSHORE	
Amagá	19,718.64
Cauca-Patía	89,509.52
Cesar-Ranchería	81,449.94
Chocó	269,310.79
Eastern Cordillera	500,943.98
Guajira	96,179.91
Sinú-San Jacinto	276,728.02
Tumaco	165,657.55
Urabá	65,955.77

Table 3-2. Production areas estimated using Vargas' approach (2009).

3.4.2 Deposit thickness

Tables 3-3 and 3-4 show the best fit distributions of thickness data used in estimating in situ resource for oil and gas.

3.4.3 Deposit porosity

Tables 3-5 and 3-6 gives the parameters obtained for porosity distribution.

3.4.4 Water saturation

Tables 3-7 and 3-8 show the distributions obtained regarding water saturation for in situ resources.

3.4.5 Volumetric factors

Tables 3-9 and 3-10 give the statistical parameters calculated for the volumetric factors for oil and gas.

Basin	Distribution	Estimated parameters						Goodness-of-fit test			
		$\hat{x}$	Confidence interval		$\hat{y}$	Confidence interval		Null hypothesis	P	Statistical value	G.L
CAG-PUT	Weibull	34.49	29.79	39.96	1.23	1.09	1.40	Was not rejected	0.30	3.70	3
CAT	Lognormal	3.81	3.48	4.15	0.86	0.68	1.18	Was not rejected	M.B	1.17	0
LLA	Lognormal	3.17	2.88	3.46	1.23	1.05	1.47	Was not rejected	M.B	9.31	0
VMM	Lognormal	4.11	3.86	4.36	0.89	0.75	1.11	Was not rejected	0.38	1.94	2
VSM	Lognormal	4.38	4.11	4.65	0.86	0.70	1.09	Was not rejected	0.48	0.49	1
Remaining basins	Triangular	30	0	825	N/A	N/A	N/A	N/R	N/R	N/R	N/R

Table 3-3. Goodness-of-fit test distributions, fit parameters and results applied to the thickness data used in the OOIP estimate. CAG-PUT, CAT, LLA, VMM and VSM refer to the Caguán - Putumayo, Catatumbo, The Eastern Llanos, Middle Magdalena Valley and Upper Magdalena Valley basins. Estimated parameters $\hat{x}$ and $\hat{y}$ are Weibull distribution parameters “a” and “b”, and average and standard deviation for lognormal distribution, respectively. For triangular distribution, estimated parameter $\hat{x}$ is the most probable value and its confidence interval gives minimum and maximum values as extremes. N/A refers to parameters which did not apply to the type of distribution being considered. N/R refers to parameters which, as they went beyond the algorithm’s range of calculations, were not reported when making the statistical estimation. M.B refers to very low probability of the null hypothesis being accepted or rejected.

Estimated parameters						Goodness-of-fit test			
$\hat{x}$	Confidence interval		$\hat{y}$	Confidence interval		Null hypothesis	P	Statistical value	G.L
3.77	3.49	4.04	1.25	1.08	1.47	Was not rejected	0.13	4.14	2

Table 3-4. Lognormal distribution fit parameters and goodness-of-fit test results applied to the thickness data used in estimating IGIP.

Basin	Distribution	Estimated parameters						Goodness-of-fit test			
		$\hat{x}$	Confidence interval		$\hat{y}$	Confidence interval		Null hypothesis	P	Statistical value	G.L
CAG-PUT	Extreme max	0.16	0.15	0.17	0.05	0.04	0.05	Was not rejected	M.B	116.28	0
CAT	Beta	3.94	2.04	7.59	49.93	24.98	99.78	Was not rejected	M.B	0.11	0
LLA	Extreme min	0.25	0.24	0.26	0.04	0.04	0.05	Was not rejected	0.19	6.11	4
VMM	Beta	12.60	9.91	16.03	50.62	37.75	67.87	Was not rejected	0.22	4.46	3
VSM	Lognormal	-1.87	-1.94	-1.81	0.22	0.18	0.28	Was not rejected	0.27	3.97	3
Remaining basins	Normal	0.16	0.15	0.17	0.06	0.05	0.07	Was not rejected	M.B.	48.21	0

Table 3-5. Goodness-of-fit test distributions, fit parameters and results applied to porosity data used in estimating OOIP. Estimated parameters $\hat{x}$ and $\hat{y}$ are extreme value distribution regarding location and scale, for the Beta distribution to parameters “a” and “b” and for normal distribution to the average and standard deviation, respectively.

Estimated parameters						Goodness-of-fit test			
$\hat{x}$	Confidence interval		$\hat{y}$	Confidence interval		Null hypothesis	P	Statistical value	G.L
2.64	1.69	4.09	15.50	9.02	26.66	Was not rejected	M.B	16.19	0

Table 3-6. Beta distribution fit parameters and goodness-of-fit test results applied to porosity data used in estimating IGIP.

Basin	Distribution	Estimated parameters						Goodness-of-fit test			
		$\hat{x}$	Confidence interval		$\hat{y}$	Confidence interval		Null hypothesis	P	Statistical value	G.L
CAG-PUT	Lognormal	-1.41	-1.47	-1.34	0.39	0.35	0.45	Was not rejected	M.B	24.57	0
CAT	Weibull	0.35	0.33	0.37	6.51	4.95	8.57	Was not rejected	M.B	0.05	0
LLA	Lognormal	-1.36	-1.48	-1.24	0.51	0.44	0.61	Was not rejected	0.36	3.21	3
VMM	Logistical	0.37	0.34	0.40	0.06	0.05	0.08	N/R	N/R	N/R	N/R
VSM	Beta	4.68	3.14	6.97	10.13	6.82	15.04	Was not rejected	0.35	3.30	3
Remaining basins	Uniform	0.05	N/A	N/A	0.95	N/A	N/A	N/R	N/R	N/R	N/R

Table 3-7. Goodness-of-fit test distributions, fit parameters and results applied to water saturation data used in estimating OOIP. Estimated parameters $\hat{x}$ and $\hat{y}$ logistical distribution regarding location and scale, and maximum and minimum for uniform distribution, respectively.

Estimated parameters						Goodness-of-fit test			
$\hat{x}$	Confidence interval		$\hat{y}$	Confidence interval		Null hypothesis	P	Statistical value	G.L
3.79	N/r	N/r	0.08	N/r	N/r	Was not rejected	0.02	12.46	0

Table 3-8. Gamma distribution fit parameters and goodness-of-fit test results applied to water saturation data used in estimating IGIP. Estimated parameters $\hat{x}$ and $\hat{y}$ are Gamma distribution regarding form and scale.

Basin	Distribution	Estimated parameters						Goodness-of-fit test			
		$\hat{x}$	Confidence interval		$\hat{y}$	Confidence interval		Null hypothesis	P	Statistical value	G.L
CAG-PUT	Lognormal	0.13	0.11	0.14	0.08	0.07	0.09	Was not rejected	M.B	11.01	0
CAT	Uniform	1	N/A	N/A	1.87	N/A	N/A	N/R	N/R	N/R	N/R
LLA	Lognormal	0.09	0.06	0.12	0.13	0.11	0.15	Was not rejected	M.B	24.81	0
VMM	Pareto	-1.37	N/R	N/R	2.06	N/R	N/R	Was not rejected	M.B	16.92	0
VSM	Lognormal	0.13	0.09	0.16	0.11	0.09	0.14	Was not rejected	M.B	12.55	1
Remaining basins	Uniform	1.06	N/A	N/A	1.51	N/A	N/A	N/R	N/R	N/R	N/R

Table 3-9. Goodness-of-fit test distributions, fit parameters and results applied to the oil volumetric factor data used in estimating OOIP. Estimated parameters $\hat{x}$ and $\hat{y}$ are form and scale parameters for Pareto distribution.

Estimated parameters						Goodness-of-fit test			
$\hat{x}$	Confidence interval		$\hat{y}$	Confidence interval		Null hypothesis	P	Statistical value	G.L
1.72	1.20	2.23	0.01	0.01	0.01	Was not rejected	M.B	0.84	0

Table 3-10. Pareto distribution fit parameters and goodness-of-fit test results applied to gas volumetric factor data used in estimating IGIP.

3.4.6 Gas oil ratio (GOR)

GOR data compiled from the five basins having information for estimate OOIP led to determining distribution functions. Table 2-11 gives the results for the best fits. Due to the GOR's high variability and, consequently, the pattern of deposits in Colombian basins, it has been assumed that such function represents probable performance in quasi-stationary flow conditions. Lacking more information regarding typical GOR history concerning each deposit and each basin, such supposition represents a hypothetical situation for approximating associated gas order of magnitude.

Basin	Distribution	Estimated parameters						Goodness-of-fit test			
		$\hat{x}$	Confidence interval		$\hat{y}$	Confidence interval		Null hypothesis	P	Statistical value	G.L
CAG-PUT	Lognormal	4.39	3.41	5.38	2.27	1.76	3.21	Was not rejected	M.B	0.01	0
CAT	T. Student	1197	845.5	1394	533.4	397.2	811.7	Was not rejected	M.B	0.05	0
LLA	Lognormal	4.58	4.16	4.99	2.15	1.89	2.49	Was not rejected	M.B	0.57	0
VMM	Lognormal	5.14	4.81	5.47	1.68	1.48	1.95	Was not rejected	0.03	4.65	1
VSM	Lognormal	5.38	5.08	5.68	1.02	0.84	1.28	Was not rejected	0.08	3.05	1
Remaining basins	Gamma	0.40	0.40	0.50	1.34	1.08	1.65	Was not rejected	M.B	11.82	0

Table 3-11. Goodness-of-fit test distributions, fit parameters and results applied to GOR data used in estimating associated gas.

3.4.7 Recoverable resources

After calculating the different production areas in each basin and taking the distribution of variables contained in equations 1-1 and 1-2 into account, in situ resources for oil, associated gas and original gas were estimated; 500,000 iterations were made for original resources and another 500,000 for estimating associated gas. Tables 3-12 to 3-14 give the results obtained, already affected by aerial factors related to areas having high environmental sensitivity (hereinafter environmental factor, Table 2-1), giving 30% geological risk factor and 20% recovery factor. Figures 3-2 to 3-8 also give the results obtained.

Basin	P_{10}	P_{50}	P_{90}
	(MMbbl)		
Total OFFSHORE	276,413	75,815	12,570
Los Cayos	43,050	11,774	1,950
Chocó offshore	12,589	3,453	575
Colombia	90,992	24,923	4,138
Guajira offshore	18,721	5,131	855
Deep Pacific	92,961	25,566	4,224
Sinú offshore	8,182	2,248	377
Tumaco offshore	9,918	2,720	451
Total ONSHORE	153,952	42,148	7,436
Amagá	804	233	75
Caguán - Putumayo	419	137	34
Catatumbo	213	59	17
Cauca-Patía	4,553	1,247	208
Cesar - Ranchería	4,137	1,135	189
Chocó	13,444	3,682	607
The Eastern Cordillera	22,653	6,221	1,030
The Guajira	4,777	1,307	218
The Eastern Llanos	3,250	892	148
Sinú - San Jacinto	13,469	3,697	614
Tumaco	4,486	1,651	611
Urabá	4,413	710	159
The Lower Magdalena Valley	13,177	3,609	602
The Middle Magdalena Valley	11,885	3,252	539
The Upper Magdalena Valley	999	274	45
Vaupés - Amazonas	51,273	14,042	2,340
TOTAL	430,365	117,963	20,006

Table 3-12. Estimated recoverable oil

Basin	P_{10}	P_{50}	P_{90}
	(Tcf)		
Total OFFSHORE	83.111	6.076	0.166
Los Cayos	0.183	0.02	0.002
Chocó offshore	53.389	3.756	0.065
Colombia	1.604	0.305	0.061
Guajira offshore	2.156	0.15	0.002
Colombian Deep Pacific	0.302	0.059	0.012
Sinú offshore	5.136	0.365	0.000
Tumaco offshore	20.341	1.421	0.024
Total ONSHORE	177.813	12.415	0.242
Amagá	2.842	0.203	0.004
Choco	8.607	0.609	0.020
Caguán - Putumayo	0.570	0.041	0.002
Catatumbo	7.755	0.548	0.010
Cauca-Patía	58.586	4.107	0.071
Cesar -Ranchería	7.937	0.558	0.010
The Eastern Cordillera	35.281	2.477	0.043
The Guajira	15.408	1.076	0.018
The Eastern Llanos	7.105	0.491	0.008
Sinú - San Jacinto	11.287	0.79	0.014
Tumaco	3.130	0.219	0.004
Urabá	2.558	0.179	0.004
The Lower Magdalena Valley	6.658	0.467	0.008
The Middle Magdalena Valley	2.253	0.041	0.002
The Upper Magdalena Valley	7.531	0.528	0.008
Vaupés - Amazonas	0.305	0.081	0.016
TOTAL	260.924	18.5491	0.409

Table 3-13. Estimated associated gas.

Basin	P_{90}	P_{50}	P_{10}
	(Tcf)		
Total OFFSHORE	122.64	14.56	1.77
Los Cayos	21.58	2.56	0.31
Chocó offshore	5.52	0.65	0.08
Colombia	38.31	4.55	0.55
Guajira offshore	7.82	0.94	0.11
Colombian Deep Pacific	39.12	4.64	0.57
Sinú offshore	5.3	0.63	0.08
Tumaco offshore	4.99	0.59	0.07
Total ONSHORE	111.54	13.21	1.58
Amagá	0.43	0.06	0.01
Caguán - Putumayo	15.25	1.81	0.22
Catatumbo	1.08	0.13	0.02
Cauca-Patía	1.91	0.23	0.03
Cesar-Ranchería	1.74	0.21	0.02
The Chocó	5.6	0.67	0.08
The Eastern Cordillera	9.6	1.14	0.14
The Guajira	2.03	0.24	0.02
The Eastern Llanos	33.05	3.9	0.47
Sinú - San Jacinto	4.2	0.49	0.06
Tumaco	3.45	0.41	0.04
Urabá	1.38	0.16	0.02
The Lower Magdalena Valley	5.66	0.67	0.08
The Middle Magdalena Valley	4.93	0.59	0.07
The Upper Magdalena Valley	2.96	0.35	0.04
Vaupés-Amazonas	18.27	2.15	0.26
TOTAL	234.18	27.77	3.35

Table 3-14. Estimated initial recoverable gas.

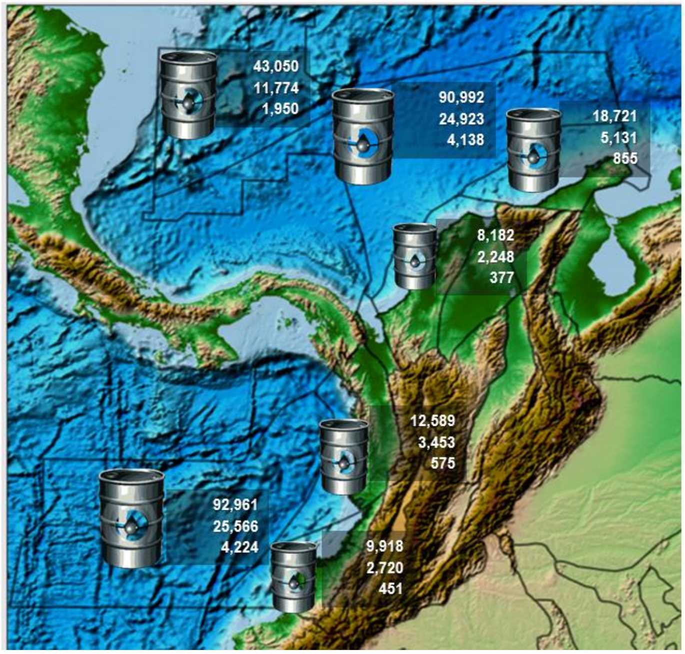

Figure 3-2. Recoverable oil (MMbbl) per basin (offshore).

Figure 3-3. Recoverable oil (MMbbl) per basin (onshore).

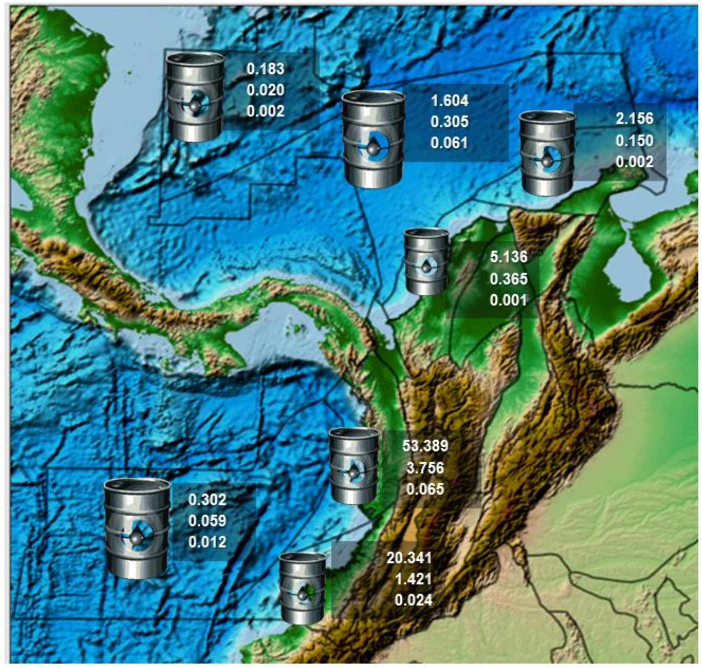

Figure 3-4. Associated gas (Tcf) per basin (offshore).

Figure 3-5. Associated gas (Tcf) per basin (onshore).

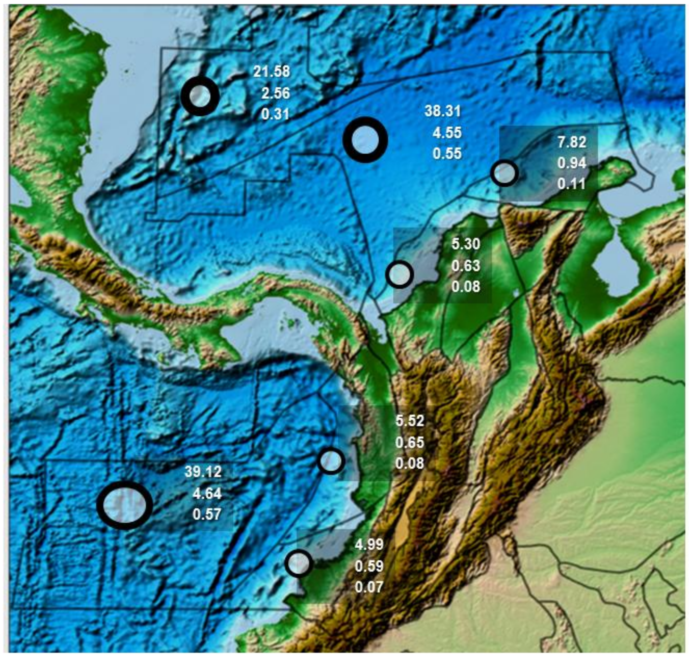

Figure 3-6. Original gas (Tcf) per basin (offshore).

Figure 3-7. Original gas (Tcf) per basin (onshore).

Evaluating total Yet-to-Find hydrocarbon volume in Colombia

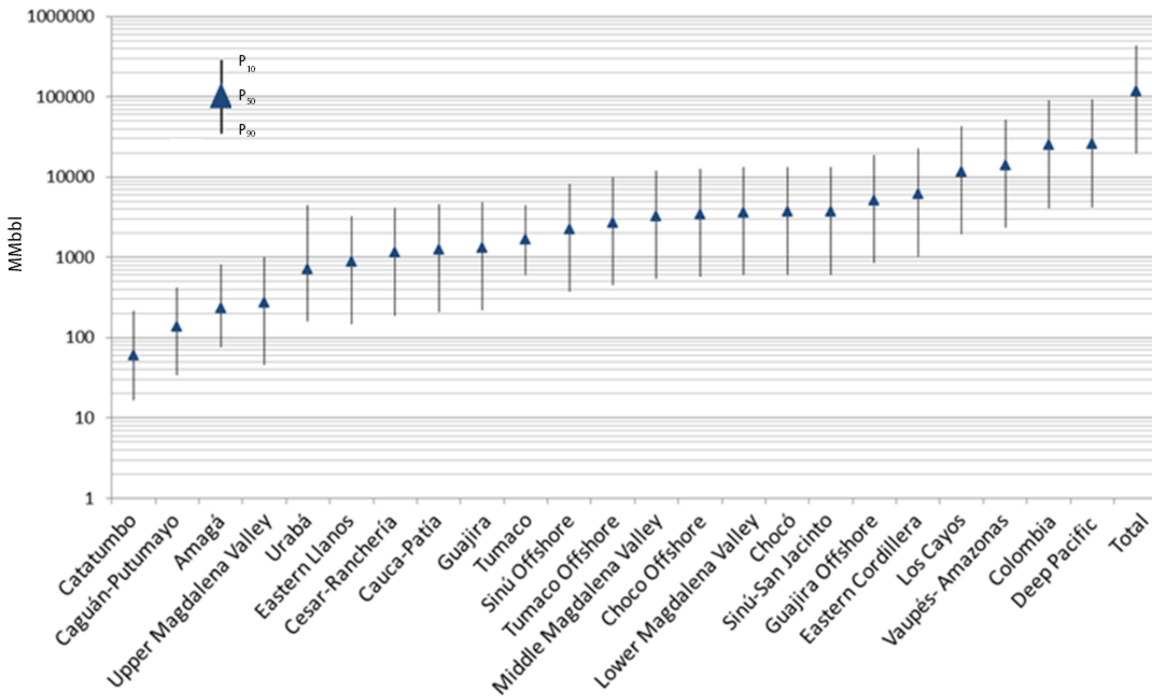

Figure 3-8. Recoverable crude per basin.

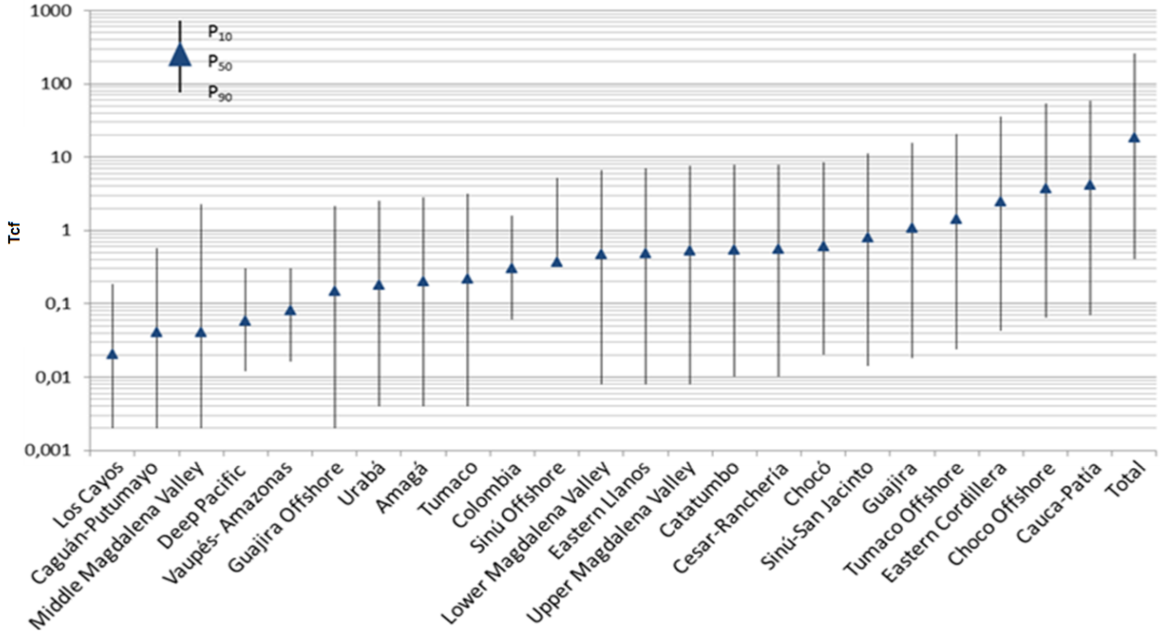

Figure 3-9. Associated gas per basin.

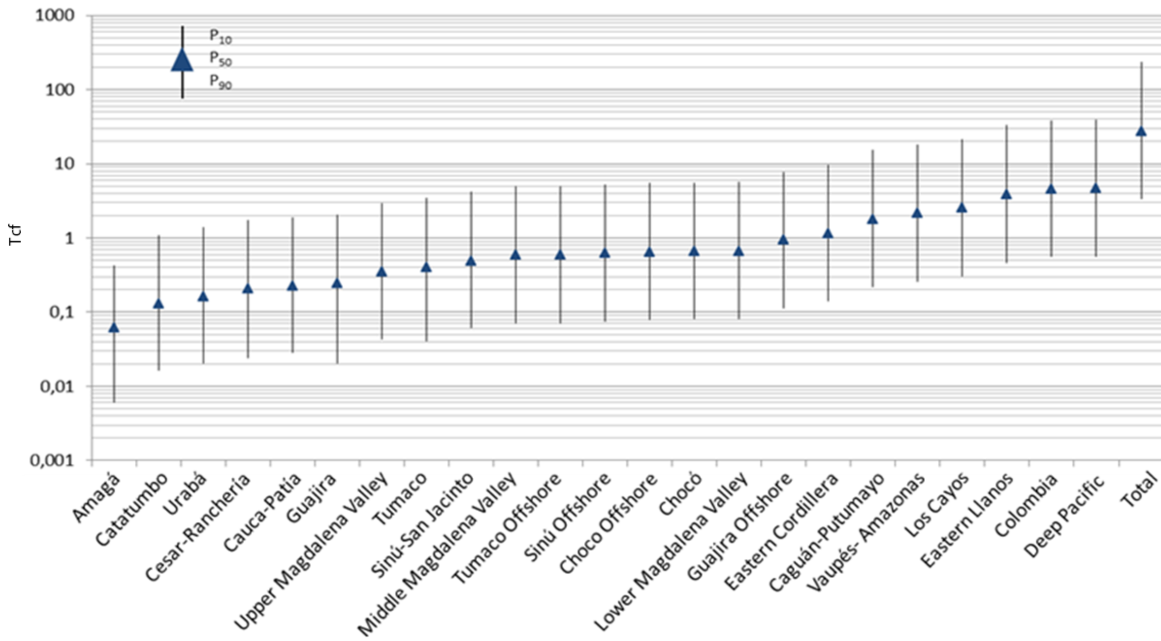

Figure 3-10. Initial recoverable gas per basin.

3.4.8 Sensitivity analysis

Table 3-15 gives sensitivity, averaged per basin for OOIP and IGIP, visualising each variables' contribution to uncertainty (i.e. thickness, porosity, water saturation and volumetric factor) in estimating the different basins' resources.

Basin	Thickness	Porosity	Sw	Bo
	Sensitivity (%)			
Amagá	92.4	5.2	1.8	0.6
Caguán - Putumayo	95.1	2.9	1.5	0.6
Catatumbo	73.3	22.9	0.7	3.2
Cauca-Patía	95.3	2.7	2.0	0.1
Los Cayos	94.0	4.1	1.8	0.2
Cesar-Ranchería	92.8	4.2	2.2	0.7
Chocó	95.1	1.7	2.7	0.5
Chocó offshore	94.4	3.8	1.2	0.5
Colombia	92.3	3.1	4.0	0.7
The Eastern Cordillera	92.7	4.3	2.0	1.0
Guajira	91.4	6.4	2.0	0.2
Guajira offshore	93.0	4.0	2.8	0.1
The Eastern Llanos	94.1	3.3	2.3	0.4
Colombian Deep Pacific	91.3	5.5	1.9	1.3
Sinú - San Jacinto	90.5	4.6	3.3	1.6
Sinú offshore	88.9	6.2	4.4	0.5
Tumaco	92.9	4.1	1.6	1.4
Tumaco offshore	93.4	3.3	2.8	0.5
Urabá	94.6	3.0	1.4	1.0
The Lower Magdalena Valley	95.1	3.5	1.2	0.1
The Middle Magdalena Valley	93.2	0.8	4.6	1.5
The Upper Magdalena Valley	90.2	5.3	3.7	0.9
Vaupés - Amazonas	93.6	4.7	1.5	0.3
Average	92.2	4.8	2.3	0.8

Table 3-15. Sensitivity of the variables involved in calculating in situ resources

Revising the values for the variables regarding each basin led to determining that the overall pattern was similar; Figure 2-9 gives such pattern.

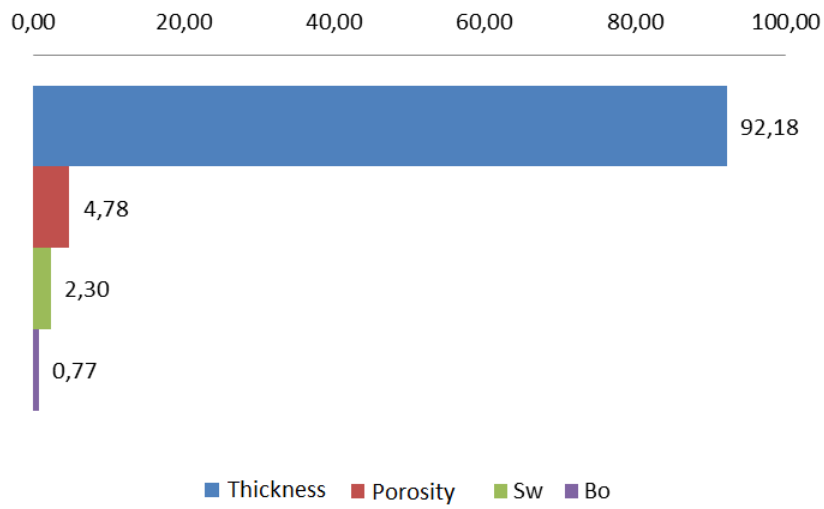

Figure 3-11. General sensitivity analysis.

3.5 Conclusions

- Estimates for recoverable oil varied from P10 to P90, ranging from 430,361.28 to 20,000.45 MMbbl;
- The range of P10 to P90 for associated gas was 260.924 to 0.410 Tcf;
- Estimating initial recoverable gas for percentiles P10 and P90 was 234.15 and 3.36 Tcf, respectively.
- Sensitivity analysis determined that thickness had the greatest influence on the calculations; and
- Ina a more conservative scenario, the percentage of a basin's area which could produce an expected 1MMbbl for each 8 Ha would be 3.44%. This would modify estimated recoverable resources, calculated for an expected 1MMbbl/Ha having 6.97%, reducing such figure by half.

3.6 Bibliography

Dean, L. (2007). Reservoir engineering for geologists. Part 3 – Volumetric Estimation. 11,. Reservoir Issue, 11, 20 - 23.

Vargas, C. A. (2009). Nuevos aportes a la estimacion del potencial de hidrocarburos en Colombia. Revista de la Academia Colombiana de Ciencias, XXXIII (126).

3.7 Appendices

Digital files in the ANH'S Document Center:

- ✓ "Areas y Produccion de Aceite.xlsx"
- ✓ "Recursos in situ.xlsx"

4 YET-TO-FIND RESOURCES

4.1 General comments

The present section evaluates yet-to-find (YTF) hydrocarbons for Colombian basins currently having sufficient data regarding reserves per field.

The fractal model was used for determining YTF resources from data regarding reserves at a determined date, thereby leading to projecting YTF hydrocarbons in actual technological conditions and prevailing political and social-environmental restrictions.

4.1.1 Fractal method

The fractal method assumes that oil field reserves have an idealised distribution which can be described by means of a parabolic or lineal function in log-log representation. As in other areas of the natural sciences, such function is determined by analysing tendency, incorporating field size and range, seeking to group fields having greater than a determined size (MMbbl). The function having the best fit with the data regarding field size and reserves suggests the total YTF subsoil resources in actual technological conditions, taking political and socio-environmental restrictions into account. Yet-to-find hydrocarbons can thus be estimated once the distribution of the reserves has been ascertained; this corresponds to the rest of the total of reserves discovered to date from the estimate of total subsoil resources defined by the best fit function.

4.2 Data and hypotheses

4.2.1 Data

Information from four basins having the minimum production and reserve data required by the method was used for the fractal approach: i.e. the Eastern Llanos, Caguán - Putumayo, the Middle Magdalena Valley and the Upper Magdalena Valley. Other basins having more limited data were incorporated for making an overall estimate for Colombia.

The information compiled from ANH reserves and resources' reports containing data regarding accumulated production and proven reserves per field, as well as the number of fields per basin having been studied provided the data for writing this chapter (such data can be found on the electronic spread-sheets referred to in the appendixes).

4.2.2 Hypothesis

Yet-to-find resources for the five basins considered in Colombia were estimated in line with the following hypothesis:

4.2.2.1 Hypothesis

A basin's reserves have a fractal distribution which may fit a parabolic or lineal function. This allows using the fractal method for determining YTF resources in a particular basin from the difference between the curve of the observed data and its theoretical fit (linear or parabolic), assuming similar exploration and production technology conditions and political and socio-environmental restrictions (Figure 4-1).

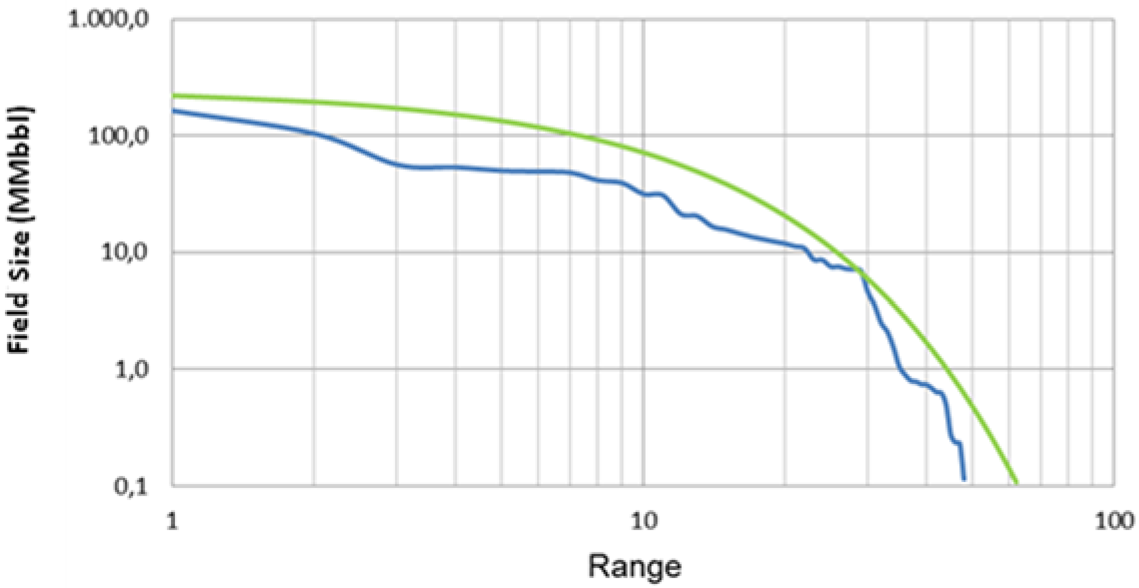

Figure 4-1. Fractal regression for a basin's YTF resources. The blue line gives the distribution, at any given moment, for fields having con a determined amount of reserves and accumulated production. The difference between the theoretical (green) and the observed curve gives the resources in actual technological conditions, regarding political and socio-environmental restrictions.

4.3 Methodology

The following steps were followed in determining yet-to-find hydrocarbon using the fractal method:

- The figures for reserves were organised by ranges. The range assigned corresponded to the number of fields having production and reserves greater than or equal to a particular figure of interest. The example shown in Figure 3-2 has only one field having production and reserves of around750 MMbbl, ten fields having production and reserves greater than 50 MMbbl and 20 fields having production and reserves greater than or equal to 135,000 bbl;

- A log-log graph was drawn presenting the range or number of fields on the abscissa, and the size of the field on the ordinate (accumulated production and reserves) in millions of barrels for the field present in the area of interest or basin; and

- The function best fitting the observed data was identified. The blue curve in the examples shown in Figure 4-2 gives the distribution of known reserves for the area of interest, and the line of fit (green) records total extractible resource in the basin in technological conditions and political and socio-environmental restrictions similar to current ones.

Field	Res +Prod
Campo 1	135.000
Campo 2	301.956.214
Campo 3	890.654
Campo 4	267.071
Campo 5	207.669.613
Campo 6	1.809.411
Campo 7	735.759.099
Campo 8	12.718.502
Campo 9	80.716.519
Campo 10	543.451
Campo 11	8.683.080
Campo 12	200.704
Campo 13	110.600.212
Campo 14	381.832.530
Campo 15	3.319.810
Campo 16	141.362.962
Campo 17	50.523.351
Campo 18	166.698.011
Campo 19	135.844.098
Campo 20	35.388.389

Field	Res +Prod	Range
Campo 1	135.000	20
Campo 12	200.704	19
Campo 4	267.071	18
Campo 10	543.451	17
Campo 3	890.654	16
Campo 6	1.809.411	15
Campo 15	3.319.810	14
Campo 11	8.683.080	13
Campo 8	12.718.502	12
Campo 20	35.388.389	11
Campo 17	50.523.351	10
Campo 9	80.716.519	9
Campo 13	110.600.212	8
Campo 19	135.844.098	7
Campo 16	141.362.962	6
Campo 18	166.698.011	5
Campo 5	207.669.613	4
Campo 2	301.956.214	3
Campo 14	381.832.530	2
Campo 7	735.759.099	1

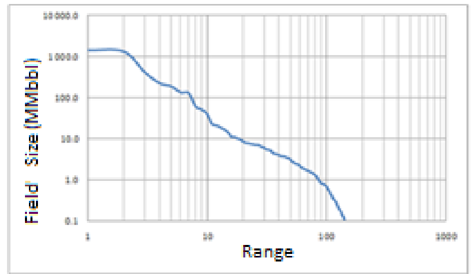

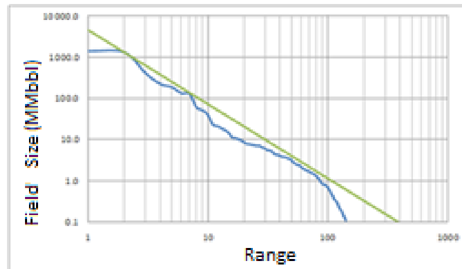

Figure 4-2. Estimating yet-to-find hydrocarbon by fractal approach.

4.4 Results

4.4.1 The Eastern Llanos

Figure 4-3 gives the fractal distribution and best fit for fields in the Eastern Llanos basin. Table 3-1 reports the values extracted from this graph.

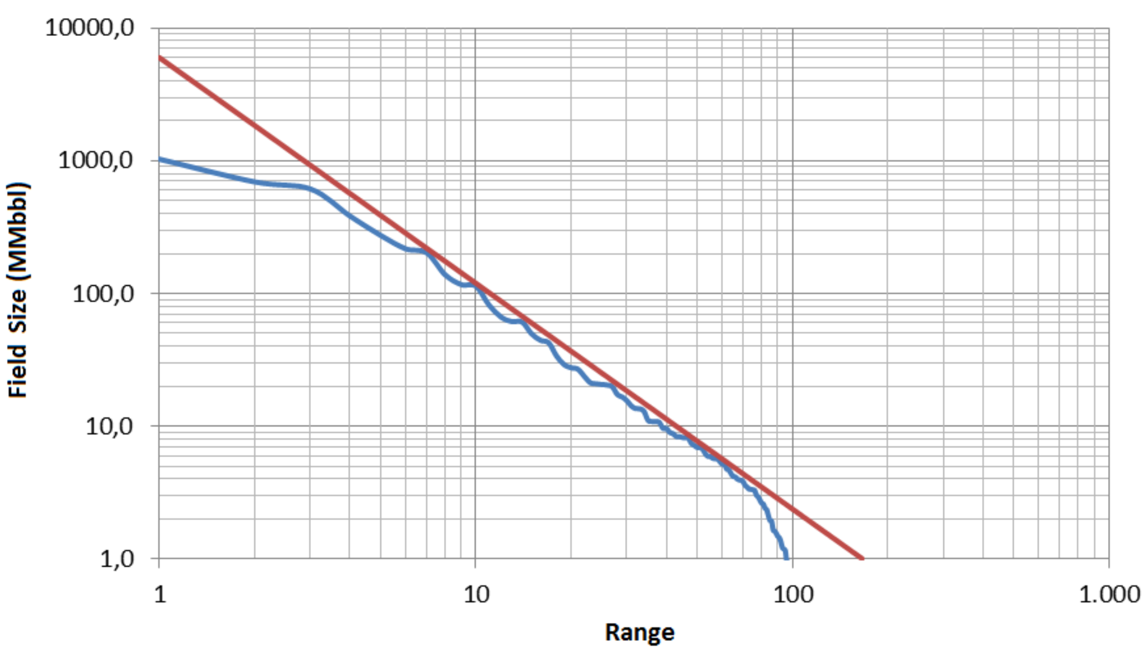

Figure 4-3. Fractal analysis of the Eastern Llanos basin. The blue line gives the fields' current distribution and the red line gives such distribution's estimated future.

A yet-to-find volume of around 7,221 MMbbl was determined for the Eastern Llanos basin in current exploration and production conditions (Table 4-1). Figure 4-3 suggests that the basin could accommodate several giant fields and a significant number of fields having a size less than 5 MMbbl.

Size (MMbbl)	Possible fields	Yet-to-find volume (MMbbl)
size ≥ 1,000	4	4,969.6
500 ≤ size < 1,000	2	1,465.1
200 ≤ size < 500	1	382.2
50 ≤ size < 200	1	130.5
20 ≤ size < 50	2	91.8
10 ≤ size < 20	2	31.3
5 ≤ size < 10	3	21.1
size < 5		129.5
	Total	**7,221.2**

Table 4-1. Distribution per size (yet-to-find resources) in the Eastern Llanos basin

It should be pointed out that the values obtained could be interpreted in line with a supposition of new findings, or re-gauging actual fields resources.

4.4.2 Caguán-Putumayo

Figure 4-4 shows the fractal analysis for the Caguán - Putumayo basin; Table 4-2 gives the values so obtained.

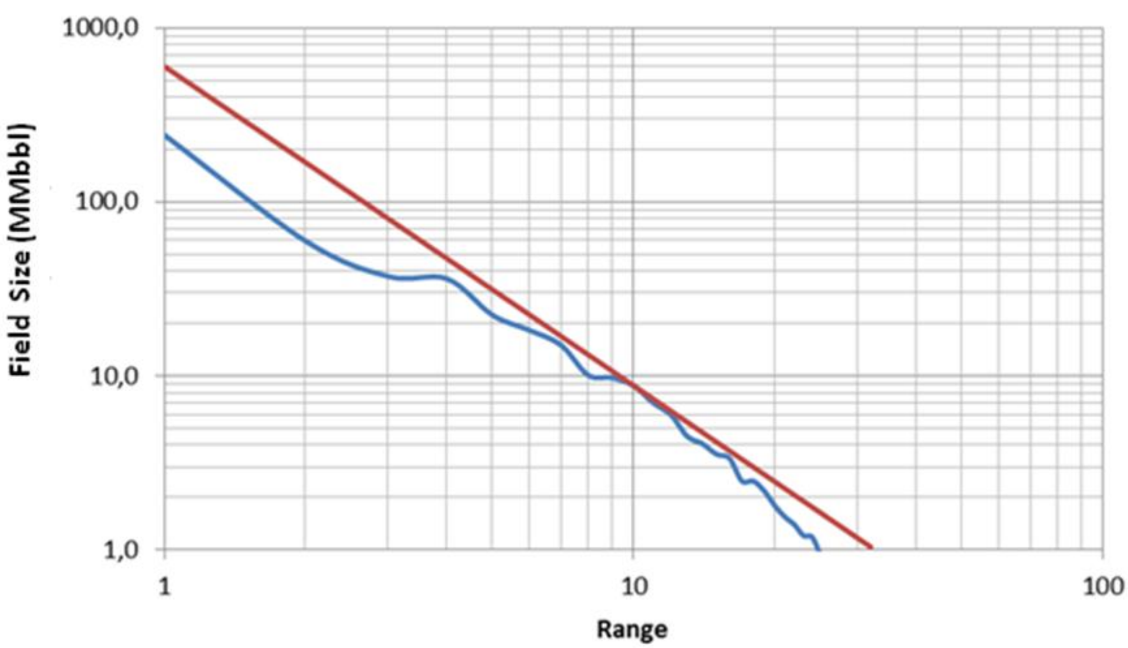

Figure 4-4. Fractal analysis for the Caguán - Putumayo basin. The blue line represents the data observed regarding accumulated production and reserves for each field and the red line represents fractal tendency from the observations.

A total of 557 MMbbl yet-to-find was determined (Table 4-2) in actual conditions for the Caguán - Putumayo basin. According to Figure 4-4, the basin could house at least two new fields having more than 50 MMbbl.

Size (MMbbl)	Possible fields	Yet-to-find volume (MMbbl)
200 ≤ size < 500	1	358.5
50 ≤ size < 200	1	108.9
20 ≤ size < 50	2	62.8
5 ≤ size < 20	2	10.7
size < 5		16.1
	Total	**557.0**

Table 4-2. Distribution per size (yet-to-find resources) in the Caguán - Putumayo basin.

4.4.3 The Middle Magdalena Valley

Figure 3-5 and Table 3-3 give the results obtained for this basin.

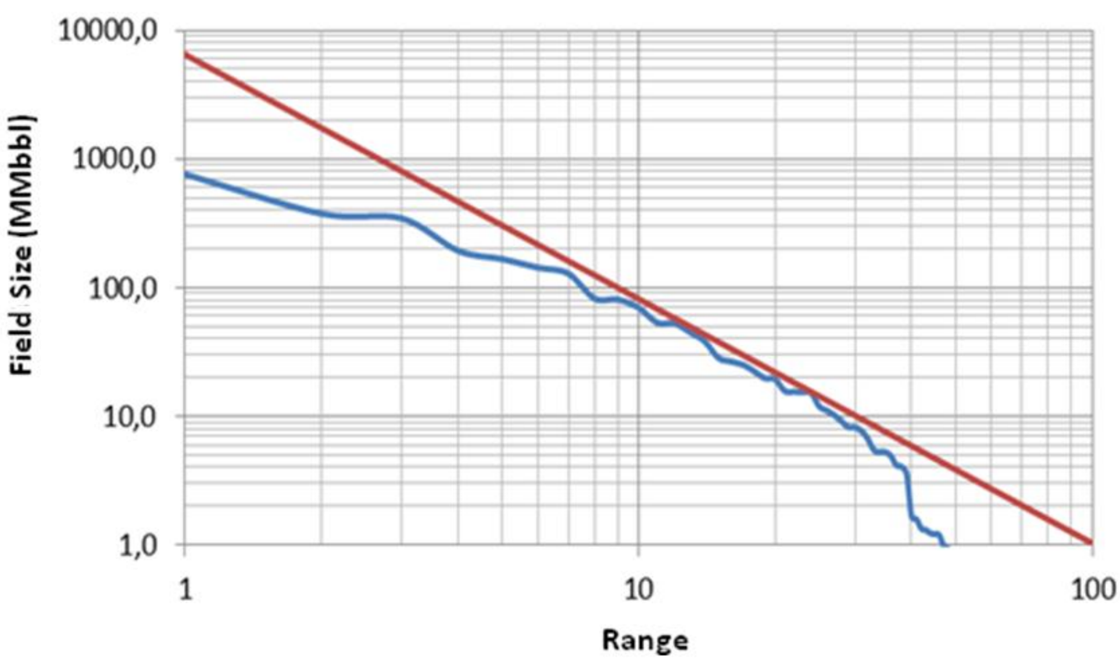

Figure 4-5. Fractal analysis for the Middle Magdalena Valley basin.

It was expected that around 8,325 MMbbl could be found for the Middle Magdalena Valley basin (Table 4-3). According to Figure 3-5, the basin could contain at least eight fields greater than 500 MMbbl.

Size (MMbbl)	Possible fields	Yet-to-find volume (MMbbl)
500 ≤ size < 1000	8	5,739.5
200 ≤ size < 500	5	1,825.8
100 ≤ size < 200	3	516.6
50 ≤ size < 100	1	93.4
20 ≤ size < 50	1	35.3
10 ≤ size < 20	2	22.4
5 ≤ size < 10	2	19.0
size < 5		73.1
	Total	**8,325.1**

Table 4-3. Distribution per size (yet-to-find resources) in the Middle Magdalena Valley basin.

4.4.4 The Upper Magdalena Valley

Figure 4-6 gives the distribution for the fields in this basin. Table 4-4 lists the data extracted from the graph in question.

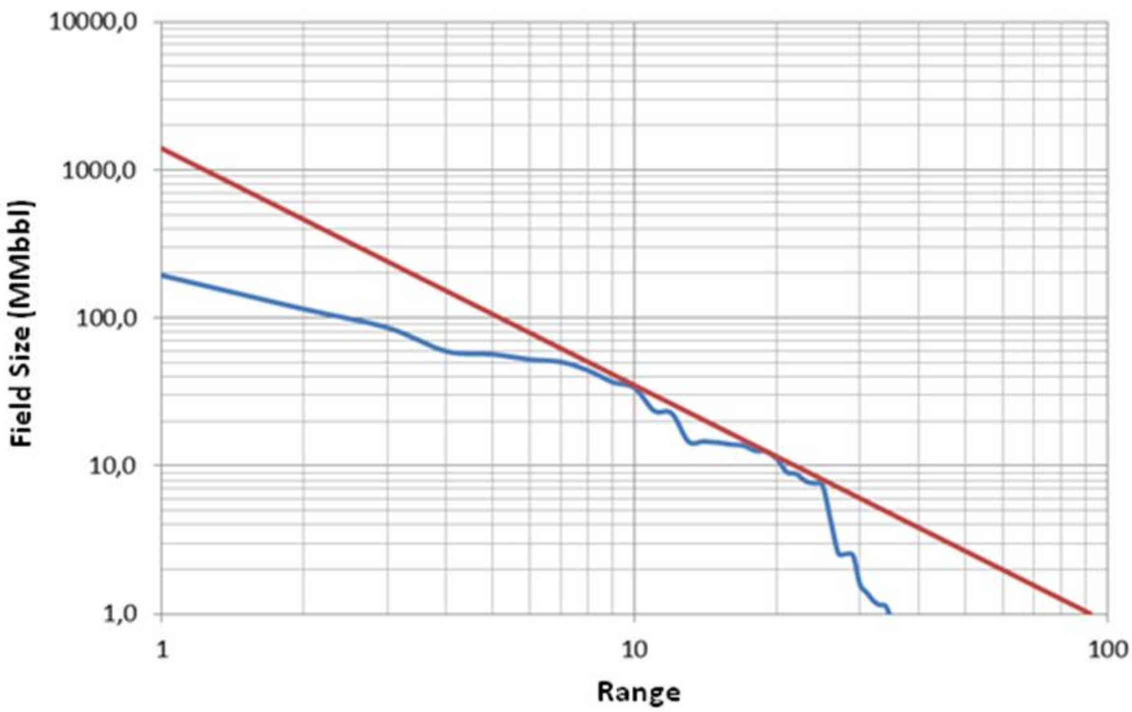

Figure 4-6. Fractal analysis for the Upper Magdalena Valley basin.

It was estimated that there could be 2,099 MMbbl in resources to be incorporated for the Upper Magdalena Valley basin. According to the distribution found, it could be expected to find at least 16 new fields having sizes greater than 100 MMbbl (Figure 4-6).

Size (MMbbl)	Possible fields	Yet-to-find volume (MMbbl)
100 ≤ size < 200	15	1,552.9
50 ≤ size < 100	4	336.4
20 ≤ size < 50	1	22.3
10 ≤ size < 20	2	23.5
5 ≤ size < 10	1	5.8
size < 5		158.5
	Total	**2,099.4**

Table 4-4. Distribution per size (yet-to-find resources) in the Upper Magdalena Valley basin.

Table 4-5 gives a summary containing information about accumulated reserves and production on 31st December 2010, compiled from data provided by ANH for the four basins considered, as well as fractal estimates made.

Basin	Accumulated production	Reserves	YTF	Reserves + YTF
	(MMbbl)			
The Eastern Llanos	3,039	1,828	7,221	9,049
Caguán - Putumayo	342	162	557	719
Middle Magdalena Valley	1,950	915	8,325	9,240
Upper Magdalena Valley	688	258	2,099	2,358
Catatumbo	3,130	4,326	7,221	14,677

Table 4-5. Summary of fractal analysis and information regarding reserves per basin.

4.4.5 Total YFT crude resources in Colombia

The information available for the four previously-mentioned basins and additional data led to estimating yet-to-find hydrocarbon for Colombia (Lower Magdalena Valley, The Eastern Cordillera and Catatumbo); 262 fields from seven basins mentioned throughout this chapter were used. Figure 4-7 and Table 4-6 gives the results obtained for the three scenarios (high, medium and low).

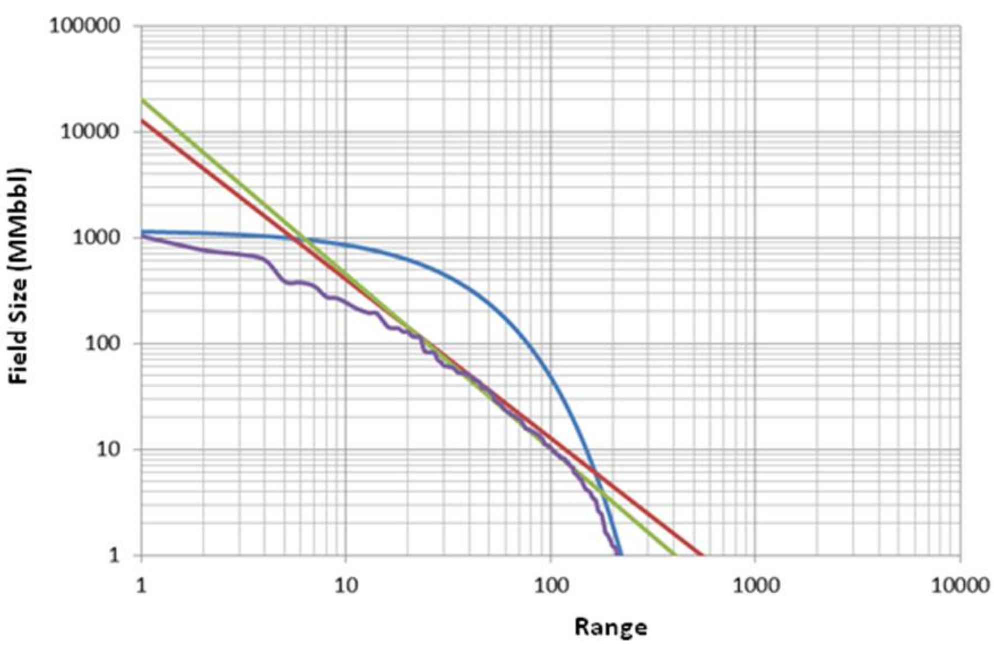

Figure 4-7. Fractal analysis for crude in Colombia. The low scenario is shown by the red line, the middle scenario by the green line and the high scenario by the blue line.

Scenario	YTF volume (MMbbl)
Low	22,797.6
Medium	26,072.4
High	33,145.9

Table 4-6. Scenarios for YTF crude resources in Colombia.

4.4.6 Total YTF gas resources in Colombia

The data regarding reserves in 48 fields from seven sedimentary basins in Colombia (Catatumbo, the Lower Magdalena Valley, the Middle Magdalena Valley, the Upper Magdalena Valley, the Eastern Cordillera, the Eastern Llanos and Guajira offshore) led to estimating yet-to-find gas. Figure 4-8 and Table 4-7 show the results of these estimations, presented in three possible scenarios (high, medium and low).

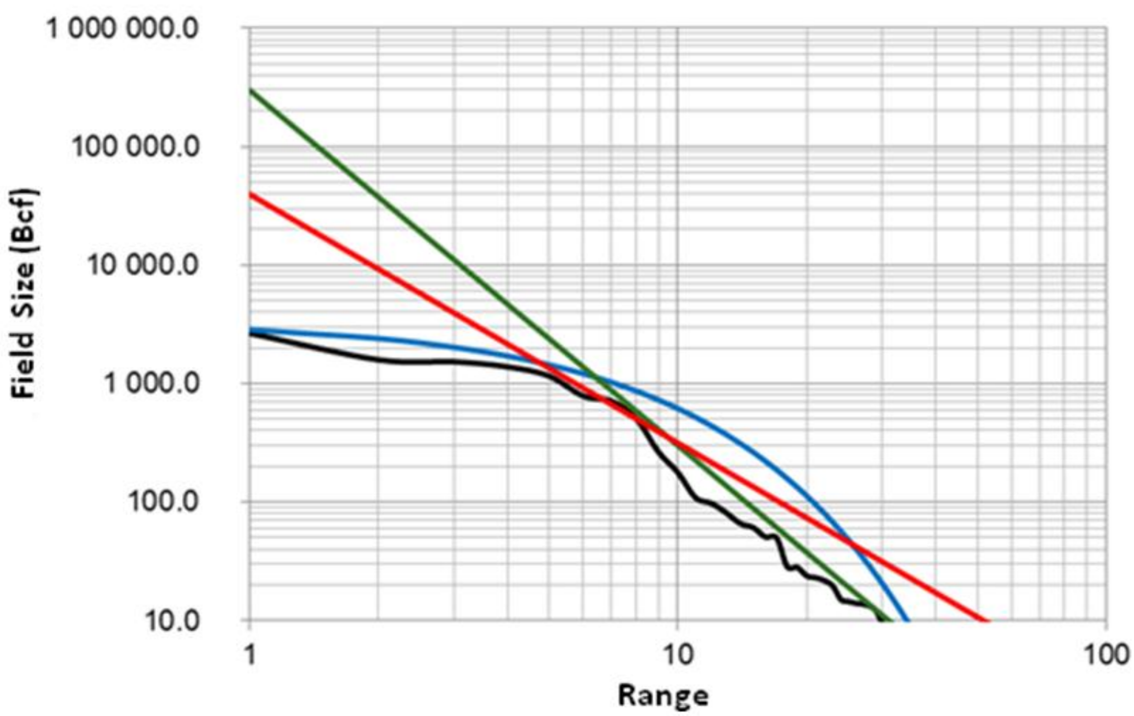

Figure 4-8. Fractal analysis for gas in Colombia.

Scenario	YTF volume (Bcf)
Low	6,615.1
Medium	49,917.9
High	348,984.6

Tabla 4-7. YTF resource scenarios for gas in Colombia.

Table 4-8 gives a summary of the fractal analysis for total crude and gas in Colombia and information regarding reserves on 31st December 2010.

Basin	Reserves	YTF	Reserves + YTF
Crude (MMbbl)	3,272	22,798	26,069
Gas (Tcf)	7.06	6.62	13.68

Table 4-8. Summary of fractal analysis and information regarding reserves for Colombia.

4.5 Conclusions

- The fractal methodology led to yet-to-find hydrocarbon resources being determined for four sedimentary basins in Colombia where minimum required information was available: the Eastern Llanos, Caguán in Putumayo, the Middle Magdalena Valley and the Upper Magdalena Valley;
- 7,221 MMbbl yet-to-find resources were estimated for the Eastern Llanos basin, 8,325 MMbbl for the Middle Magdalena Valley, 2,099 MMbbl for The Upper Magdalena Valley and 557 MMbbl for Caguán in Putumayo; and
- Likewise, and from known data for all of Colombia, yet-to-find crude and gas resources in the order of 22,798 MMbbl and 6.62 Tcf were estimated respectively.

4.6 Bibliography

Ahlbrandt, T. S. (2005). Comparison of methods used to estimate conventional undiscovered petroleum resources: world examples. Natural Resources Research, 14(3), 187-210.

Laherrere, J. (2000). Distribution of field sizes in a petroleum system: parabolic fractal, lognormal or stretched exponencial: Marine and Petroleum Geology, 7(4), 539 -546.

4.7 Appendices

Digital file in the ANH'S Document Center:

- ✓ "YTF_Fractal.xlsx"

5 METHANE GAS HYDRATES

5.1 General comments

Gas hydrates are crystalline solids consisting of a molecule of gas surrounded by water molecules; these are formed in conditions involving high pressure and low temperatures. Gas hydrates usually occur in sediments' porous spaces and can form cement, nodules, veins or layers (Popescu et al., 2006). Gas hydrates may contain different types of gases within their structures (carbon dioxide, nitrogen and hydrogen sulphate), but most natural gas hydrates mainly consist of methane (Kvenvolden, 1995).

Gas hydrates can form and remain stable in favourable pressure and temperature conditions and when free methane and water are available (Sloan, 1990).

5.1.1 Origin and formation

Hydrate formation needs an anoxic environment which is saturated by methane gas and water molecules so that gas hydrates may begin to form spontaneously in conventional deposit pore spaces and fractures, in temperature and pressure conditions leading to these two phases' stable integration.

Such conditions are usually present in continental shelf sediments along ocean margins or in high latitudes (Kvenvolden, 1988). Biogenic gas, formed during the early diagenesis of organic matter, or thermogenic gas associated with migration from deeper accumulations, is forced to become solubilised in the water present (Sloan & Carolyn, 1998). Pressure increases if the deposition of sediments and organic matter continues, and the potential area for hydrate accumulation could achieve suitable depth and thickness as the methane generation and dissolution cycle progresses.

The change of the liquid phase composed of water and gas to solid hydrate only occurs at low temperatures and/or high pressure in an area called the methane hydrate stability area (Figure 5-1). The thickness of this area will thus depend on the geothermal gradient and the water column and rock covering it (Kvenvolden, 1988). Other parameters controlling the stability area are seabed temperature, gas composition, salinity and the local geology.

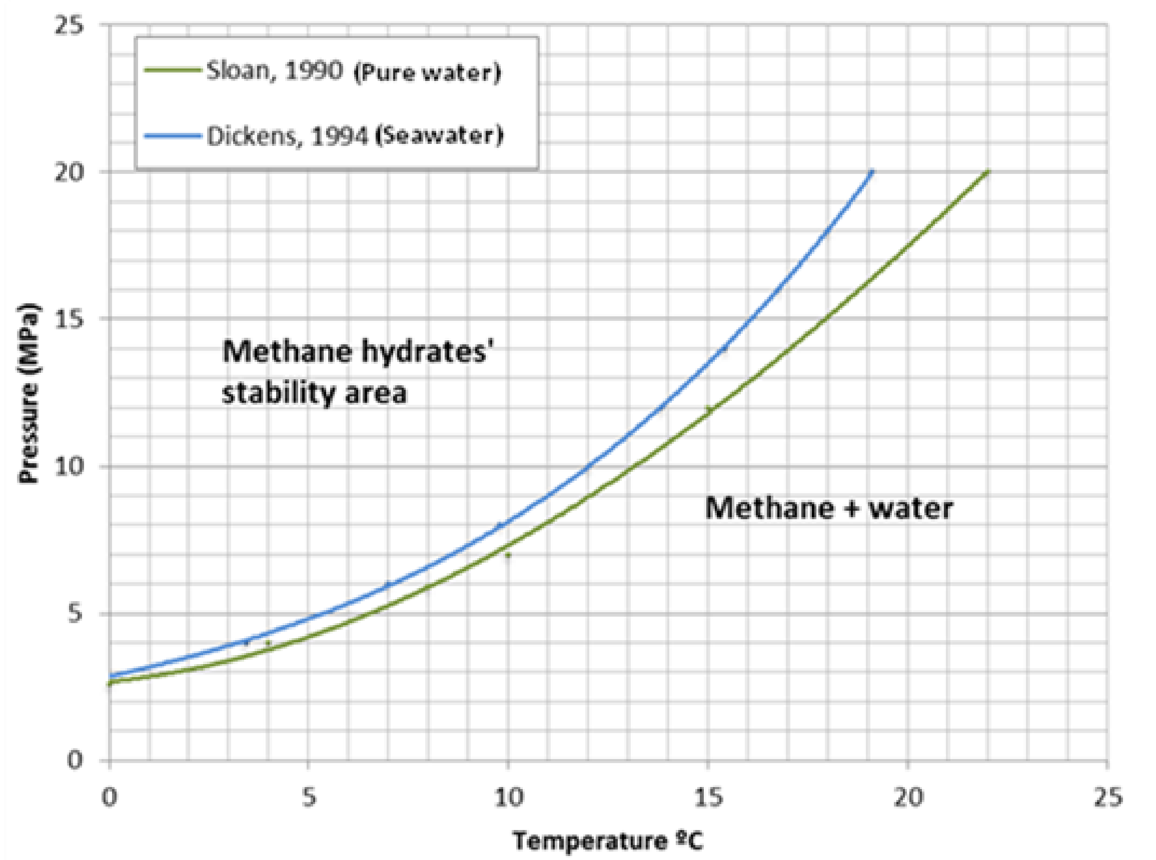

Figure 5-1. Pressure and temperature stability curves for the base of the gas hydrates area. Both curves are just for methane gas in the hydrate.

5.1.2 Bottom simulating reflector (BSR)

The first indicator regarding the presence of hydrates in marine sediments is the bottom simulating reflector (BSR) observed in seismic reflection sections. This reflector marks the base of the hydrate stability area below the seafloor.

The BSR results from the contrast in negative impedance between sediments containing hydrates and lower hydrate-free sediments; this reflector marks the base of the stability area below the seafloor.

The BSR lies approximately parallel to the seafloor and can be easily seen in slope areas (gradient) by cutting the stratigraphic reflectors; it usually has reverse polarity to that of the seafloor reflector (Figure 5-2); however, if this lies parallel to the strata then it can be difficult to identify. Some authors have stated that gas hydrates can be present even when the BSR has not been identified in seismic reflection (Yuan et al., 1998).

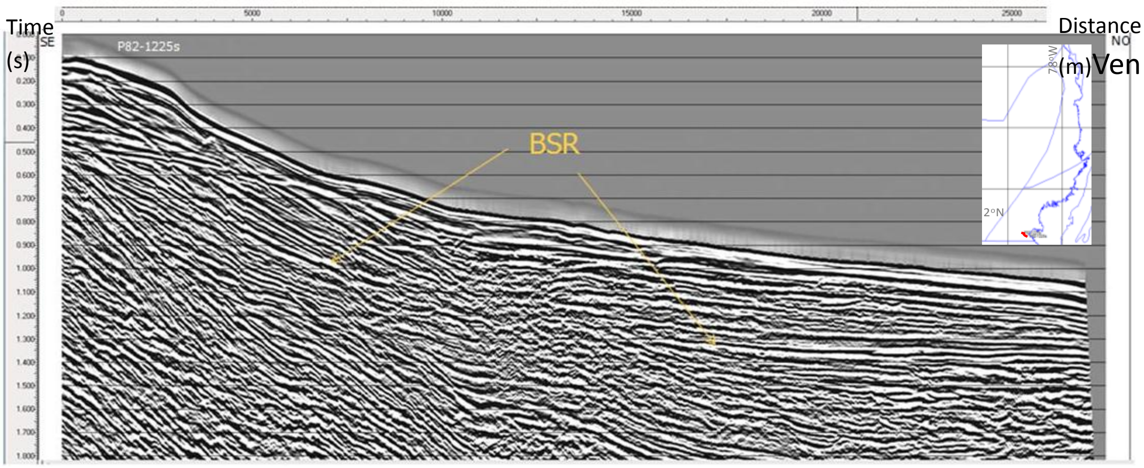

Figure 5-2. BSR characteristics identified in a seismic section to the south of the Colombian Pacific. The red mark on the map in the upper right-hand corner indicates the location of this line. The BSR, suggested by the orange arrows, shows strong amplitude, inverse to that of the seafloor reflector. It can also be seen how this crosses the upper and lower stratigraphic reflectors.

BSR characteristics leads to obtaining a map of hydrates' regional distribution; analysing the BSR and the speed of structures provides semi-quantitative information about the amount of hydrates and their distribution, as well as the amount of free gas under the hydrate stability area (Yuan et al., 1998).

5.1.3 Gas hydrate distribution around the world

The presence of gas hydrates has been inferred in 50 areas around the world (Figure 5-3). However, only a limited number of gas hydrate accumulations have been examined in detail; 5 gas hydrate accumulations have been very well studied. Such accumulations are found in marine and permafrost areas, as follows: the Blake Ridge along the south-eastern continental margin of the USA, the Cascadian bioregion along the continental margin of the Pacific coast of Canada, on the eastern coast of Japan, Nankai, northern Alaska and in the Mackenzie River delta in northern Canada (Collet, 2002).

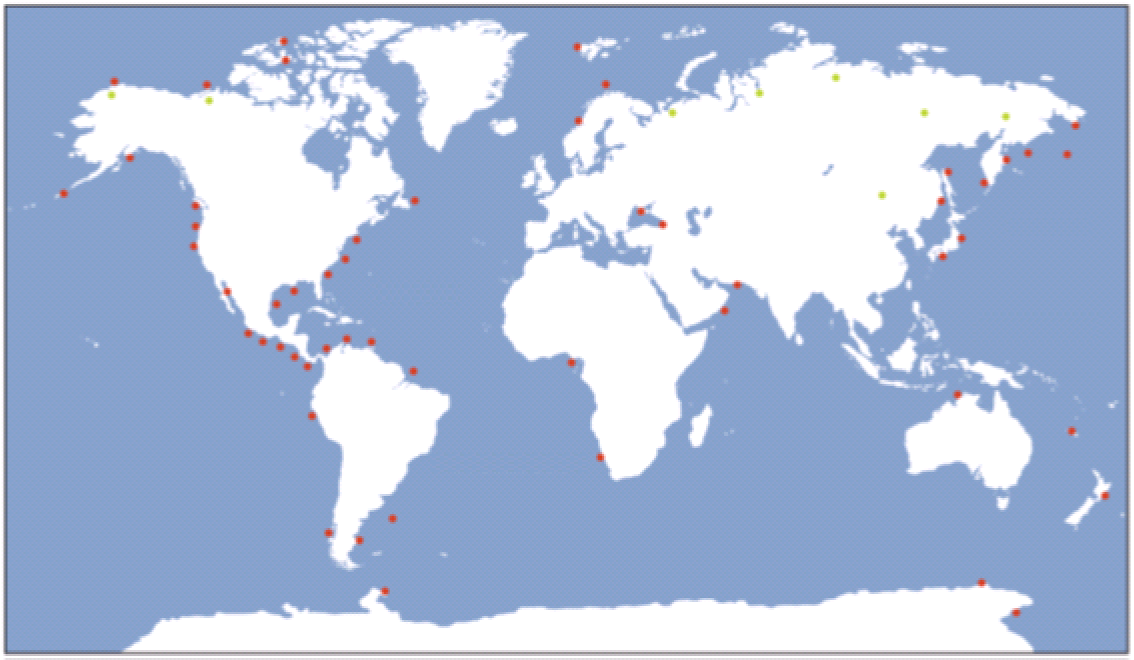

Figure 5-3. Location of inferred and known gas hydrate areas around the world. The red circles show continental margins and continental areas are shown in greens, modified from Collet (2002).

Worldwide estimations of the amount of methane in hydrate deposits vary from 14 to 34,000 trillion m^3 in permafrost areas and from 3,100 to 7,600,000 trillion m^3 in oceanic sediments (Table 5-1) It can be observed that the estimated amount is much greater than the reserves of remaining natural gas which were estimated at 187.1 trillion m^3 for 2010 by BP (BP Global, 2011).

Amount of gas	Reference
Gas contained in gas hydrates in terrestrial areas	
$1.4x10^{13}$	Meyer (1981)
$3.1x10^{13}$	McIver (1981)
$5.7x10^{13}$	Trofimuck *et al.*, (1977)
$7.4x10^{13}$	MacDonald (1900)
$3.4x10^{16}$	Dobrynin *et al.*, (1981)
Gas contained in gas hydrates in oceans	
$3.1x10^{15}$	Meyer (1981)
5-25 x 10^{15}	Trofimuck *et al.*, (1977)
$2x10^{16}$	Kvenvolden (1988)
$2.1x10^{16}$	MacDonald (1900)
$4x10^{16}$	Kvenvolden & Claypool (1988)
$7.6x10^{18}$	Dobrynin *et al.*, (1981)

Table 5-1. Worldwide estimates of gas in hydrates. All values shown in m^3, modified from Collet (2002).

5.2 Data and hypotheses

5.2.1 International data

Several databases worldwide which compile information about the distribution of gas hydrates' saturation and volumetric yield were reviewed for estimating gas in hydrates resources. The data reported by Collett (1995) for estimating USA resources, specifically in the Golf of México area, was used for making a genetic and environmental analogy.

5.2.2 National data

Seismic data and information about wells along Colombian continental margins was compiled from ANH's oil database; it revealed 807 seismic lines (around 39,000 km) and 24 wells with their corresponding registries (Figure 5-4).

A search was also made for seismic information about the Caribbean and Colombian Pacific coast corresponding to international scientific cruises and projects being carried out in this area. Fifty-five seismic lines (about 3,000 km) were incorporated into the study (Figure 5-4); such lines refer to data from the University of Texas Institute for Geophysics' projects DSDP93GC, IG2408, IG2401 and IG2901 and data from the British Oceanographic Data Centre's Charles Darwin project CD40 (1989).

All the information so compiled was integrated into a digital project run in Kingdom Suite, (GasHydrates.tks), forming an integral part of this study. The aforementioned seismic project includes BSR maps, the upper limit for the hydrate area, the seafloor, the speed used for converting horizons to depths and the polygons of the areas where BSR presence was interpreted.

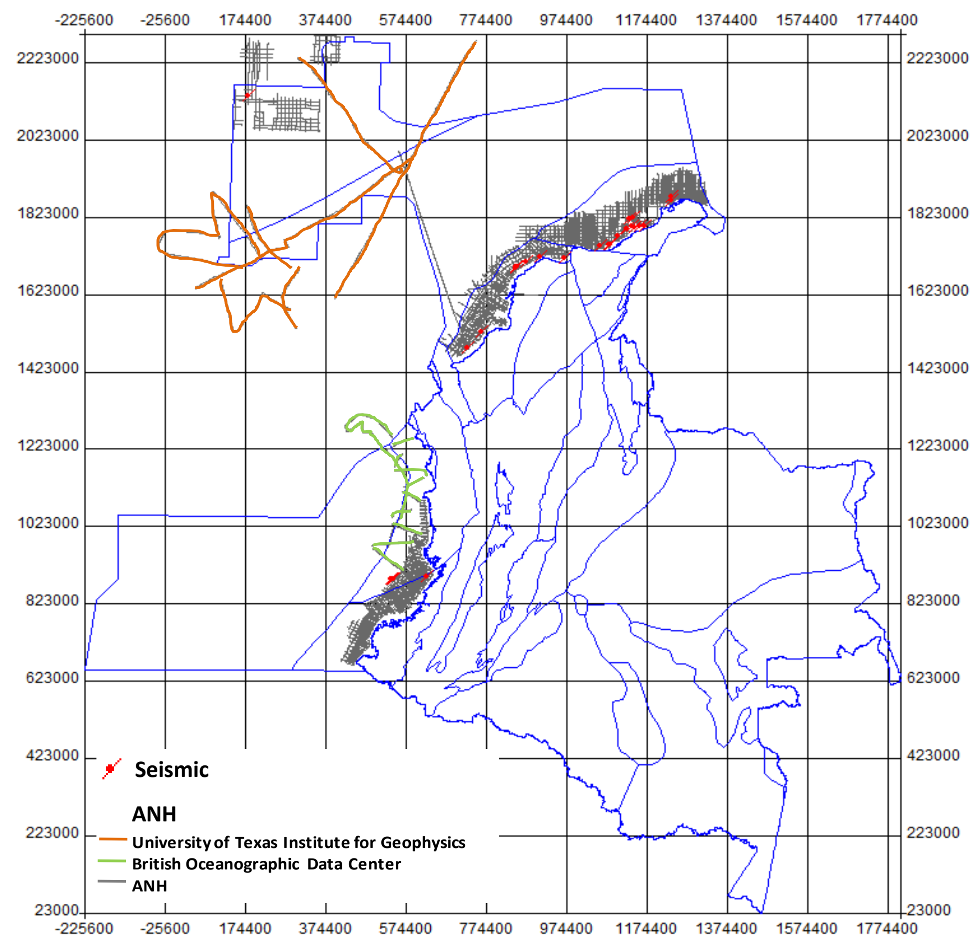

Figure 5-4. Seismic lines and wells used for estimating gas hydrates' potential

5.2.3 Hypotheses

Gas hydrates resources in Colombian marine basins have been evaluated in line with the following hypotheses:

5.2.3.1 Hypothesis 1

Areas containing gas hydrates are restricted to areas where bottom simulating reflector (BSR) can be interpreted;

5.2.3.2 Hypothesis 2

The thickness of the gas hydrate area can be obtained with a BSR-generated isopach map base of the hydrate stability area and an estimated limit for estimated seafloor pressure and temperature conditions guaranteeing molecule stability; and

5.2.3.3 Hypothesis 3

The distribution of gas hydrate saturation values and their volumetric yield can be taken from analogous gas hydrate areas.

5.3 Methodology

The following equation was used for estimating the volume of gas which could be contained in gas hydrate accumulations in Colombian marine basins:

$$HG = 0.035 * A * h * \varphi * s_{hg} * G_{hg} \tag{5-1}$$

HG : gas volume (Tcf)

A : area of gas hydrate occurrence (km2)

h : deposit thickness (m)

φ : deposit porosity (v/v)

s_{hg} : degree of gas hydrate saturation (v/v)

G_{hg} : volumetric yield of gas in hydrates (v/v)

The following activities were carried out in each marine basin for this estimate:

- Seismic and well information was loaded into a Kingdom Suite project; The coordinates for seismic lines were estimated from files regarding navigation and scientific cruise reports for loading the seismic lines obtained from the Charles Darwin project CD40 (1989);
- The BSR and seafloor were interpreted;

- Polygons were drawn for the areas where the BSR was interpreted;
- Conversion to depth was done and maps of the surface were interpreted. The speeds used for converting to depth were:
    - ✓ A constant 1,500 m/s speed was used in all areas for converting seafloor to depth;
    - ✓ Time-depth curves regarding available wells were used for the Colombian Caribbean for obtaining a map of BSR speed;
    - ✓ Regarding the Colombian Pacific coast, the speed functions obtained from the work of Minshull et al., (1994) were used as well as a well located in the area for obtaining a map of BSR speed. Such procedure was chosen due to the scarce information regarding wells in this area (Figure 5-5).

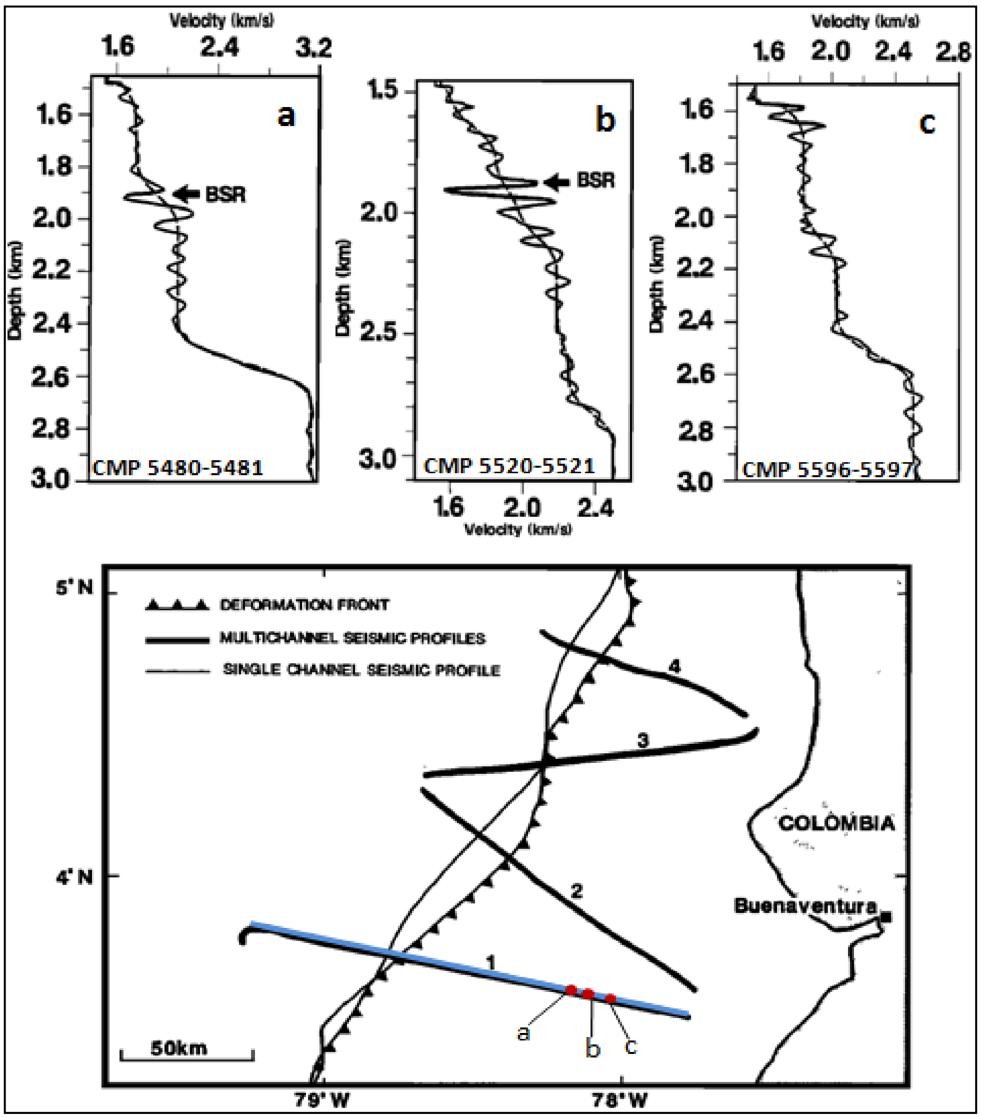

Figure 5-5. Speed functions taken for conversion to depth in the Colombian Pacific. Speed functions were obtained by inverting the wave equation in some CMP from line 1 (blue line on the lower map). The approximate location of the CMP can be seen with the red circles on the lower map, modified from Minshull et al., (1994)

- The gas hydrate area's upper limit was estimated using equation 5-4 modified from Dickens et al., (1994), defining pressure and temperature stability conditions for methane hydrates in seawater, as follows:
  - ✓ Seafloor depth values were taken from the map generated for this reflector in marine basins;
  - ✓ Seafloor pressure and temperature were calculated from equations 5-2 and 5-3:

$$P_{fo} = P_{atm} + \rho_{water} * g * h_{fo} \quad \textbf{(5-2)}$$

$$T_{fo} = 295.1 * {h_{fo}}^{-0.6} \quad \textbf{(5-3)}$$

P_{fo}: seafloor pressure (MPa)

T_{fo} : seafloor temperature normalised to 3 °C < T_{fo} < 6.5 °C

P_{atm} : atmospheric pressure (Mpa)

ρ_{agua} : water density (1,030 Kg/m^3)

h_{fo} : seafloor depth (m)

g : gravity (m/s^2)

✓ The depth to which the seafloor (due to its pressure and temperature conditions) may be considered the limit of the gas hydrates area was estimated (equation 5-4). Figure 5-6 gives an example of the pressure and temperature obtained for the Colombian Caribbean seafloor and the base of the hydrate stability area, also defined by equation 5-4.

$$\frac{1}{T+273.15} = 3.79 \cdot 10^{-3} - 2.83 \cdot 10^{-4} \log(P) \quad \textbf{(5-4)}$$

T : temperature (°C)

P : pressure (MPa)

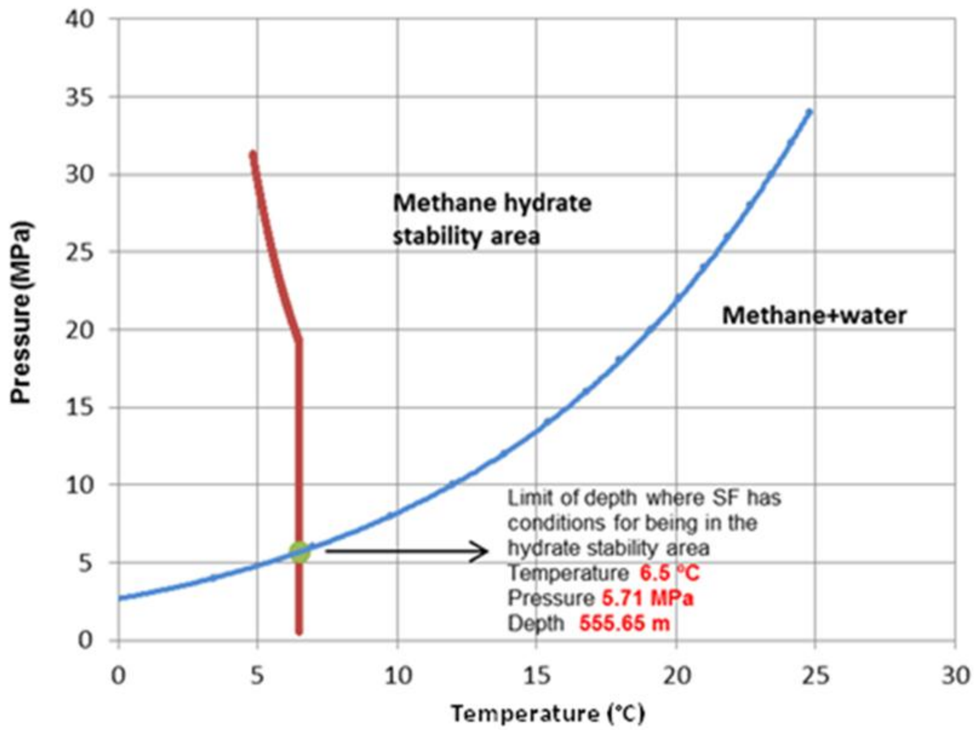

Figure 4 6. Seafloor (SF) pressure and temperature in the Colombian Caribbean and hydrate stability conditions defined by the equation proposed by Dickens et al., (1994). The blue line gives the base of the stability area inferred by equation 4-4. The red line represents SF pressure and temperature in the area where the BSR was interpreted. It was observed that hydrate stability cannot be guaranteed from certain SF depth.

- Seafloor depths greater than 555.65 m complied with pressure and temperature conditions for being within the hydrate stability area; the seafloor could thus be established as the upper limit for hydrates in this area (Figure 5-6).
  - ✓ The foregoing suggested that in these areas the hydrostatic pressure slope was sufficient to guarantee stability; the pressure was very low or the temperature very high for guaranteeing this in the other areas.
  - ✓ For all points on the seafloor map in which depth was less than 555.65 m, the Δh was calculated for entering the area of stability using equation 5-5 (Figure 5-7).

$$\Delta \boldsymbol{h} = \frac{\rho_{water}}{\rho_{marine\ sediment}} * \left(555.56 - \boldsymbol{h}_{fo}\right) \qquad \textbf{(5-5)}$$

  - ✓ There was minimum variation regarding the depth required for points on the seafloor above 555.65 m in the area of stability. The hydrate area limit in these points should have been deeper in the middle of sediment layers, incorporating the lithostatic slope at stability pressure.
  - ✓ Equation 5-5 applied a factor derived from the ratio between water density and that of marine sediments. This factor ranged from 0.52 to 0.6 and tried to affect the thickness considered below the seafloor, having a pressure slope greater than the hydrostatic one (marine sediments) so that total pressure in such areas increased proportionally.

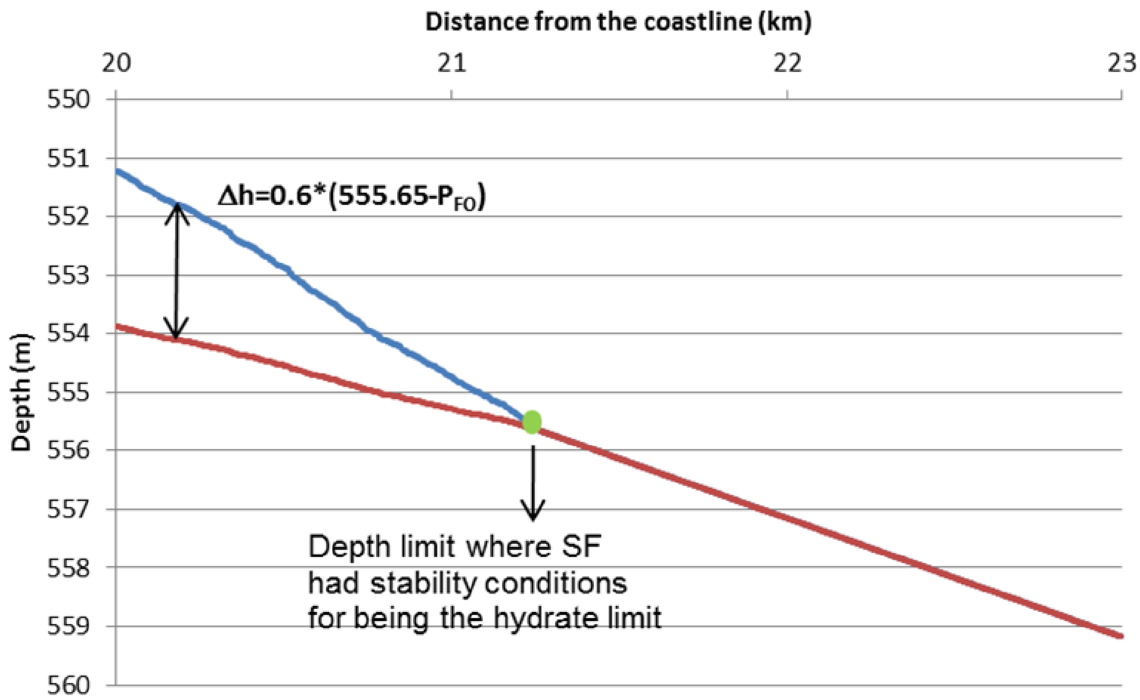

Figure 5-7. Estimating hydrate area limit for less than 555.65 m seafloor depths. Blue represents the seafloor (SF). Red is the hydrate stability limit for the methane area. From 555.65 m onwards, the SF may be considered the stability area limit.

- ✓ Pressure and temperature regarding gas hydrate area limit were estimated again from equations 5-6 and 5-7 once the Δh had been calculated at all points where the seafloor had a depth less than 555.65 m (Figure 5-8).

$$P_{tzh} = P_{fo} + \rho_{sediments} * g * \Delta h \quad \textbf{(5-6)}$$

$$T = \frac{1}{3.79 \cdot 10^{-3} - 2.83 \cdot 10^{-4} \log(P_{tzh})} + 273.15 \quad \textbf{(5-7)}$$

P_{tzh} : pressure in hydrate area limit (Mpa)

$\rho_{sedimentos}$: marine sediment density, around 1900 kg/m³

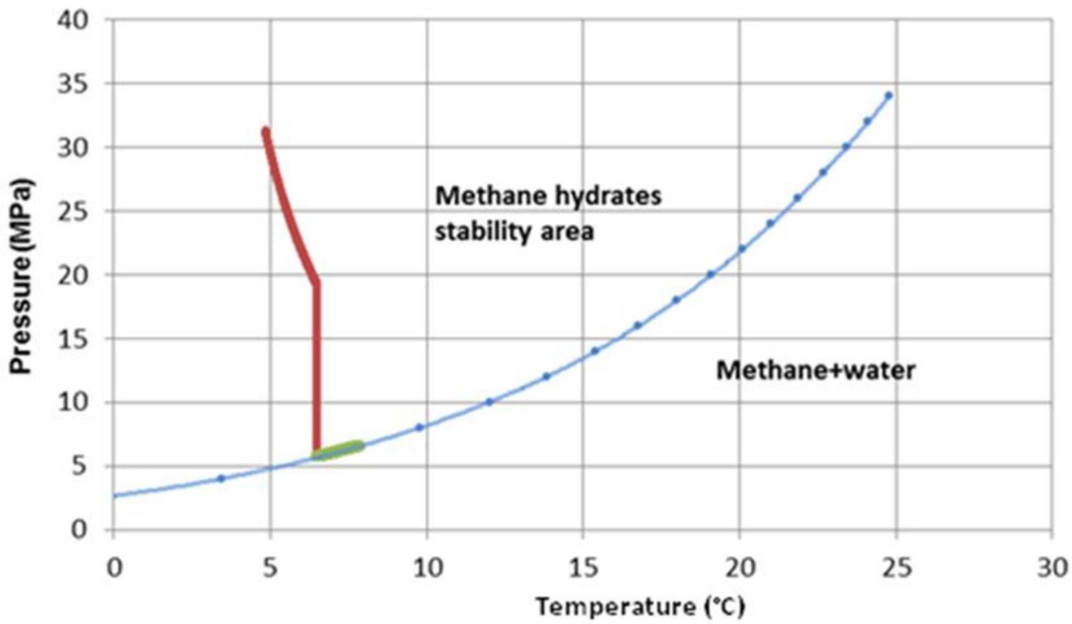

Figure 5-8. Pressure and temperature for hydrate area limit in the Colombian Caribbean and hydrate stability conditions defined by the equation proposed by Dickens et al., (1994). The red line represents SF pressure and temperature in the areas where the BSR was interpreted. The green line shows the estimated points, including the Δh.

- ✓ The map for the gas hydrates limit was calculated from the points at which seafloor depth was greater than 555.65 m and the points recalculated below the seafloor (the green line in the example shown in Figure 5-8) in areas where the latter was above 556.65 m depth:
    - The isopach was calculated between the BSR and the gas hydrate area limit;
    - The volume of the gas hydrate area was estimated from the polygon of the area and the isopach;
    - The distribution of probability was adjusted to effective porosity values in records concerning wells in the Colombian Caribbean, considering just the depth interval defined by the limit and the base of the gas hydrate stability area. This distribution was used for making calculations for all the basins;
    - A bibliographic review was made for determining the distribution of values regarding the degree of gas hydrate saturation and volumetric yield of gas in hydrates, since data regarding this area was lacking, and
    - Monte Carlo simulation involved using porosity, gas hydrate saturation and gas hydrates' volumetric yield as random variables. The volume derived from analysing the seismic sections was incorporated as a constant parameter in the simulation.

5.4 Results

Equation 5-1 was used for calculating some variables deterministically and others were assigned probability functions by statistical analysis. Random variables were produced from analysing the distribution of known data concerning the area or by analysing the values used in studies around the world.

5.4.1 Gas hydrate occurrence areas

The areas considered in the calculations were those where seismic lines led to identifying the presence of the BSR (Table 5-2, Figure 5-9).

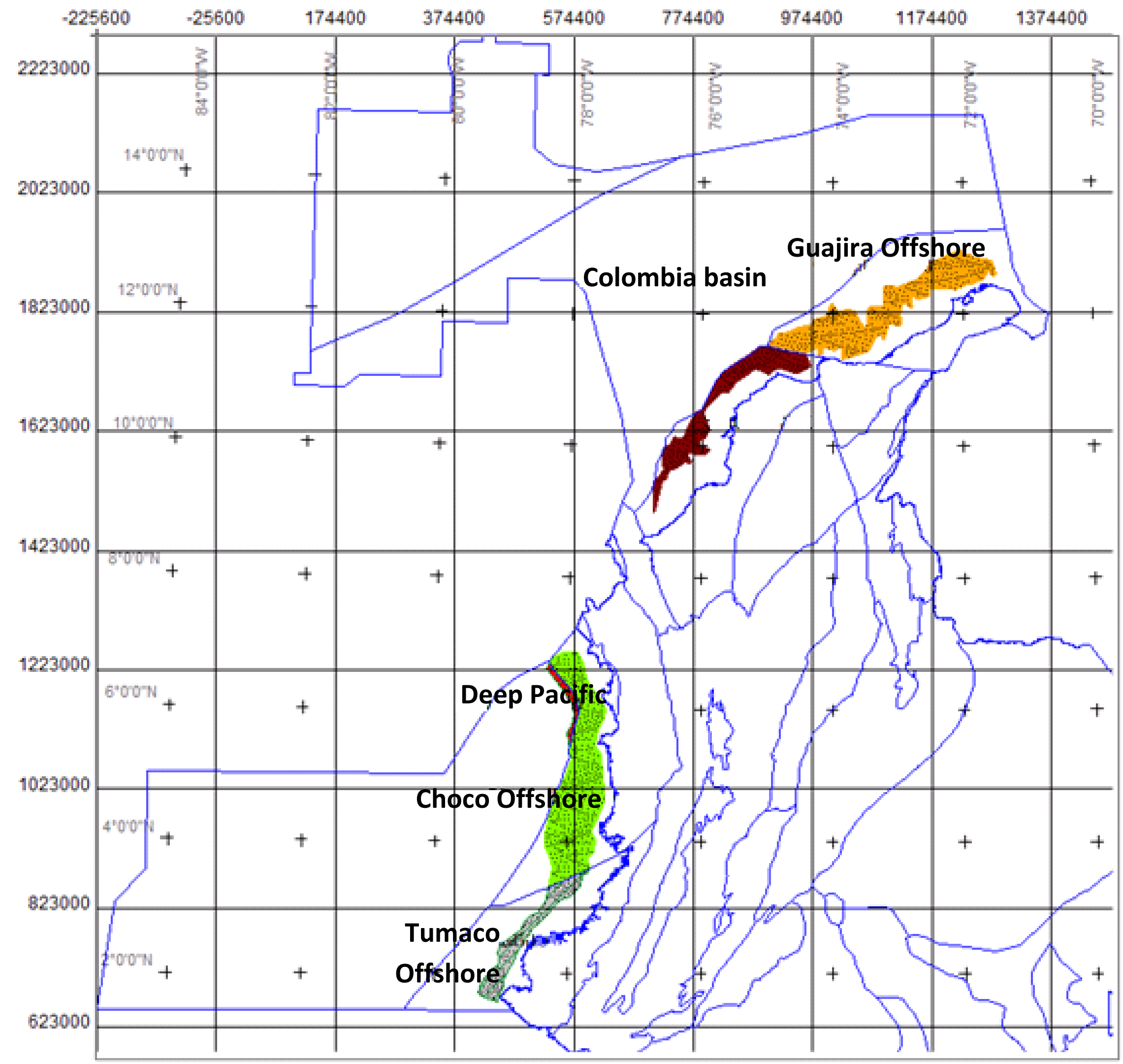

Figure 4 9. Polygons for the areas where the BSR was interpreted. Caribbean area: the polygon for the Guajira offshore basin is shown in orange, Sinú offshore in brown and the Colombia basin in pink. These defined a strip parallel to the coast which became thinner towards the southeast, giving a width varying from around 60 km to 1 Km from northeast to southwest. Pacific area: the polygon for the Chocó offshore basin is shown in green, Tumaco offshore in gray and Deep Pacific in red; likewise, a strip was defined parallel to the coast which became thinner from north to south, having a width which varied from around 80 km to 20 km from north to south.

5.4.2 Deposit thickness

The resources' potential distribution was restricted to the continental slopes, becoming reduced as the seafloor gradient increased. The BSR in the Caribbean and Colombian Pacific gave a strip parallel to the coast (Figures 5-10 and 5-11), reaching widths of up to 80 km in some areas. It was observed in both cases that the BSR became deeper in a direction perpendicular to the coast.

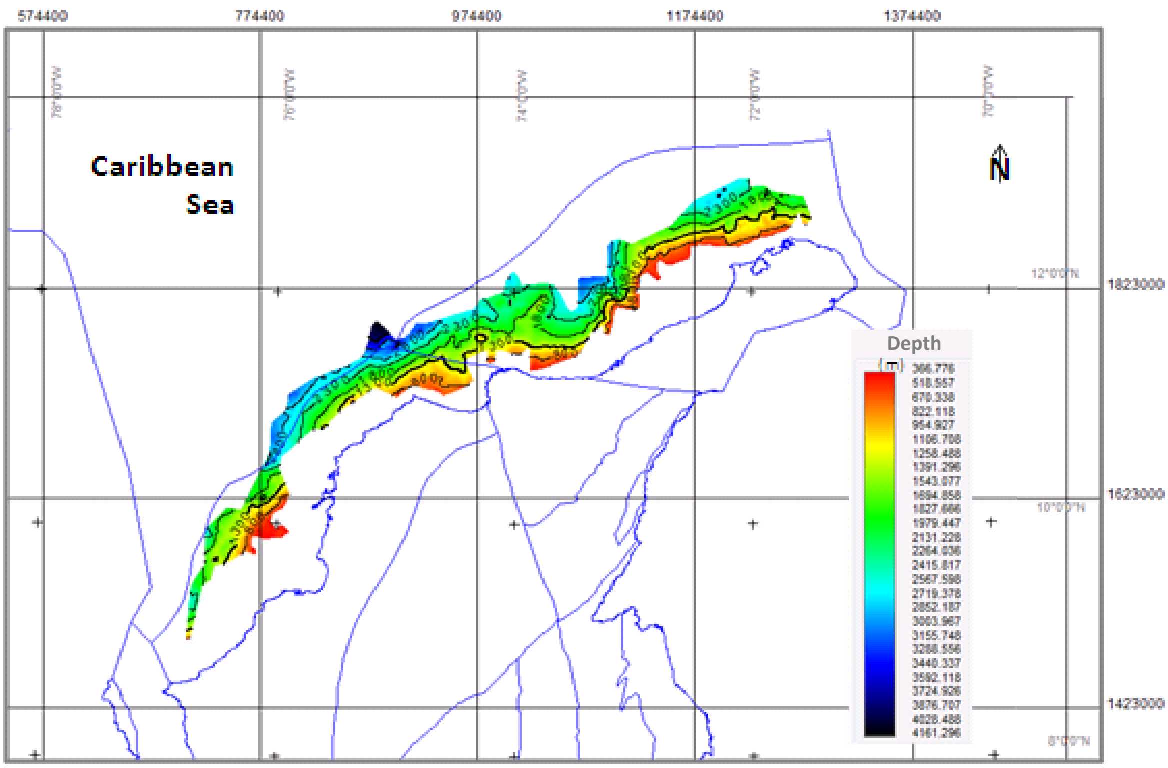

Figure 5-10. Map of the BSR for the Colombian Caribbean. It can be observed that the BSR was restricted to a strip parallel to the coast which became thinner towards the southeast of the Sinú offshore basin. Its depth varied from 0.3 km in the area closest to the coast and, as it became further from the coast line, it became deeper, reaching around 4 km in the Colombia basin.

ANH
AGENCIA NACIONAL DE HIDROCARBUROS

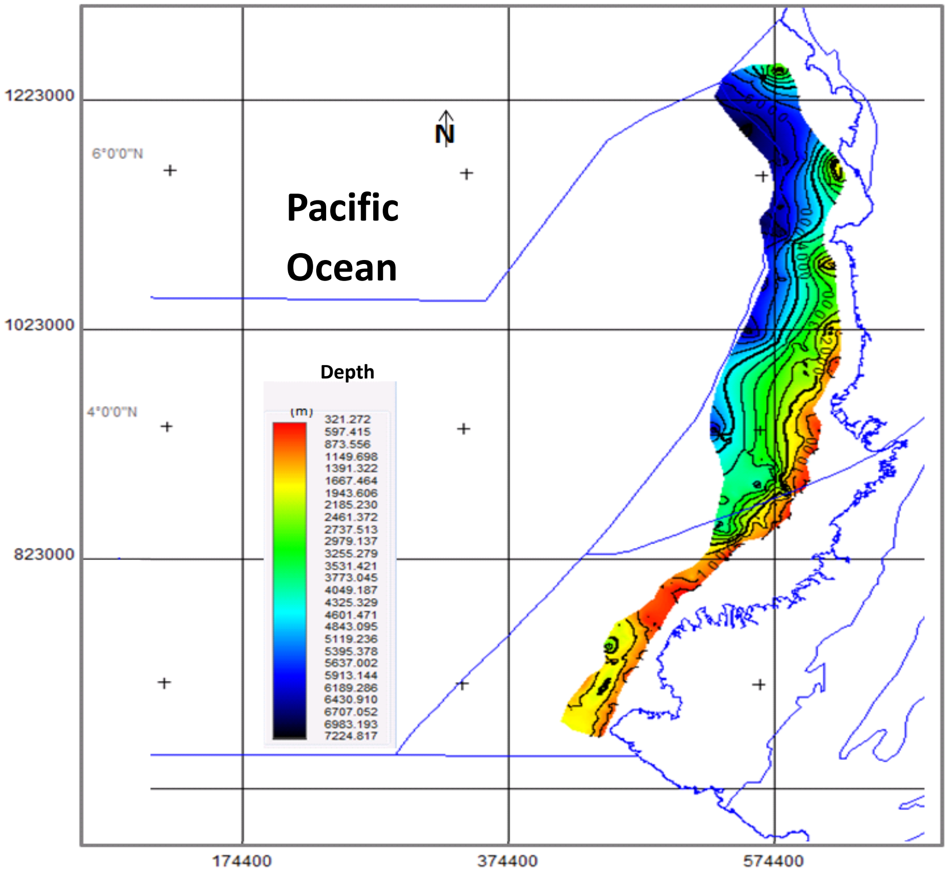

Figure 5-11. Map of the BSR for the Colombian Pacific. The BSR gave a strip parallel to the coast which became thinner towards the south; its depth varied from 0.3 km in the area closest to the coast, which became deeper as it became further away from the coastline, reaching 7 km to the north in the Deep Pacific basin.

Figures 5-12 to 5-29 give the BSR distribution maps and isopach hydrate area limit for Colombian marine basins. The volumes used for estimating resources in each basin were calculated from thickness data and BSR aerial distribution; Table 5-2 gives this data.

Basin	Area (km²)	Minimum-maximum thickness (km)	Volume (km³)
Chocó offshore	22,404.33	0.004 - 4.81	40,731.63
Colombia Basin	2,042.33	0.397 - 1.27	1,635.12
Guajira offshore	18,873.14	0.0002 - 1.46	10,529.41
Deep Pacific	1,308.37	1.97 - 3.17	3,271.65
Sinú offshore	10,248.28	0.0009 -1.14	5,189.15
Tumaco offshore	6,374.35	0.009 - 2.49	4,623.07

Table 5-2. Dimensions of the areas considered for gas hydrate potential calculations.

5.4.2.1 Guajira offshore

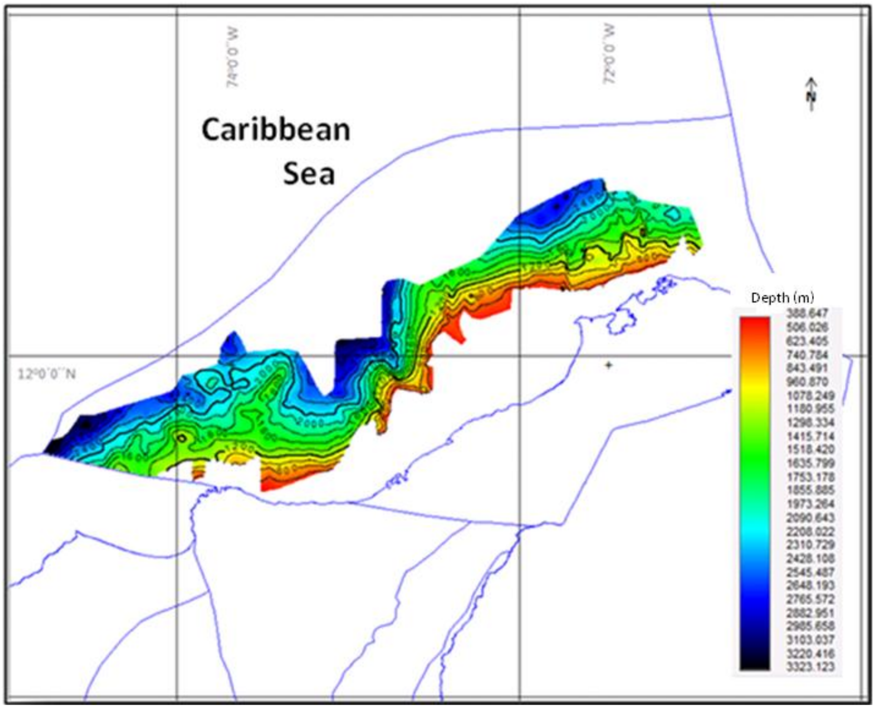

Figure 5-12. Map of the BSR for the Guajira offshore basin. The BSR in this basin gave depths between 0.4 km in the area close to the coast and 3 km in the most far off area.

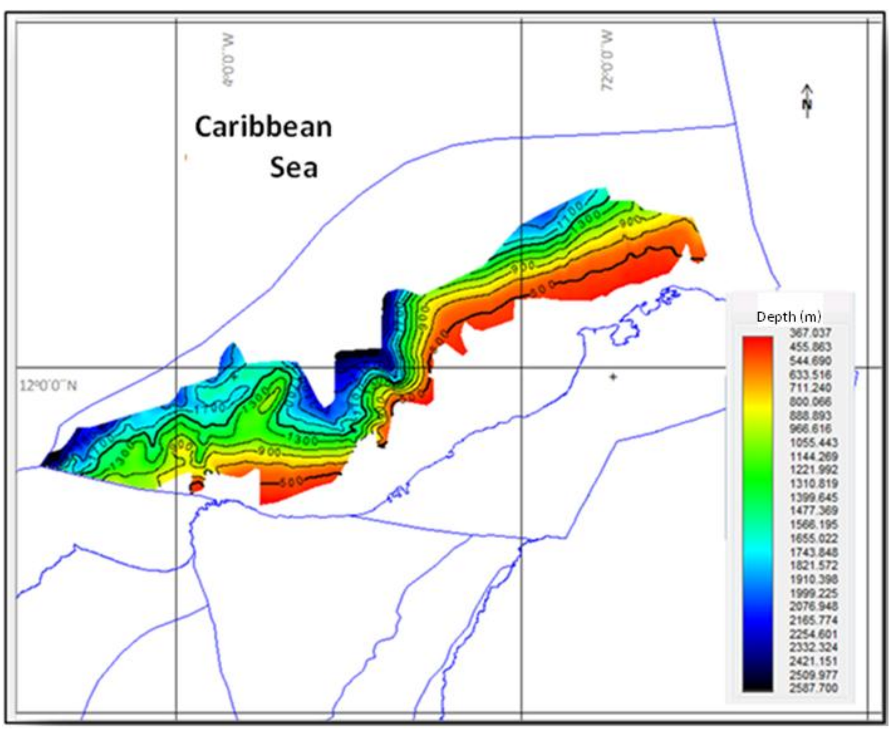

Figure 5-13. Map of the hydrate area limit for the Guajira offshore basin. The hydrate limit followed the BSR tendency having depths from 0.3 km to around 2.5 km.

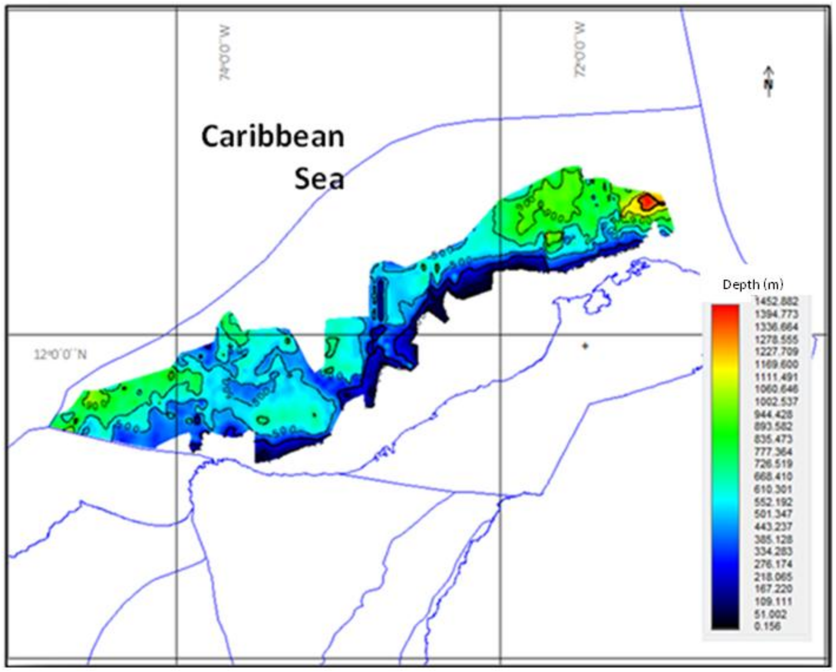

Figure 5-14. Isopach map of the hydrate area for the Guajira offshore basin. This basin's thickness had a broad range of variation, from a few metres in the area close to the coast to around 1000 m towards the north where the BSR and hydrate limit were deeper.

5.4.2.2 Sinú offshore

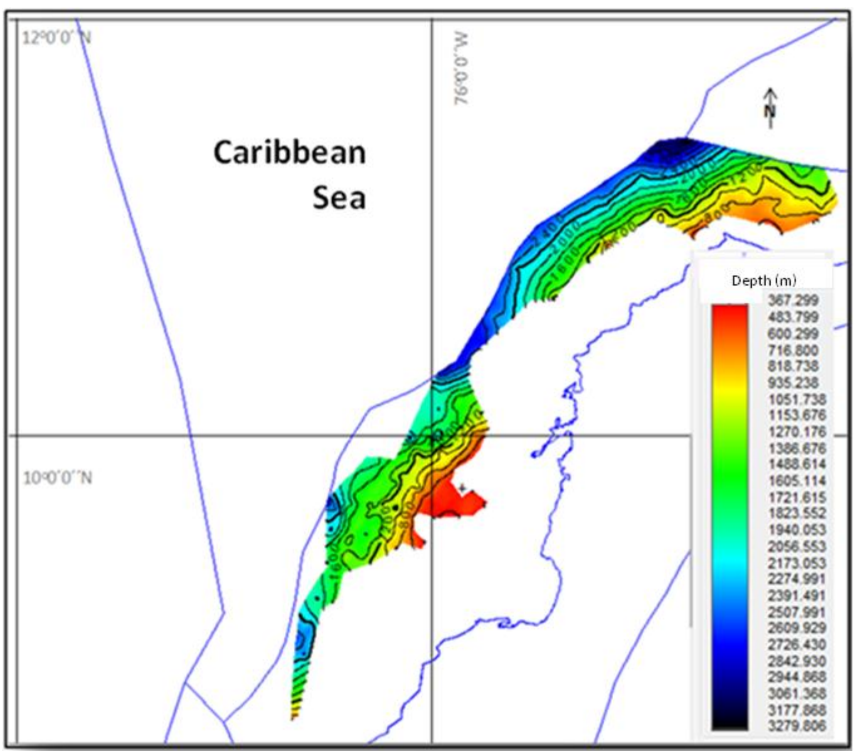

Figure 5-15. Map of the BSR for the Sinú offshore basin. In this basin the BSR gave depths varying from 0.4 km in the area closest to the coast to around 3 km to the north.

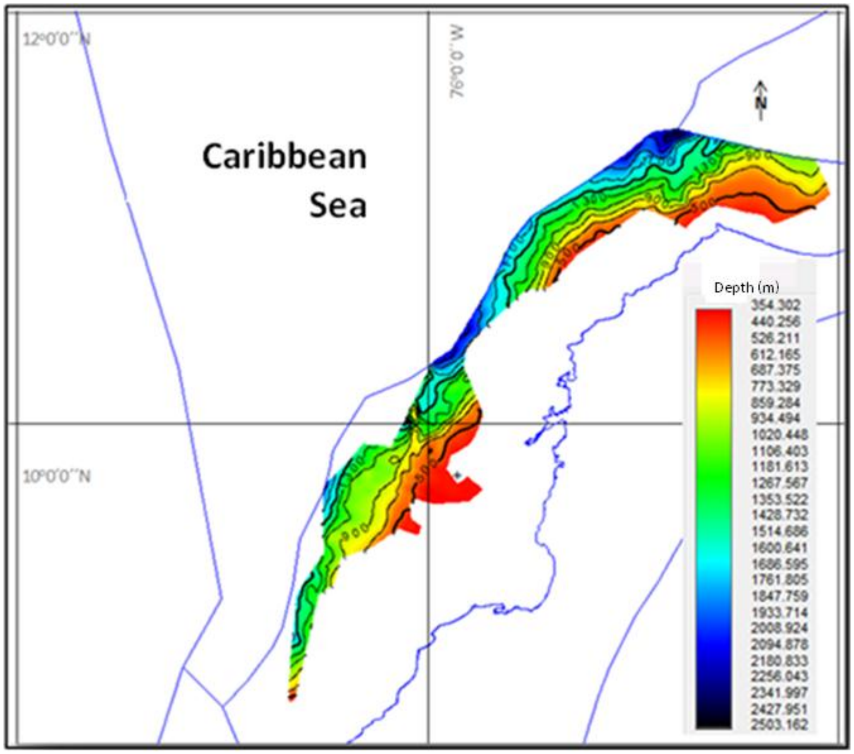

Figure 5-16. Map of the hydrate area limit for the Sinú offshore basin. The hydrate limit had the same tendency as the BSR, having depths varying from 0.3 km to around 2.5 km.

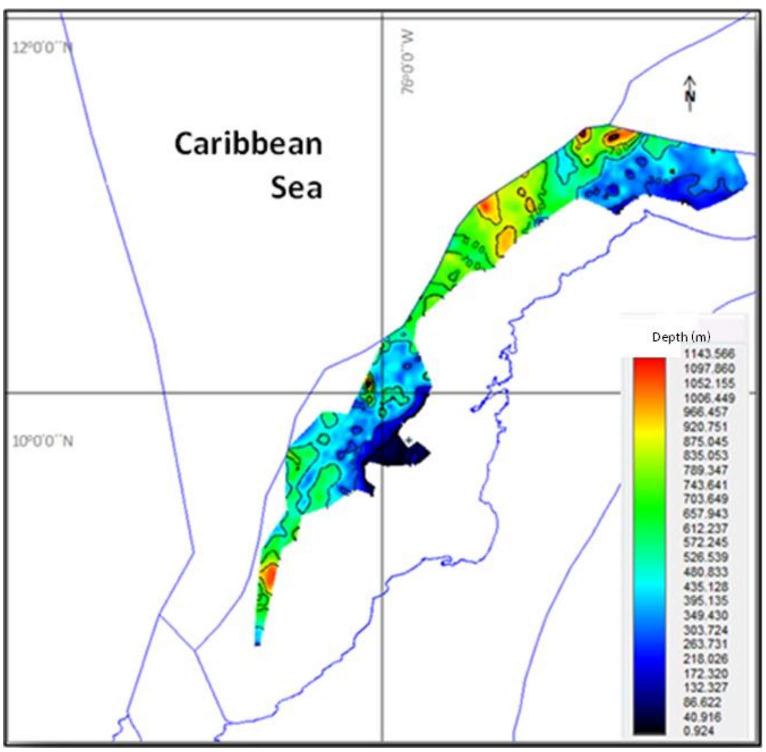

Figure 5-17. Isopach map of the hydrate area for the Sinú offshore basin. Thickness ranged from a few metres in the area closest to the coast to around 1,000 m, the greatest thickness being presented in the basin's central area.

5.4.2.3 Colombia basin

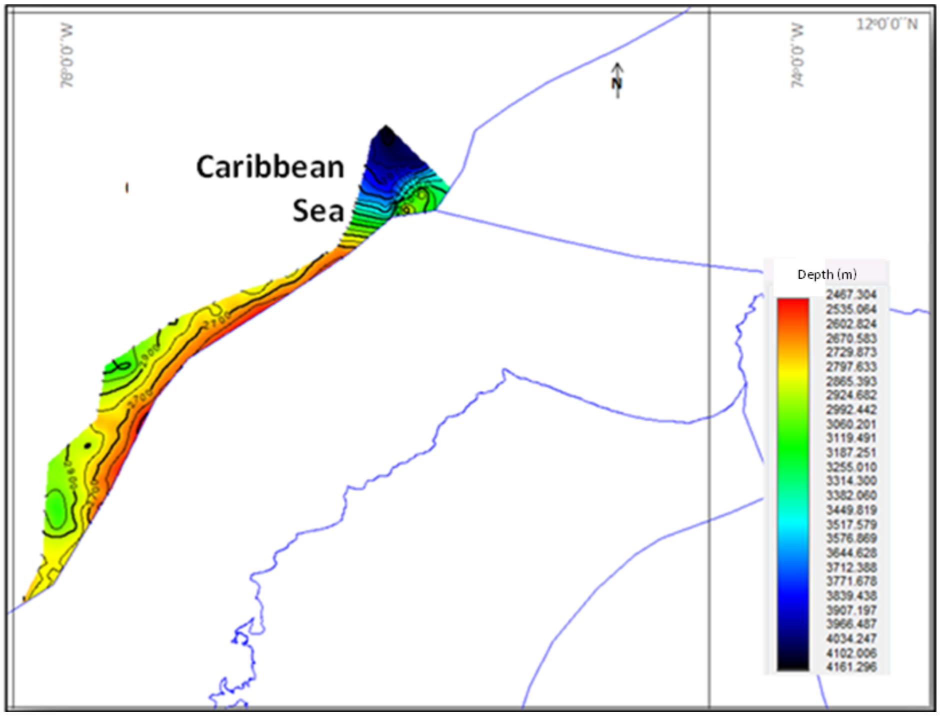

Figure 5-18. Map of BSR for the Colombia basin. It may be observed that the BSR becomes deeper as it became father away from the coast in a perpendicular direction, reaching around 4 km in the deepest areas.

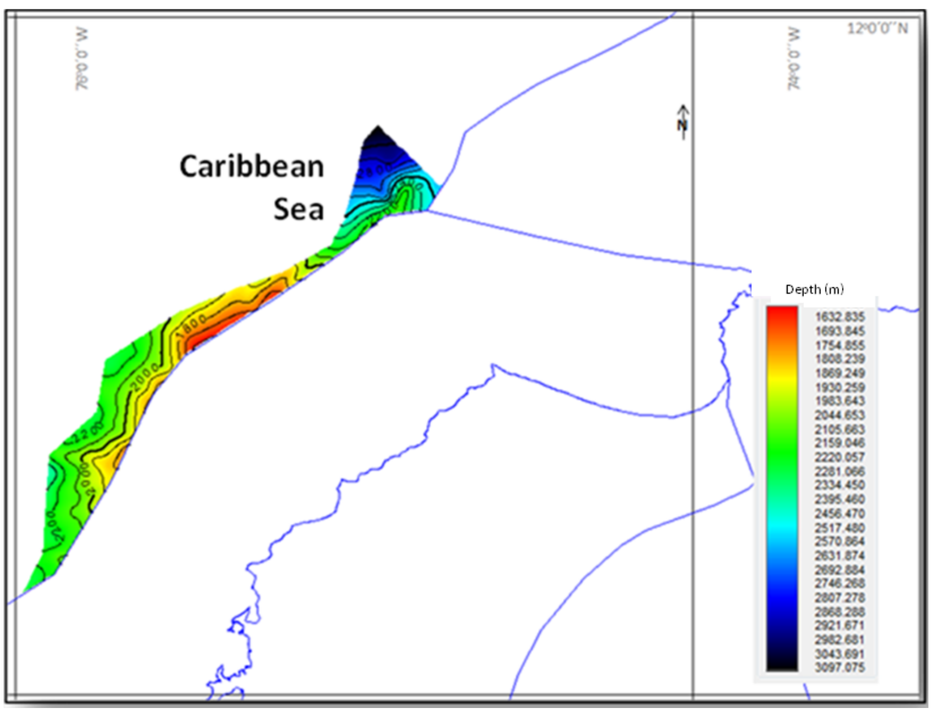

Figure 5-19. Map of hydrate area limit for the Colombia basin. The hydrate area limit gave the same tendency as the BSR, reaching depths of 3 km around the area farthest away from the coast.

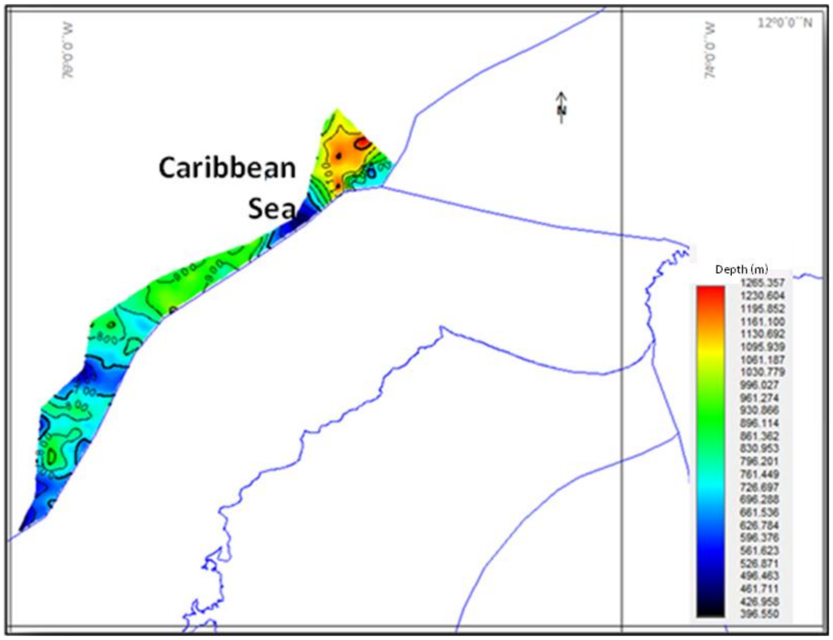

Figure 5-20. Isopach map of the hydrate area for the Colombia basin. The thicknesses in this area varied from 300 m to around 1200 m. The greatest thicknesses occurred in the north where the BSR and hydrate area limit were deepest.

5.4.2.4 Chocó offshore

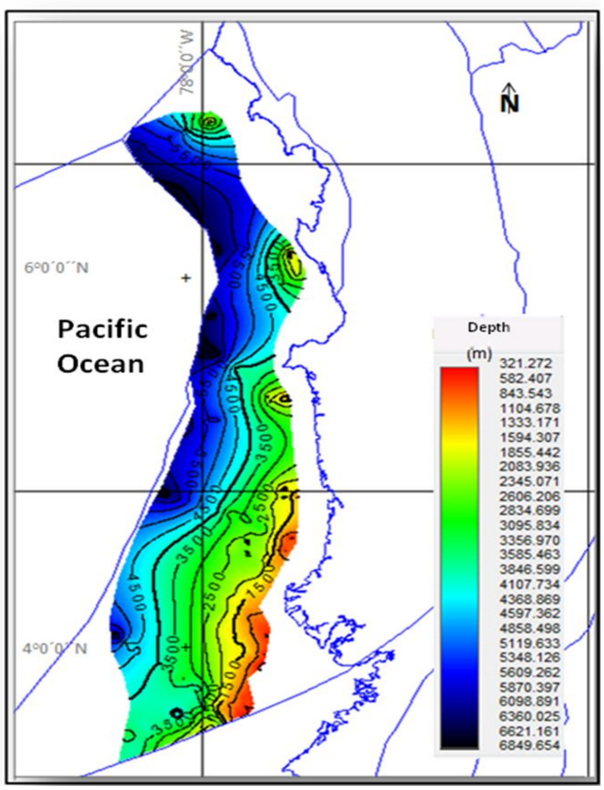

Figure 5-21. Map of the BSR for the Chocó offshore basin. The BSR gave depths varying from 0.3 km in the area close to the coast, increasing in a perpendicular direction until reaching around 6.5 km.

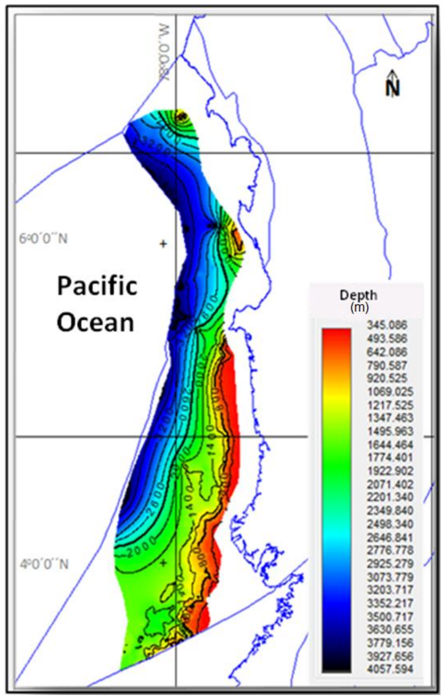

Figure 5-22. Map of hydrate area limit for the Chocó offshore basin. The hydrate area limit had the same tendency as the BSR, varying in depth from 0.3 km in the area close to the coast to 4 km in the area farthest away from it.

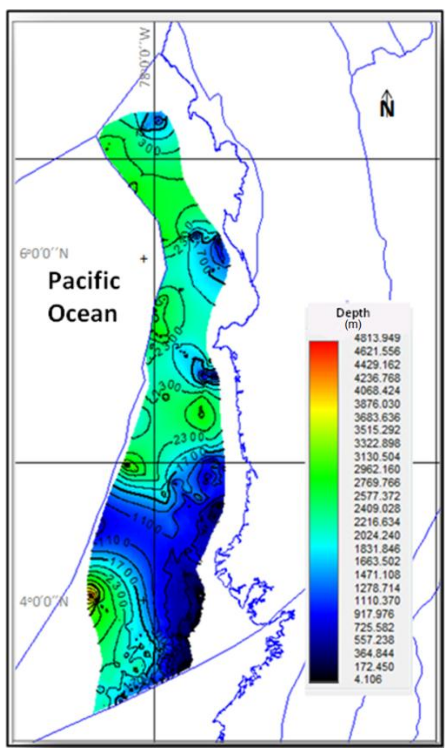

Figure 5-23. Isopach map for the Chocó marine basin. The thickness of the hydrate area varied from a few metres in the area close to the coast, reaching around 3,000 m to the southeast.

5.4.2.5 Tumaco offshore

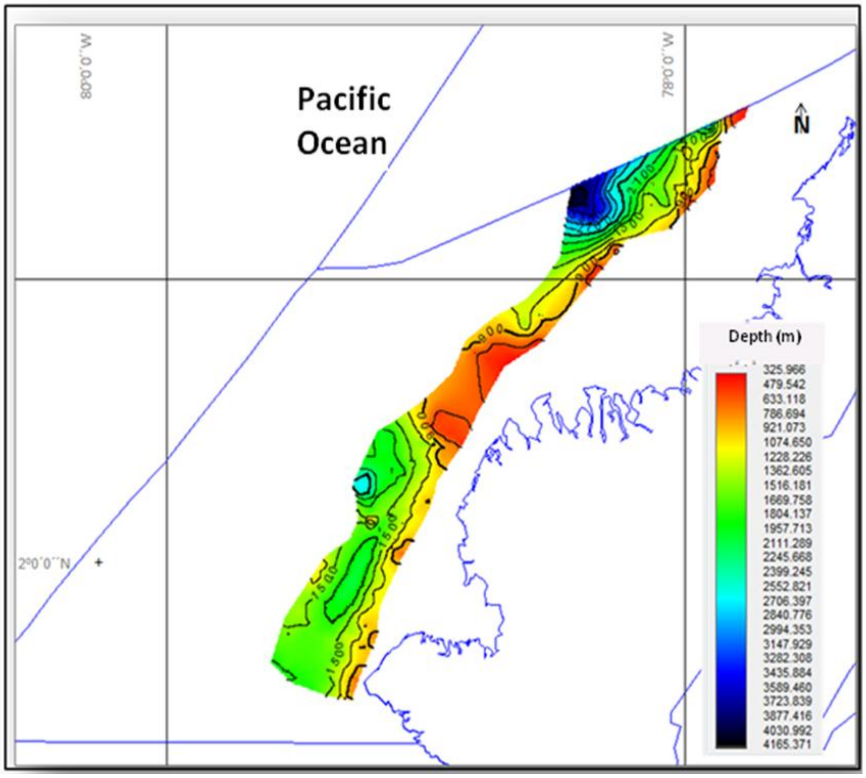

Figure 5-24. Map of the BSR for the Tumaco offshore basin. The BSR ranged from depths of 0.3 km in the area close to the coast to around 4 km to the northeast. A high spot was observed in the central part of the basin.

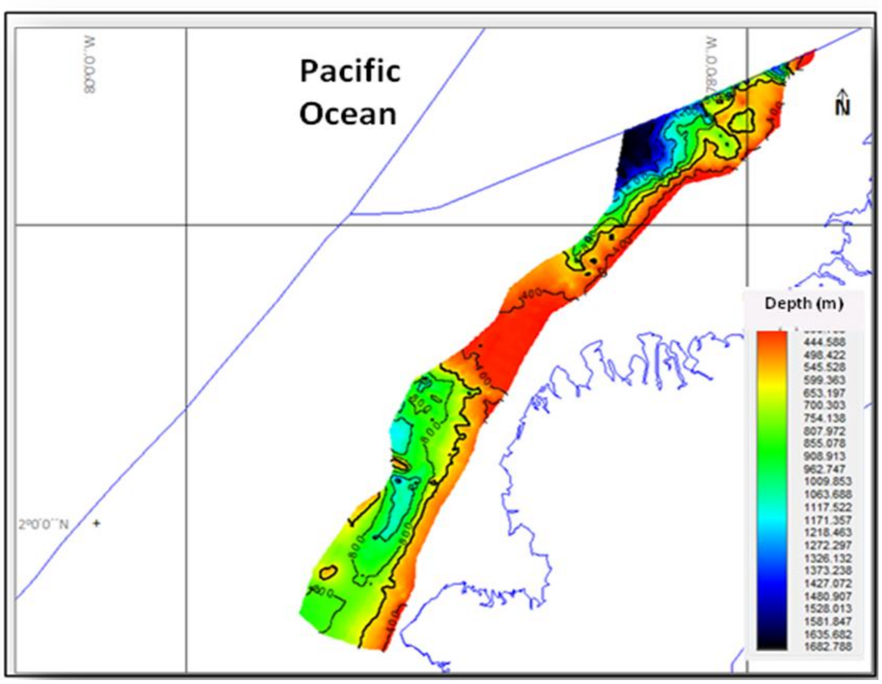

Figure 5-25. Map of hydrate area limit for the Tumaco offshore basin. The hydrate area limit also gave a high spot in the central part of the basin, and varied in depth from 0.3 km to 1.5 km.

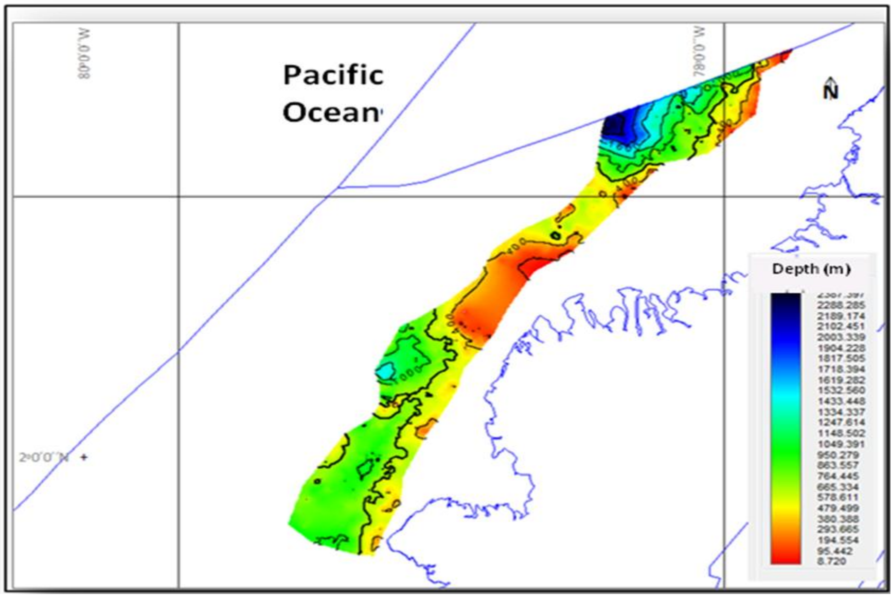

Figure 5-26. Isopach map for the Tumaco offshore basin. Thicknesses varied from a few metres in the area close to the coast to around 2 km to the northeast where the BSR and the limit were at their deepest. A reduction in thickness was identified in the central part.

5.4.2.6 Deep Pacific

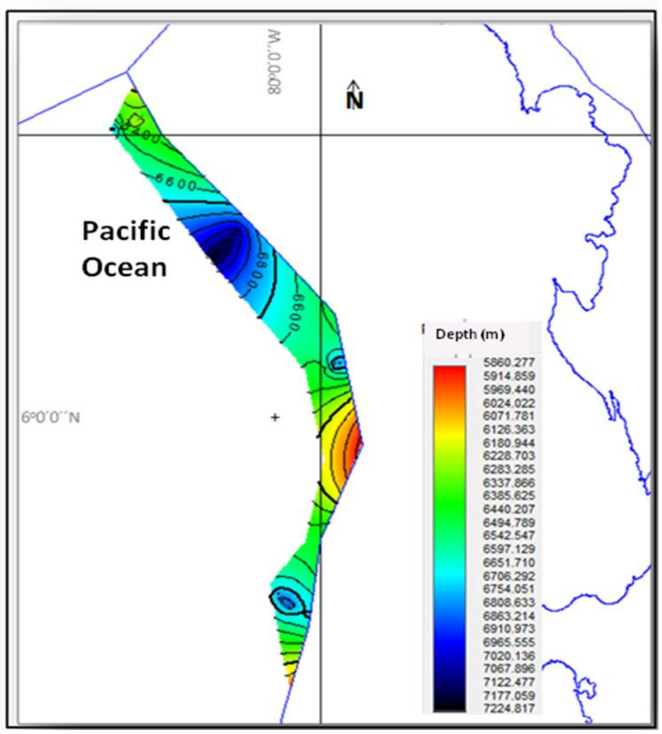

Figure 5-27. Map of the BSR for the Deep Pacific basin. The BSR in this basin was deeper, varying from around 6 km to 7 km, this being due to finding it in the part farthest away from the coast where depths were greater.

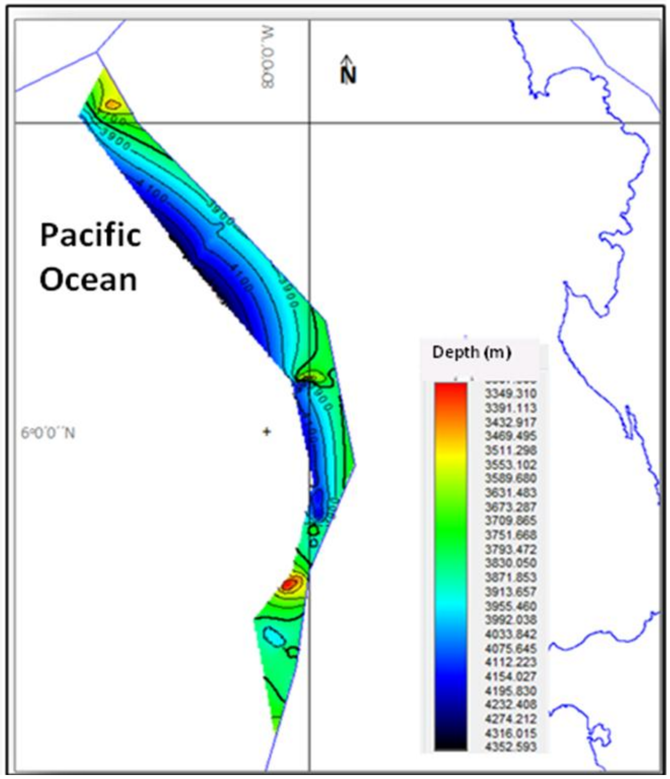

Figure 5-28. Map of the hydrate area limit for the Deep Pacific basin. This gave the same relief as the BSR, varying from 3 km to 4 km in depth.

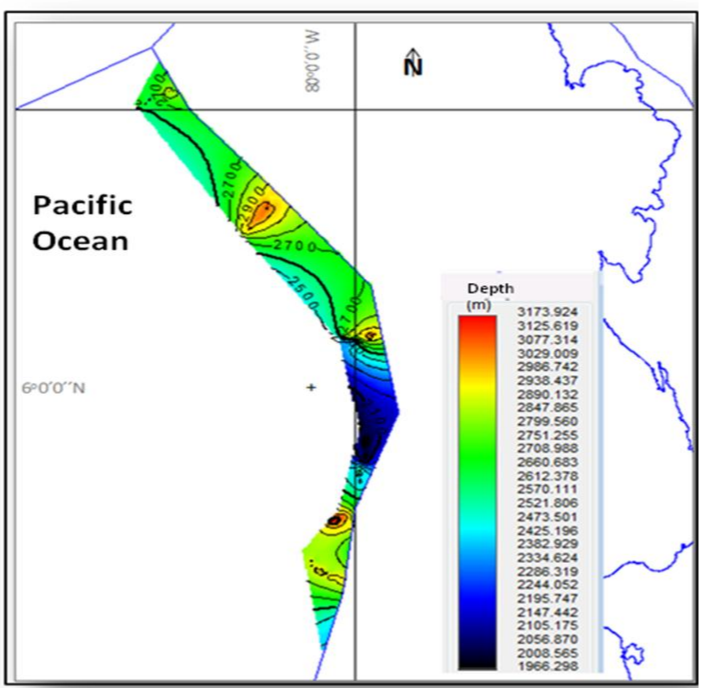

Figure 4 29. Isopach map for the Deep Pacific basin. The thickness of hydrate area in this basin varied from 2 km to around 3 km. This gave the greatest thickness due to it being found in the area where the BSR was deepest.

5.4.2.7 Deposit porosity

Porosity value distribution was estimated according to the data concerning the effective porosity records for 22 wells. However, most available wells did not come within hydrate occurrence areas (Figure 5-30). Nevertheless, such wells represented the only information available for calculating porosity distribution. A variation in porosity was observed with similar depth throughout the whole area being analysed, being assumed to be representative of the whole area having hydrates.

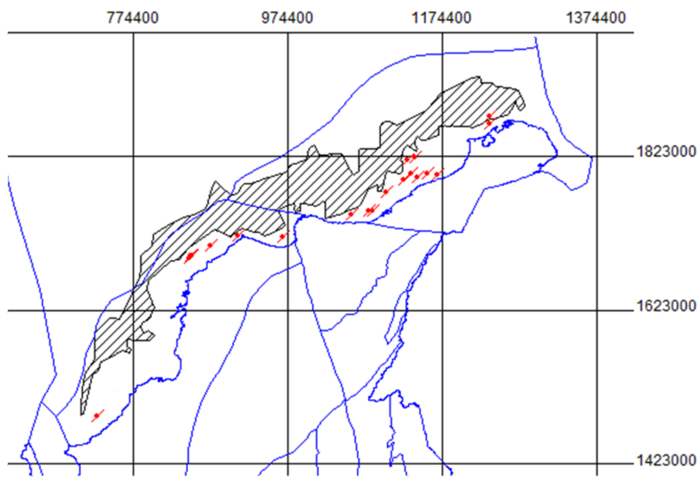

Figure 5-30. Wells having effective porosity records

The interval for the values analysed covered the interval between 4,161.3 m and 354.3 m depth, being the maximum depth estimated for the BSR and the minimum depth for the hydrate areas' upper limit, respectively. Porosity values less than 3% were not taken for estimating distribution as they were not considered to be expected values in rock and could have been due to errors in record taking or when calculating effective porosity. The distribution best fitting the data was a Weibull-type distribution (Table 5-3).

Estimated parameters						Goodness-of-fit test			
$\hat{x}$	Confidence interval		$\hat{y}$	Confidence interval		Null hypothesis	P	Statistical value	G.L
0.12	0.12	0.12	1.67	1.66	1.68	Was not rejected	M.B.	5.01	0

Table 5-3. Goodness-of-fit parameters and test results applied to porosity data for determining statistical distribution used in estimating gas hydrates potential. Estimated parameters $\hat{x}$ and $\hat{y}$ are Weibull distribution regarding "a" and "b" respectively. M.B refers to very low probability of the null hypothesis being accepted or rejected.

5.4.3 Degree of gas hydrate saturation

Gas hydrate saturation values estimated in work carried out around the world was reviewed; the distribution used for calculating USGS hydrate resources in the Gulf of México (Collet, 1995) was taken, considering that this covered the whole range of variation found in analogous gas hydrate areas (Table 5-4).

Fractile	100	95	75	50	25	5	0
Gas hydrate saturation	2	3.2	8	14	20.5	25.7	27

Table 5-4. Gas hydrates saturation distribution parameters, taken from Collet (1995).

5.4.4 Volumetric yield of gas in hydrates

Volumetric yield describes when free gas is stored in gas hydrates. If gas hydrate structure is completely full of methane, 1m³ of hydrate could contain 172 m³ of methane in standard pressure and temperature conditions. However, many researchers consider that such scenario cannot be found in nature; nevertheless, gas hydrates are not stable if a structure contains less than 70% gas, thereby implying a production of at least 139 m³ of methane (Collet, 1995).

A pessimistic to moderate range was chosen in the present work, i.e. a variation from 139 m³ (70% methane occupation of gas hydrates) to 164m³ (representing 90%), using the distribution range used for calculating USGS hydrate resources in the Gulf of México (Collet, 1995). Table 4-5 shows the variable random fractals associated with describing gas hydrate volumetric yield.

Fractile	100	95	75	50	25	5	0
Volumetric yield of gas in hydrates	139	140.3	145.3	151.5	167.8	162.8	164

Table 5-5. Gas hydrates volumetric yield distribution parameters, taken from Collet (1995).

5.4.5 Gas hydrate potential

Considering the aforementioned hypotheses and all the variables described in equation 5-1, associated gas hydrates potential in Colombian marine basins was calculated using the Monte Carlo probabilistic approach. Table 5-6 gives the results obtained, not counting restricted areas due to the presence of environmental reserves.

Basin	Gas in hydrates (Tcf)		
	P_{10}	P_{50}	P_{90}
Marine Chocó	46.87	11.79	3.03
Colombia basin	1.91	0.48	0.12
Marine Guajira	12.18	3.08	0.79
Deep Pacific	3.68	0.93	0.24
Marine Sinú	5.75	1.45	0.37
Marine Tumaco	5.23	1.32	0.34
Total Colombia	75.63	19.04	4.89

Table 5-6. Estimating gas potential n hydrates. These results were affected by environmental factors shown in Table 2-1.

The results for the Colombia and Deep Pacific basins were underestimated due to not having adequate seismic coverage allowing a more precise estimate of methane hydrates' potential.

The Hess escarpment lies to the south of Los Cayos basin, on the border with the Colombia basin. Depths in this area varied from 0.5 km to 3 km from northeast to southeast in a strip of around 200 km (Figure 5-31) which could store gas hydrates, as has been found on the Colombian Caribbean coast. However, due to the few north-east to south-east seismic lines covering the Hess escarpment, the presence of gas hydrates could not be validated with total certainty by interpreting the BSR, since no reflector was found fulfilling the necessary conditions with certainty.

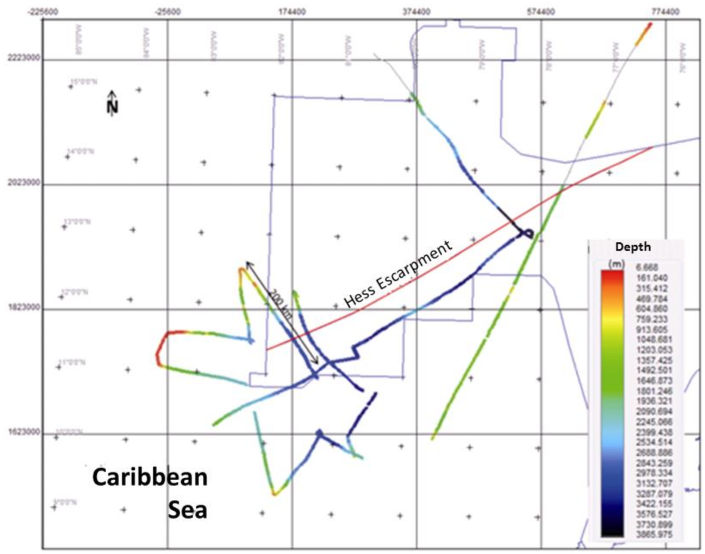

Figure 5-31. Seísmic lines available in the area limiting Los Cayos and Colombia basins. It can be seen that there was an increase in depth in a northeast-southeast direction all along the slope procuced by the Hess escarpment (red line).

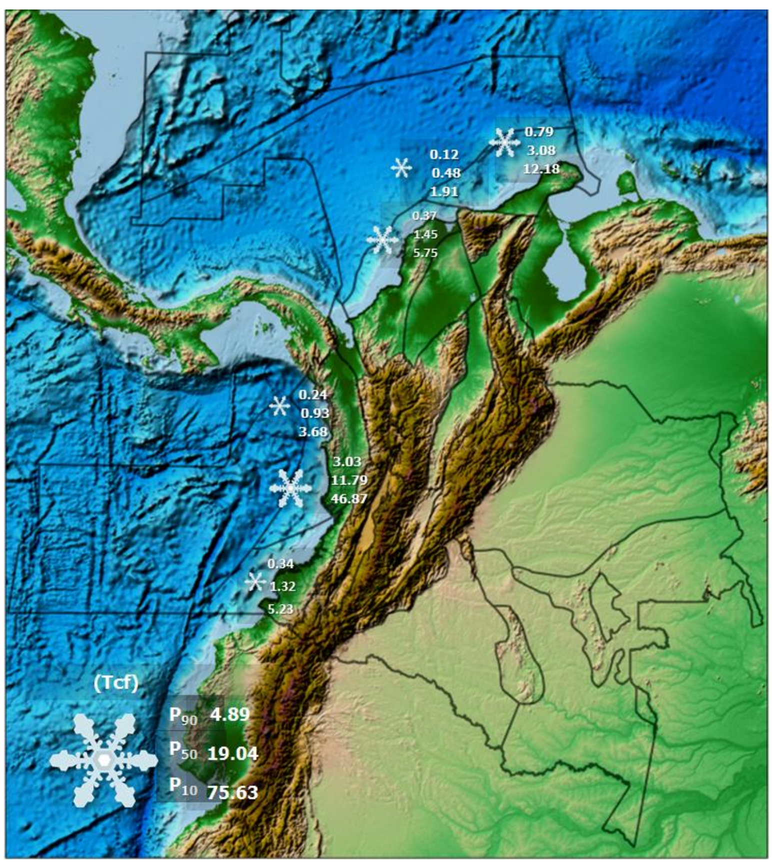

Figure 5-32. Gas hydrates' potential for Colombia marine basins.

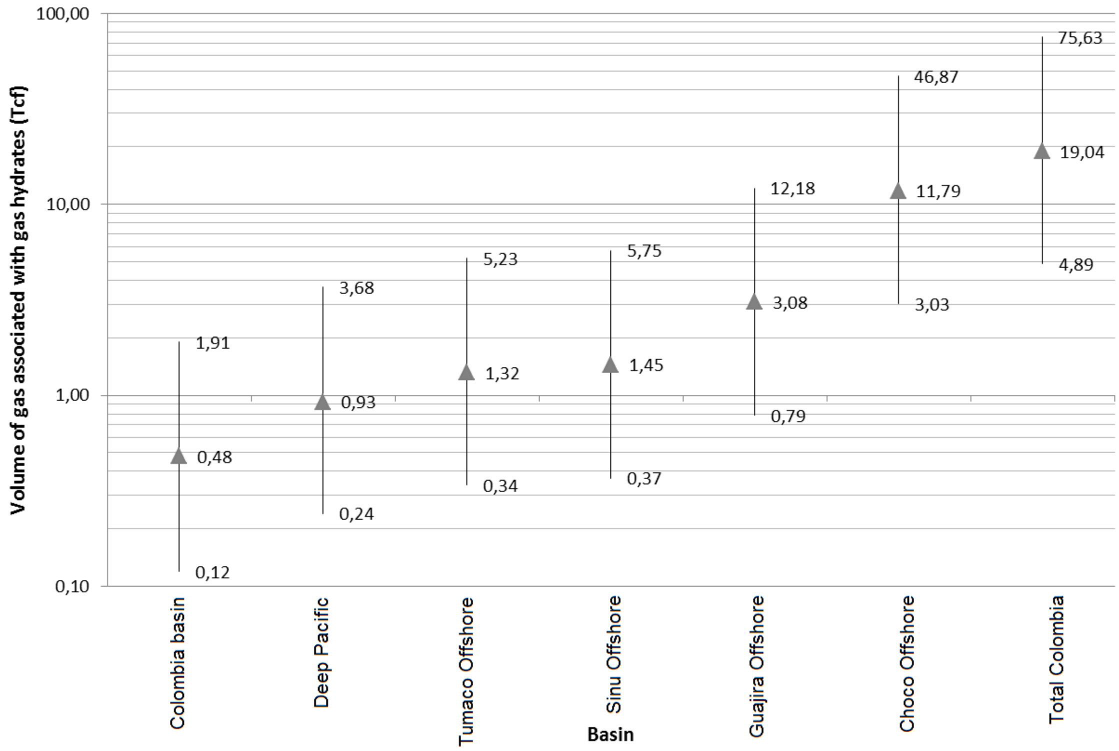

Figure 5-33. Gas hydrate potential for Colombian marine basins

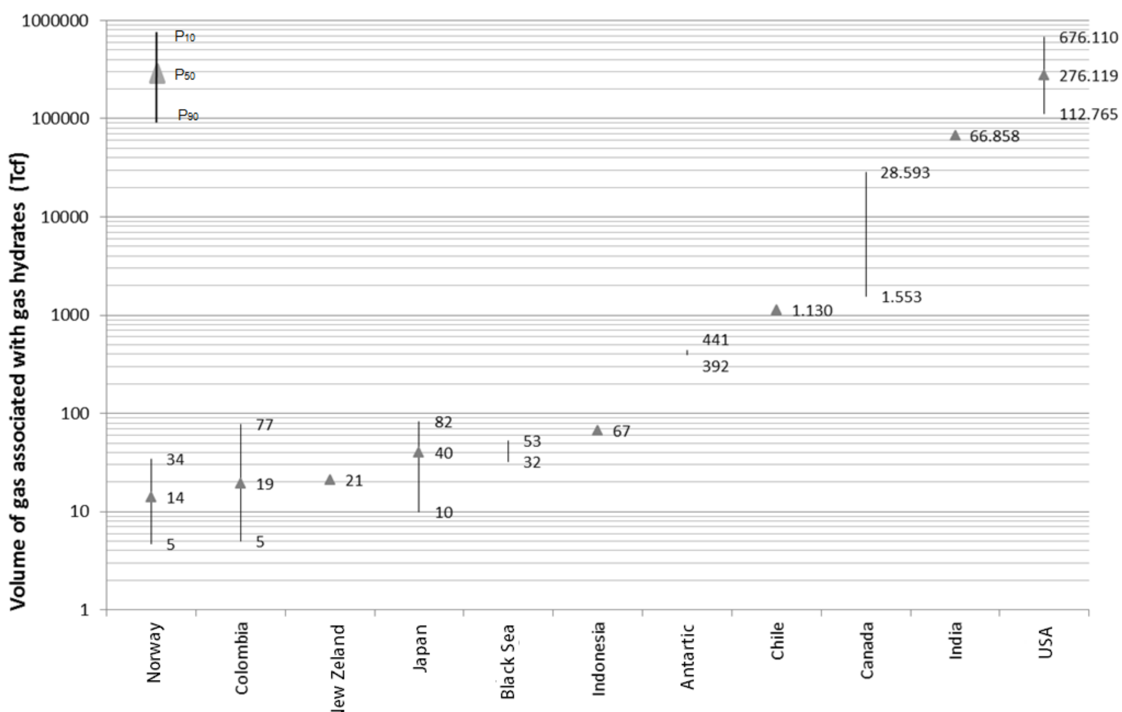

Figure 5-34. YTF gas hydrates in Colombia compared to estimated resources in other parts of the world changes Colombia's upper amenities.

5.4.6 Sensitivity analysis

The degree of influence or weighting of each random variable in equation 5-1 in calculating the potential for Colombian marine basins can be seen in Figure 5-35.

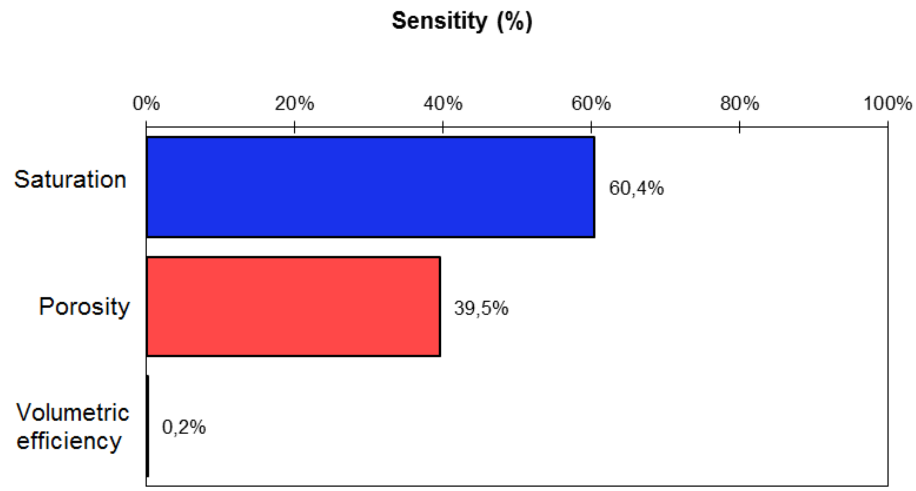

Figure 5-35. Sensitivity analysis for the variables used in estimating gas hydrates potential.

Sensitivity analysis for all the basins analysed suggested that gas hydrate exploration studies in Colombian basins should pay more attention to hydrate saturation (60.4%) and porosity (39.5%) than to the degree of volumetric yield.

5.5 Conclusions

- According to the calculations regarding gas hydrates' potential, the most prospective basin would be the Chocó offshore basin, followed by Guajira offshore and Sinú offshore basins;
- The results obtained in this work for the potential of methane gas in gas hydrates (75.63 – 4.89 Tcf) were considerably less than the values estimated by D. Little (2008), reaching 400 Tcf;
- Methane gas in gas hydrates was found in Colombian park system areas (1.4 Tcf, 0.35 Tcf and 0.09 Tcf for P10, P50 and P90, respectively);
- Potential for the Colombia and Deep Pacific basins was underestimated due to scarce seismic and well information being available for them; and
- There could be gas hydrates in the area bordering Los Cayos and the Colombia basins. Analysis of their potential requires more and pertinent information.

5.6 Bibliography

BP Global. (2011). Statistical Review 2011. Consulted on 30th June 2011 at, http://www.bp.com/statisticalreview

Camerlenghi, A. (2009). Hidratos de Metano: Cambio climatico, energia y riesgo submarino. IX Trobada de Professorat de Ciències de la Terra i del medi ambient del Batxillerat.

Collet, T. (1995). Gas hydrate resources of the United States. U.SG.S. Digital Data Series, 30.

Collet, T. (2002). Energy resource potential of natural gas hydrates. American Association of Petroleum Geologists' Bulletin, 86(11), 1971-1992.

D. Little, A. (2008). Evaluation of potential of unconventional energy resources in Colombia. Agencia Nacional de Hydrocarbons. Houston: Arthur D. Little Inc.

Dickens, G., & Quinby Hunt, M. (1994). Methane hydrates stability in seawater. Geophysical Research Letters, 21 (19), 2115-2118.

Jackson, B. (2004). Seismic evidence for gas hydrates in the North Makassar Basin, Indonesia. Petroleum Geoscience, 10(3), 227-238.

Kvenvolden, K. (1988). A primer on the geological occurrence of gas hydrate. Geological Society London Special Publications, 137, 9-30.

Kvenvolden, K. (1995). A review of the geochemistry of methane in natural gas hydrates. Organic Geochemistry, 23(11), 997-1008.

Lüdman, T., Wong, H., Konerding, P., Zillmer, M., Peterson, J., & Flüh, E. (2004). Heat flow and quantity of methane deduced from a gas hydrate field in the vecinity of the Dnieper Canyon, northwestern Black Sea. Geo-Marine Letters, 24(3), 182-193.

Majorowicz, J., & Osadetz, K. (2001). Gas hydrate distribution and volume in Canada. American Association of Petroleum Geologists' Bulletin, 85 (7), 1211-1230.

Master, C., & Root, D. (1991). Resource constraints in petroleum production potential. Science, 253(5016), 146-152.

Milkov, A., & Sassen, R. (2001). Estimate of gas hydrate resource, northwestern Gulf of Mexico continental slope. Marine Geology, 179(1), 71-83.

Minshull, T., Singh, S., & Westbrook, G. (1994). Seismic velocity structure at a gas hydrate reflector, offshore western Colombia, from full waveform inversion. Journal Of Geophysical Research, 99(B3), 4715-4734.

Morales, E. (2003). Methane hydrates in the Chilean continental margin. Electronic Journal of Biotechnology, 6(2), 80-84.

Pecher, I., Henry, S., Gorman, A., & Fohrmann, M. (2004). Gas hydrates on the Hikurangi and Fiordland margins, New Zealand. American Association of Petroleum Geologists Hedberg conference. Vancouver.

Popescu, I., De Marc, B., Leericolais, G., Nouze, H., Poort, J., & Panin, N. (2006). Multiple bottom-simulating reflections in the Black Sea: potential proxies of past climate conditions. Marine Geology, 227(3), 163-176.

Sain, K., & Gupta, H. (2009). Gas hydrates; a future major potential source of energy in India. Glimpses of Geoscience Research in India, 244-250.

Senger, K. (2010). First order estimation of in-place gas resources at the Nyegga gas hydrate prospect. Norwegian Sea Energies, 3, 2001-2026.

Sloan, E. (1990). Natural gas hydrate phase equilibria and kinetics; understanding the state of the art. Revue de l'Institut Français du Pétrole, 45(2), 245-266.

Sloan, E., & Carolyn, K. (1998). Clathrate hydrates of natural gases. New York: Dekke.

Tanahashi , M. (2011). Present satus of Japanese Methane Gas Hydrates Research and Development Program. Hydrate in Japan. CCOP Hydrate Workshop. Vietman.

Thakur, N., & Rajput, S. (2010). Exploration of Gas Hydrates. New York: Springer.

Yuan, T., Nahar, K., Chand, R., Hyndman, R., Spence, G., & Chapman, N. (1998). Marine gas hydrates: seismic observations of bottom-simulating reflectors off the West Coast of Canada and the East Coast of India. Geohorizons, 3(1), 1-11.

5.7 Appendixes

Digital files in the ANH'S Document Center:

- "Hidratos de gas Colombia.xlsx"
- "YTF_GasHydrates.zip"

6 COALBED METHANE

6.1 General comments

Methane gas is a constituent element of coal in high concentrations, depending on its composition and external factors such as temperature, pressure and geological conditions (Ortega, 2008). This kind of gas is called coalbed methane (CBM).

Extracting gas from coal requires dewatering a coal seam by lowering the pressure to enable the release of more mobile molecular species, including methane and ethane mixtures (and some traces of C_3, N_2 and CO_2).

6.1.1 Origin and formation

Coal originates from the decomposition of plants and vegetable material, such as leaves, wood and bark. It becomes accumulated in reducing environments, in swamps, lagoons and shallow marine areas. Carbon transformation and vegetable material enrichment occurs as time elapses, accompanied by a rapid burial rate leading to layers being formed having high organic content. Overlying levels must have sufficiently low porosity and permeability to maintain a proper anaerobic environment and continue carbonisation. It should be stressed that more than ten meters of silt coal are needed to produce a one-meter-thick coal layer.

6.1.2 Types of coal

Several classifications of coal are related to the degree of carbonisation or maturation of the source vegetable material, depending on the type of organic matter, age, depth, pressure, temperature and geological conditions in the basin where it has been formed. Coal and peat are the carbon forms having the lowest maturation values and little alteration of parental vegetal material; lignite and anthracite are coal forms having greater evolution.

The category of coal is measured in terms of physical and chemical parameters, such as volatile matter, fixed carbon, ash, humidity, calorific value and sulphur content. The higher the grade/rank, the greater the fixed carbon content and calorific value whilst natural humidity and the amount of volatile matter becomes reduced. Figure 6-1 illustrates the classification of coal based on rank and chemical properties (Stach, 1982).

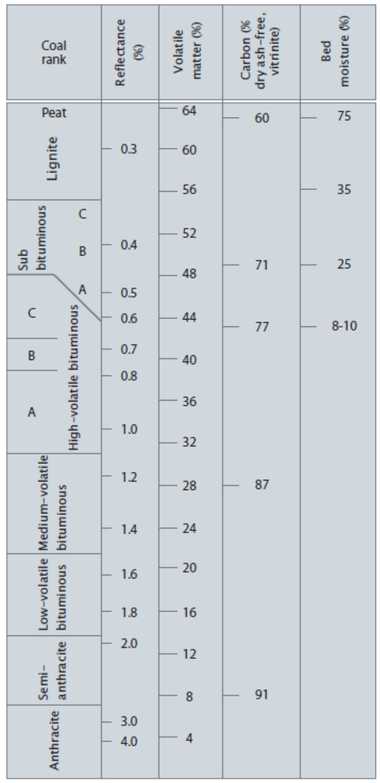

Figure 5 1. Classification of coal based on ranks and chemical properties such as vitrinite reflectance percentage, volatile matter, ash and humidity, taken from (Stach, 1982).

6.1.3 Coalbed methane (CBM) deposits

Gas in coalbed methane (CBM) deposits is stored in the micropores and internal discontinuity planes in coal. Two porosity systems can be distinguished:

- Primary porosity is that which is developed or originates at the moment of strata formation and consists of just the matrix's porous space. It is able to absorb a large amount of gas but contributes very little towards permeability; and
- Secondary porosity or that caused by natural fractures, cracks and fissures called cleats is that contributing most to permeability (Figure 6-2).

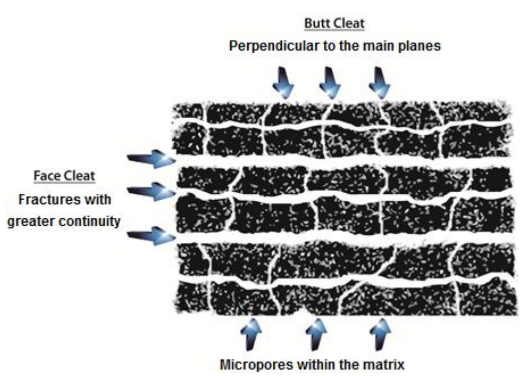

Figure 6-2. Diagram of coal matrix, micropores and the natural fracture system.

6.1.4 CBM around the world

More than 40 countries have investigated resources of CBM, but commercial projects have only been developed in Australia, Canada, China and India. Estimated CBM resources around the world are greater than 9,000 Tcf (Table 6-1).

Country	Coal (10^9 ton)	CBM (Tcf)
Russia	6,500	600 – 4,000
China	4,000	1,060 – 1,240
USA	3,970	400
Canada	7,000	200 – 2,700
Australia	1,700	300 - 500
Germany	320	100
England	190	60
Kazakhstan	170	40
Poland	160	100
India	160	30
South Africa	150	30
The Ukraine	140	60

Table 6-1. CBM reserves around the world, taken from Tonnsen & Miskimins (2010).

6.1.5 Coal in Colombia

The main characteristics of Colombian coal are given below regarding its distribution, composition and reserves as reference point in evaluating the CBM potential. A map of Colombian coal-bearing provinces is given in Appendix 6-1.

6.1.5.1 Colombian coal-bearing provinces

Coal is evident throughout Colombia, from the sandy Guajira in the north to Leticia in the Amazonian region in the south. Variation in its properties has led to 12 provinces or coal-bearing areas being differentiated, evaluated according to the amount of knowledge and geological conditions regarding mines and outcrops (INGEOMINAS, 2004). Figure 6-3 and Table 6-2 give a summary of Colombia's coal-bearing provinces.

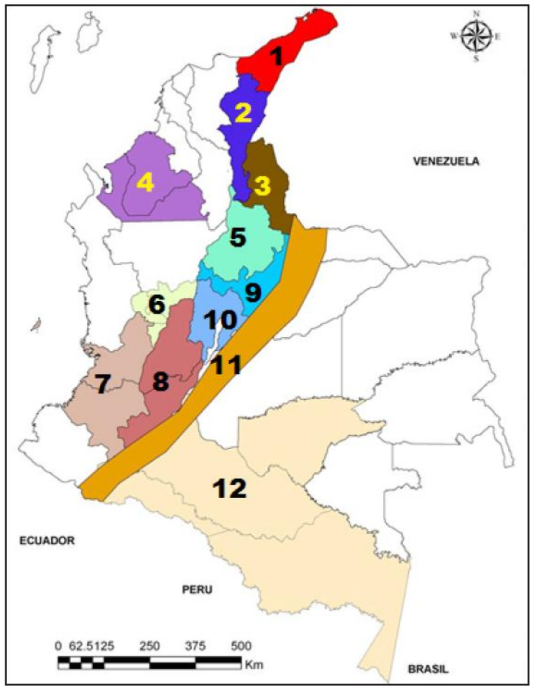

Figure 6-3. Colombian coal-bearing provinces, modified from (INGEOMINAS, 2004): 1. Guajira; 2. Cesar; 3. Norte de Santander; 4. Cordoba – Norte de Antioquia; 5. Santander; 6. Antiguo Caldas – Antioquia; 7. Valle del Cauca – Cauca; 8. Huila – Tolima; 9. Boyacá; 10. Cundinamarca; 11. Borde Llanero; 12. Llanura Amazónica.

Each region or province is divided into areas, sectors, blocks and coal mines. Mining resources' classification categories are based on geological certainty and their degree of technical economic safety (INGEOMINAS, 2004). The physical and chemical properties of coal (humidity (%), Cz - ash (%) MV - volatile matter (%), CF - fixed carbon, St - sulphur content and PC - calorific power) described in Table 6-2 can be related to the coal classification proposed by Stach (1982) shown in Figure 6-1.

Part of Colombia	Area	Sector	Humidity (%)	Cz (%)	MV (%)	CF (%)	St (%)	PC (BTU/lb)
La Guajira	Cerrejón Norte		11.94	6.94	35.92	45.2	0.43	11,586
	Cerrejón Central							
	Cerrejón Sur							
Cesar	La Loma	La Loma syncline	11.39	10.32	33.37	66.63	0.72	10,867
		El Boquerón	10.29	5.61	36.79	47.31	0.59	11,616
		El Descanso Sur						
	La Jagua de Ibirico	La Jagua	7.14	5.32	35.7	51.84	0.62	12,606
		Cerro Largo						
Córdoba-Norte de Antioquia	Alto San Jorge	San Pedro Sur	14.49	9.24	37.55	38.73	1.31	9,280
		San Pedro Norte	14.49	9.24	37.55	38.73	1.31	9,280
		Alto San Jorge	14.49	9.24	37.55	38.73	1.31	9,280
Antioquia-Antiguo Caldas	Venecia-Fredonia		11.64	8.11	40.06	40.2	0.48	10,426
	Amagá-Angelópolis	Amagá-Nechí	13.16	11.96	36.69	38.18	0.55	9,682
		Angelópolis						
	Venecia-Bolombolo	Rincón Santo	9.84	11.1	38.45	40.61	1.04	10,090
		Bolombolo	8.49	7.9	37.77	45.91	1.09	11,113
	Titiribí	Corcovado	7.25	7.92	37.99	46.84	0.72	11,767
		El Balsal						
	Río Sucio-Quinchía		4.08	15.56	31.75	48.61	1.8	10,713
	Aranzazu-Santágueda	Aranzazu	22.22	28.69	30.33	18.76	0.67	5,451
		Santágueda	19.03	25.05	37.32	18.6	0.43	6,230
Valle del Cauca-	Yumbo-Asnazú	Golondrinas-Río	2.69	22.38	28.15	46.79	2.85	

Cauca		Cañaveralejo						11,088
		Cañaveralejo-Río Pance						
		Río Pance-Río Guachinte						
		Río Guachinte-Río Asnazú						
	Río Dinde-Quebrada Honda		2.83	20.63	36.72	39.84	4.02	11,138
	Mosquera-El Hoyo	Pedregosa-Mosquera	8.11	16.3	35.18	40.42	1.42	
		Limoncito-Yeguas						
		El Vergel						10,058
		Quilcacé-El Hoyo						
Cundinamarca	Jerusalén-Guataquí		5.19	5.34	39.09	50.38	0.58	13,044
	Guaduas-Caparrapí	Caparrapí	4.12	5.61	22.43	67.83	0.59	12,829
		Guaduas						
	Guatavita-Sesquilé-Chocóntá	Suesca-Chocóntá	1.98	11.23	34.88	51.91	0.91	12,682
		Guatavita						
	Tabio-Río Frío-Carmen de Campa	Carmen de Campa	3.42	12.67	20.8	63.10	1.53	13,041
		Tabio-Río Frío	4.12	9.76	18.01	68.11	0.93	13,390
	Checua-Lenguazaque	Cogua-Sutatausa-Guachctá	3.66	9.46	26.8	60.07	0.80	13,433
		Lenguazaque-Cucunubá-Nemocón	4.67	10.62	33.85	50.86	1.06	12,718
	Suesca-Albarracín		3.92	10.43	33.53	52.12	0.69	12,738
	Zipaquirá-Neusa	Zipaquirá-Embalse del Neusa	1.04	14.42	24.33	60.21	1.38	12,993
		Embalse del Neusa-Vereda Lagunitas						
	Páramo de la Bolsa-Machetá		4.42	14.21	35.7	45.67	1.04	11,309
	Checua-Lenguazaque		3.56	10.00	25.19	61.25	0.80	13,439
	Suesca-Albarracín		4.69	12.18	33.71	49.42	1.07	12,420
Boyacá	Tunja-Paipa-Duitama		9.48	11.4	38.03	41.09	1.53	11,268
	Sogamoso-Jericó		4.29	9.57	30.19	55.96	1.23	13,099
	Betania		1.47	8.36	30.94	59.25	1.00	13,859
	Úmbita-Laguna de Tota		5.75	13.10	38.34	42.8	1.21	11,699
Santander	San Luis	Western flank	2.70	25.95	28.11	43.23	1.76	10,913
			1.63	7.65	33.38	57.33	1.37	13,994
		Eastern flank	1.18	18.72	30.48	49.62	2.01	12,284
			1.18	10.09	29.05	59.67	2.15	13,893
	Cimitarra Sur		4.61	4.61	29.77	61.01	0.62	13,021
	Capitanejo-San Miguel		6.33	7.51	19.00	67.16	0.93	11,782
	Miranda		1.81	14.47	15.13	68.59	3.46	12,803
	Molagavita		0.80	8.58	32.25	58.37	0.70	14,161
	Páramo del Almorzadero		5.18	4.71	14.23	75.88	0.75	12,889
	Chitagá		3.29	12.59	12.9	71.22	1.44	12,804
	Pamplona-Pamplonita	Pamplonita	2.96	9.97	36.15	50.92	1.34	13,199
		Pamplona						
	Herrán-Toledo	Toledo	2.31	7.46	26.99	63.24	0.83	14,120
		Herrán						
		North						
	Salazar	Centre	3.76	9.46	36.81	49.96	0.62	12,762
		South						
Norte de Santander	Tasajero	East	2.84	10.17	34.82	52.18	0.85	13,326
		West	2.56	7.65	33.67	56.12	0.85	13,925
		South	2.42	17.10	34.59	45.89	0.89	12,291
	Zulia-Chinácota	Zulia Sur	3.36	11.90	35.29	49.45	1.27	12,967
		Santiago	2.71	5.95	30.55	60.80	0.71	14,153
			8.33	17.06	28.67	47.33	0.62	9,911
		San Cayetano	2.02	12.12	26.66	59.20	1.43	13,324
			2.17	18.05	36.61	43.17	0.78	11,410
		San Pedro	2.53	11.30	35.63	50.54	0.81	13,290
			2.69	14.88	38.49	43.94	0.83	12,436
		Villa del Rosario	2.74	7.50	36.70	53.06	0.70	13,588
	Catatumbo	Zulia Norte-Sardinata	3.67	9.18	37.57	49.59	0.95	12,602
		El Carmen	4.31	8.64	39.17	47.88	0.95	12,316
Llanura Amazónica	Leticia		10.39	30.89	36.09	22.63	3.67	6,662

Table 6-2. Colombian coal-bearing provinces with their classification into areas and sectors, Key: Cz- ash (%), MV - volatile material (%), CF fixed carbon, St – sulphur content and PC – calorific power, modified from (INGEOMINAS, 2004).

6.1.5.2 Geology

Chronostratigraphically, there is a broad range of ages within which the most significant accumulations of coal developed: Maastrichtian-Upper Oligocene, Albian-Cenomanian and Cretaceous (INGEOMINAS, 2004). Table 6-3 gives a summary of the main coal-bearing formations in Colombia.

Formation	Age	Area
Cerrejón	Eocene	La Guajira
Los Cuervos	Paleocene - Lower Eocene	El Cesar, Norte de Santander and western Santander
Guaduas	Upper Maastrichtian - Paleocene	Cundinamarca and Boyacá
Umir	Campanian - Maastrichtian	Western Cundinamarca, Boyacá and Santander
Cerrito	Miocene - Pliocene	Córdoba and northern Antioquia
Amagá	Upper Oligocene - Lower Miocene	Caldas, Antioquia and Córdoba
Guachinte and Ferreira	Eocene - Oligocene	Valle del Cauca and Cauca
Floresanto and Maralú	Oligocene - Lower Miocene	Antioquian Urabá
Ciénaga de Oro	Oligocene	Córdoba
Tarazá	Oligocene	Northern Antioquia
Pepino – the middle	Oligocene	Putumayo
Carbonera	Upper Eocene - Lower to Middle Oligocene	Norte de Santander
San Fernando	Upper Eocene - Lower Oligocene	The fringe of the Eastern Llanos
Margua	Middle to Upper Eocene	The fringe of the Eastern Llanos
Socha	Paleocene	Eastern Boyacá
Clays of El Limbo and Limbo	Paleocene – Middle Eocene	The fringe of the Eastern Llanos
Catatumbo and Mito Juan	Upper Maastrichtian	Santander and Norte de Santander
Grupo Palmichal	Upper Maastrichtian - Upper Paleocene	The fringe of the Eastern Llanos
Seca	Maastrichtian	Southern and western Cundinamarca
Córdoba	Maastrichtian	Eastern Cundinamarca and south-eastern Boyacá
Chipaque	Cenomanian	Localities in Cundinamarca
Une	Albian	Meta and Boyacá
Caballos	Albian	Huila and Tolima

Table 6-3. The most important coal-bearing units in Colombia (INGEOMINAS, 2004).

6.1.5.3 Coal reserves and resources

Table 6-4 gives measured, indicated, inferred and hypothetical resources and reserves and their potential for each coal-bearing area in Colombia.

Part of Colombia	Area	Resources plus reserves			Resources	Potential (YTF)
		Measured	Indicated	Inferred	Hypothetical	
La Guajira	Cerrejón Norte	3,000.00				3,000.00
	Cerrejón Central	670				670.00
	Cerrejón Sur	263.3	448.86	127.50	27.16	866.82
	Total	3,933.30	448.86	127.50	27.16	4,536.82
Cesar	La Loma	1,777.10	1,563.98	1,963.18	993.50	6,297.76
	La Jagua de Ibirico	258.30				258.30
	Total	2,035.40	1,563.98	1,963.18	993.50	6,556.06
Córdoba - Norte de Antioquia	Alto San Jorge	381.00	341.00			722.00
	Total	381.00	341.00			722.00
Antioquia-Antiguo Caldas	Venecia-Fredonia	8.94	40.14	16.87		65.95
	Amagá-Angelópolis	11.84	63.64	92.33	25.38	193.19
	Venecia-Bolombolo	57.95	84.80	18.75		161.50
	Titiribí	11.33	37.25	4.45	1.07	54.10
	Total	90.06	225.83	132.40	26.45	474.74
Valle del Cauca - Cauca	Yumbo-Asnazú	30.7	56.42	47.49	10.98	145.59
	Río Dinde-Quebrada Honda	4.37	16.66	19.69		40.72
	Mosquera-El Hoyo	6.38	19.06	30.72		56.16
	Total	41.45	92.14	97.9	10.98	242.47
Cundinamarca	Jerusalen-Guataquí	1.81	5.73	5.28	3.23	16.05
	Guaduas-Caparrapí	6.76	32.68	21.36	0.91	61.71

	San Francisco-Subachoque-La Pradera	11.35	48.2	60.89	6.46	126.9
	Guatavita-Sesquilé-Chocóntá	21.9	64.31	106.88	10.14	203.23
	Tabio-Río Frío-Carmen de Carupa	19.43	55.82	54.84	24.78	154.87
	Checua- Lenguazaque	140.42	345.44	210.66	16.25	712.77
	Suesca-Albarracín	32.92	87.71	68.90		189.53
	Zipaquirá-Neusa	1.64	4.96	10.41		17.01
	Total	236.23	644.85	539.22	61.77	1,482.07
Boyacá	Checua-1enguazaque	35.69	129.87	115.84		281.4
	Suesca-Albarracín	7.81	43.29	106.26		157.36
	Tunja-Paipa-Duitama	24.03	97.21	171.41		292.65
	Sogamoso-Jericó	102.84	412.25	473.71		988.8
	Total	170.37	682.62	867.22		1,720.21
Santander	San Luis	56.08	108.64	123.44		288.16
	Capitanejo-San Miguel		18	1.43		19.43
	Miranda		5.49			5.49
	Molagavita		7.95			7.95
	Páramo del Almorzadero		118.24	24.37		142.61
	Total	56.08	258.32	149.24		463.64
Norte de Santander	Chitagá	0.66	1.98	7.4		10.04
	Mutiscua-Cácota	1.56	0.66	0.16		2.38
	Pamplona-Pamplonita	2.79	6.25	4.83		13.87
	Herrán-Toledo	4.78	14.63	9.17		28.58
	Salazar	7.71	15.5	5.8		29.01
	Tasajero	14.18	29.51	50.23		93.92
	Zulia-Chinácota	40.05	124.15	103.2		267.4
	Catatumbo	47.96	121.66	179.98		349.59
	Total	119.69	314.34	360.77		794.79
Total		**7,063.58**	**4,571.94**	**4,237.43**	**1,119.86**	**16,992**

Table 6-4. Coal resources and reserves in Colombia in millions of tons (INGEOMINAS, 2004).

6.2 Data and hypotheses

6.2.1 International data

The set of compiled data attached as part of this document in a file labelled “Appendix 6-2 – CBM database Alberta - Canada.xlsx” consists of 1,511 samples from deposits distributed throughout the coal-bearing basins of Alberta in Canada. This information has been used for estimating the distribution of in-situ gas content (G_C).

6.2.2 National data

The compiled set of data attached as part of this document in a file labelled “Appendix – Colombian CBM database.xlsx” (Appendix 6-3) contains the information used for calculating the CBM potential, thickness, density and mapped coal-bearing areas, the results of each statistical analysis for areas having little or no information available and the information used for estimating the distributions of in-situ gas (G_C) content.

6.2.3 Hypotheses

Effective CBM potential in Colombian basins was evaluated in line with the following hypotheses:

6.2.3.1 Hypotheses 1

Areas having CBM in Colombian sedimentary basins are represented by areas identified on the available cartography regarding coal (i.e. INGEOMINAS, 2004).

6.2.3.2 Hypotheses 2

Values regarding thickness, density and other properties in all coal-bearing provinces are considered to be representative of the values expected for the sedimentary basins in which they are located.

6.2.3.3 Hypotheses 3

Gas concentration (Gc) for areas having effective CBM potential per basin in Colombia may be estimated in line with some of the following scenarios:

- Evaluation Scenario 1: pattern for coal-bearing basins in Alberta, Canada
- Evaluation Scenario 2: G_C pattern expected for Colombian basins (UPTC, 2010)
- Evaluation Scenario 3: G_C pattern obtained from pithead field data (UPTC, 2010).

6.3 Methodology

Coalbed methane potential in Colombia was estimated by means of Equation 6-1:

$$G = 1 \cdot 10^{-9} * A * h * \rho_b * G_c \tag{6-1}$$

G: in situ gas (Bcf)

A: drainage area (m^2)

h: deposit thickness (m)

ρ_b: apparent average coal density (g/cm^3)

G_c: gas concentration (ft^3/ton)

The following steps were followed when estimating CBM for all Colombian sedimentary basins:

- Outcrop areas were extracted from the polygons representing coal-bearing formations of interest. These polygons were contoured showing mining conditions, geological and/or structural contacts, changes of thickness, geological certainty and local characteristics such as municipal limits, rural areas or mining blocks of relevance for a particular sector:
  - ✓ Polygons were drawn from Colombian Geological Service information (INGEOMINAS, 2004), digitalising all coal manifestations recorded in Colombian coal-bearing areas, regardless of their condition regarding other study variables in Equation 6-1;
  - ✓ The polygons were discretised by geological unit, province, area and coal-bearing block for each basin.

- Coal-bearing levels' thickness and density were obtained from stratigraphic columns, levels reported in mines and data inferred regarding outcrops registered by INGEOMINAS (2004). Only coal-bearing levels of up to a maximum 300 m sequence thickness was established for evaluating the CBM resources:
  - ✓ Thickness and density were discretised regarding the polygons by geological unit, province, area and coal-bearing block for each basin;
  - ✓ Known data regarding density and thickness by block or province was statistically analysed. Values were assigned to non-producing areas having coal manifestations according to the analysis of producing areas;
  - ✓ A zero thickness value was assigned for mapped areas regarding formations considered as being coal-bearing but for which no coal manifestations had been reported;
  - ✓ A database was produced with the information from the thickness and density polygons for the areas having coal manifestations for Colombia (Appendix 6-3);
  - ✓ Distributions were found for G_C from the proposed hypotheses describing three different scenarios; and
  - ✓ Monte Carlo simulations were then used with equation 6-1 for calculating in situ gas by assuming thickness, area, density as constants and gas concentration (G_C) as random values.
- CBM resources were then evaluated in all three proposed scenarios.

6.4 Results

Statistical analysis of some of the variables in equation 6-1 led to ascertaining their representativity and identifying the distribution of probability best fitting the data. Such tests led to ascertaining the degree of certainty (probability), i.e. whether there were greater deviations. Specific values were determined for such equation's other parameters and it was not necessary to associate any statistical distribution with their pattern.

6.4.1 Drainage area

The study took all the areas reported as having cartographic information available for coal into account into account. Table 6-5 gives the values considered per basin.

Basin	Area (km²)
Amagá	159.39
Non-prospective areas	2,811.15
Caguán - Putumayo	1,517.23
Catatumbo	793.09
Cauca - Patía,	279.12
Cesar - Ranchería	499.39
The Eastern Cordillera	3,434.02
Guajira	17.42
The Eastern Llanos	188.35
Sinú - San Jacinto,	4,962.37
The Lower Magdalena Valley	938.66
The Middle Magdalena Valley	1,525.13
The Upper Magdalena Valley	585.96
Vaupés Amazonas	5,854.03

Table 6-5. Coal-bearing areas per basin. Some coal-bearing areas were found which were outside the limits defined by ANH for Colombian basins; these were located in non-prospective areas according to ANH's definition for such areas.

6.4.2 Deposit thickness

The thickness considered in each polygon (contoured by geological unit, province, area, and coal-bearing block for each basin) is given in the file attached as Appendix 6-3. Thickness could be considered as being a deterministic variable from such information. Distribution functions were defined from the most genetically apt data in areas having cartographic information but lacking thickness referents. Table 6-6 gives the results of the statistical analysis for this variable.

Estimated parameters						Goodness-of-fit test			
$\hat{x}$	Confidence interval		$\hat{y}$	Confidence interval		Null hypothesis	P	Statistical value	G.L
0.84	0.73	0.95	1.65	1.58	1.74	Was not rejected	M.B.	12.6	0

Table 6-6. Lognormal distribution fit parameters and goodness-of-fit test results applied to the thickness data used in estimating CBM. Estimated parameters $\hat{x}$ and $\hat{y}$ are lognormal distribution regarding the mean and standard deviation, respectively. M.B refers to very low probability of the null hypothesis being accepted or rejected.

6.4.3 Average apparent density of coal

The same as thickness values were applied in equation 6-1, density values were applied in each polygon where the value was reported for this parameter. This data also led to identifying a distribution function which could then be used for areas lacking density data. Table 6-7 gives the results for the best fit and pertinent goodness-of-fit tests.

Estimated parameters						Goodness-of-fit test			
$\hat{x}$	Confidence interval		$\hat{y}$	Confidence interval		Null hypothesis	P	Statistical value	G.L
0.29	0.29	0.30	0.04	0.04	0.04	Was not rejected	M.B.	51.6	0

Table 6-7. Lognormal distribution fit parameters and goodness-of-fit test results applied to the density data used in estimating CBM.

Estimated thickness and density distributions were thus used for the Eastern Llanos, Vaupés in the Amazonas and Caguán in Putumayo basins and for some blocks in the Eastern Cordillera and the Upper Magdalena Valley.

6.4.4 Gas concentration (Gc)

6.4.4.1 Scenario 1

G_C was estimated by correlating information regarding coal-bearing basins in Alberta, Canada (Appendix 6-2), considering their similarity with Colombian basins. A gamma-type distribution gave the best fit according to statistical analysis (Table 6-8).

Estimated parameters						Goodness-of-fit test			
$\hat{x}$	Confidence interval		$\hat{y}$	Confidence interval		Null hypothesis	P	Statistical value	G.L
0.92	N/R	N/R	139.6	N/R	N/R	Was not rejected	M.B.	36.9	0

Table 6-8. . Gamma distribution fit parameters and goodness-of-fit test results applied to the gas concentration data used in estimating CBM in Scenario 1. Estimated $\hat{x}$ and $\hat{y}$ are Gamma distribution regarding form and scale parameters.

6.4.4.2 Scenario 2

The UPTC (2010) has proposed a range of G_C obtained by means of canister desorption tests, this also being supported by information from basins around the world and by estimates for producing methane from different types of coal. Such average range is moderate (60-100 ft^3/ton) and weights all Colombian coal at a maximum depth of 300 m (Figure 6-4). Table 6-9 gives some of the results which UPTC (2010) obtained for the samples analysed. A uniform G_C distribution was selected in this scenario according to the nature of the UPTC data (2010).

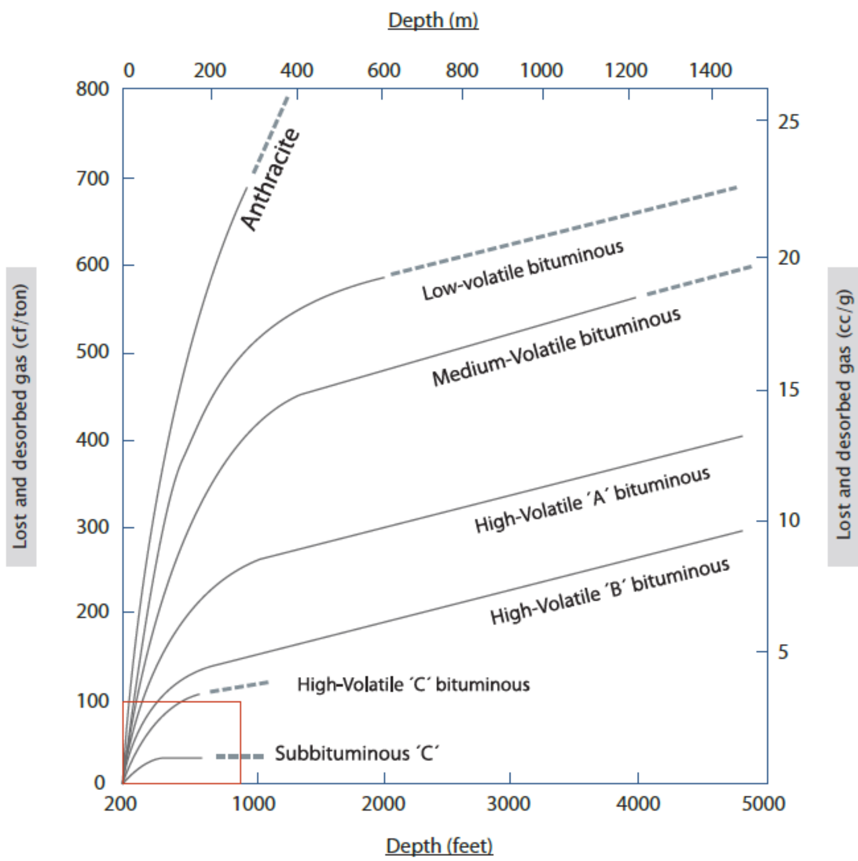

Figure 6-4. Estimating maximum methane production regarding type of coal and depth. Modified from Eddy et al. (1982).

Parameter	Range
Permeability	0.5 – 50.0mD
Porosity	5 – 12 %
Range of coal	High-volatile bituminous B – sub-bituminous A
Coal thickness x strata	30 cm – 2 m
Net thickness	6 – 8 m
Expected gas concentration	*60-100 foot³/ton*

Table 6-9. Values for some parameters analysed regarding pithead coal samples in Boyaca. (UPTC, 2010).

6.4.4.3 Scenario 3

The values reported by the UPTC (2010) were very low, being obtained from pithead samples. Such information could reflect altered strata as a consequence of mining activity in the exploitation front from which the samples were extracted.

A triangular Gc distribution having extreme and average data regarding pithead Gc pattern was estimated from these observations, associated with Gc pithead pattern (Table 5-10).

Parameter	Value (ft^3/ton)
Minimum	0.29
Most probable	1.90
Maximum	1.14

Table 6-10. Estimated parameters for gas concentration used in calculating the CBM. A triangular distribution was assumed.

6.4.5 CBM in Colombia

Using the Monte Carlo method for evaluating resources the coalbed methane (CBM) for Colombian basins, according to the assumed hypotheses and equation 6-1 in this document, led to the following results for the three scenarios considered here (Tables 6-11, 6-12 and 6-13. These have already been affected by the environmental factors listed in Table 2-1. Figure 6-5 gives the results for Scenario 2 and Figure 6-6 compares them to estimates for other countries.

Basin	P_{10} (Bcf)	P_{50} (Bcf)	P_{90} (Bcf)
Amagá	516	96	4
Non-prospective areas	2,557	480	24
Caguán - Putumayo	167	31	2
Catatumbo	682	128	7
Cauca - Patía	721	135	7
Cesar - Ranchería	17,713	3,296	161
The Eastern Cordillera	4,585	867	44
Guajira	832	156	8
The Eastern Llanos and Amazonía	573	107	5
Sinú - San Jacinto	33,287	6,339	313
The Lower Magdalena Valley	252	47	2
The Middle Magdalena Valley	4,448	830	42
The Upper Magdalena Valley	11,178	2,100	107
TOTAL	**77,511**	**14,612**	**725**

Table 6-11. CBM in Scenario 1.

Basin	P_{10} (Bcf)	P_{50} (Bcf)	P_{90} (Bcf)
Amagá	147	123	98
Non-prospective areas	721	599	480
Caguán - Putumayo	47	39	31
Catatumbo	193	161	128
Cauca - Patía	204	170	136
Cesar - Ranchería	4,994	4,160	3,327
The Eastern Cordillera	1,297	1,080	865
Guajira	233	195	156
The Eastern Llanos and Amazonía	162	135	108
Sinú - San Jacinto	9,499	7,913	6,332
The Lower Magdalena Valley	71	60	48
The Middle Magdalena Valley	1,259	1,049	840
The Upper Magdalena Valley	3,163	2,636	2,107
TOTAL	**21,990**	**18,319**	**14,655**

Table 6-12. CBM in Scenario 2.

Basin	P_{10}	P_{50}	P_{90}
	(Bcf)	(Bcf)	(Bcf)
Amagá	2.0	1.8	1.0
Non-prospective areas	12.1	8.8	5.2
Caguán - Putumayo	0.9	0.6	0.0
Catatumbo	2.8	2.4	0.9
Cauca - Patía	3.0	2.5	1.0
Cesar - Ranchería	82.0	60.7	35.0
The Eastern Cordillera	21.4	15.8	8.9
Guajira	3.9	2.8	2.0
The Eastern Llanos and Amazonía	2.3	2.0	1.5
Sinú - San Jacinto	156.1	115.5	67.3
The Lower Magdalena Valley	1.0	0.9	1.0
The Middle Magdalena Valley	21.0	15.3	9.0
The Upper Magdalena Valley	52.0	38.4	22.3
TOTAL	**360.6**	**267.4**	**155.1**

Table 6-13. CBM in Scenario 3.

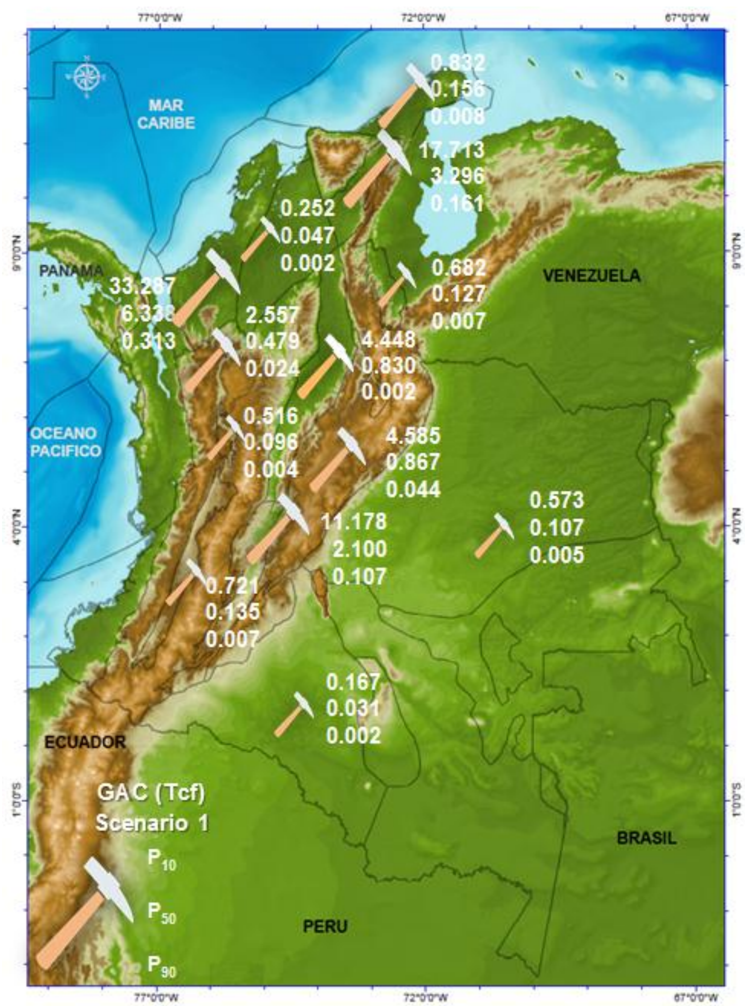

Figure 6-5. Map of CBM for Colombian basins in Scenario 1.

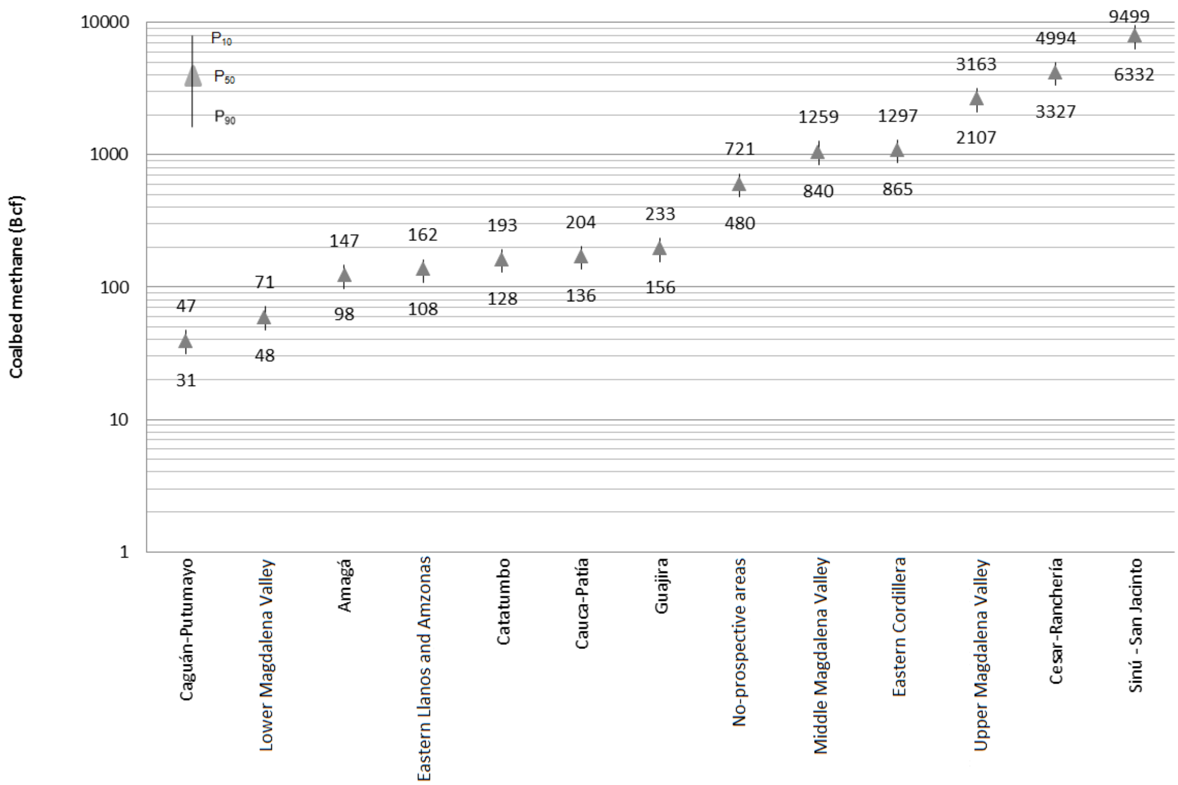

Figure 6-6. CBM for the Colombian basins in Scenario 1.

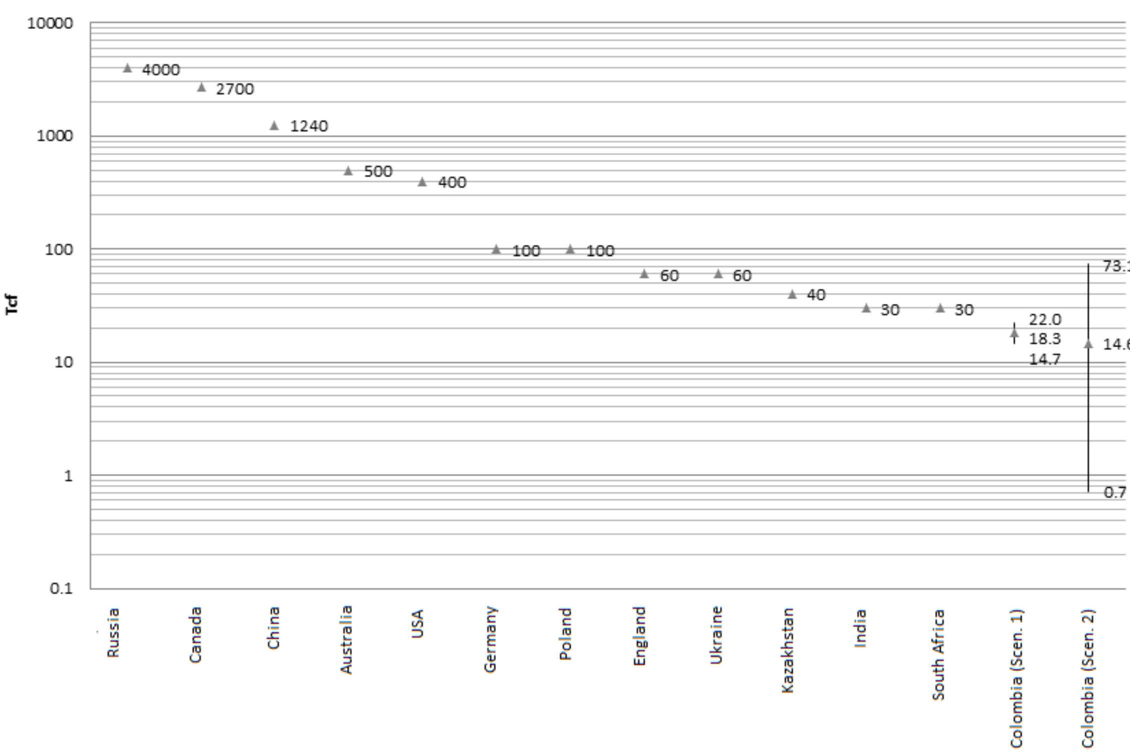

Figure 6-7. Comparing CBM in Colombia in the first two Scenarios with that for other countries.

6.5 Conclusions

- The San Jacinto basin in Sinú, Cesar - Ranchería, the Upper Magdalena Valley, The Eastern Cordillera, the Middle Magdalena Valley and the Guajira basins has the greatest resources of CBM;
- P_{50} values for the three scenarios were 18,319.0, 14,612.0 and 267.4 Bcf. The last value was most improbable given that the Gc values measured for coal mine exploitation underestimate resources CBM production. Such data, however, could be used as reference for industrial safety; and
- The CBM resources estimated in this work (14,612-18,319 Bcf) were comparable with values estimated by D. Little (2008); (17,800 Bcf).

6.6 Bibliography

Beaton, A. (2003). Production potential of coalbed methane resources in Alberta. Alberta Geological Survey, Alberta Energy and Utilities Board, Alberta.

Beaton, A., Pana, C., Chen, D., Wynne, D., & Langenberg, C. W. (2002). Coalbed methane potential of Upper Cretaceous - tertiary strata, Alberta Plains. Alberta Geological Survey, Alberta Energy and Utilities Board, Alberta.

INGEOMINAS. (2004). El carbón Colombiano: recursos, reservas y calidad. Bogota.

Ortega, J. (2008). Reservorios de gas asociado al cabon (CBM). Contacto SPE(30), 8-11.

Rottenfusser, B., Langenberg, W., Mandryk, G., Richardson, R., Fildes, B., Olic, J., et al. (2002). Regional evaluation of the coalbed methane potential in the plains and foothills of Alberta, stratigraphy and rank study (digital version). Alberta G. S., A. Energy and Utilities Board, Alberta.

Stach, E. (1982). Stach's Textbook of Coal Petrology. Berlin: Borntraeger.

Tonnsen, R. R., & Miskimins, J. L. (2010). A conventional look at an unconventional reservoir: coalbed methane production potential in deep environments. Search and Discoveries(80122), 5.

UPTC. (2010). Mediciones de gas metano asociado al carbón mediante pruebas de desorción con canister. Tunja: Universidad Pedagógica and Tecnológica de Colombia.

Wynne, D., & Beaton, A. (2003). Alberta Geological Survey. Visited on the 4th of March 2011: CBM - Coal Database for the Alberta Plains Area: http://www.ags.gov.ab.ca/publications/abstracts/DIG_2003_0001.html

6.7 Appendixes

Digital files in the ANH'S Document Center:

- ✓ "Áreas carboniferas por cuenca.klm"
- ✓ "Base de Datos GAC Alberta - Canadá.xlsx"
- ✓ "Base de Datos GAC Colombia.xlsx"

7 TAR SANDS

7.1 General comments

The organic material present in the subsoil may become submitted to alteration such as maturing or degradation; maturing involves its thermal transformation and degradation involves chemical changes produced by bacterial activity or washing by water (Chillingarian & Yen, 1978).

Maturing leads to an increase in saturated hydrocarbons (HC) and a reduction in NSO compounds (involving nitrogen, sulphur and oxygen). Degradation, on the other hand, leads to a reduction in saturated HC content, especially n-paraffin and increased NSO and asphaltenes (Figure 7-1).

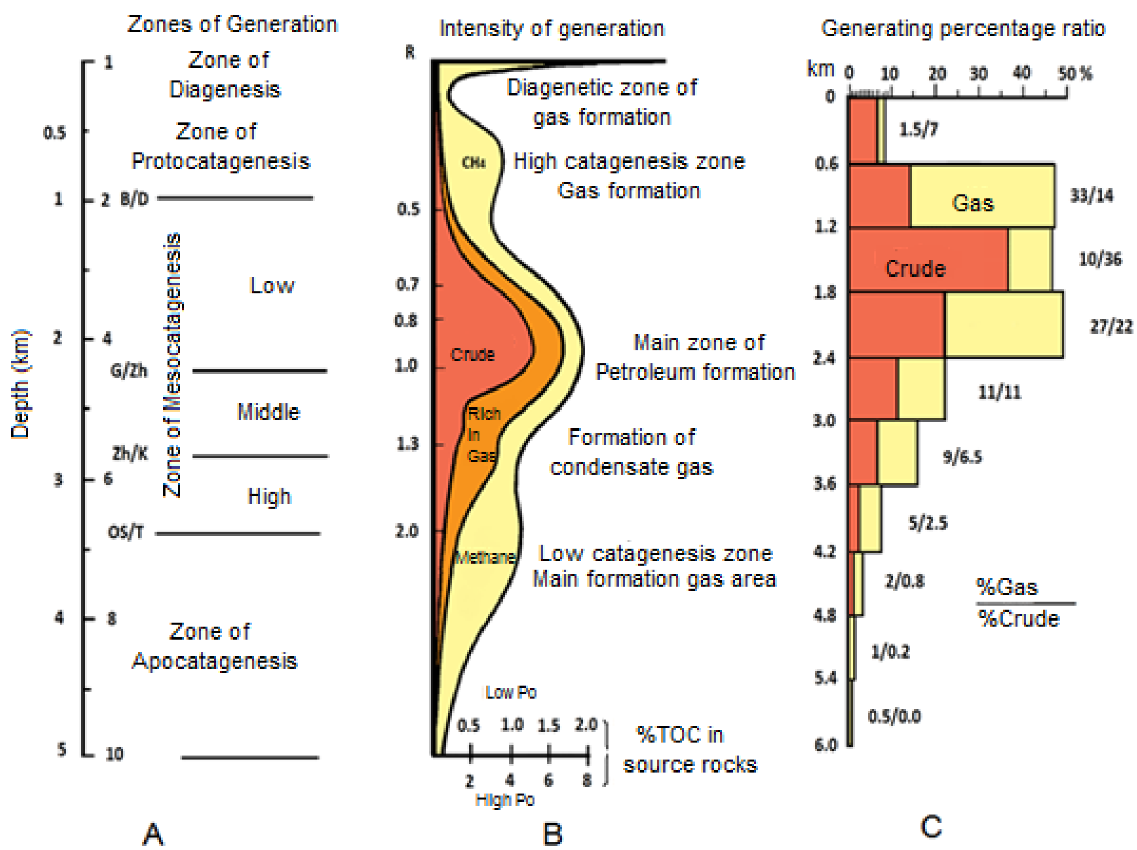

Figure 7-1. Diagram of gas and oil generation from organic material during lithogenesis. A) Shows production areas regarding depth; the letters in each area indicate the coal ranges used as catagenesis stage indicators (D – sub-bituminous to bituminous having abundant volatile matter, C, G – bituminous having abundant volatile matter, C to B, Zh – bituminous with abundant volatile matter, K –bituminous having intermediate volatile matter, OS – bituminous having intermediate to low-volatile matter, T – bituminous having low- anthracitic volatile matter). B) Gas and oil generation intensity regarding vitrinite reflectance where Po is source-rock from the H/C ratio. C) is the percent ratio for gas and oil generation regarding depth (modified from Chillingarian and Yen, 1978).

7.1.1 Bitumens

Organic material in bituminous substances has been considered to be residue from organic life occurring in the form of viscous impregnations in sand, limonites, shale and carbonates (dolomites and limestones). It could be said that kerogen (the insoluble organic material incorporated in source-rock sediments) consists of small units which are similar to asphaltic bitumens and thus lead to describing bitumens as low-mature (or extremely degraded) hydrocarbons.

Figure 7-2. Bitumen outcrop in the Middle Magdalena Valley, sector between Honda and Norcasia.

Bituminous substances vary from liquid petroleum to heavy crude oil, from viscous asphalts to solid asphaltites and asphaltic pyrobitumens. The types of organic compounds which can be extracted by solvents (especially when the solvent is carbon dioxide) are called bitumens (Figure 7-2). Actually, the amount of these bitumens is low compared to the large amount of insoluble kerogenic material which remains in the rock (Chillingarian & Yen, 1978).

Properties such as viscosity and n-paraffin (n-alkane) content can indicate whether the bitumen is a residue from low level thermal maturing or degradation.

7.1.2 Asphalts

Asphalt represents a compound material containing asphaltenes, waxes and resins. These can be converted into asphaltites or asphaltides during meteorisation and metamorphism. Deposits of this type as such are not the product of biodegradation; their formation is due to the incompatibility of two simultaneously produced liquid phases: light paraffin and asphaltene during thermal processes, such as normal maturing. Such phases cannot coexist and the asphalthenic phase becomes separated from the liquid phase (Chillingarian & Yen, 1978).

In terms of hydrocarbon type, conventional oil contains 30% paraffin, 50% naphthene, 15% aromatic and 5% asphalt hydrocarbons (Figure 7-3). Asphalts are also produced as direct residues from the distillation of conventional oil, thermal fragmentation and thinning or the oxidation of crude residues by exposure to the air (Chillingarian & Yen, 1978).

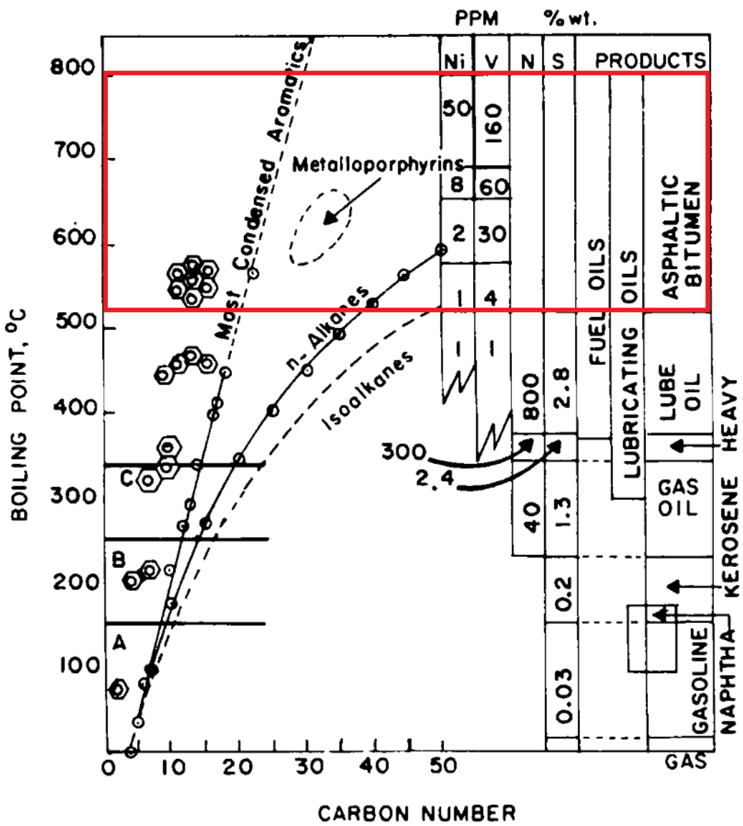

Figure 7-3. The ratio between boiling point and the number of carbons for pure hydrocarbons (left), and the composition of several petroleum fractions (right). Red square corresponds to area of Asphaltic bitumen. Modified from Chillingarian & Yen (1978).

7.1.3 Tar sands

The term tar sands (even though being inappropriate, since tar refers to a substance produced by destructive distillation) attempts to group bitumen-bearing sedimentary rocks (whether consolidated or not), consisting of highly viscous solids or semisolid hydrocarbons.

Even though tar sands' hydrocarbons are extremely viscous, their synthesis is relatively simple and leads to conventional light oil being obtained. Traditional processes can be modified in refineries for treating these types of substances.

7.1.4 Classifying tar sands

The classification of asphalts and bitumens' physical properties remains ambiguous. Viscosity is variable in each type of compound; the H/C ratio becomes reduced when ranging from natural gas and conventional oil to asphalts and then to kerogen, but this is not a weighty parameter for differentiating them. Environmental factors determine how this is done, whether by degradation (e.g. oxidation, bacteria, being washed by water) or maturing, allowing such ambiguity to be resolved. Figure 7-4 shows a conventional classification.

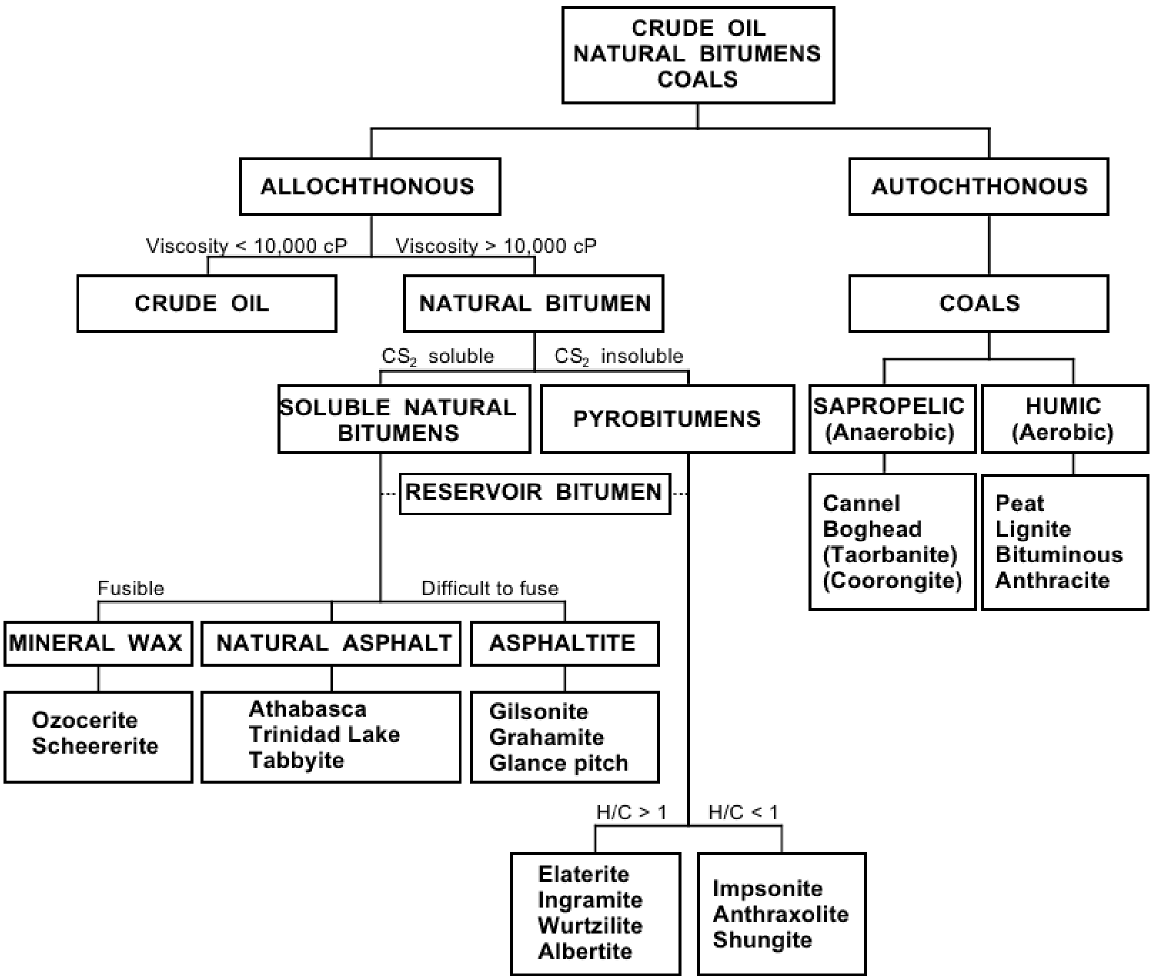

Figure 7-4. Classification of bituminous substances, from Meyer & Witt (1990).

Geologically, tar sands deposits may be broadly classified into two members: large updip deposits just below the surface of the water on the edge of foreland basins and small- and medium-sized deposits associated with loss of seal rock integrity. Both types are usually linked to faults and inconformity and can also be associated with oozes, springs, tufa deposits and mud volcanoes.

Tar sands deposits often occur on the surface or at depths just below the surface (<200 m) where hydrocarbon deposits come into contact with the atmosphere, surface aquifers or surface water (Chillingarian & Yen, 1978).

7.1.5 The nature of the impregnation

- Asphaltic arenites: are mainly presented in strata a few metres wide, having high clay or fine sand content. The amount of bituminous material in rock ranges from 3% to 15%, having penetration at temperatures above 15.6°C. The main deposits of this type are found in Canada (i.e. Athabasca) and Venezuela (Chillingarian & Yen, 1978);
- Asphalt having an appreciable amount of inert and organic materials: 36% mineral concentration and 54% bitumen, with 10% water and organic material. There are deposits of this type in Trinidad, off the coast of Venezuela (Chillingarian & Yen, 1978); and
- Asphaltites: naturally-occurring complex hydrocarbons, where bitumen percentage is around 90% (Chillingarian & Yen, 1978).

7.1.6 Tar sand accumulation in Colombia

During phases involving multiple hydrocarbon production and expulsion from basins, large volumes migrated towards their margins, leading to the accumulation of heavy crude oil at relatively superficial depths on the Eastern Llanos and in Putumayo. Large areas of tar sands (bitumens, asphalts, etc) were also formed as hydrocarbons migrated, reached the surface and became exposed to biodegradation and evaporation. Such deposits extend from Florencia all along the front of the mountains as far as San Vicente and cross La Macarena until reaching the southern part of the Llanos basin (Figures 7-5 and 7-6).

The manifestations are mainly found in the Eastern Cordillera area, in the Boyacá, Santander and Cundinamarca departments and their respective piedmont areas, in both the Upper and Middle Magdalena Valley, Putumayo (the Garzón massif) and parts of Meta (La Macarena) and Casanare.

Bitumen deposits are usually found in Cretaceous (Guadalupe, Guaduas, La Luna, Villeta, Une and Chipaque), Palaeogene and Neogene units (Picacho, Socha and Cacho) and some Quaternary deposits associated with active oozes and exhumed deposits where the light fraction escaped. Lithologically, they are found in medium-grained arenites to conglomeratic facies and, to a lesser extent, in siliceous limonites to carbon-bearing shale and schist. Table 7-1 shows some geochemical parameters regarding manifestations in Colombia.

	Tuta Boyaca	Velez Santander	Chaparral Tolima	San Jose Guaviare	Tado Chocó
Ash	84.44	5.01	0.55	N/R	7.26
Sulphur	0.51	0.75	3.2	0.49	N/R
Volatile material	7.76	12.31	N/R	N/R	46.77
Fixed carbon	N/R	80.72	N/R	N/R	44.9
Nickel	N/R	N/R	185	12.8	N/R
Vanadium	N/R	N/R	89	N/R	N/R
Iron	N/R	N/R	N/R	0.22	N/R

Table 7-1. Chemical parameters regarding some tar sands manifestations in Colombia, taken from INGEOMINAS reports (see associated bibliography). N/R not recorded.

Figure 7-5. Asphalt outcrop, La Cristal rural area - San José del Guaviare, taken from Duque (2002).

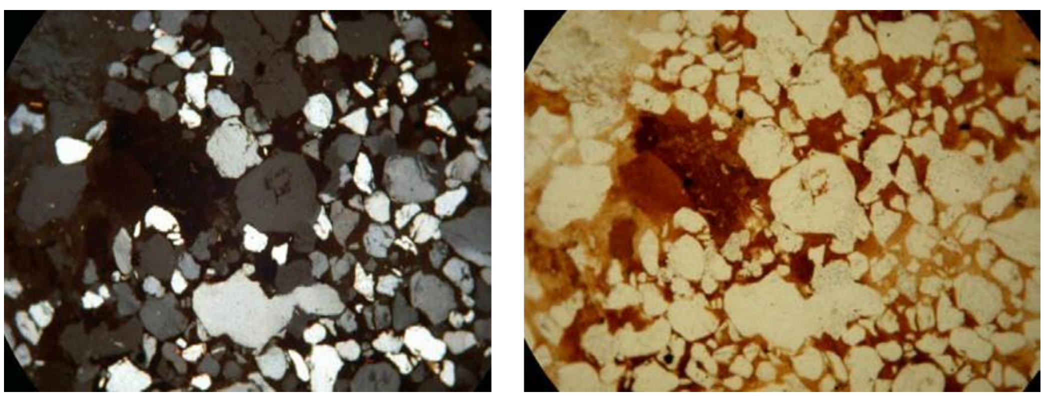

Figure 7-6. Thin sections of asphaltic sample from La Cristal rural area - San José del Guaviare. A. crossed Nicols (x 25) and B. parallel Nicols (x 25), taken from Duque (2002).

7.1.7 Extraction in Colombia

Information regarding bitumen exploitation has been available since the beginning of the 20th century. For example, 1928 reports mention an analysis of their quality in Boyacá and Cundinamarca (Grosse, 1928). Later studies dealt with the Colombian Cretaceous period and the inventory of manifestations. The Colombian Geological Service (Servicio Geológico Nacional) made a national mining inventory during the 1940s which identified and sampled occurrences in other departments (Instituto Geologico Nacional, 1948).

Currently, the Colombian Geology and Mining Institute (Instituto Colombiano de Geología and Minería - INGEOMINAS) has catalogued asphalts (Table 6-2), using the Official Classification of Minerals in Colombia (Colombian Ministry of Mines and Energy, 2003). Exploration and exploitation licences are granted according to the Mining Code and regulations laid down by the Ministry of Mines and Energy, the Ministry of the Environment and autonomous corporations monitoring the environmental impact of mining/farming techniques on each region.

Official classification of minerals (INGEOMINAS)			
Group	153 Sandstones, conglomerates, sands, boulders, gravels, crushed sandstone, split or crushed rock or stones, bitumen and natural asphalts		
Class	1533 Bitumen and natural asphalts		
Subclass	**1533000**	**1533001**	**153300**
Title	Bitumen and natural asphalt; asphaltites asphaltic and rocks.	Natural asphalt or asphaltites.	All other asphaltic rocks (except for subclass 2030).
Unit	ton	ton	ton
CIIU rev. 3 A.C.	1490		
Harmonised system	2714.90		
CIIU DANE		29091200	

Table 7-2. Official classification of minerals - bitumen and natural asphalt (Ministry of Mines and Energy, Sistema Nacional de Information Minero Colombiano-SIMCO, 2003).

7.1.8 Tar sand accumulations throughout the world

There are large deposits around the world; the main reserves are located in Canada (Athabasca) and Venezuela (Faja del Orinoco), each having reserves almost equal to the reserves of conventional crude in the rest of the world. Tar sand reserves could represent up to two thirds of crude from hydrocarbons, accounting for around 3.6 trillion barrels of recoverable oil compared to 1.75 trillion barrels in the world for conventional oil (Dyni, 2010). The map in Figure 7-7 and Table 7-3 show the main tar sand deposits in the world.

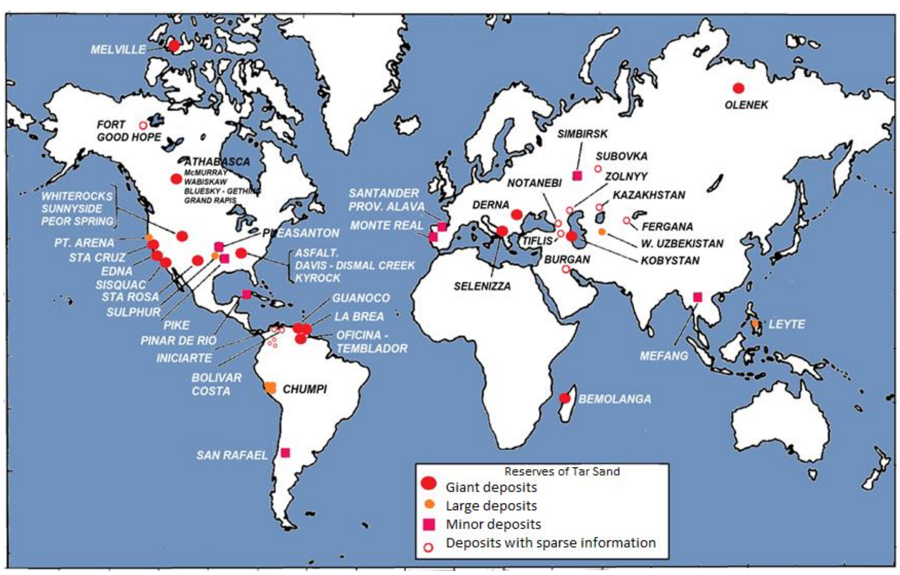

Figure 7-7. Main tar sand deposits around the world modified from Chillingarian & Yen (1978).

Country	Deposit	Reservoir rock age	Area	Thickness			Bitumen		
			(ha)	Sq. mi	ft	Average	Sat. (wt%)	°API 60°F	(%) Sulphur
Canada	McMurray - Wabiskaw, Alberta		2,326,942	9,000	0-300	175	...	...	...
	Bluesky - Gething, Alberta		485,623	1,875	0-400		...	...	...
	Grand Rapids, Alberta		445,154	1,625	400	280	...	...	...
	Total "Athabasca" *tar sands*	L. Cretaceous	3,237,485	12,500		150	2-18	10.5	4.5
	Melville Island N.W.T	Triassic	?	?	60-80		?-16	10	0.9 - 2.2
Eastern Venezuela	Oficina - Temblador tar belt	Oligocene	2,326,942	9,000	3-10			10	
Malagasy	Bemolanga	Triassic	38,850	150	80-300	100	10		0.7
U.S.A	Asphalt Ridge, Utah	Oligocene and U. Cretaceous	4,452	...	11-254 24-200	98 100	11	8.6 - 12	0,5
	Sunnyside, Utah	U. Eocene	13,881	...	10-350		9	10 - 12	0.5
Albania	Selenizza	Mio - Pliocene	2,147	8	33-330	50	8-14	4.6 - 13.2	6,1
U.S.A	Whiterocks, Utah	Jurassic	769	3	900-1,000		10	12	0,5
	Edna, California	Mio-Pliocene	2,669	10	0-1,200	250	9-16	13	4.2
	Peor Springs, Utah	U. Eocene	702	3	1-250	34	9		
Venezuela	Guanoco	Recent (alluvial)	405	2	2, 9	4	64	8	5.9
Trinidad	La Brea	U. Miocene	51	...	0-270	135	54	1 - 2	6.0 - 8.0
U.S.A	Santa Rosa, New Mexico	Triassic	1,874	7	0-100	20	4- 8		
	Sisquoc, California	U. Pliocene	71	...	0-185	85	14- 18	4 - 8	
	Asphalt, Kentucky	Pennsylvanian	2,833	11	5-36	15	8 - 10		
Rumania	Derna	Pliocene	186	...	6- 25		15-22		0.7
U.S.S.R	Cheildag, Kazakhstan	M. Miocene	33	...		200	5 - 13		
U.S.A	Davis - Dismal Creek, Kentucky	Pennsylvanian	769	3	10- 50	15	5		
	Santa Cruz, California	Miocene	486	2	5 - 50	11	10- 12		
	Kyrock, Kentucky	Pennsylvanian	364	...	15- 40	20	6- 8		

Table 7-3. Main tar sands deposits around the world, taken from Chillingarian & Yen (1978).

7.2 Data and hypotheses

7.2.1 International database

The set of compiled data appended as part of this document in a file labelled Appendix 7-1 contains information regarding different oil sands deposits in Alberta Canada. The data contain information about wells, cores, lithological, stratigraphical and geochemical analysis as well as forms of exploration and exploitation of the resource in this region. Some of this database's contents were used when estimating tar sands potential in Colombia for establishing a comparative reference framework.

7.2.2 National (Colombian) database

The set of data so compiled appended as part of this document in a file labelled Appendix 7-2 contains the information used for calculating weighting factors per resource scenario and evaluation category, that used for evaluating the tar sands areas, the data used for estimating bitumen, thickness, density and content distribution and the results for each test of goodness of fit and correlations.

The information about tar sand occurrences in Colombia was obtained from three sources:

- The Colombian Geological Atlas (INGEOMINAS, 2007) and Mining Land Registry information concerning mining titles and requests up to 2008, as well as publications regarding mining studies, manifestations, occurrences and inventories in Colombia;
- Undergraduate theses from the Universidad Nacional de Colombia and other universities associated with asphalt manifestations in Colombia; and
- The ANH Seeps Inventory, as well as information from the Colombian Geochemical Atlas (Agencia Nacional de Hidrocarburos, 2010).

7.2.3 Hypotheses

All this information was sifted for identifying representative areas having asphalt and bitumen manifestations which were considered as evidence of areas having YTF tar sands. A weighting factor was then applied to these areas thereby reducing uncertainty regarding the effective presence of tar sands in line with the following hypotheses.

7.2.3.1 Hypothesis 1

The control points associated with tar sand manifestations, derived from available information (INGEOMINAS, ANH, Universities, etc), becomes a factor representing effective tar sands potential in Colombia; and

7.2.3.2 Hypothesis 2

Areas of representativity are derived from control points from a system for classifying resources and reserves as being either identified (measured 0-250 m, indicated 250-750 m and inferred 750–2,250 m) or tar sands resources (hypothetical 2,250-5,000 m). Figure 7-8 illustrates the scenarios which had to be evaluated;

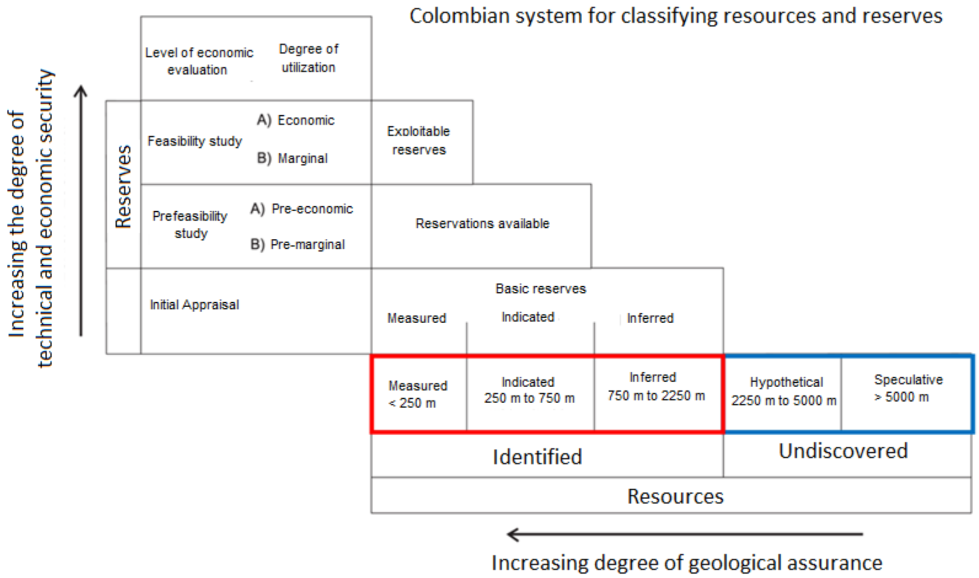

Figure 7-8. System for classifying resources and reserves (ECOCARBON, 1995).

7.2.3.3 Hypothesis 3

The thickness, density and bitumen content values for tar sands units in Colombia have a pattern which fits a statistical distribution supported by data regarding manifestations throughout Colombia (Figure 7-9). Such distribution is shown in the digital file in Appendix 7-2.

7.2.3.4 Hypothesis 4

A ratio between a particular basin's total asphalt area and its total area may be defined from the available information regarding tar sand occurrences; this ratio will lead to defining the area of the resource in on-shore (continental) basins lacking tar sands information. Figure 7-9 illustrates this hypothesis.

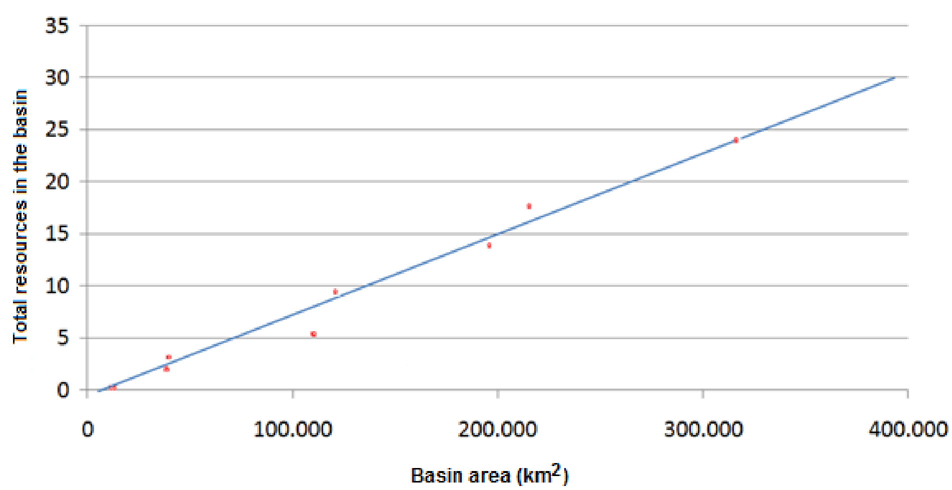

Figure 7-9. The graph shows the ratio between each basin's area regarding a specific resource's total area (measured, indicated, inferred and hypothetical) for a particular basin (red dots), determined from central tendency (blue line).

7.3 Methodology

The following equation was used for evaluating the tar sands potential in each Colombian basin:

$$V_{tar} = 6,29 \cdot 10^{-2} * A * h * \rho_{Roca} * P_{Bitumen} * \frac{1}{\rho_{Bitumen}} \quad \textbf{(6-1)}$$

V_{tar}: original in situ oil (MMbbl)

A: area of the resource (m^2)

h: tar sand layer thickness (m)

ρ **Roca:** rock density (g/cm^3)

$P_{bitumen}$: percentage of bitumen (p/p)

ρ **bitumen:** total bitumen density (g/cm^3)

The procedure for estimating the resource consisted of the following stages:

- A bibliographic review of different sources was made: international data regarding tar sand deposits was used as reference information for evaluating manifestations in Colombia. Mining data regarding wells, records, lithology, manifestations, occurrences or mining inventories for the different regions of Colombia were then reviewed.
  - ✓ A database was then compiled from the inventory of manifestations. The compiled information contained coordinates, place of occurrence, year of report and bitumen thickness, percentage, lithology and chemical properties (Appendix 7-2);
  - ✓ A map of tar sands occurrences per basin was drawn.
- Frequency histograms were drawn for evaluating the pattern and associating distributions with data regarding bitumen thickness, density and percentage of bitumen concerning occurrences in the inventory.
  - ✓ Different sedimentary environments were considered for rock density, according to the inventory, in an attempt to define a range of values for bitumen-bearing rock; and
  - ✓ Goodness-of-fit tests were used, considering the best distribution for each variable, and parameters were estimated for such distribution and their respective confidence intervals.
- The map of occurrences was used for classifying resources and reserves, producing areas having a ratio defined by identified (measured 0-250 m, indicated 250-750 m and inferred 750-2,250 m) and resources (hypothetical 2,250-5,000 m).
  - ✓ Overlying areas were eliminated for calculating the total area containing the resource; and

- ✓ A ratio between basin area and total area was established for the resource in a particular basin. Such estimation led to establishing areas of the resource in basins for which there was only minimal or zero information.
- o Monte Carlo simulations were made using Equation 7-1 for calculating tar sands potential, taking rock thickness and density and bitumen density and percentage as distribution factors.

The indicated and hypothetical categories were chosen for presenting the results after having observed the estimated resources' pattern in the four evaluation categories (measured, indicated, inferred and hypothetical) in the proposed scenarios. Figure 7-10 gives an example of these evaluation ratios.

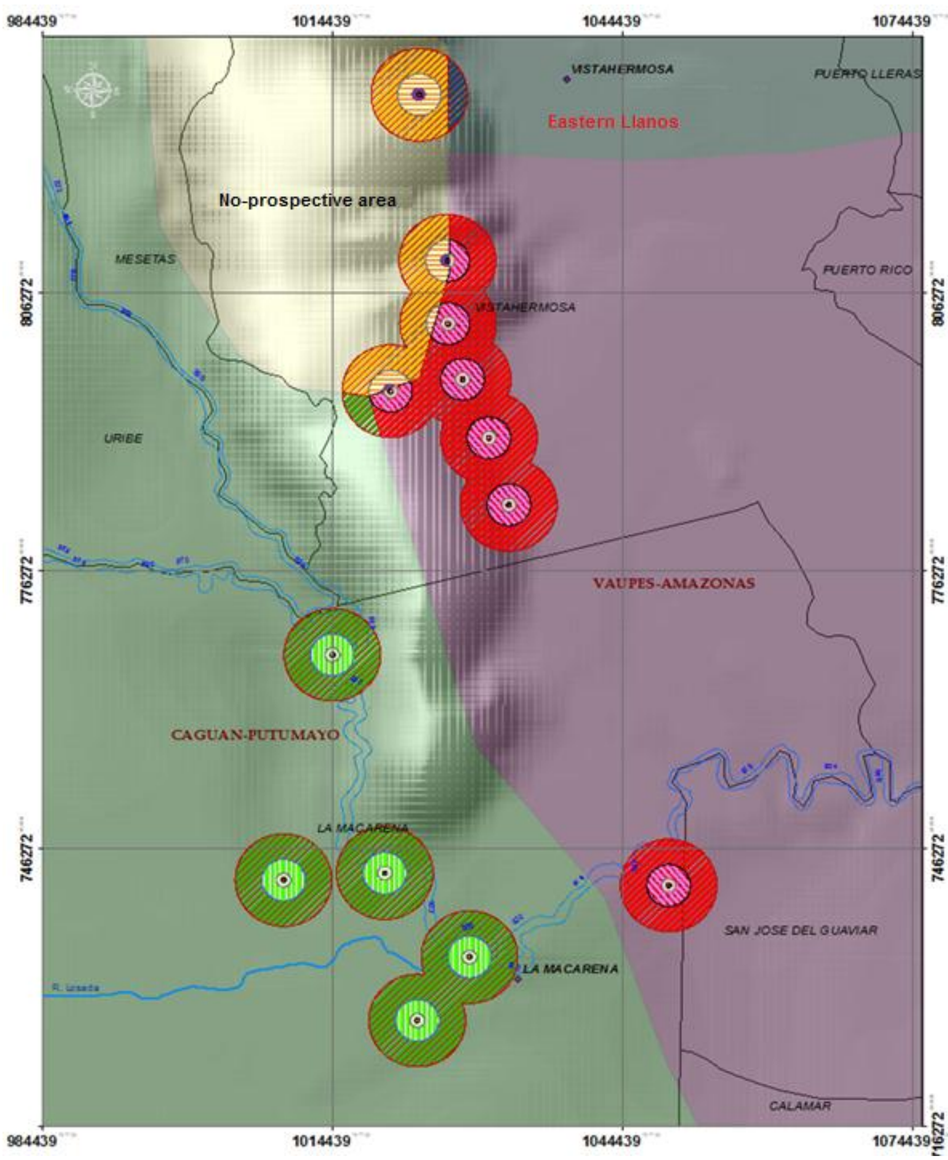

Figure 7-10. A map illustrating the areas associated with the resource in an area limited to three basins (La Macarena). Four circles in each tar sand occurrence site indicate projections for measured (0–250 m), indicated (250–750 m), inferred (750–2,250 m) and hypothetical resources (2,250–5,000 m). The colours represent different basins.

ANH AGENCIA NACIONAL DE HIDROCARBUROS

7.4 Results

The random variables used in Equation 7-1 were subjected to statistical analysis leading to ascertaining their representativity and identifying the distribution of probability best fitting the data. These tests led to establishing confidence intervals for the distribution parameters and degree of certainty when calculating goodness-of-fit (test statistic).

This report only contains information concerning the results for the best fits and estimations; the rest are reported in the appended digital files in Appendixes 7-1 and 7-2.

7.4.1 Tar sand occurrences

The manifestations are shown on the tar sands occurrence map (Figure 7-11). Manifestations have been discriminated on this map according to the source for the information.

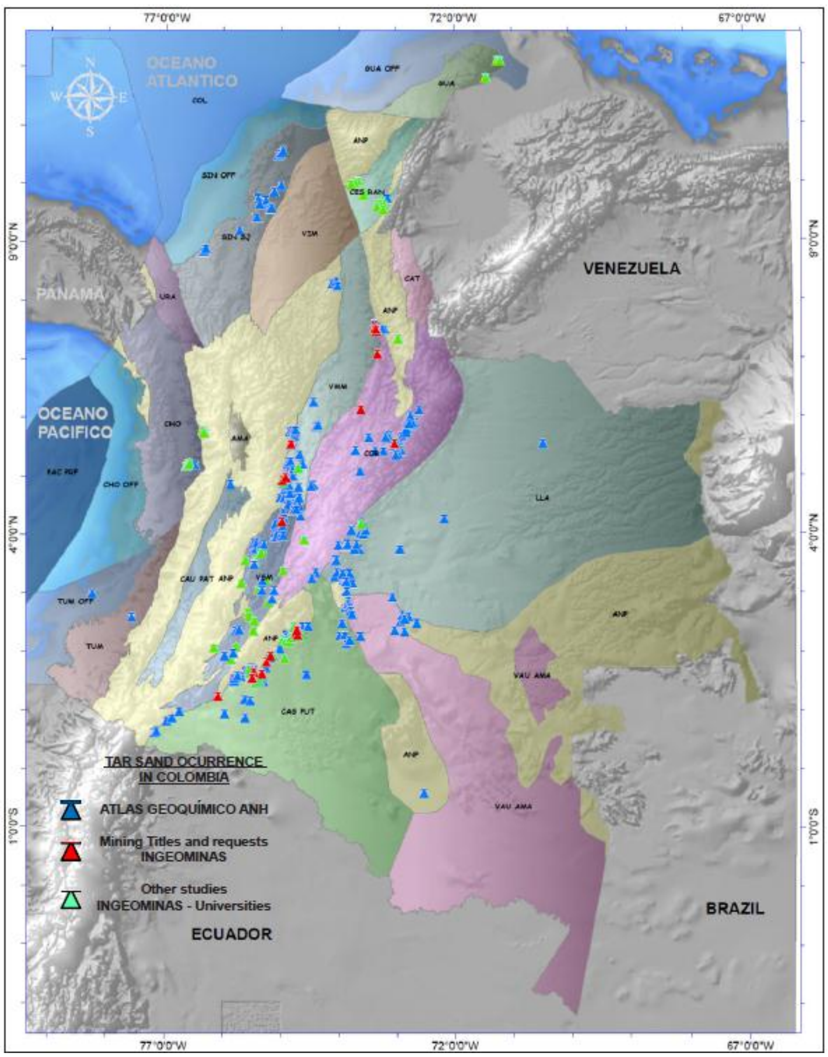

Figure 7-11. Tar sand occurrences per basin in Colombia, indicating the type of source.

7.4.2 Thickness

Analysing thickness in the manifestations inventory suggested a logistical-type distribution from the parameters shown in Table 7-4; 30 m maximum thickness, 5 m mean and 7 m standard deviation were found.

Estimated parameters						Goodness-of-fit test			
$\hat{x}$	Confidence interval		$\hat{y}$	Confidence interval		Null hypothesis	P	Statistical value	G.L
3.41	2.21	4.61	3.26	2.67	3.98	N/R	N/R	N/R	N/R

Table 7-4. Goodness-of-fit parameters regarding logistical distribution and goodness-of-fit test results applied to the thickness data used in estimating tar sand potential. Estimated parameters $\hat{x}$ and $\hat{y}$ are logistical distribution regarding location and scale. "N/R" refers to parameters which, as they went beyond the algorithm's range of calculations, were not reported when making the statistical estimation.

7.4.3 Bitumen density

Analysing the data regarding bitumen density in the manifestations inventory revealed a lognormal pattern for occurrence frequency (Table 7-5).

Estimated parameters						Goodness-of-fit test			
$\hat{x}$	Confidence interval		$\hat{y}$	Confidence interval		Null hypothesis	P	Statistical value	G.L
0.12	0.09	0.16	0.09	0.07	0.12	Was not rejected	M.B.	2.70	0

Table 7-5. Lognormal distribution parameters and goodness-of-fit test results applied to the bitumen density data used in estimating tar sand potential. Estimated parameters $\hat{x}$ and $\hat{y}$ are lognormal distribution regarding the mean and standard deviation, respectively. M.B refers to a very low probability of the null hypothesis being accepted or rejected.

7.4.4 Rock density

According to the aforementioned inventory, different sedimentary environments were considered having different porosity for establishing a range of density for bitumen-bearing rock. A uniform distribution was considered ranging from 2.21 g/cm^3 to 2.73 g/cm^3.

7.4.5 Area

The areas were defined according to criteria for evaluating identified and resources per basin (Figures 7-9 and 7-10; Table 7-6).

Basin	Area (ha)	Measured (ha)	Indicated (ha)	Inferred (ha)	Hypothetical (ha)
Non-prospective area	32,837,455	3,135	18,622	109,001	274,009
Caguán - Putumayo	11,030,407	541	3,925	33,060	127,556
Cauca - Patía	1,282,331	20	157	1,414	5,900
Los Cayos	14,475,501	20	157	1,414	6,263
Cesar - Ranchería	1,166,868	20	157	1,414	6,263
Chocó	3,858,198	196	1,142	6,471	18,513
The Eastern Cordillera	7,176,620	1,240	8,977	66,868	205,519
The Eastern Llanos	22,560,327	1.120	7,443	46,401	140,138
Tumaco offshore	3,455,268	20	157	1,414	6,263
Sinú - San Jacinto	3,964,459	314	2,513	22,070	83,724
Tumaco	2,373,242	32	183	1,491	6,405
The Middle Magdalena Valley	3,294,942	1,008	7,684	54,802	154,503
The Upper Magdalena Valley	2,151,284	941	7,210	61,963	226,707
Vaupés - Amazonas	15,486,731	266	1,932	15,969	50,227

Table 7-6. Areas of the resource per basin in Colombia.

A ratio was then established between the area of a particular basin's resources and such basin's total area for determining maximum the area of YTF resources for basins lacking such information (hypothesis 4).

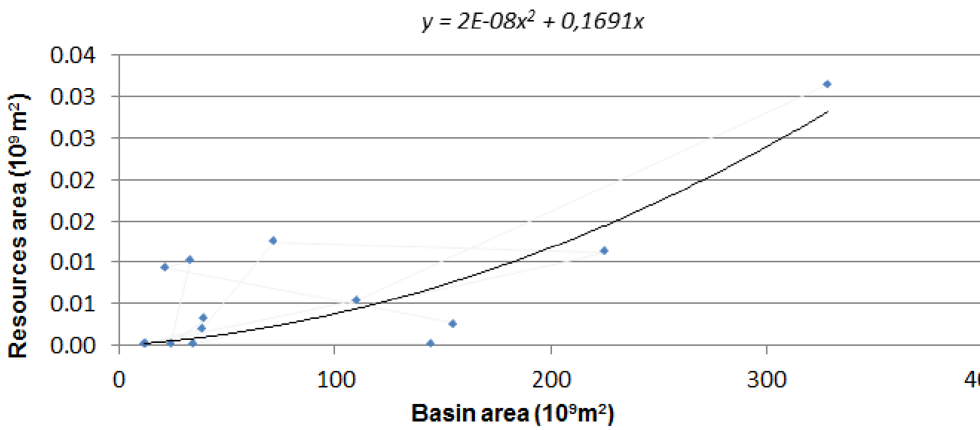

Figure 7-12. Ratio between areas of the resource per basin in Colombia regarding function and area per basin.

Basin	Area (ha)	Measured (ha)	Indicated (ha)	Inferred (ha)	Hypothetical (ha)
Amagá	282,493	5	60	644	2,639
Catatumbo	771,501	14	167	1,767	7,181
Guajira	1,377,892	27	306	3,173	12,767
Urabá	944,895	18	206	2,168	8,784
The Lower Magdalena Valley	3,801,740	93	927	8,940	34,581

Table 7-7. Areas of resource projected for those basins lacking occurrence data

7.4.6 Potential of tar sands in Colombia

The results of the Monte Carlo simulation for calculating the tar sands potential are shown below, as well as the parameters defined in equation 7-1 and the previously-defined distributions. These results were previously weighted with environmental factors shown in Table 2-1.

Basin	Indicated (MMbbl)		
	P_{10}	P_{50}	P_{90}
Amagá	7.2	1.0	0.2
Non-prospective area	1,949.0	263.4	44.6
Caguán - Putumayo	437.0	59.1	10.0
Catatumbo	19.0	2.6	0.4
Cauca - Patía	19.0	2.6	0.4
Cesar - Ranchería	19.0	2.6	0.4
Chocó	134.9	18.2	3.1
The Eastern Cordillera	965.8	130.5	22.1
Guajira	36.1	4.9	0.8
The Eastern Llanos	877.7	118.6	20.1
Sinú - San Jacinto	272.2	36.8	6.2
Tumaco	21. 6	2.9	0.5
Urabá	24.1	3.3	0.6
The Lower Magdalena Valley	111.9	15.1	2.6
The Middle Magdalena Valley	927.5	125.3	21.2
The Upper Magdalena Valley	807.9	109.2	18.5
Vaupés - Amazonas	182.8	24.7	4.2
TOTAL	**6,812.6**	**920.6**	**155.7**

Table 7-1. Potential of tar sands for the indicated resources evaluation category.

Basin	Hypothetical (MMbbl)		
	P_{10}	P_{50}	P_{90}
Amagá	318.6	43.1	7.3
Non-prospective area	28,678.4	3,875.4	655.5
Caguán - Putumayo	14,203.0	1,919.3	324.6
Catatumbo	816.9	110.4	18.7
Cauca - Patía	711.9	96.2	16.3
Cesar - Ranchería	756.1	102.2	17.3
Chocó	2,187.7	295.6	50.0
The Eastern Cordillera	22,109.1	2,987.7	505.3
Guajira	1,035.9	140.0	23.7
The Eastern Llanos	16,526.0	2,233.2	377.7
Sinú - San Jacinto	9,067.2	1,225.3	207.2
Tumaco	753.9	101.9	17.2
Urabá	1,027.7	138.9	23.5
The Lower Magdalena Valley	4,174.3	564.1	95.4
The Middle Magdalena Valley	18,650.3	2,520.3	426.3
The Upper Magdalena Valley	25,404.0	3,432.9	580.6
Vaupés - Amazonas	4,752.8	642.3	108.6
TOTAL	**151,173.9**	**20,428.5**	**3,455.1**

Table 7-2. Potential of tar sands for the hypothetical resources evaluation category.

Figure 7-1. Map of tar sands potential for the indicated resources evaluation category.

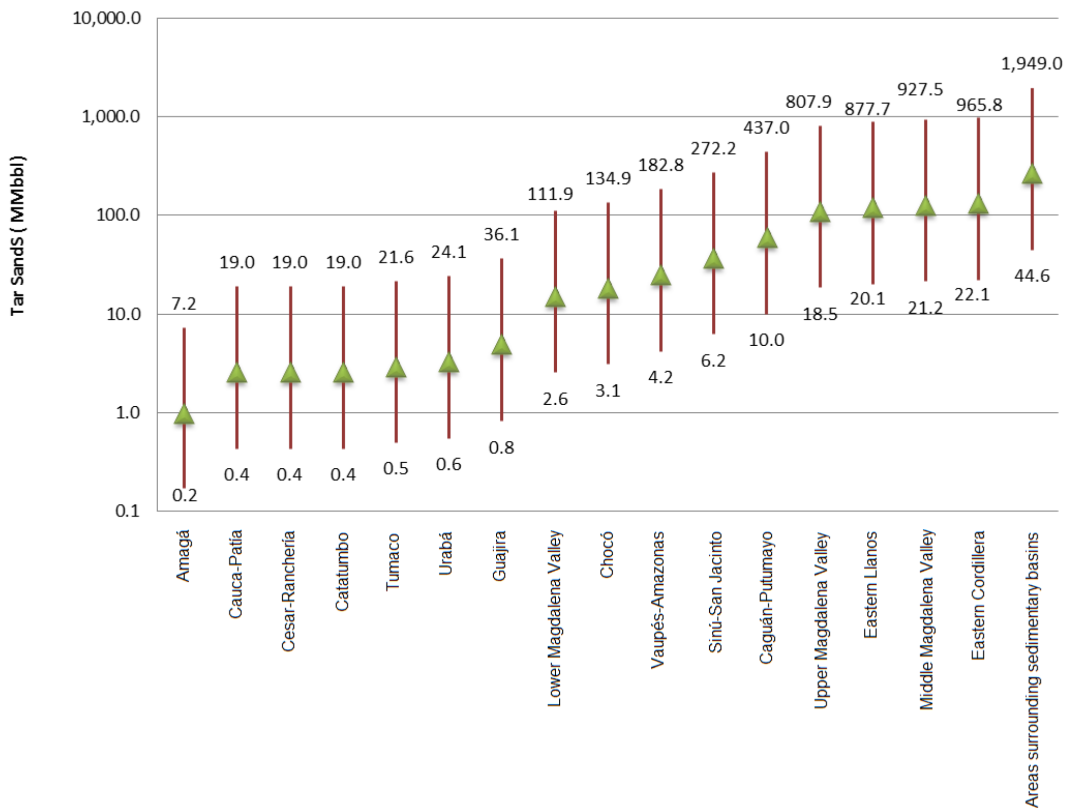

Figure 7-14. Potential of tar sands for the indicated resources evaluation category.

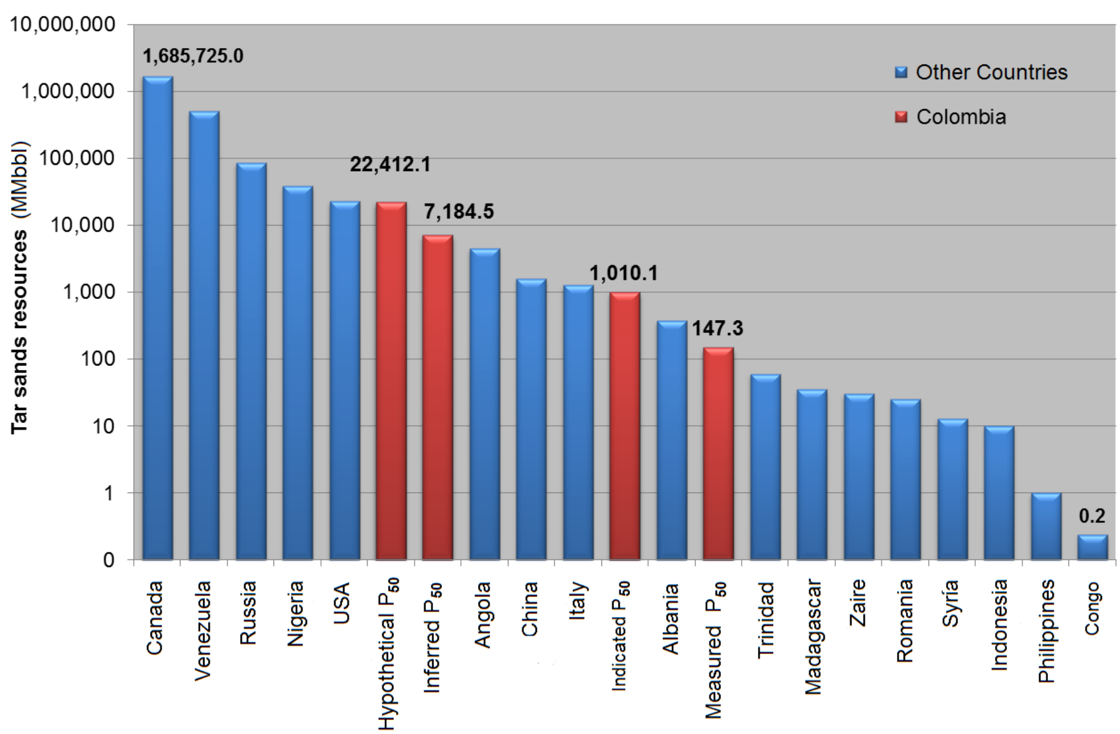

Figure 7-2. Comparing the resources estimated for Colombia with those published for other countries.

7.4.7 Sensitivity analysis

It was established that target formation thickness was the random variable having the greatest weighting on the simulation from the data compiled concerning manifestations in Colombia, and according to the nature of distribution functions (rock thickness and density, bitumen density and percentage) (Figure 7-16); exploratory exercises will consequently have to make greater efforts at defining them (followed by bitumen content and rock density). The areas' representativity will also have to be validated due to the nature of the hypotheses used in this work.

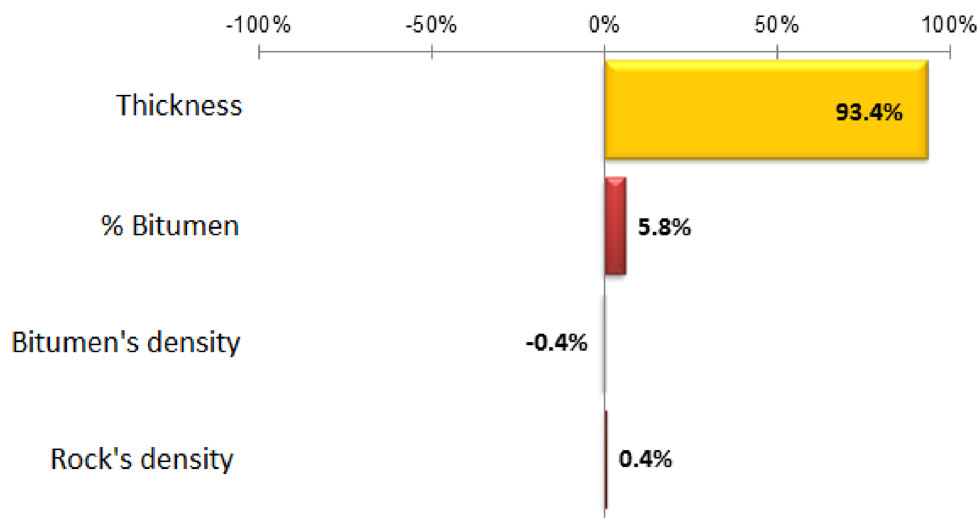

Figure 7-3. Percentage analysis of the sensitivity of variables used for calculating the tar sands potential in each basin of Colombia.

7.5 Conclusions

The sensitivity analysis showed that thickness was the most sensitive variable when calculating the tar sands potential (67,889);

The Eastern Cordillera basin had the greatest prospectivity for tar sands;

Tar sands potential for the whole of Colombia, ranging from 156 to 6,813 MMbbl (P_{10} to P_{90}), was lower than that reported by D. Little (2008) (67,889 MMbbl); and

The potential of the plains areas, such as the Eastern Llanos' basin, could lie on the eastern flank; however, information regarding bitumen manifestations is still lacking for this area in particular.

7.6 Bibliography

Agencia Nacional de Hidrocarburos. (2010). Organic Geochemistry Atlas of Colombia. Bogotá: Universidad Nacional de Colombia.

Bachu, S. (1987). Subsurface disposal related to in situ oil sands projects. Alberta Research Council, Alberta.

CARBOCOL. (1992). Reconocimiento geológico del area de Tadó, Departamento de Chocó: Mapa de estaciones y afloramientos de asfaltita. Bogota.

Chillingarian, G. V., & Yen, T. F. (1978). Bitumens, Asphalts and Tar Sands. New York: Elsevier Scientific Publishing Company.

Duque, H. R. (2002). Estudio geológico y geoquímico de un prospecto de arenitas asfálticas en la región del Capricho, Municipio de San José del Guaviare, Departamento del Guaviare, Colombia. Undergraduate thesis, Universidad Nacional de Colombia, Facultad de Ciencias, Bogotá.

Dyni, J. R. (2010). Survey of Energy Resources. World Energy Council.

ECOCARBON. (1995). El carbón, normas generales sobre muestreo y analysis de carbones. Bogotá.

Grosse, E. (1928). Informe sobre los asfaltos en la parte central y meridional del Departamento de Boyacá. Ministerio de Minas y Petroleos, Servicio Geológico Nacional, Bogotá.

Gulf Canada Resources Limited. (1993). Phase I. Study to asses the potential of minerals and metals in Alberta oil sands deposits. Calgary.

Hein, F. J. (2006). Subsurface Geology of the Athabasca Wabiskaw-McMurray Succession: Lewis-Fort McMurray Area, Northeastern Alberta. Earth Sciences Report 6, Alberta Geological Survey, Alberta.

Hitchon, B. (1993). Geochemical Studies - 4 Physical and chemical properties of sediments and bitumen from some Alberta oil sands deposits. Alberta Research Council.

INGEOMINAS. (1933). Estructura geologica de la parte suroriente de la conseción Chaux Fulson, Santander del Norte. Colombia. Bogotá.

INGEOMINAS. (1970). Ocurrencias minerales en el nororiente Antioqueño. Medellín.

INGEOMINAS. (1970). Recursos minerales de parte de los departamentos de Norte de Santander y Santander. Boletin Geológico XVIII N°3, Bogotá.

INGEOMINAS. (1972). Ocurrencias minerales en los cuadrangulos J-11 (Chiquinquira), J-12 (Tunja), J-13 (Sogamoso) y parte del J-10 (La Palma) y el K-10 (Villeta) . Bogotá.

INGEOMINAS. (1976). Informes de minerales no metalicos en el departamento de Tolima. Ibague.

INGEOMINAS. (1976). Ocurrencias minerales en el departamento del Huila. Neiva.

INGEOMINAS. (1976). Ocurrencias minerales en las regiones sur y oriental del departamento del Tolima. Ibagué.

INGEOMINAS. (1988). Estandarizacion del metodo de asfaltenos, de bitumen y de carbón . Bogotá.

INGEOMINAS. (1995). Visita técnica a la manifestación de asfalto en el municipio de Santa Rosa, Vereda Concepción. Cauca. Bogotá.

INGEOMINAS. (1999). Inventorio Minero Nacional - Departamento de Norte de Santander. Bogotá.

INGEOMINAS. (1999). Proyecto Minero Nacional - Departamento de Boyacá. Bogotá.

INGEOMINAS. (2006). Inventorio Minero - Macizo de Garzón. . Bogotá.

INGEOMINAS. (2007). Mapa Geológico de Colombia. Escala 1:2,800.000. Bogotá.

Instituto Geologico Nacional. (1948). Estudio Economico de los asfaltos de Guaní, en Chaparral-Tolima. Bogotá.

Instituto Geológico Nacional. (1954). Descubrimiento de petroleo en Tolu, Bolivar. Bogotá.

Instituto Geologico Nacional. (1957). Carbones de Landazari Asfaltita de Gualio Municipio de Velez, Departamento de Santander. Bogotá.

Instituto Geologico Nacional. (1960). Informe de investigación de yacimientos minerales en Colombia. Bogotá.

Laboratorio de Minas y Petroleos. (1932). Informe sobre los resultados de la analisis de dos muestras de Fuel Oil y una de Asfalto. Bogotá.

Meyer, R.F. & Witt, W. (1990). Definition and World Resources of Natural Bitumens. U.S. Geological Survey Bulletin No. 1944.

Ministerio de Minas y Energía. (2003). Sistema Nacional de Información Minero Colombiano - SIMCO. Consulted on the 7th xxx 2011, de Clasificación Oficial de Minerales: http://www.simco.gov.co/simco/Politicasdelsector/FormatoB%C3%A0sicoMinero/tabid/90/Default.aspx

Servicio Geologico Nacional. (1942). Combustibles minerales del Departamento de Santander. Ministerio de Minas and Petróleos, Bogotá.

Servicio Geologico Nacional. (1946). Manifestacions de petroleo y asfalto en las rocas eruptivas y esquitos cristalinos del Valle Medio del Magalena, Colombia. Ministerio de Minas and Petróleos , Bogotá.

Servicio Geologico Nacional. (1950). Comision a las Carboneras del Guatiquía Limitada - Municipio de Villavicencio. Ministerio de Minas and Petróleos.

Servicio Geologico Nacional. (1950). Estudios de los yacimientos de asfalto de Nemal - Cundinamarca. Ministerio de Minas and Petróleos, Bogotá.

Servicio Geologico Nacional. (1950). Informe sobre los asfaltos de Guaduas - Cundinamarca. Ministerio de Minas and Petróleos, Bogotá.

Servicio Geologico Nacional. (1959). Sobre la geologia de la parte sur de la Macarena . Ministerio de Minas and Petróleos, Bogotá.

Servicio Geológico Nacional. (1961). Roca asfaltica al norte de Villavicencio, Meta. Ministerio de Minas and Petróleos, Bogotá.

Servicio Geologico Nacional. (1966). Informe sobre la cuenca Hullera "Tunja - Paipa - Duitama". Ministerio de Minas and Petróleos, Bogotá.

Servicio Geologico Nacional. (1969). Mapa de yacimientos de asfalto. Ministerio de Minas and Petróleos, Bogotá.

Servicio Geológico Nacional. (1976). Ocurrencias minerales en el Departamento de Cundinamarca - Compilation. Ministerio de Minas and Petróleos, Bogotá.

7.7 Appendixes

Digital files in the ANH'S Document Center:

- ✓ “Base de Datos Athabasca Tar Sands.xlsx”
- ✓ “Base de Datos Tar Sands Colombia.xlsx”

8 OIL SHALE

8.1 General comments

Oil shale is a fine-grained, organic matter-containing, sedimentary rock, producing substantial quantities of oil and gas when it is subjected to destructive distillation. Most of the organic matter contained in oil shale is insoluble in ordinary organic solvents; it must therefore become decomposed by heating to enable it to be extracted.

The amount of oil which can be recovered from oil shale deposits by conventional extraction varies from 4% to just over 50% of the rock's total weight or between 10 and 150 gallons of oil per ton of rock and, although not all oil shale has good output/yield, most have small amounts of soluble organic matter (bitumen) and many contain seams, veins or cavities saturated with solid or viscous hydrocarbons, thereby making them attractive (Dyni, 2006).

The oil shale market was not competitive with coal, oil or natural gas until 2004; however, the extraction of this resource is very common in countries having easily-exploitable deposits and which lack other fossil fuel resources. Some oil shale deposits also contain minerals and metals such as alum, nahcolite, dawsonite, sulphur, vanadium, zinc, copper and uranium thereby providing them with added value (Yen & Chillingarian, 1976).

8.1.1 Origin and formation

The main oil shale formation environments would include large lakes, shallow seas on continental shelves and continental shields and small lakes, marshes and lakes associated with producing coal. The contemporary deposit of fine-grained minerals and the degradation of biota-derived organic products in such settings have led to oil shale formation.

An abundance of organic matter, the early development of anaerobic conditions and the absence of destructive organisms, together with continuous sedimentation sometimes accompanied by subsidence, provide the necessary conditions for the compaction and diagenesis of organic matter-rich strata. Chemical activity at low temperatures (around 150° C) causes a loss of the volatile fraction, eventually producing a sedimentary rock rich in refractory organic residues (Yen & Chillingarian, 1978).

8.1.2 Types of oil shale

Oil shale has been given different names over the years such as cannel coal, boghead coal, alum shale, stellarite, albertite, bituminite, wolongite, bituminous schiates, torbanite and kukersite; some of these names are still used for certain kinds of oil shale.

Hutton (1991), who pioneered the use of fluorescence microscopy in studying oil shale deposits in Australia, devised a classification which was mainly based on the origin of organic matter by adapting petrographic terms from the terminology used for coals. This has proved very useful in correlating the different kinds of organic matter present in oil shale with the chemistry of the hydrocarbons derived from them (Dyni., 2006).

Hutton (1991) divided organic matter-rich sedimentary rocks into three different groups: humic coal and carbonaceous shale, bitumen-impregnated rocks and oil shale. He then subdivided the latter group into three subgroups based on the setting for their deposition: terrestrial, lacustrine (related to lakes) and marine (Figure 8-1).

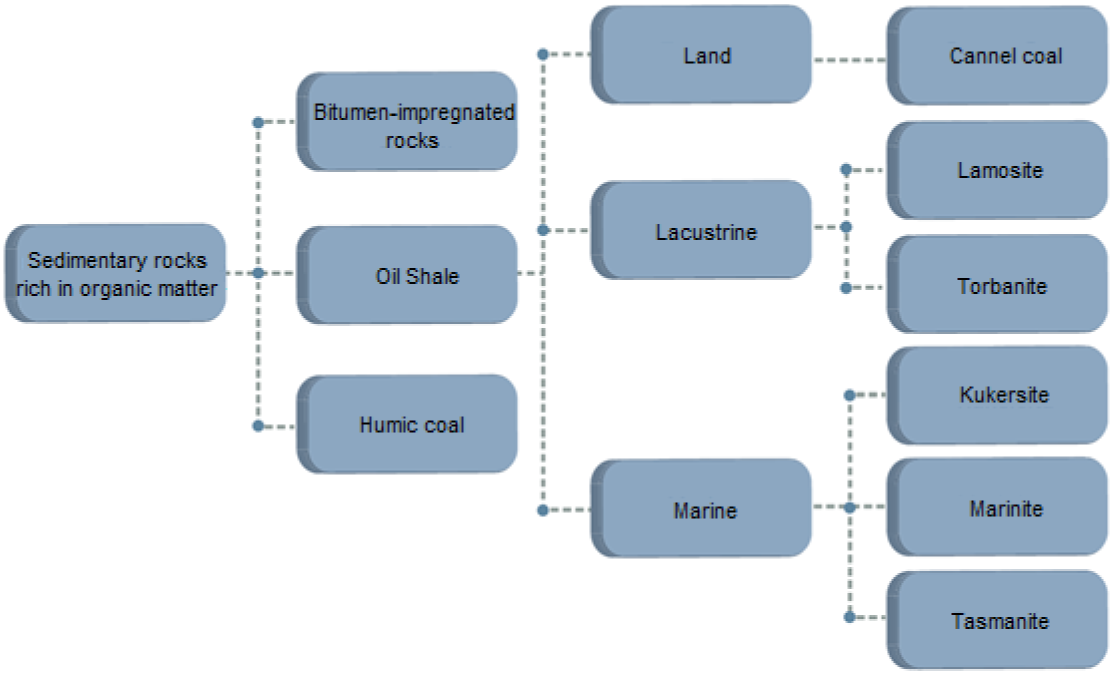

Figure 8-1. Oil shale classification, adapted from Hutton (1991).

Hutton (1991) recognised six specific types within the above three oil shale groups: cannel coal, lamosite, marinite, torbanite, tasmanite and kukersite.

Lamosite is brownish, greyish or dark grey to black. Its main organic component is lamalginite derived from lacustrine plankton seaweed. Minor compounds would include vitrinite, inertite, telalginite and bitumen.

Marinite has a marine origin and is a grey to dark grey. Its main organic components are lamalginite and bitumen, mainly derived from marine phytoplankton. It contains small amounts of telalginite and vitrinite. Marinites are usually deposited in epicontinental seas, such as shallow marine shelves or inland seas, where wave action is restricted and currents are minimal.

Torbanite, tasmanite and kukersite are related to specific kinds of seaweed originating the organic matter. Torbanite is black and its organic matter mainly consists of telalginite derived from lipid-rich seaweed (Botryococcus and related forms) found in freshwater or brackish lakes. It may contain small amounts of vitrinite and inertite. Tasmanite is brown to black and its organic matter is mainly telalginite derived from unicellular seaweed called Tasmanitid. Kukersite is light-brown marine seaweed. Its main organic component is telalginite derived from Gloeocapsomorpha prisca, green seaweed (Dyni, 2006).

8.1.3 Determining the grade of oil shale

Oil shale's volumetric yield can be determined by different methods, their results being expressed in a variety of units. Their calorific value (power) is obtained by using calorimeters. The calculated values are reported in units such as British thermal units (BTU) per pound, calories per gram (cal/g), kilocalories per kilogram (kcal/kg) and megajoules per kilogram (MJ/kg).

Although oil shale's calorific value is a useful and fundamental property of rock, it does not provide information regarding the amount of oil or gas that can be produced by destructive distillation. The grade of oil shale can be determined in laboratory retort tests by measuring the amount of oil produced from a shale sample. The Modified Fischer Assay is a commonly used method for this task in the USA; it was first developed in Germany and later adapted by the U.S. Bureau of Mines for oil shale analysis regarding the Green River formation in western USA (Stanfieldet & Frost, 1949). The technique later became standardised as ASTMD-3904-80.

Fischer's method does not necessarily indicate the maximum amount of oil that can be produced by a given oil shale. Other retorting methods for producing oil, such as the Tosco II process, can increase production by up to 100%. In fact, the Hytort process can increase such production threefold to fourfold in some oil shale (Schora, 1983; Dyni JR, 2010). The Fischer Assay only gives an approximation of a deposit's potential energy.

Rock-Eval and mass balance represent the newest techniques for oil shale evaluation; both of them give more complete information regarding the grade of a particular oil shale. Despite this, the modified Fischer assay remains the most widely used one (Yen & Chillingarian, 1976).

8.1.4 Oil shale exploitation

Extracting oil from oil shale is essentially a mining process, whether it be opencast or underground (fracturing), which is subsequently accompanied by surface or in situ distillation. The liquid product so obtained in such distillation is then enhanced to produce synthetic crude which can be processed at a refinery (Figure 8-2).

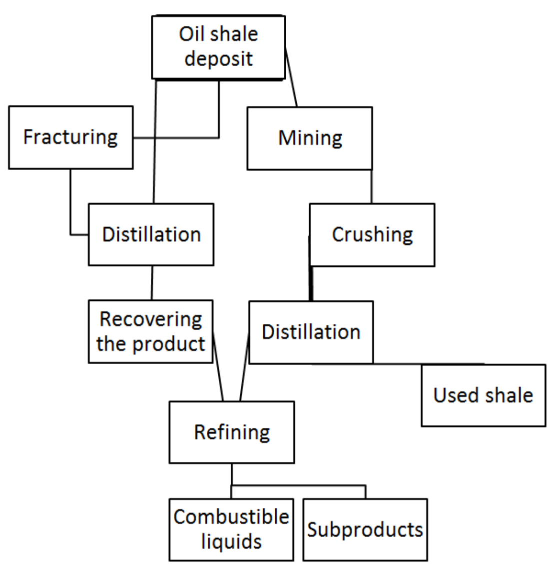

Figure 8-2. Oil shale exploitation, modified from Johnson & Crawford (2004).

The most developed technologies to date are those regarding opencast exploitation for both direct combustion and obtaining synthetic oil, whilst only pyrolysis is available for in situ distillation. This is the case of one of the most innovative processes called in situ conversion (patented by Shell) where the oil shale temperature is raised by electric heaters located in vertical boreholes throughout the thickness of a particular deposit and fluid secreted by the rock is led to the surface through production wells drilled for such purpose. This process is currently being investigated and developed.

8.1.5 Deposits around the world

Early Palaeozoic deposits formed in marine shelf environments have been reported in Northern Europe, Northern Asia and eastern and central North-America. Middle Palaeozoic oil shale deposits have also been reported in eastern and central USA and Central Europe; thin marine sequences have found in Russia. Accumulations have been found on every continent in late Palaeozoic rocks, many of them being associated with coal belts which have been exploited on a small scale in Scotland, France, Spain, South Africa, Australia, Russia and other countries. There are Ordovician kukersite deposits in Estonia and Leningrad in Russia (Yen & Chillingarian, 1976).

The older lacustrine deposits are found in Eastern Canada (Albert shale) and were formed during the early Carboniferous age. One of the largest late Permian deposits in the world (Irati shale) is located in Southern Brazil. Similar aged shale is also present in Southern Argentina, Uruguay and Southern Montana in the USA having a smaller expanse and lower grade. Low-grade Mississippian deposits are found in Northern Alaska.

Mesozoic oil shale has been reported on all continents except Australia. The Stanleyville basin in the Congo in Africa has Triassic age oil shale deposits from lacustrine environments. Northern and Eastern Asia have Jurassic to Cretaceous age deposits in coal belts.

Black Cretaceous age shale has been reported in large marine shelf accumulations in Israel, Jordan, Syria and the southern Arabian Peninsula. There are widely distributed Jurassic black shale deposits in Europe; there are also some minor Triassic deposits in central and southern Europe. Large Triassic age deposits are present in North America in Alaska and Jurassic and Cretaceous age deposits in the central part of Canada; these have small thicknesses but are high grade.

Many Tertiary age oil shale deposits are not of marine origin, but are rather associated with a lacustrine environment and coal belts. Small accumulations of this type have been reported in New Zealand, several parts of Europe, South America in the Andes and on the western coast of North America. Oil shale in Colombia is mainly restricted to late Mesozoic and Cenozoic rocks (Appendix 8-2).

The greatest oil shale accumulations in the world have a lacustrine environment and are from the early or middle Tertiary ages. These would include the Green River formation and other deposits in the Western USA, the Paraiba Valley oil shale deposits in Southern Brazil and those in eastern China. Many of the aforementioned deposits are being commercially exploited.

8.2 Data and hypotheses

The set of data attached as part of this document in a file in Appendix 8-1 consists of 120 samples from different deposits distributed throughout the world. Although the initial database contained information about more than 200 deposits, it had to be refined by selecting only those deposits which had complete information for all the designated fields. The distribution of thickness was taken from this database for estimating the shale oil potential.

8.2.1 National (Colombian) database

The set of data which is attached as part of this document in a file labelled Appendix 8-2 includes the information used for calculating the weighting factors by scenario and category for evaluating the resource, that used for estimating oil shale areas, the data used for estimating hydrocarbon content distribution (S_2P) and the results of each goodness-of-fit test and pertinent correlation.

8.2.2 Hypotheses

8.2.2.1 Hypothesis 1

The ratio between the total control area, defined from sampling presented in the Geochemical Atlas of Colombia (ANH, 2010) and shale surface/outcrop area by basin, shown in the Geological Atlas of Colombia (INGEOMINAS, 2007), represents the oil shale's effective area regarding both surface and depth. The following expression illustrates this hypothesis:

$$f_A = \frac{Total\ control\ area}{Total\ shale\ area}$$

8.2.2.2 Hypothesis 2

Total control area will be significant if total organic carbon (TOC) content favours commercial scenarios. It is considered that TOC values in this work regarding kerogen quality ranging from very good to excellent (≥ 4%) favour commercial occurrences of the resource (Figure 8-3).

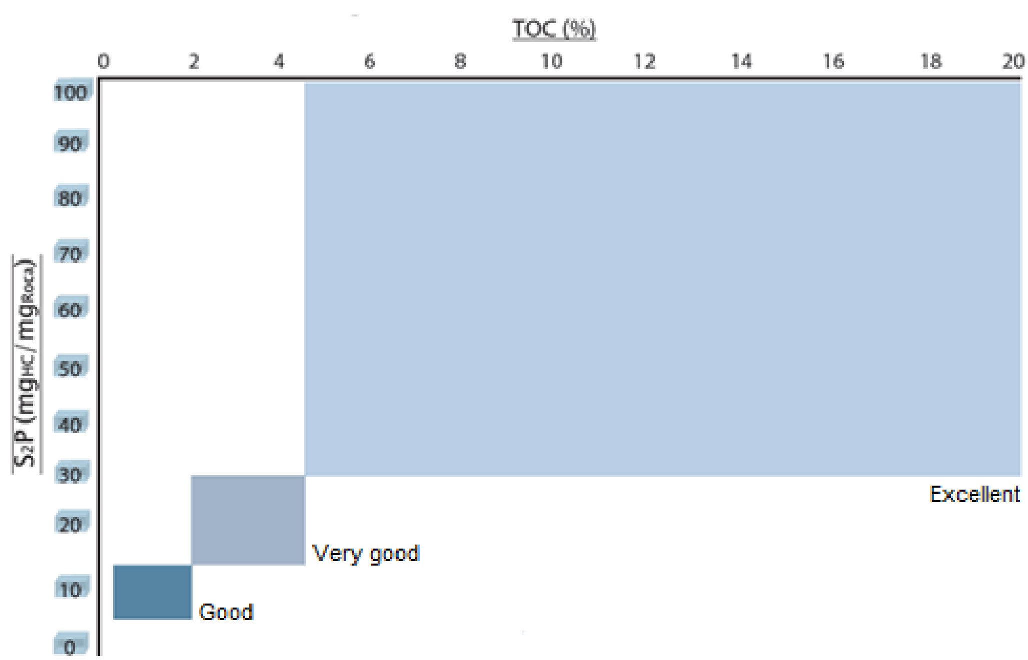

Figure 8-3. Kerogen quality in particular regions.

8.2.2.3 *Hypothesis 3*

Conditions representing control areas must be evaluated. Each control point derived from selecting representative observations of the resource, and compiled in the Geochemical Atlas of Colombia (ANH, 2010), can help to ascertain resource areas for assessing the resource from measured (250 m evaluation radius) to hypothetical areas (5,000 m evaluation radius). Figure 8-4 illustrates the scenarios which had to be evaluated.

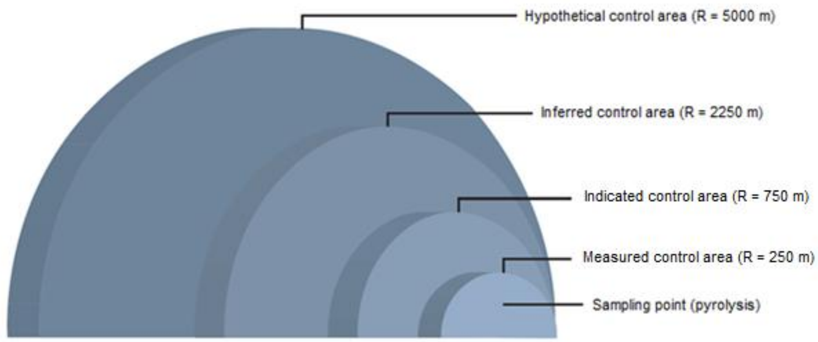

Figure 8-4. Representative diagram for control areas produced from the sampling points used for calculating weighting factors f_A

8.2.2.4 *Hypothesis 4*

The thickness of oil shale units in Colombia follows a lognormal distribution supported by data regarding deposits around the world (Figure 8-5). Such distribution is supported by Appendix 8- 1.

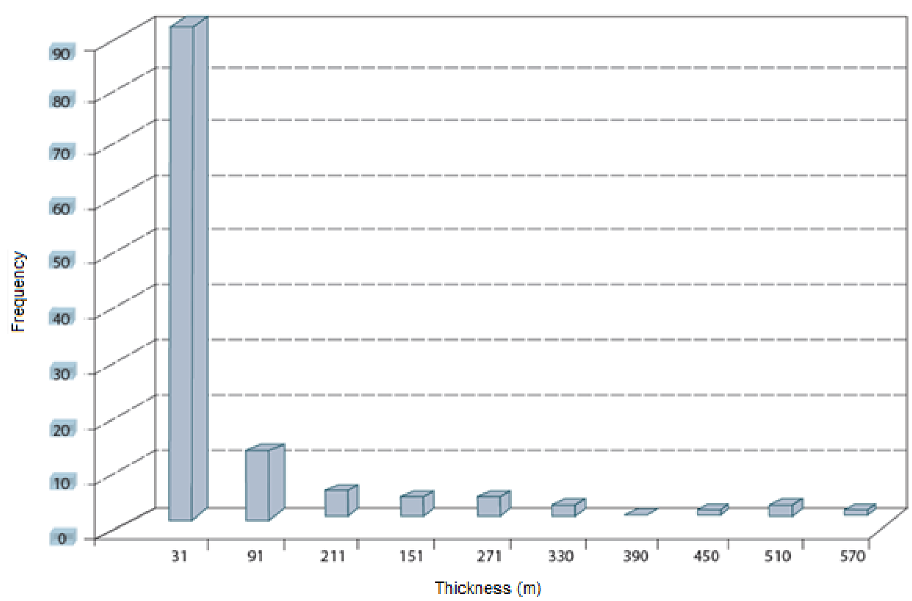

Figure 8-5. Histogram of lognormal thickness frequency used for estimating the oil shale potential.

8.2.2.5 *Hypothesis 5*

The pattern of S_2P hydrocarbon content in basins having no report for this parameter is equal to that presented in geologically analogous basins.

8.3 Methodology

The following equation was used for evaluating the oil shale potential in each Colombian basin:

$$OSOIP = 6.2905 \cdot 10^{-9} * h * A * f_A * \rho * S_2P * \frac{1}{\rho_{HC}} \tag{8-1}$$

OSOIP: original oil shale in place (i.e. in situ) (MMbbl)

h: oil shale unit thickness (m)

A: shale area (m^2)

f_A: deposit area weighting factor (m^2/m^2)

ρ : total rock density (g/cm^3)

S_2P: hydrocarbons generated by kerogen distillation –hydrocarbon content (mg_{HC} /g_{Roca})

ρ **HC**: oil shale density (g/cm^3)

The procedure for estimating the resource considered the following stages:

- A database containing characteristics such as age, tonnage, thickness, area, yield, potential, and density regarding oil shale deposits worldwide was compiled after a bibliographic review had been made (Appendix 8-1):
  - ✓ Frequency histograms were drawn for visualising the pattern and associating a particular distribution to thickness;
  - ✓ Goodness-of-fit tests (i.e. Lilliefors, Student's t-test and Chi^2) were applied for accepting or rejecting the hypothesis regarding thickness distribution; and
  - ✓ Parameters were estimated for such distribution as well as the pertinent confidence intervals.
- A database was compiled containing information about areas, organic matter content and assessment scenarios for Colombia (Appendix 8-2):
  - ✓ The cartography presented in the Geological Atlas of Colombia (Ingeominas, 2007) was used for estimating the surface area of mudstone, shale and mud having organic matter in each basin. Polygons were then drawn showing the oil shale potential areas;
  - ✓ The pattern of hydrocarbon content (S_2P) in each basin was analysed by taking information concerning the pyrolysis test presented in the Geochemical Atlas of Colombia (ANH, 2010), thereby obtaining a distribution for this property per basin;
  - ✓ Statistical analysis was performed to support such distribution; and
  - ✓ Weighting factors were calculated regarding four categories for evaluating the resource, distributed into four scenarios for controlling the oil shale area.
- Monte Carlo simulations were made using the OSOIP formulation; thickness, area, total rock density, organic matter content and shale oil density were used as random variables and the area as fixed parameter.

8.3.1 Scenario 1

The weighting factors were calculated in this scenario by dividing the sum of the control areas within each shale polygon by the sum of the polygons having control points; this was done basin by basin:

$$f_A = \frac{\sum sum\ of\ control\ areas\ in\ each\ shale\ polygon}{\sum shale\ area\ having\ control\ points}$$

Shale areas lacking control points were not taken into account in the way that this denominator was presented nor were excesses of area in the numerator (arising from control points within a given polygon) which should fall outside such polygon. Figure 8-6 shows the issues raised for the weighting factors for each basin in this scenario.

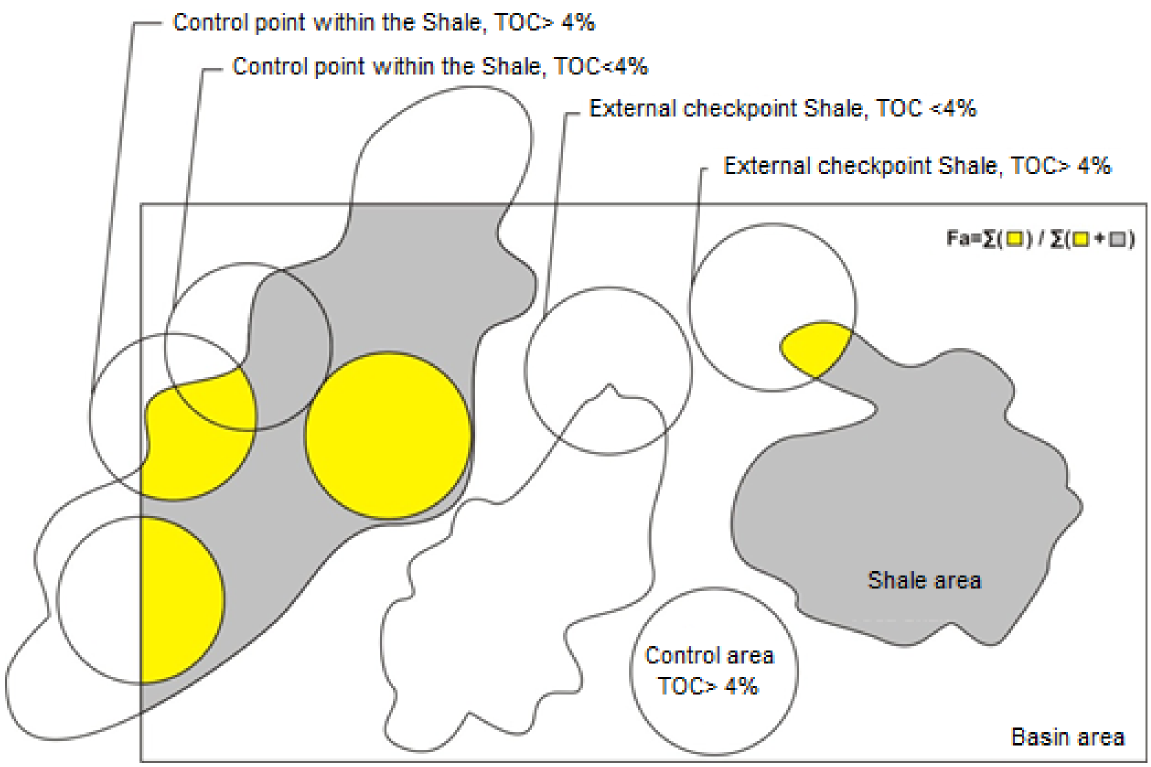

Figure 8-6. Diagram for calculating the weighting factor per basin "f_A" for Scenario 1.

8.3.2 Scenario 2

Figure 8-7 shows a diagram for calculating the ratio of areas in this scenario. This approach can lead to factors greater than unity, which is not surprising, since it is possible that (as shown in the Figure below) just the numerator's yellow areas exceed the sum of the denominator, especially when dealing with inferred or hypothetical evaluation categories.

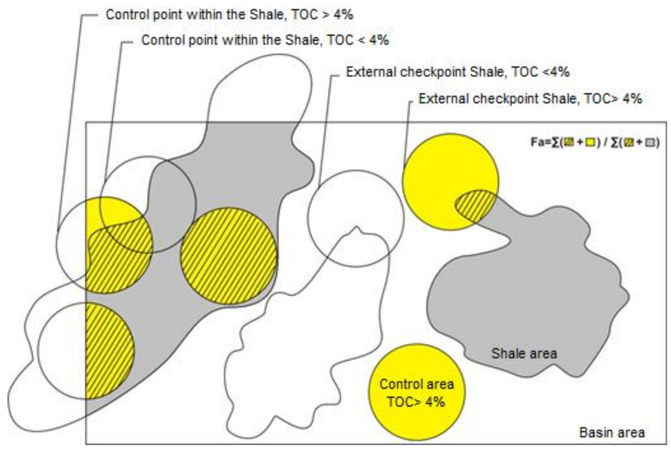

Figure 8-7. Diagram for calculating the weighting factor per basin “f_A” for Scenario 2.

8.3.3 Scenario 3

The concept of Thiessen polygons was used for calculating the weighting factors in this scenario. This led to generating an area from the distances measured between a control point and its neighbours. Such areas were summed per basin and then divided by total basin area.

$$f_A = \frac{\sum \textit{Thissen polygon areas in each basin}}{\textit{Basin area}}$$

8.3.4 Scenario 4

A simple polygon to polygon ratio was obtained in this scenario regarding the area of shale to that defined by control points, leading to more than one factor per basin. It was intended to find a distribution of probability using all the factors calculated for Colombia.

$$f_A = \frac{\textit{Sum of control areas within each shale polygon}}{\textit{Shale areas having control points}}$$

Figure 8-8 gives a diagram of the calculations used.

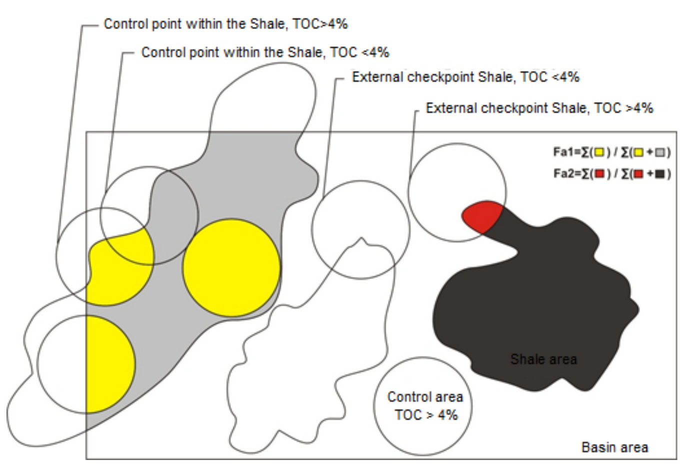

Figure 8-8. Diagram for calculating the weighting factor per basin “f_A” for Scenario 4

Weighting factor/basin area curves were made for the first 3 scenarios regarding each resource assessment category (measured, indicated, inferred and hypothetical). Occurrence probability distribution was found for all basins by category for the last scenario. The indicated and hypothetical categories were chosen for presenting the results after having observed the pattern for the estimated resources in the assessment categories (measured, indicated, inferred and hypothetical) in the proposed scenarios.

8.4 Results

Different distributions were tested for the random variables; parameters regarding distribution patterns were first estimated according to each distribution, and then goodness-of-fit tests were made for identifying the best value (least deviation). This report only shows the results of the best fits and estimates; the remaining results are reported in the digital files in Appendixes 8-1 and 8-2.

8.4.1 Oil shale unit thickness

Regarding data for deposits around the world, it was found that oil shale unit thickness ranged from 1 m to 600 m, having 68 m average and 113 m standard deviation. The histogram so produced (Figure 8-5) suggested a log-normal pattern regarding occurrence frequency; graphs were thus drawn showing this variable's lognormal probability (Figure 8-9) and three goodness-of-fit tests: the Lilliefors and Student-t and Chi^2 tests. The Table below gives the results obtained for the last mentioned test.

Estimated parameters						Goodness-of-fit test			
$\hat{x}$	Confidence interval		$\hat{y}$	Confidence interval		Null hypothesis	P	Statistical value	G.L
3.11	2.82	3.40	1.6	1.42	1.83	Was not rejected	0.07.	0.08	0

Table 8-1. Lognormal distribution fit parameters and goodness-of-fit test results applied to the thickness data used in estimating OSOIP.

Estimated parameters $\hat{x}$ and $\hat{y}$ are lognormal distribution regarding the mean and standard deviation, respectively.

8.4.2 Total rock density

Density values were not reported in many cases investigated in the pertinent literature about particular deposits. Due to such lack of data it was decided to take the minimum and maximum values which could be extracted for constructing a triangular distribution.

Parameters	Value (g/cm^3)
Minimum	2.1
Maximum	2.4
Most probable	2.36

Table 8-2. Parameters estimated for total oil shale density, considering an asymmetrical triangular distribution.

8.4.3 Oil shale density

Oil shale density distribution parameters were determined in the same way as the values shown in Table 8-2 for rock density in view of the scarcity of data for this variable (Table 8-3).

Parameters	Value (g/cm^3)
Minimum	0.9
Maximum	0.97
Most probable	0.91

Table 8-3. Parameters estimated for total oil shale density, considering an asymmetrical triangular distribution.

8.4.4 Shale areas

Table 8-4 shows the shale area value estimated per basin. Figure 8-9 shows these areas' national coverage.

Basin	Shale area (m^2)
Amagá	10,930.008
Non-prospective areas	44,122,937.434
Caguán - Putumayo	25,842,949.353
Catatumbo	4,051,256.044
Cauca - Patía	770,194.542
Cesar - Ranchería	1,691,905.112
Chocó	14,723,778.122
The Eastern Cordillera	39,404,970.408
Guajira	2,124,744.030
The Eastern Llanos	2,436,354.892
Sinú - San Jacinto	21,920,971.043
Tumaco	7,385,534.349
Urabá	246,010.452
The Lower Magdalena Valley	10,676,780.807
The Middle Magdalena Valley	5,937,422.714
The Upper Magdalena Valley	3,016,913.891
Vaupés - Amazonas	758,654.554

Table 8-4. Areas of shale per basin in Colombia.

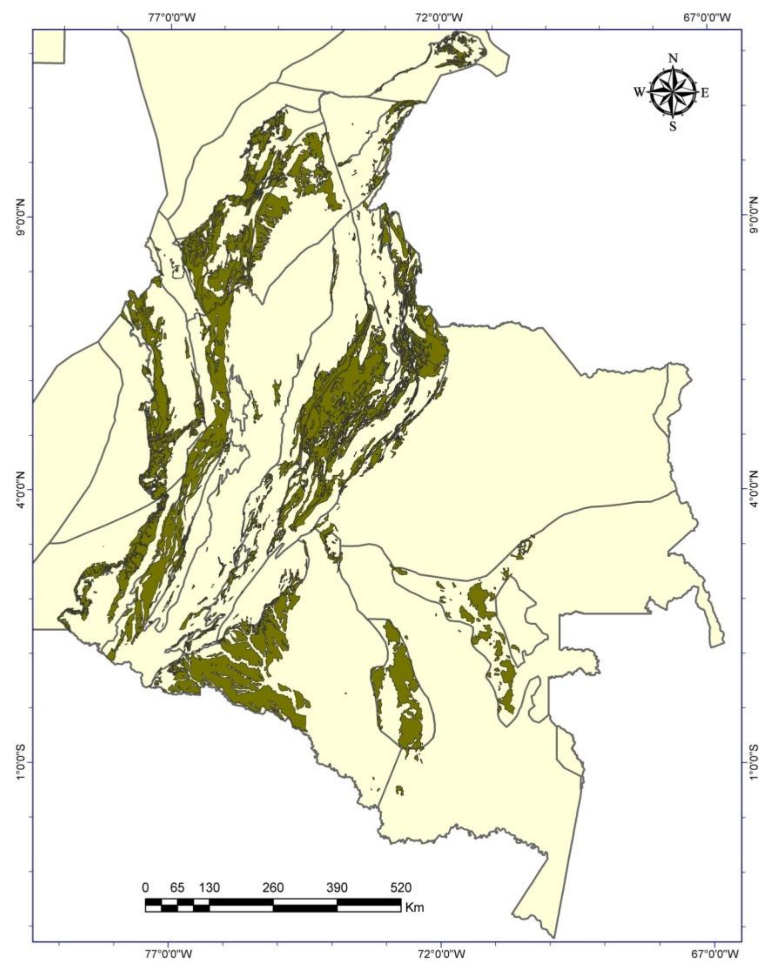

Figure 8-9. Shale outcrop cartography (green).

8.4.5 Deposit area weighting factor

Tables 8-5 to 8-8 se shows the weighting factors obtained per basin for the four resource evaluation categories regarding the four proposed scenarios.

An attempt was made to obtain a ratio for finding factors for those basins lacking them regarding the first three scenarios (graphs showing weighting factor to basin area ratio); however, the resulting correlations did not lead to extracting any type of tendency. Calculating effective oil shale area thus had to be approached from another angle. A probability distribution was thus sought in the fourth scenario so that all basins could be associated in estimating the oil shale potential (Equation 8-1).

Figures 8-10 to 8-12 show the aforementioned ratios for the indicated resources category in the first three scenarios; the pattern for the rest was very similar and their graphs/Figures have been included in the attached digital files.

Basin	Scenario 1	Scenario 2	Scenario 3	Scenario 4
Caguán - Putumayo	$1.784*10^{-2}$	$1.992*10^{-2}$	$1.719*10^{-3}$	$8.080*10^{-3}$
				$4.844*10^{-2}$
The Eastern Cordillera	$1.416*10^{-4}$	$2.061*10^{-4}$	$1.060*10^{-1}$	$1.290*10^{-3}$
				$4.092*10^{-5}$
				$2.890*10^{-3}$
				$6.181*10^{-3}$
				$6.868*10^{-5}$
				$3.364*10^{-4}$
				$4.457*10^{-4}$
				$4.535*10^{-3}$
				$9.553*10^{-4}$
Sinú - San Jacinto	$2.352*10^{-2}$	$1.185*10^{-1}$	$3.221*10^{-1}$	$2.352*10^{-2}$
The Middle Magdalena Valley	$2.258*10^{-4}$	$3.388*10^{-4}$	$3.907*10^{-2}$	$1.479*10^{-4}$
				$3.921*10^{-4}$
				$7.683*10^{-4}$
The Upper Magdalena Valley	$1.605*10^{-3}$	$5.340*10^{-3}$	$1.295*10^{-1}$	$1.056*10^{-3}$
				$1.961*10^{-2}$

Table 8-5. Measured factors used in estimating OSOIP. These factors were calculated in the Methodology section for the first three scenarios to obtain a single factor per basin; however, one shale unit was obtained for each basin in the last scenario.

Basin	Scenario 1	Scenario 2	Scenario 3	Scenario 4
Caguán - Putumayo	$8.873*10^{-2}$	$1.349*10^{-1}$	$1.719*10^{-3}$	$7.989*10^{-2}$
				1.164E-1
The Eastern Cordillera	$1.226*10^{-3}$	$1.744*10^{-3}$	$1.060*10^{-1}$	$8.588*10^{-3}$
				$3.891*10^{-4}$
				$8.333*10^{-2}$
				$2.383*10^{-2}$
				$5.565*10^{-2}$
				$5.458*10^{-4}$
				$2.985*10^{-3}$
				$3.795*10^{-3}$
				$1.182*10^{-4}$
				$5.358*10^{-2}$
				$6.794*10^{-3}$
Sinú - San Jacinto	$3.194*10^{-1}$	1.067	$3.221*10^{-1}$	$3.194*10^{-1}$
The Middle Magdalena Valley	$2.033*10^{-3}$	$3.050*10^{-3}$	$3.907*10^{-2}$	$1.332*10^{-3}$
				$3.948*10^{-3}$
				$5.482*10^{-3}$
The Upper Magdalena Valley	$1.440*10^{-2}$	$3.763*10^{-2}$	$1.295*10^{-1}$	$7.338*10^{-3}$
				$1.743*10^{-2}$
				$2.281*10^{-1}$

Table 8-6. Indicated factors used in estimating OSOIP. As stated in the Methodology section, values were obtained which were above those per unit for weighting factors in scenario 2 (highlighted in red) when areas

outside the shale polygons were greater than such area (it should be stressed that the ratio sought with this scenario's values was not good).

Basin	Scenario 1	Scenario 2	Scenario 3	Scenario 4
Caguán - Putumayo	$3.474*10^{-1}$	1.073	$1.719*10^{-3}$	$3.079*10^{-1}$
				$4.711*10^{-1}$
The Eastern Cordillera	$8.132*10^{-3}$	$1.406*10^{-2}$	$1.060*10^{-1}$	$5.565*10^{-2}$
				$2.707*10^{-3}$
				$1.946*10^{-2}$
				$9.707*10^{-1}$
				$5.868*10^{-3}$
				$5.176*10^{-1}$
				$8.078*10^{-2}$
				$1.264*10^{-1}$
				$3.703*10^{-1}$
				$3.968*10^{-3}$
				$2.433*10^{-2}$
				$2.239*10^{-4}$
				$2.249*10^{-2}$
				$6.900*10^{-2}$
				1
				$4.290*10^{-1}$
				$2.160*10^{-2}$
Sinú - San Jacinto	$5.251*10^{-3}$	$2.359*10^{-2}$	$3.221*10^{-1}$	1
				$4.511*10^{-1}$
				$2.174*10^{-3}$
The Middle Magdalena Valley	$1.410*10^{-2}$	$2.731*10^{-2}$	$3.907*10^{-2}$	$6.067*10^{-3}$
				$1.380*10^{-1}$
				$2.859*10^{-2}$
				$5.249*10^{-2}$
				$6.094*10^{-1}$
The Upper Magdalena Valley	$1.259*10^{-1}$	$2.598*10^{-1}$	$1.295*10^{-1}$	$6.355*10^{-2}$
				$1.327*10^{-1}$
				$3.725*10^{-1}$
				$6.558*10^{-1}$

Table 8-7. Inferred factors used in estimating OSOIP

Basin	Scenario 1	Scenario 2	Scenario 3	Scenario 4
Caguán - Putumayo	$4.811*10^{-1}$	7.332	1.719*10-3	$5.628*10^{-1}$
				$9.936*10^{-1}$
				$1.293*10^{-3}$
Cesar - Ranchería	$1.166*10^{-1}$	3.479	0	$1.166*10^{-1}$
The Eastern Cordillera	$3.082*10^{-2}$	6.227*10-2	1.060*10-1	$1.225*10^{-1}$
				$7.314*10^{-3}$
				$2.955*10^{-1}$
				$8.535*10^{-1}$
				1
				$5.574*10^{-2}$
				$3.336*10^{-1}$
				$2.786*10^{-2}$
				$9.720*10^{-1}$
				$1.541*10^{-1}$
				$2.960*10^{-1}$
				$3.022*10^{-1}$
				$6.101*10^{-1}$
				$1.535*10^{-1}$
				$5.368*10^{-3}$
				$1.794*10^{-2}$
				$9.834*10^{-2}$
				$1.387*10^{-2}$
				$8.131*10^{-2}$
				$8.017*10^{-1}$
				$2.492*10^{-1}$
				1
				$6.990*10^{-1}$
				$4.469*10^{-2}$
				$1.521*10^{-1}$
				$5.479*10^{-1}$
The Eastern Llanos	$7.077*10^{-2}$	5.137*10-1	3.122*10-2	$7.077*10^{-2}$
Sinú - San Jacinto	$2.212*10^{-2}$	8.651*10-2	3.221*10-1	$1.391*10^{-2}$
				$1.787*10^{-2}$
				$6.382*10^{-3}$
				$6.855*10^{-1}$
				1
				$3.692*10^{-1}$
				1
				$1.323*10^{-2}$
The Middle Magdalena Valley	$6.894*10^{-2}$	1.087*10-1	3.907*10-2	$3.473*10^{-2}$
				$5.957*10^{-2}$
				$2.297*10^{-2}$
				$5.608*10^{-1}$
				$7.177*10^{-1}$
				$1.784*10^{-2}$
				$4.893*10^{-2}$
				$3.217*10^{-1}$
				$1.864*10^{-1}$
				$7.286*10^{-2}$
				$2.036*10^{-1}$
				1
				$5.549*10^{-2}$
The Upper Magdalena Valley	$2.190*10^{-1}$	5.290*10-1	1.295*10-1	$1.328*10^{-1}$
				$4.981*10^{-1}$
				$6.831*10^{-3}$
				$9.889*10^{-2}$
				$8.578*10^{-1}$
				1

Table 8-8. Hypothetical factors used in estimating OSOIP

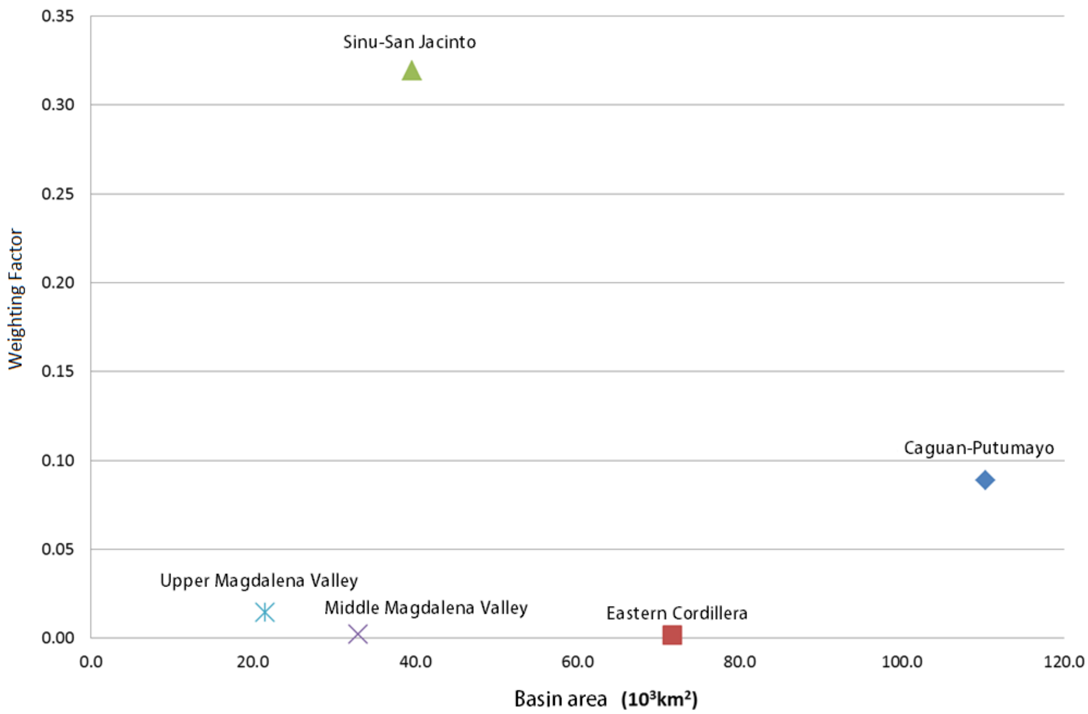

Figure 8-10. Ratio between indicated weighting factors in Scenario 1 and basin area. As can be seen, it was not possible to extract a particular tendency allowing factors to be estimated in other basins from their areas. The other factors' patterns (measured, inferred and hypothetical) were similar in this scenario.

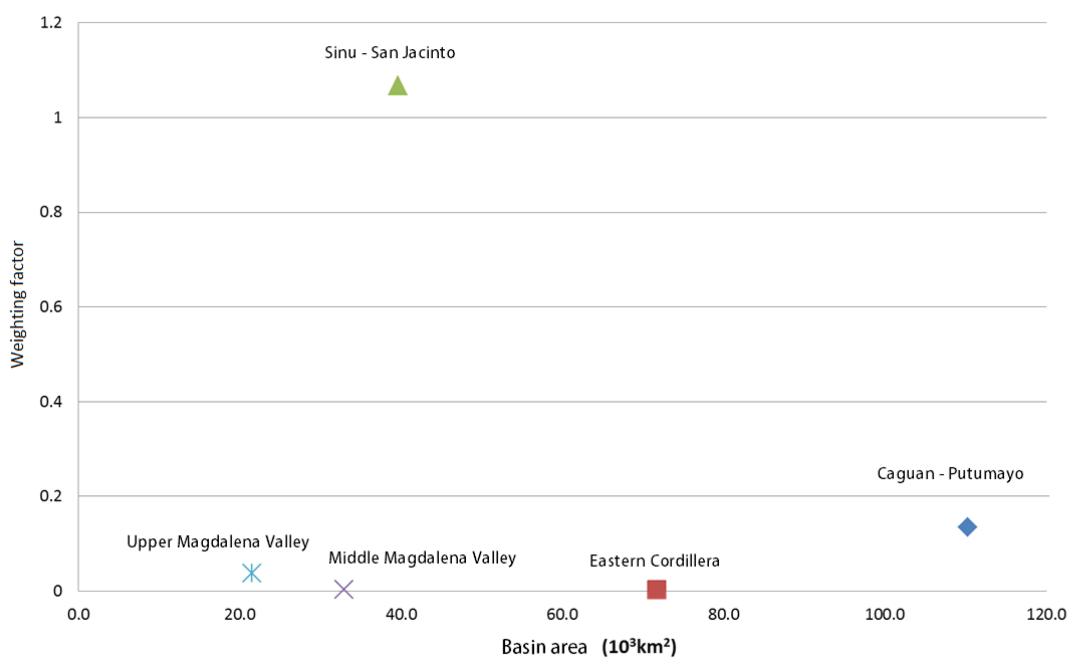

Figure 8-11. Ratio between indicated weighting factors in Scenario 2 and basin area. The other factors' patterns (measured, inferred and hypothetical) were similar in this scenario.

Figure 8-12. Ratio between indicated weighting factors in Scenario 3 and basin area. The other factors' patterns (measured, inferred and hypothetical) were similar in this scenario and did not lead to any sort of tendency being established.

Tables 8-9 and 8-10 show the results of the statistical analysis for best fit distribution regarding indicated and hypothetical factors in Scenario 4. Such scenario was finally chosen for calculating the oil shale potential, and the final results given in this chapter are for the resource evaluation categories applying the two aforementioned factors.

Estimated parameters						**Goodness-of-fit test**			
$\hat{x}$	Confidence interval		$\hat{y}$	Confidence interval		**Null hypothesis**	P	**Statistical value**	G.L
0.41	0.25	0.68	0.12	0.05	0.29	Was not rejected	M.B	0.20	0

Table 8-9. Gamma distribution fit parameters and goodness-of-fit test results applied to the indicated weighting factors in Scenario 4 used in estimating OSOIP. Estimated parameters $\hat{x}$ **and** $\hat{y}$ are the Gamma distribution regarding form and scale. M.B refers to a very low probability of the null hypothesis being accepted or rejected.

Estimated parameters						**Goodness-of-fit test**			
$\hat{x}$	Confidence interval		$\hat{y}$	Confidence interval		Null hypothesis	P	Statistical value	G.L
0.65	0.48	0.88	0.52	0.24	0.82	Was not rejected	0.14	2.16	1

Table 8-10. Gamma distribution fit parameters and goodness-of-fit test results applied to the hypothetical weighting factors in Scenario 4 used in estimating OSOIP.

Comparisons were made with aerial weighting factors from other parts of the world to ensure that the figures for estimating resources represented realistic scenarios.

8.4.6 S_2P hydrocarbon content

The information from pyrolysis tests contained in the Geochemical Atlas of Colombia (ANH, 2010) was used as input for estimating S2P hydrocarbon content per basin. The data regarding outcrop samples was used as the resource being evaluated is mainly exploited by mining opencast deposits, even though new cutting-edge technologies point to their in-depth exploitation. It was only necessary to use well information regarding the Ranchería (Cesar), San Jacinto (Sinú), Tumaco and Urabá basins as no surface data was available for them.

8.4.6.1 Caguán – Putumayo

The 23 items of data available gave 6.02 mg_{HC}/g_{Rock} average value and 11.03 mg_{HC}/g_{Rock} standard deviation. Gamma distribution presented the best data fit. Table 8-11 shows the results of such fit.

Estimated parameters						Goodness-of-fit test			
$\hat{x}$	Confidence interval		$\hat{y}$	Confidence interval		Null hypothesis	P	Statistical value	G.L
0.36	0.23	0.58	16.5	7.28	37.6	Was not rejected	M.B	0.20	0

Table 8-11. Goodness-of-fit test results and parameters applied to the S2P data in the Caguán basin, Putumayo, for determining the statistical distribution used in estimating OSOIP.

8.4.6.2 Catatumbo

The 62 items of data used gave 1.34 mg_{HC}/g_{Rock} average value and 1.78 mg_{HC}/g_{Rock} standard deviation. Lognormal data pattern was normal. Table 8-12 shows the results of such fit.

Estimated parameters						Goodness-of-fit test			
$\hat{x}$	Confidence interval		$\hat{y}$	Confidence interval		Null hypothesis	P	Statistical value	G.L
-0.7	-1.2	-0.3	1.63	1.38	1.98	Was not rejected	M.B	0.88	0

Table 8-12. Goodness-of-fit parameters and test results applied to the S_2P data in the Catatumbo basin for determining the statistical distribution used in estimating OSOIP.

8.4.6.3 Cauca – Patía

No information was available regarding S2P hydrocarbon content for this basin. The distribution for this variable in a neighbouring basin was thus used; the parameters found for the Tumaco basin given were thus taken, given their similar geological evolution.

8.4.6.4 Cesar - Ranchería

249 data items were used, giving 1.69 mg_{HC}/g_{Rock} average value and 2.34 mg_{HC}/g_{Rock} standard deviation. Normal logarithm distribution in this basin gave the best fit. Table 8-13 shows the results of such fit.

Estimated parameters						Goodness-of-fit test			
$\hat{x}$	Confidence interval		$\hat{y}$	Confidence interval		Null hypothesis	P	Statistical value	G.L
-0.3	-0.5	-0.1	1.37	1.26	1.50	Was not rejected	0.07	5.34	2

Table 8-13. Goodness-of-fit parameters and test results applied to the S_2P data in Cesar - Ranchería basin, for determining the statistical distribution used in estimating OSOIP.

8.4.6.5 Chocó

49 items of data were analysed, giving 34.56 mg_{HC}/g_{Rock} average value and 47.57 mg_{HC}/g_{Rock} standard deviation. Again, normal logarithm distribution gave the best fit (Tables 8-14).

Estimated parameters						Goodness-of-fit test			
$\hat{x}$	Confidence interval		$\hat{y}$	Confidence interval		Null hypothesis	P	Statistical value	G.L
1.86	1.17	2.55	2.40	2.00	3.00	Was not rejected	M.B	0.8	0

Table 8-14. Goodness-of-fit parameters and test results applied to the S_2P data in the Chocó basin for determining the statistical distribution used in estimating OSOIP.

8.4.6.6 Eastern Cordillera

The 196 items of data gave 2.28 mg_{HC}/g_{Rock} average value and 5.58 mg_{HC}/g_{Rock} standard deviation. Pareto distribution gave the best data fit (Table 8-15).

Estimated parameters						Goodness-of-fit test			
$\hat{x}$	Confidence interval		$\hat{y}$	Confidence interval		Null hypothesis	P	Statistical value	G.L
1.47	1.13	1.81	0.12	0.16	0.29	Was not rejected	M.B	1.53	0

Table 8-15. Goodness-of-fit parameters and test results applied to the S_2P data in the Eastern Cordillera basin for determining the statistical distribution used in estimating OSOIP. Estimated parameters $\hat{x}$ and $\hat{y}$ are the Pareto distribution form and scale parameters.

8.4.6.7 Guajira

Since no information was available about S2P hydrocarbon content in the basin, the distribution presented for this variable regarding the Cesar - Ranchería basin, was taken, given their geological similarity.

8.4.6.8 Eastern Llanos

The 75 items of data used gave 3.03 mg_{HC}/g_{Rock} average value and 6.23 mg_{HC}/g_{Rock} standard deviation. A Pareto distribution gave the best fit for Eastern Llanos data, like that for the Eastern Cordillera (Tables 8-16).

Estimated parameters						Goodness-of-fit test			
$\hat{x}$	Confidence interval		$\hat{y}$	Confidence interval		Null hypothesis	P	Statistical value	G.L
1.14	0.69	1.58	0.56	0.36	0.86	Was not rejected	M.B	3.41	0

Table 8-16. Goodness-of-fit parameters and test results applied to the S_2P data in the Eastern Llanos basin for determining the statistical distribution used in estimating OSOIP

8.4.6.9 Sinú - San Jacinto

290 items of data were used, giving 0.71 mg_{HC}/g_{Rock} average value and 2.07 mg_{HC}/g_{Rock} standard deviation. An exponential distribution gave the pattern best fitting the data (Table 8-17).

Estimated parameters						Goodness-of-fit test			
$\hat{x}$	Confidence interval		$\hat{y}$	Confidence interval		Null hypothesis	P	Statistical value	G.L
0.71	0.63	0.79	N/A	N/A	N/A	Was not rejected	M.B	0.47	0

Table 8-17. Goodness-of-fit parameters and test results applied to the S2P data in the San Jacinto basin, Sinú, for determining the statistical distribution used in estimating OSOIP. For exponential distribution, estimated parameter $\hat{x}$ represented the mean. N/A refers to parameters which did not apply to the type of distribution being considered.

8.4.6.10 Tumaco

92 items of data were analysed, giving 1.35 mg_{HC}/g_{Rock} average value and 2.34 mg_{HC}/g_{Rock} standard deviation. Again, normal logarithm distribution gave the best fit. Table 8-18 gives the results of such fit.

Estimated parameters						Goodness-of-fit test			
$\hat{x}$	Confidence interval		$\hat{y}$	Confidence interval		Null hypothesis	P	Statistical value	G.L
-0.3	-0.5	-0.1	0.95	0.83	1.11	Was not rejected	0.09	4.84	2

Table 8-18. Goodness-of-fit parameters and test results applied to the S2P data in the Tumaco basin for determining the statistical distribution used in estimating OSOIP.

8.4.6.11 Urabá

Only three items of data were available for this basin, meaning that it was decided to use triangular distribution. Table 8-19 lists the distribution parameters.

Parameters	Value
Minimum	0.08
Maximum	0.33
Most probable	0.18

Table 8-19. Parameters considered for S2P in the Urabá basin.

8.4.6.12 Lower Magdalena Valley

5 items of data regarding outcrops were available for this basin and thus triangular distribution was assumed (Table 8-20).

Parameters	Value
Minimum	0.09
Maximum	3.58
Most probable	1.274

Table 8-20. Parameters estimated for S2P in the Lower Magdalena Valley basin.

8.4.6.13 Middle Magdalena Valley

The 49 items of data gave 2.92 mg_{HC}/g_{Rock} average value and 10.51 mg_{HC}/g_{Rock} standard deviation. Normal logarithm distribution gave the best data fit (Table 8-21).

Estimated parameters						Goodness-of-fit test			
$\hat{x}$	Confidence interval		$\hat{y}$	Confidence interval		Null hypothesis	P	Statistical value	G.L
-0.9	-1.5	-0.4	1.88	1.57	2.35	Was not rejected	M.B.	0.001	0

Table 8-21. Goodness-of-fit parameters and test results applied to the S_2P data in the Middle Magdalena Valley basin for determining the statistical distribution used in estimating OSOIP.

8.4.6.14 Upper Magdalena Valley

The 282 items of data gave a 20.88 mg_{HC}/g_{Rock} average value and 18.26 mg_{HC}/g_{Rock} standard deviation. An extreme value distribution was associated with lognormal data. Table 8-22 shows the results of such fit.

Estimated parameters						Goodness-of-fit test			
$\hat{x}$	Confidence interval		$\hat{y}$	Confidence interval		Null hypothesis	P	Statistical value	G.L
3.04	2.92	3.17	0.98	0.89	1.08	Was not rejected	0.11	5.93	3

Table 8-22. Goodness-of-fit parameters and test results applied to the S_2P data in the Upper Magdalena Valley basin for determining the statistical distribution used in estimating OSOIP. Estimated parameters $\hat{x}$ and $\hat{y}$ are extreme value distribution regarding location and scale parameters.

8.4.6.15 Vaupés – Amazonas

As no information was available regarding S_2P hydrocarbon content in this basin, it was decided to associate it with the same distribution parameters found for the Caguán - Putumayo basin, due to their similarity in terms of geological evolution.

8.4.7 Oil shale in Colombia

Monte Carlo simulation results for calculating the oil shale potential are given below, along with the parameters defined in equation 8-1 and the previously defined distributions. These results had already been weighted by the environmental factors shown in Table 2-1 for excluding those possibly present in environmental conservation areas.

Basin	Indicated oil shale resources (MMbbl)		
	P_{10}	P_{50}	P_{90}
Amagá	3.48	0.06	0.01
Non-prospective areas	5.52	0.29	0.01
Caguán - Putumayo	259.06	4.95	0.03
Catatumbo	85.03	3.57	0.13
Cauca - Patía	240.15	7.77	0.23
Cesar - Ranchería	622.91	13.94	0.28
Chocó	412.19	10.91	0.27
The Eastern Cordillera	294.64	9.54	0.28
Guajira	10,443.25	198.65	1.16
The Eastern Llanos	798.88	33.31	1.24
Sinú - San Jacinto	1,135.06	47.48	1.88
Tumaco	2,678.01	99.34	2.96
Urabá	1,950.33	97.09	4.13
The Lower Magdalena Valley	12,165.96	220.42	3.75
The Middle Magdalena Valley	39,432.19	549.61	7.34
The Upper Magdalena Valley	5,986.40	240.93	8.45
Vaupés - Amazonas	14,564.94	682.19	28.32
TOTAL	91,077.98	2,220.05	60.47

Table 8-23. OSOIP for the indicated resources evaluation category.

It was estimated that there could be 179.86 MMbbl of oil shale (6,291.36 MMbbl in P_{10} and 5.39 MMbbl in P_{90}) for the indicated resources evaluation category in areas forming part of the Colombian Park System (Parques Nacionales Naturales).

Basin	Hypothetical oil shale resources (MMBbl)		
	P_{10}	P_{50}	P_{90}
Amagá	26.47	0.54	0.01
Non-prospective areas	38.53	2.59	0.11
Caguán - Putumayo	1,952.38	44.25	0.23
Catatumbo	612.76	31.64	1.11
Cauca - Patía	1,737.96	68.73	1.95
Cesar - Ranchería	4,644.63	118.44	2.40
Chocó	2,967.84	94.76	2.27
The Eastern Cordillera	2,132.84	83.32	2.38
Guajira	79,469.45	1,809.20	9.63
The Eastern Llanos	5,712.77	296.63	10.41
Sinú - San Jacinto	8,015.75	422.47	16.07
Tumaco	19,007.30	889.21	24.51
Urabá	13,597.94	862.95	34.62
The Lower Magdalena Valley	90,189.61	1,894.28	31.18
The Middle Magdalena Valley	300,054.28	4,792.46	62.47
The Upper Magdalena Valley	43,068.00	2,153.04	70.91
Vaupés - Amazonas	104,516.63	6,005.43	241.42
TOTAL	677,745.15	19,569.94	511.67

Table 8-24. OSOIP for the hypothetical resources evaluation category.

It was estimated that there could be 1,584.85 MMbbl of oil shale for the hypothetical resources evaluation category (46,345.60 MMbbl in P_{10} and 45.61 MMbbl in P_{90}) in areas forming part of the Colombian Park System (Parques Nacionales Naturales).

Figure 8-13 gives graphs of indicated resource distribution per basin. Figure 8-14 gives a comparison of the resources calculated for Colombia within a global framework.

Figure 8-13. Map of the Oil shale potential for the indicated resources evaluation category.

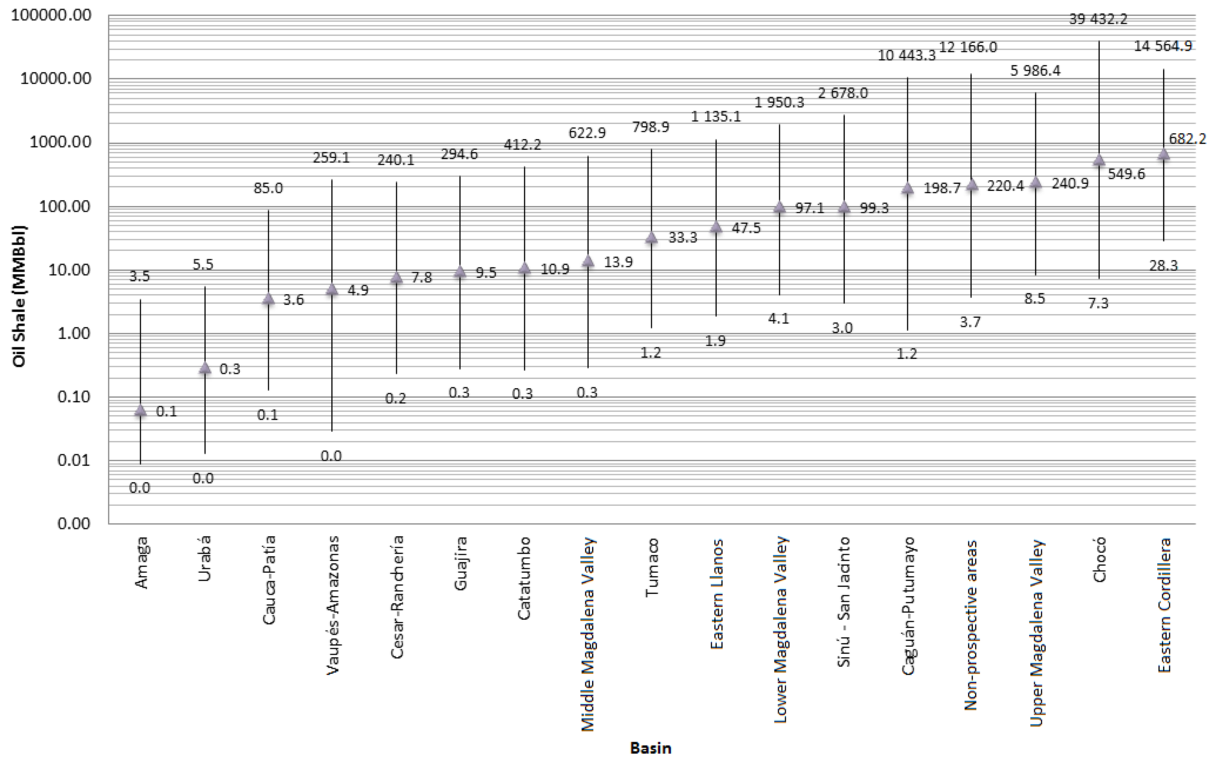

Figure 8-14. Oil shale potential for the indicated resources evaluation category.

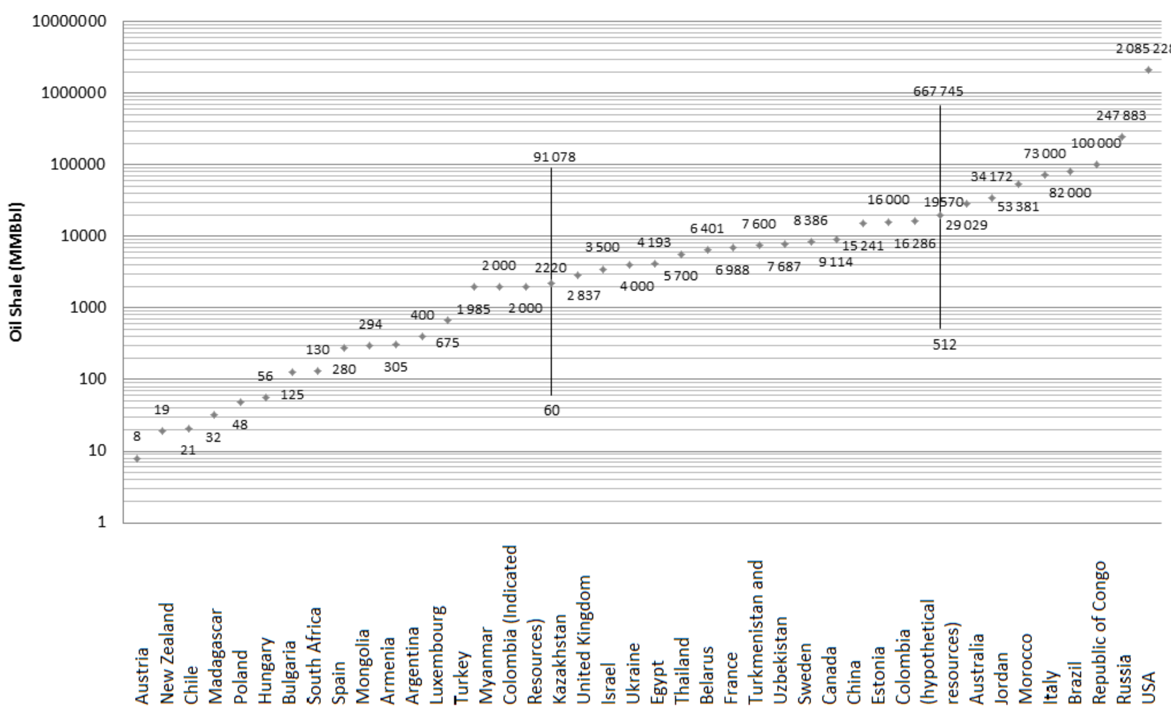

Figure 8-15. Comparing OSOIP for Colombia with that for other countries throughout the world.

8.4.8 Sensitivity analysis

The three variables to which the process was most sensitive were hydrocarbon content, aerial weighting factor and thickness. The order of sensitivity percentages for these three parameters varied according to the basin and resources evaluation category.

- Figure 8-16 shows the first pattern for the indicated resources category.

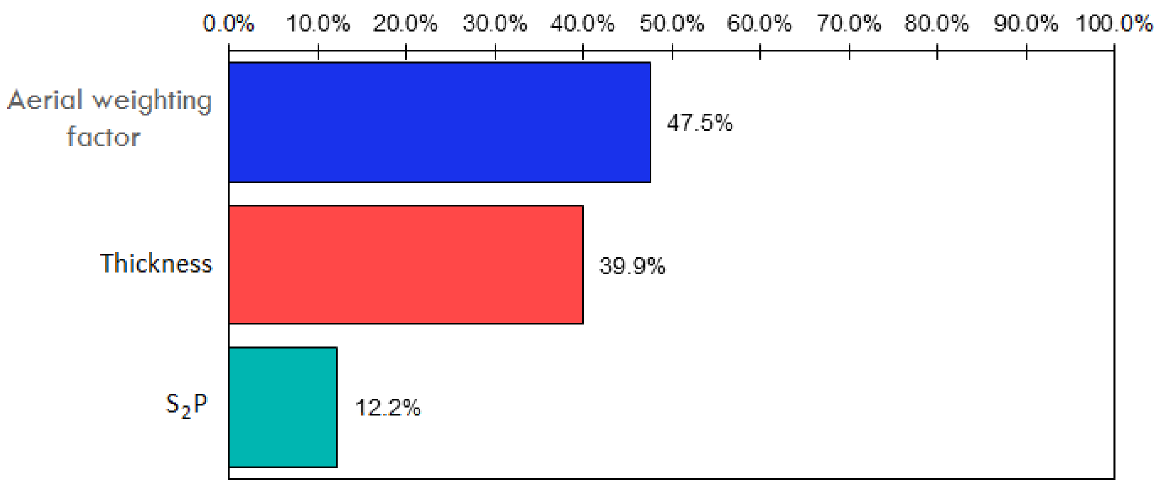

Figure 8-16. Sensitivity average 1 for the indicated resources category. This pattern was present in the Patía (Cauca), Ranchería (Cesar), the Eastern Cordillera, Guajira, the Eastern Llanos, San Jacinto (Sinú), Tumaco, Urabá, the Lower Magdalena Valley and the Upper Magdalena Valley basins

- Figure 8-17 shows the second pattern for the same category.

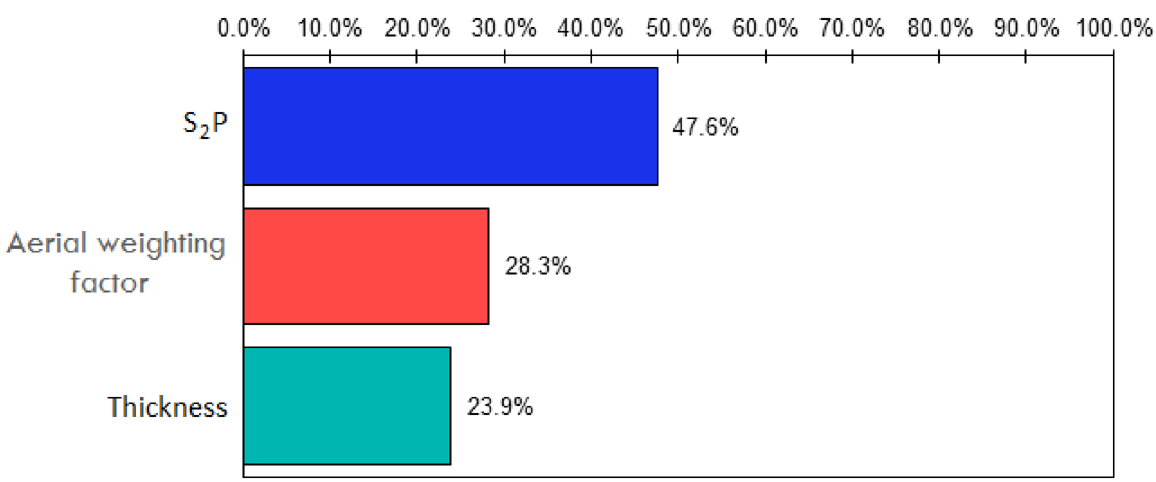

Figure 8-17. Sensitivity average 2 for the indicated resources category. This pattern was present in the Amagá, Caguán (Putumayo), Catatumbo, Chocó, the Middle Magdalena Valley and Vaupés (Amazonas) basins and in the so-called non-prospective areas.

- Likewise, sensitivity evaluated for the hypothetical resources category gave the first pattern shown in Figure 8-18.

ANH
AGENCIA NACIONAL DE HIDROCARBUROS

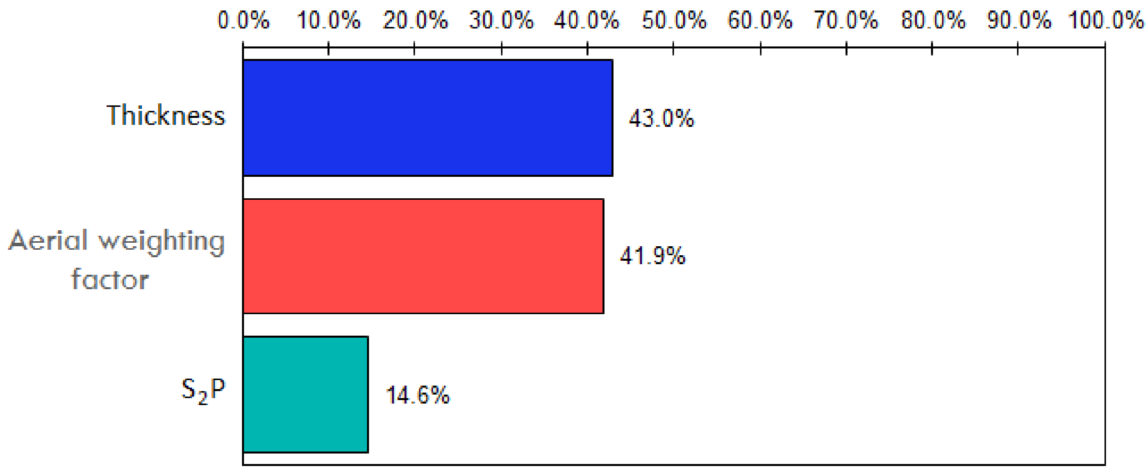

Figure 8-18. Sensitivity average 3 for the hypothetical resources category. This pattern was present in the Patía (Cauca), Ranchería (Cesar), the Eastern Cordillera, Guajira, the Eastern Llanos, San Jacinto (Sinú), Tumaco, Urabá, the Lower Magdalena Valley and the Upper Magdalena Valley basins.

- Figure 8-19 gives the second pattern for the hypothetical resources evaluation category.

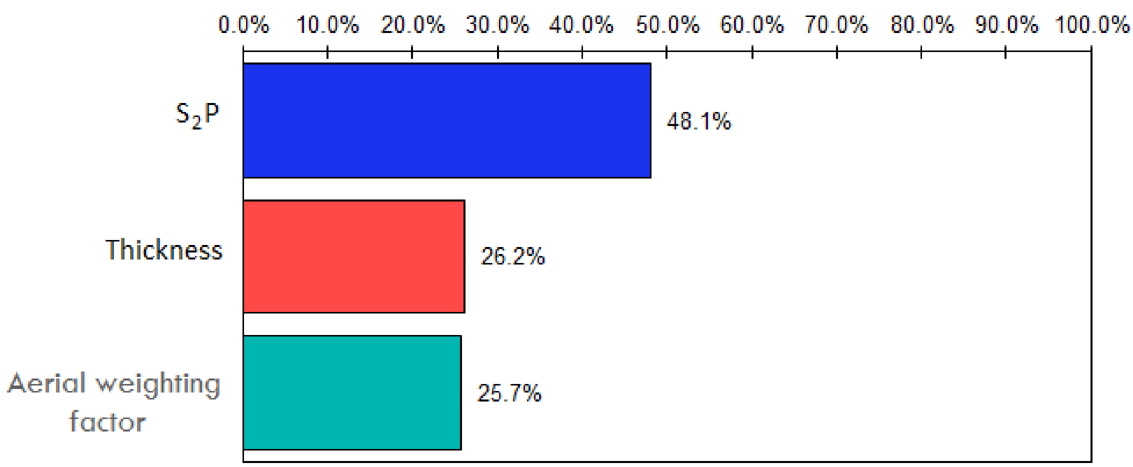

Figure 8-19. Sensitivity average 4 for the hypothetical resources category. This pattern was present in the Amagá, Caguán (Putumayo), Catatumbo, Chocó, Middle Magdalena Valley and Vaupés (Amazonas) basins and in the so-called non-prospective areas.

8.5 Conclusions

- The Eastern Cordillera was the basin having the greatest prospectivity in P_{90}, regarding the presence of oil shale, followed by the Upper Magdalena Valley and the Chocó basin (Figure 8-13);
- The previous order changed in P_{50}, showing the Eastern Cordillera basin to be most prospective, but placing the resources present in the Chocó above those for the Upper Magdalena Valley; and
- The prospectivity of the Lower Magdalena Valley, Caguán - Putumayo and Sinú - San Jacinto basins was also high, even though variability in the range of estimating the resource in the Caguán - Putumayo basin in should be considered.

8.6 Bibliography

Abercrombie, F. N. (1984). Chemical characterization of an oil shale bed lying within the Heath Formation, Fergus County, Montana. American Chemical Society.

Agencia Nacional de Hidrocarburos. (2010). Organic Geochemistry Atlas of Colombia. Bogotá: Universidad Nacional de Colombia.

Altius Minerals. (2009). Albert Oil Shale Project: Exploration Overview. New Brunswick.

Altun , N. E. (2006). Oil Shales in the World and Turkey; reserves, current situation and future prospects: A Review. Oil Shale (23), 211-227.

Anatoly , K. B. (2007). Oil shale as a prospective raw material for fuel, energy and chemical industries – to be or not to be? Oil Shale (24), 5-7.

Andersson, A. (1985). The Scandinavian Alum Shale. Sérvicio Geológico Sueco.

Australian Goverment. (2009). Condor Deposit. Consulted on the 6th January 2011, de Geosciences Australia: http://www.ga.gov.au/oceans/ea_ons_hills_Summ.jsp

Australian Goverment. (2009). Dauringa Deposit . Consulted on the 6th January 2011, de Geosciences Australia: http://www.ga.gov.au/provexplorer/provinceDetails.do?eno=20298

Australian Goverment. (2009). Mersey River Deposit. Consulted on the 6th January 2011, de Geosciences Australia: http://dbforms.ga.gov.au/pls/www/geodx.strat_units.sch_full?wher=stratno=25424

Bacon, C. A. (2000). The petroleum potential of onshore Tasmania: A review. Mineral Resources Tasmania. Geological Survey Bulletin (71), 93.

Bamburak, J. D. (1999). Cretaceous black shale investigations in the northern part of the Manitoba Escarpment. Consulted on the 6th January 2011, de Geological Services; Manitoba Industry Trade and Mines. Report of Activities: www.gov.mb.ca/stem/mrd/geo/field/roa99pdf/gs-28-99.pdf

Bellanca, A. (2001). Transition from marine to hypersaline conditions in the Messinian Tripoli formation from the marginal areas of the Central Sicilian Basin. Sedimentary Geology (140), 87-105.

Bencherifa, M. (2009). Moroccan Oil Shale, Research and Development. Office National Des Hydrocarbures Et Des Mines.

Blue Ensign Technologies. (2009). The Julia Creek Shale Oil Resource > [Consulted on the 6th January 2011]. Consulted on the Enero de 2011, de http://www.blueensigntech.com.au/

Chonglong, W. (2002). Study on dynamics of tectonic evolution in the Fushun Basin, Northeast China. Science in China, D Series (45), 14.

Clarey, M., & Thompson, M. (2010). Study Area. In D. Copeland, & M. Ewald, Available ground water determination, Green River Basin Water Plan II (page 35). Wyoming.

Connah, T. H. (1964). Torbanite Deposit - Alpha, Central Queensland. Department of Mines, Geological Survey of Queensland, Queensland.

Coxhell, S., & Fehlberg, B. (2000). Julia Creek Vanadium and Oil Shale Deposit. Applied Geoscientific Research and Practice in Australia (11), 13.

Draut, A. (2005). The Geology of Central and Southeastern Utah. Penrose Conference Field Trip Guide. Geological Society of America. University of California, (page 20). Utah.

Dyni, J. R. (2006). Geology and resources of some world oil shale deposits. USGS. Virginia: USGS Publication Warehouse.

Dyni, J. R. (2010). Survey of Energy Resources. World Energy Council.

Engel, M. A. (2006). Miocene Halictine Bee from Rubielos de Mora Basin: Spain. Novitates(3503), 10.

European Academies Science Advisory Council. (2007). Study on the E.U. oil shale industry viewed in the light of the Estonian Experience. Committee on Industry, Research and Energy of the European Parliament.

Fekry, Y. (2010). Potentiality of Black Shales in Egypt. Consulted on the Febrero de 2011 de www.medemip.eu/.../Oil%20Shale%20.../POTENTIALITY_OF_BLACK_ SHALES_IN_EGYPT.pdf, de Undersecretary for Mineral Resources. Ministry of Petroleum, Egypt: 18

Foster, C. B. (1982). Illustration of early tertiary (Eocene) plant microfossils from de Yaamba Basin. Geological Survey of Queensland, Department of Mines, Queensland.

Garetskii, R. G. (2004). Pripyat Trough: Tectonics, Geodynamics, and Evolution. Russian Journal of Earth Sciences(6), 217–250.

Garside, L. J. (1983). Nevada Oil Shale. Nevada Bureau of Mines and Geology, Nevada.

Gerta, K. (2004). Low Diversity, Late Maastrichtian and Early Danian Planktic Foraminiferal Assemblages of Eastern Tethys. Journal of foraminiferal Research(34), 49-73.

Glennie, K. W. (1998). Petroleum Geology of the North Sea: Basic Concepts and Recent Advances. Oxford: Wiley-Blackwell.

Graham, J. P. (2000). An Application of Sequence Stratigraphy in Modeling Oil Yield Distribution: The Stuart Oil Shale Deposit, Queensland, Australia. , 146 p. Work de grado (M.Sc. Applied Geology), . School of. Tesis M.Sc: Applied Geology, Queensland University of Technology, School of Natural Resouce Science, Queensland.

Gross, S. (1977). The Mineralogy of the Hatrurim Formation, Israel. Geological Survey of Israel Bulletin(70), 1-80.

Gurov, E. (2003). Ejecta of the Boltysh Impact Crater in the Ukrainian Shield. Impact Markers in Stratigraphic Records(3), 179-202.

Harrington, E. (2005). Technical Report on the Poker Flats Property, Carlin Mining District, Elko County, Nevada, USA. Reliance Geological Services Inc.

Harvie, B. A. (2010). The Shale-Oil Industry in Scotland 1858–1962. I: Geology and History. Oil Shale(27), 354-358.

Hassaan, M., & Ezz-Eldin, M. (2007). The Black Shale in Egypt: A Promising Tremendous Resource of Organic Matter. CSPG-CSEG Convention. Calgary.

Ho, A. (2009). Oil Shale Annual Report. Esperance Minerals N.L, Sydney.

Holger, L., Bernhard , S., Hans, J., & Josef , P. (2000). Trace Element Distribution in Palaeozoic Black Shales:"Kupferschiefer" (Germany) and Exshaw Formation (Canada). Journal of Conference Abstracts, 52(2), 656.

Hutton, A. C. (1990). Classification, Organic Petrography and Geochemistry of Oil Shale. Lexington University of Kentucky, Institute for Mining and Minerals Research., Kentucky.

INGEOMINAS. (2007). Mapa Geológico de Colombia. Escala 1:2'800.000. . Bogotá.

Israel Goverment. (2010). Mineral Resources - Oil Shale. Consulted on the 21 de Febrero de 2011, de Geological Survey of Israel: http://www.gsi.gov.il/Eng/Index.asp?CategoryID=113&ArticleID=160

James, H. G. (1980). An Assessment of Oil Shale Technologies. Washington, D.C: U.S Government Printing Office.

Johnson, H., & Crawford, P. (2004.). Strategic Significance of America's Oil Shale Resource. US Department of Energy.

Jordan Goverment. (2010). The Hashemite Kingdom of Jordan, Hydrocarbons, Oil Shale. Consulted on the 21 de Febrero de 2011, de Natural Resource Authority: http://www.nra.gov.jo/index.php?option=com_content&task=view&id=34&Itemid=44

Kara, G., & Korkmaz, S. (2008). Organic Geochemistry, Depositional Environment And Hydrocarbon Potential of the Tertiary Oil Shale Deposits in NW Anatolia, Turkey. Oil Shale(25), 444–464.

LeMone, D. (2008). Uraniferous Phosphates: Resource, Security Risk, or Contaminant. . Annual Waste Management Conference, Waste Management Symposia, (pág. 15). Phoenix.

Loughnan, F. C., & Roberts, I. F. (1983). Buddingtonite (NH4-feldspar) in the Condor Oil Shale Deposit, Queensland, Australia. Mineralogical Magazine(47), 327-334.

Louw, S. J., & Addison, J. (1985). Studies of the Scottish Oil Shale Industry. History of the Industry, Working Conditions, and Mineralogy of Scottish and Green River Formation Shales. Final report Vol. 1., US Department of Energy.

Macualey, G. (1984). Cretaceus Oil Shale Potential of the Prairie Province, Canada. Consulted on the 28 de Enero de 2011, de Geological Survey of Canada : www.gov.mb.ca/stem/.../shales/shale_cretaceous_potential2.pdf

Matthews, R. D., & Feldkirchner, H. (1983). The Distribution and Regional Correlation of Devonian Oil Shales in the Eastern United States. Symposium on Geochemistry and Chemistry of Oil Shale, (pág. 12). American Chemical Society.

Mukhopadhyay, P. K. (2008). Mississippian Lacustrine Horton Formation Source Rocks from Nova Scotia and New Brunswick, Eastern Canada: Major Shale Gas and Oil Shale Resource Plays. Search and Discovery(10167), 33.

Mukhopadhyay, P. K. (2004). Evaluation of Petroleum Potential of the Devonian-Carboniferous Rocks from Cape Breton Island, Onshore Nova Scotia. Nova Scotia Department of Energy, Antigonish.

Newell, N. (1948). Key Permian Section, Confusion Range, Western Utah. Geological Society of America Bulletin(59), 1053-1058.

Nizar, A.-J. (2009). Geomorphological and Geological Constraints on the Development of Early Bronze Chert Industries at the Northern Rim of the Al Jafr Basin, Southern Jordan. Mediterranean Archaeology and Archaeometry(9), 17-27.

Pápay, L. (2001). Comparative Analysis of Hungarian Maar-Type Oil Shales (Alginites) on the Basis of Sulfur Content. Oil Shale(18), 139-148.

Peter, F. F. (1996). Tertiary Basins of Spain, the Stratigraphic Record of Crustal Kinematics ,. Cambridge University Press.

Raseroka, A. L. (2009). Natural Gas and Conventional Oil Potential in South Africa's Karoo Basins. Search and Discover(90100).

Regina, B. (1990). Aromatic Hydrocarbons in the Paraiba Valley Oil Shale. Organic Geochemistry(15), 351-359.

Russell, P. L. (1990). Oil Shales of the World, their Origin, Occurrence and Exploitation. New York: Pergamon Press.

Schmitt, L. J. (1989). Aerial Distribution of Oil Shales with Associated Mineral Resources and Metal Anomalies in the Western United States and Alaska. Consulted on the 21 de Febrero de 2011, de U.S.G.S Miscellaneous Field Studies Map 2091: http://pubs.er.usgs.gov/usgspubs/mf/mf2091/

Schora, F. C. (1983). Progress in the commercialization of the Hytort Process. Eastern Oil Shale Symposium (págs. 183–190). Lexington: University of Kentucky, Institute for Mining and Minerals Research.

Smith , W. D., & Naylor , R. D. (1990). Oil Shale Resources on Nova Scotia. Economic Geology Series Nova Scotia, 59.

Smith, J. W. (1983). The Chemistry which Created Green River Formation Oil Shale. Symposium on Geochemistry and Chemistry of Oil Shale (págs. 9-11). American Chemical Society .

Stanfield, K. E., & Frost, I. C. (1949). Method of Assaying Oil Shale by a Modified Fischer Retort. U.S. Bureau of Mines .

Steele, H. (1979). The Economic Potentialities of Synthetic Liquid Wasls from Oil Shale. Massachesetts: Arno Press Inc.

Suwannathong, A., & Khummongkol, D. (2007). Oil Shale Resource in Mae Sot Basin, Thailand . 27th Oil Shale Symposium Memories. Colorado: CERI Mines.

Ventura, R. (2009). Geochemical and Thermal Effects of a Basic Sill on Black Shales and Limestones of the Permian Irati Formation. Journal of South American Earth Sciences(28), 14–24.

Viive , V. (2006). Conodonts of the Kiviõli Member, Viivikonna Formation (Upper Ordovician) in the Kohtlasection, Estonia. En. Proceedings of the Estonian Academy of Sciences, 213–340.

Vizmap. (2010). Map of resources de Australia. Consulted on the 6th January 2011, de Yaamba Deposit: http://www.vizmap.com.au/NRM/Commodities/493580.htm

Yen, T. F., & Chilingarian, G. V. (1976). Oil Shale. Amsterdam: Elsevier Scientific Publishing Company.

Zhu, J. (2006). Resource Status and Development Application Stratagem of Oil Shale in Maoming Basin. 26th Oil Shale Symposium Memories. Colorado: College of Earth Science, Lilin Univerity. Oil and gas Resource Stratagem Research Center.

8.7 Appendixes

Digital files in the ANH'S Document Center:

- ✓ “Base de Datos Oil Shale Internacional.xlsx”
- ✓ “Base de Datos Oil Shale Colombia.xlsx”

9 SHALE GAS AND SHALE OIL

Shale gas and shale oil may be defined as hydrocarbons associated with shale formations (US Department of Energy, 2009). Organic material-rich shale formations which were previously considered simply as source rocks or seals for accumulations of gas in stratigraphically-associated sands and carbonates are now defined as shale formations (US Department of Energy, 2009). Such deposits are composed of sedimentary rocks having predominantly clay-sized particle content and also considerable percentages of organic material, making them prone to generate and store important amounts of gaseous hydrocarbons.

The amount of hydrocarbons which could be present in shale usually depends on the rock's wealth of organic material and the degree of maturity reached. Resources of around 3,350 MMbbl and 20.81 Tcf have been estimated in Eagle Ford shale, one of the basins having the greatest development regarding the exploitation of this resource (US Department of Energy, 2011).

The effects of the emergence of this type of production began to become evident at the end of 2005, since when the price of natural gas has become decoupled from crude prices (i.e. they are no longer linked) (Rios, 2010). This resource's development has undoubtedly been intensifying in many nations since that time. These countries' energy profile has changed regarding their estimates of yet-to-find shale gas and shale oil, their investment in exploration, and eagerness to break with traditional schemes tied to conventional production horizons regarding hydrocarbons in an attempt to migrate towards prospecting non-conventional resources.

9.1.1 Classification

Shale is included in a varied group of deposits called continuous-type (unconventional) hydrocarbon accumulations (Schmoker, 2005). These consist of large volumes of oil- or gas-bearing rock in which the presence of hydrocarbon does not depend on the water column. These belts cannot be evaluated in view of the foregoing regarding bottom contacts (i.e. water-oil contact (WOC) or gas-oil contact (GOC)), as in conventional deposits.

These deposits usually have a large aerial extension and could occur below rocks totally saturated by water below WOC or GOC. Their hydrocarbon load covers the whole belt, lacks a trap or seal and has extremely low matrix permeability. Shale deposits also develop abnormal pressure (whether high or low) and are normally associated with source rocks.

The areas in which these accumulations give the best production characteristics are known as "sweet spots", a term in some ways comparable with that of "fields" for conventional deposits.

9.1.2 Origin and formation

The clays in shale were initially deposited in the form of mud, in low energy settings such as lake- or ocean-type environments having low or zero water circulation. Fine particles suspended in these environments could fall slowly together with small microorganisms, the remains of algae, plants and animals. However, an imbalance in the oxygen supply may have developed if they became buried rapidly, transforming the environment into an anoxic one inhibiting the chemical or biological sequestrators responsible for organic material degradation. Favourable preservation conditions for hydrocarbon development would thus become produced.

Pressure and temperature gradually increase whilst sediment load becomes buried over shale-forming materials. Compaction is responsible for transforming the clays (normally tabular) into thin layers which then become laminated shale stratifications during lithification. The preserved organic material becomes decomposed during initial heating under pressure (diagenesis), thereby producing an insoluble material called kerogen.

If burial increases, the rock and its constituents undergo catagenesis in which kerogen slowly becomes converted into bitumen and then into a liquid or gaseous hydrocarbons (wet gas). Additional heat becoming incorporated may cause the remaining kerogen to react producing carbon and the change from liquid phases to hydrocarbon phases (dry gas), thus entering a stage called metagenesis (Figure 9-1).

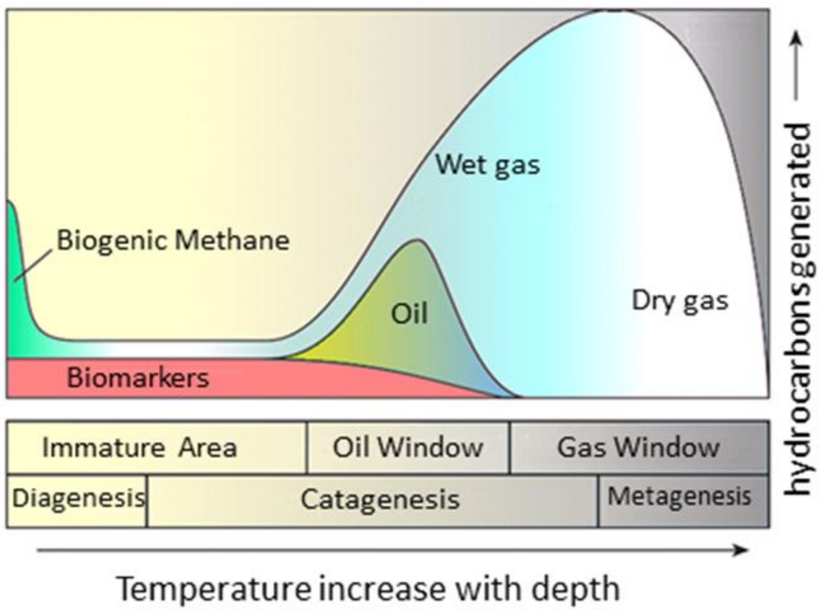

Figure 9-1. Kerogen transformation, modified from Boyer et al., (2006).

All processes involved in transforming kerogen into hydrocarbons are usually known as "maturing". Oil, wet gas or dry gas would thus be generated depending on how this process evolves and the type of kerogen involved. Kerogen types I and II are associated with generating liquids and type III with gases (Figure 9-2).

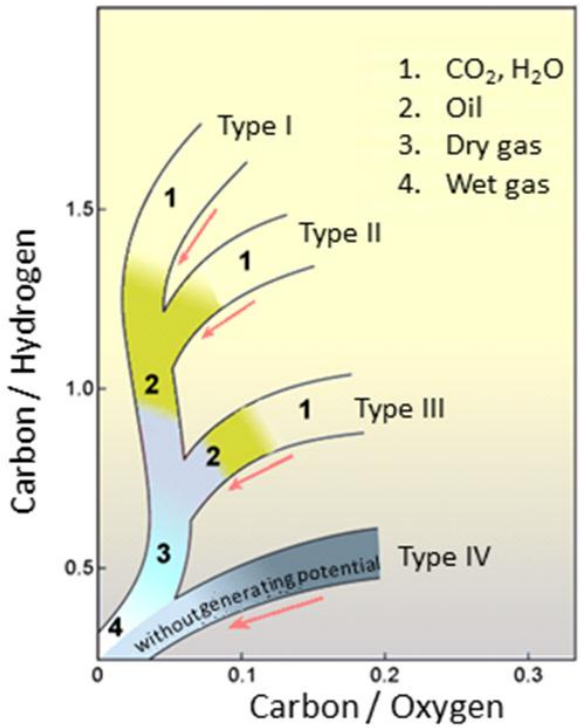

Figure 9-2. Van Krevelen diagram, modified from Boyer et al., (2006). The pale red lines indicate the direction of increased maturity.

All processes involved in transforming kerogen into hydrocarbons are usually known as "maturing". Oil, wet gas or dry gas would thus be generated depending on how this process evolves and the type of kerogen involved. Kerogen types I and II are associated with generating liquids and type III with gases (Figure 9-2).

9.1.3 Shale characterization

Rock's potential for storing and producing economic volumes of gas can be evaluated by identifying specific characteristics such as the type of kerogen, maturity, total organic content, the matrix's mineralogy, porosity, permeability and gas concentration.

9.1.3.1 Some fundamental geochemical analysis

Total organic content (TOC) is directly related to the amount of hydrocarbons possibly generated and thus its importance; TOC values between 0.5% and 2.0% are usually considered the lowest limit for defining prospective background intervals. This range of values is associated with gas shale quality between "very poor" and "regular" (Boyer et al., 2006).

Vitrinite reflectance tests (Ro) on maceral material in gas shale are fundamental when establishing thermal maturity. These tests give an indirect measurement of the temperatures to which rock has been submitted, thereby leading to identifying the generation window which could be entered (Figure 9-1) and thus the type of hydrocarbon generated. Gas shale thermal maturity could vary from marginal (0.4% Ro to 0.6% Ro) to mature/post-mature (0.6% Ro to 2% Ro) and these could also contain gas ranging from biogenic to thermogenic.

9.1.3.2 Some fundamental petrophysical analysis

Considering the form of the clays and their deposition and lithification, then it is to be expected that shale would develop almost zero vertical permeability and extremely low horizontal permeability (in the nano Darcy order). Permeability is thus one of the most sensitive variables and one of the most important production parameters to be determined. Figure 9-3 gives a comparative scheme for the order of magnitude of permeability in shale.

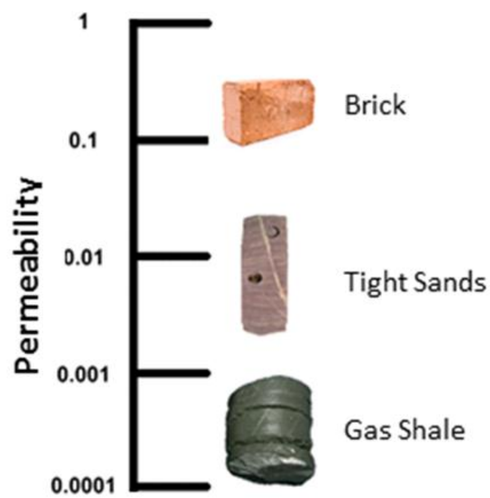

Figure 9-3. Comparative scheme for shale permeability.

The hydrocarbons in shale could be stored in rock in three ways: in the local porous system, as gas in solution in intraporal water and absorbed in minerals or organic material within pores, micropores and microfractures in the rock matrix. The latter form of retention is usually responsible for the accumulation of the greatest amount of gas.

Characterising porosity and identifying the type which could support production are essential when evaluating future recovery scenarios and defining the appropriate stimulation mechanism. Figure 9-4 compares conventional porosity in an arenite and that in shale.

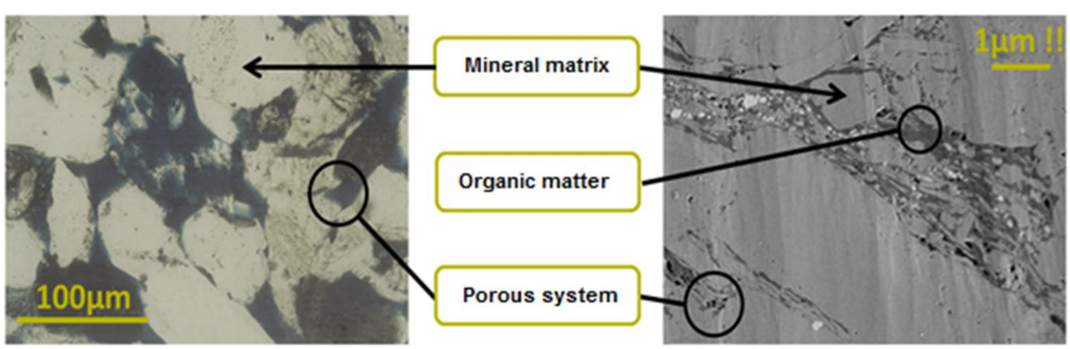

Figure 9-4. Comparing the porosity of a conventional arenite (left panel) and that of gas shale (right panel), modified from Loucks et al., (2009).

Filtering cartridge desorption tests carried out on nucleus fragments are amongst the traditional forms of measuring gas content in rock, but these do not reflect interstitial gas or dependence on pressure (Boyer et al., 2006). Measuring desorption isotherms (such as the Langmuir isotherm) leads to more realistic results regarding maximum gas content related to deposit pressure.

Mineralogical description and identifying the type of clay predominating in rock play a basic role in shale exploitation. Designing stimulation treatments and selecting the areas of rock in which such work could be carried out are affected by such characterisation, in turn, affecting assessment of a particular play's technical prospectivity.

9.1.3.3 Identifying prospective intervals

The methodology proposed by Passey et al., (1990) led to identification in organic material-rich well areas, from a set of basic records such as sonic (DT), deep resistive (ILD) and gamma ray (GR) records. The cross between the DT and pseudo-sonic (DtR) curves obtained from ILD records led to inferring the type of fluid saturating the porous space. Both these curves are parallel in rocks saturated by water and lacking organic material, and could even become overlapped, since both respond to variations in rock porosity; however, such curves cross in hydrocarbon-saturated or organic material-rich rocks, resulting in their notable separation (Figure 9-5).

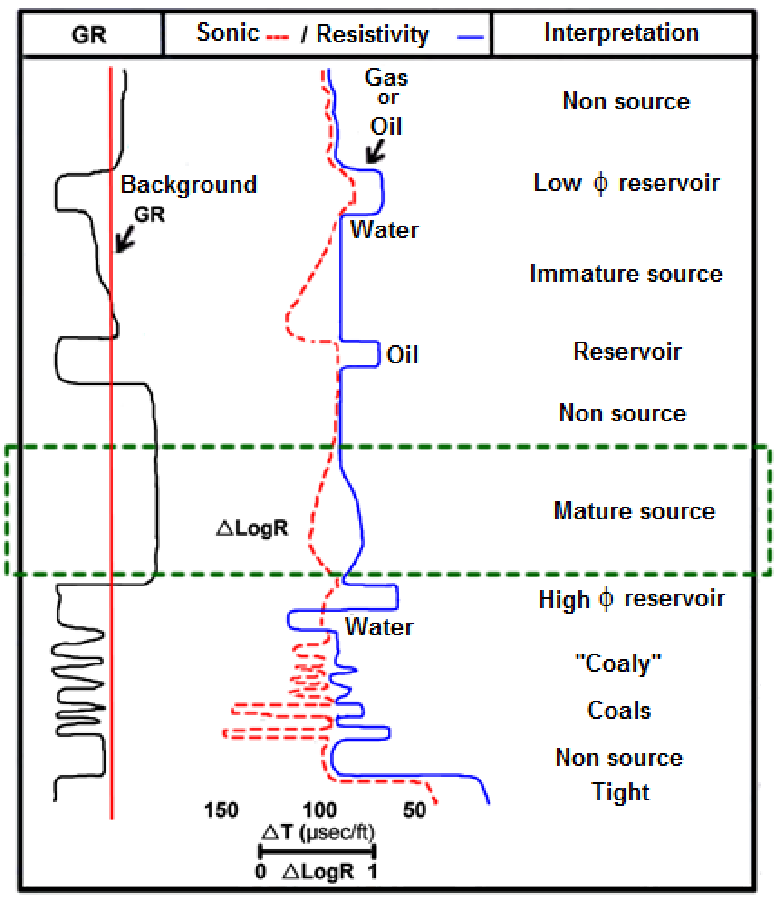

Figure 9-5. A diagram showing the form given by DT and ILD records in organic material-rich areas, modified from Passey *et al.*, (1990). The green dashed area shows the possible presence of associated hydrocarbons.

The separation occurring in the intervals of organic material-rich source rock and prospectivity for generating shale gas and shale oil is produced by two effects; the sonic curve responding to the presence of kerogen, low density and low speed and the resistive curve responding to the fluid in a particular formation. Separation is only due to slow curve response in low maturity or immature areas. As well as the effect of the sonic record, the resistivity curve increases in mature areas due to the presence of the hydrocarbons so generated.

The distinction between the intervals of sand saturated with hydrocarbons in conventional deposits and organic material-rich matures areas in non-conventional deposits is shown in the gamma ray record. As this is a lithological record it allows differentiating the areas of clay. Passey et al., (1990) have thus provided a methodology facilitating prospective net thickness to be obtained for shale deposits.

9.1.3.4 Exploitation methods

Hydraulic fracturing (fracking) is one of the well stimulation techniques used for developing shale projects because it allows connecting a deposit's well areas to be hydraulically isolated. The amount of recovered hydrocarbon is directly related to the good management of these techniques. The volume of stimulated rock depends on the complexity of the induced fracture and thus the expected recovery; such recovery also depends on the number of frackings made in the same interval.

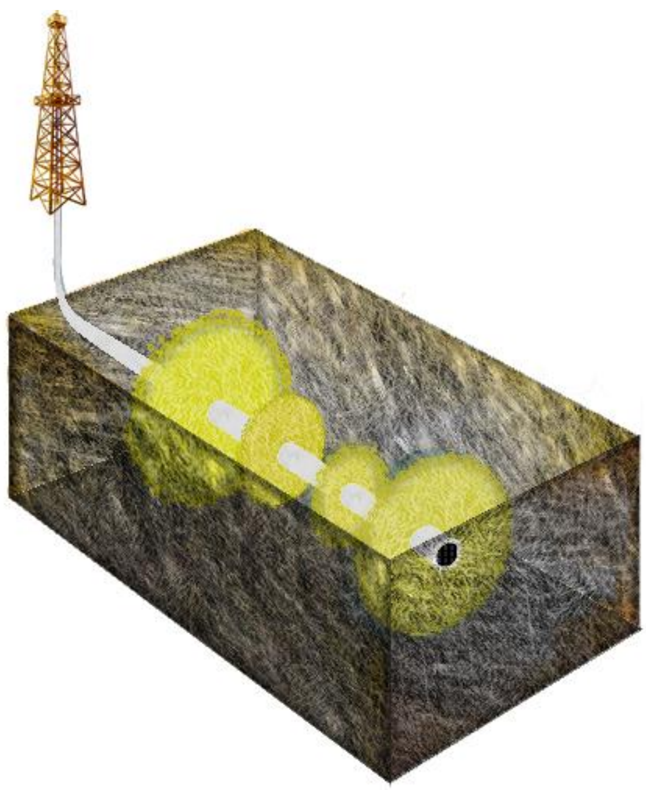

Figure 9-6. Illustrative diagram of multi-stage fracking.

Figure 9-6 illustrates multistage fracking in which the fractures are simultaneously induced in the same pumping. Combining this stimulation method with horizontal perforation technologies and geo-navigation (geosteering) in shale formations provides viability dad techniques for such exploitation projects.

9.1.3.5 Worldwide panorama

The largest shale reserves are found in the USA (the leading country in developing this resource). Some eastern and northern European countries are in a stage aimed at assessing prospects, the same as other countries like China and India. The presence of this resource has already been evaluated in Australia and southern South-America and development plans for already identified plays are already in place. Table 9-1 shows the potential identified for some countries on different continents.

Country	Shale gas resources (Tcf)	Country	Shale gas resources (Tcf)
USA	3,284	Germany	33
Canada	1,490	Holland	66
Mexico	2,366	Sweden	164
Colombia	78	Norway	333
Venezuela	42	Denmark	92
Argentina	2,732	The UK	97
Bolivia	192	Algeria	812
Brazil	906	Libya	1,147
Chile	287	Tunes	61
Paraguay	249	Morocco	108
Uruguay	83	South Africa	1,834
Poland	792	China	5,101
Lithuania	17	India	290
Kaliningrad	76	Pakistan	206
The Ukraine	197	Turkey	64
France	720	Australia	1381
			Total
			25,300

Table 9-1. Shale gas resources, taken from US Department of Energy (2011).

9.1.4 Some source rock packages in Colombia

The most well-known generating (source) rock belts in Colombia date from the Cretaceous and Palaeogene ages, even though there is evidence concerning the possible existence of Palaeozoic rocks. Such rocks were deposited in marine environments in conditions involving little circulation (anoxic) and high precipitation of organic material (Ryan and Cita, 1977; Thiede and Van Andel, 1977; Arthur et al., 1987; Erbacher et al., 2001).

Some of the formations present in the Middle Magdalena Valley (Rosablanca, Paja, Tablezo, Simití, La Luna and Umir), Cesar - Ranchería (Lagunitas, Aguas Blancas, Laja – La Luna and Molino) and Catatumbo (Tibú, Mercedes, Aguardiente, Capacho, La Luna, Colon, Mito - Juan) basins, deposited during the Cretaceous period and associated with events affecting their organic material enrichment are considered as being sources of Colombia's (or even the world's) most prolific hydrocarbon deposits (West, 1996).

La Luna, Simiti and Tablezo formations are amongst the most fertile source rocks of the Middle Magdalena Valley, giving 3.5% TOC and 0.9% Ro on average.

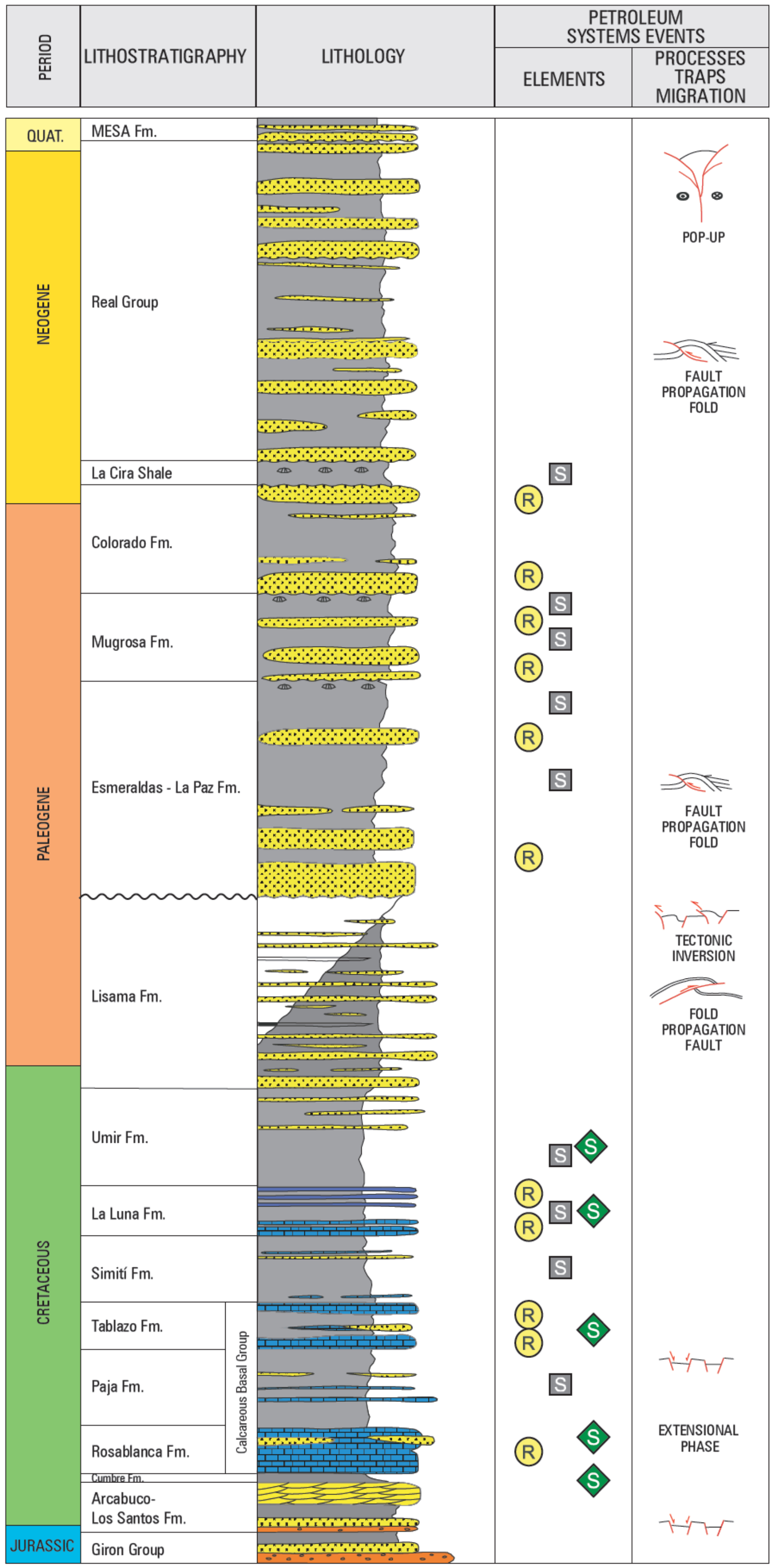

Figure 9-7. Petroleum system in the Middle Magdalena Valley basin, modified from Mojica, Arévalos, & Castillo (2009).

The Molino, Laja - La Luna, Lagunitas and Aguas Blancas formations in the Cesar - Ranchería, basin are in a generation phase, giving an average 1% to 1.4% TOC.

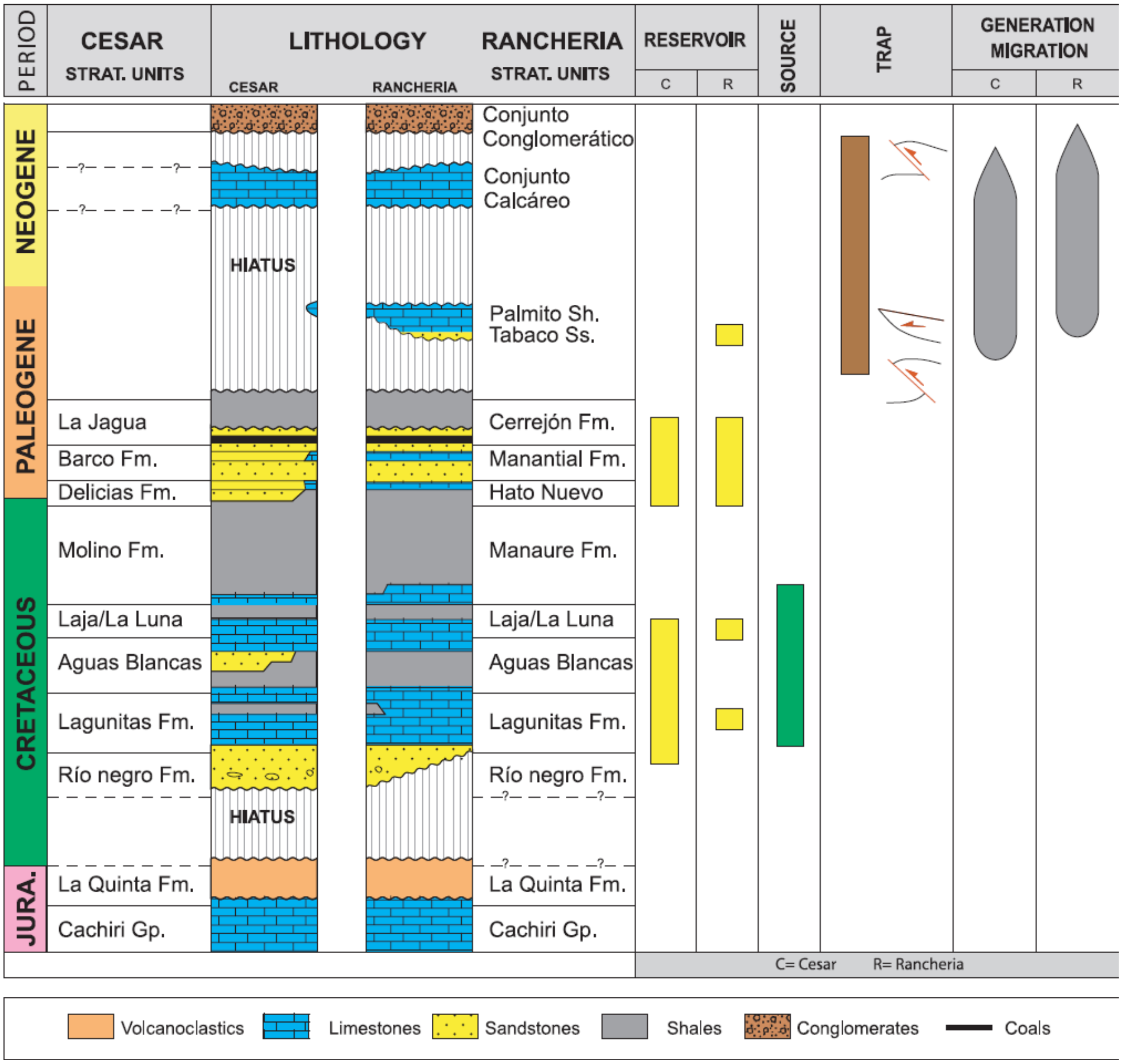

Figure 9-8. Petroleum system in the Cesar - Ranchería basin, modified from Mojica, Arévalos, & Castillo (2009).

La Luna formation is the main source in the Catatumbo basin, having a 1.5% to 9.6% TOC and 200 ft average thickness (Agencia Nacional de Hidrocarburos, 2007).

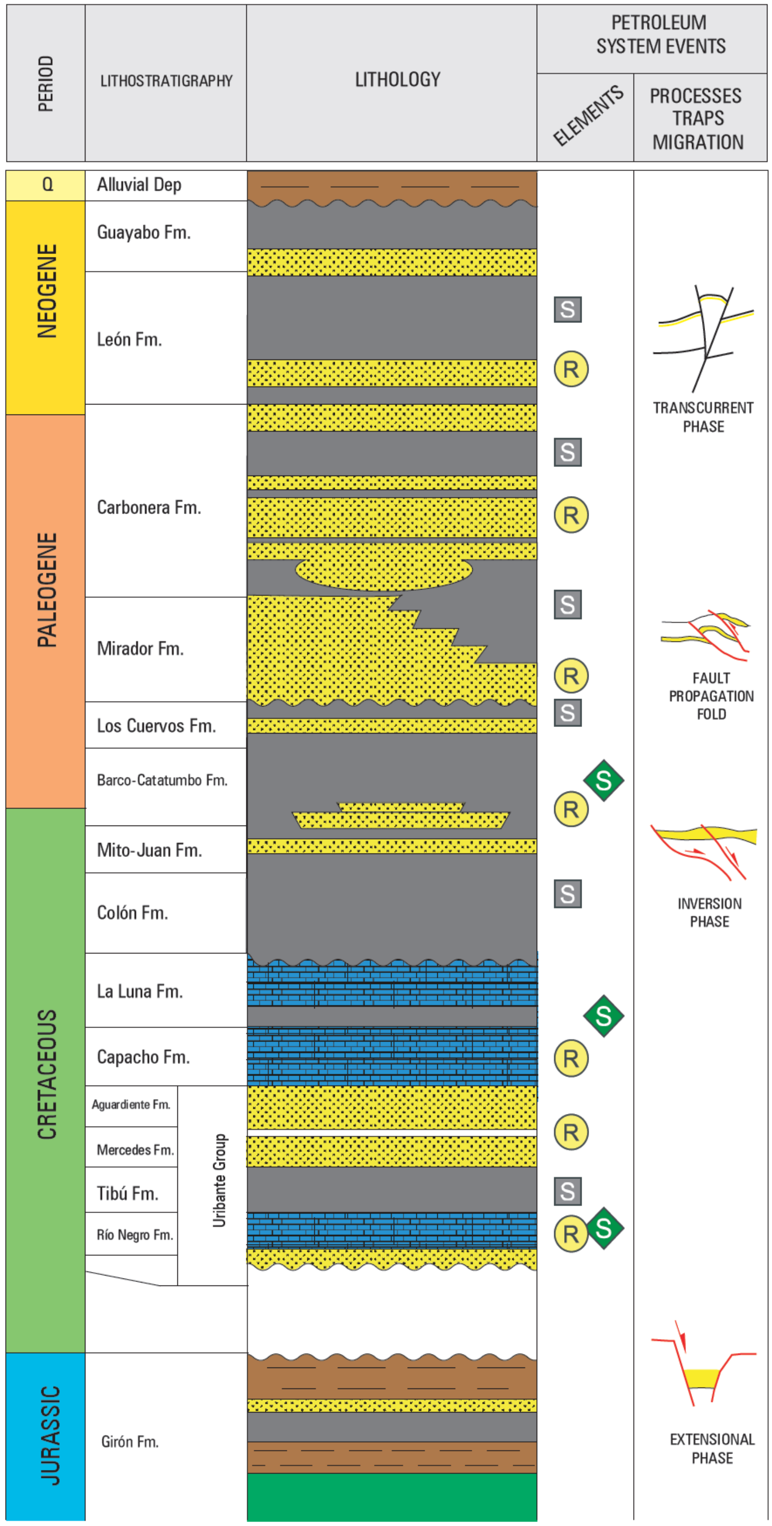

Figure 9-9. Petroleum system in the Catatumbo basin, modified from Mojica, Arévalos, & Castillo (2009).

Features identified in seismic profiles and corroborated by well data have led to delimiting source rock belts in three basins. Continuous reflectors in them may be associated with certain non-conformities and stratigraphic sequence limits, such as maximum regressive surfaces (MRS) or maximum flooding surfaces (MFS). Pre-Cretaceous non-conformity and Turonian MFS for the aforementioned basins (Figures 9-7, 9-8 and 9-9) could be taken as the limit and base for the main rock source package, as well as their associated seismic reflectors being easily interpretable. Similar operational concepts may be extended to other basins, even those having a different age.

9.2 Data and hypotheses

Appendix 9-1 contains files from the "ShaleGas.tks" project which were loaded with seismic and well information supplied by ANH for the Middle Magdalena Valley, Cesar - Ranchería and Catatumbo basins and also provide all the necessary interpretations.

This project shows the horizons interpreted, the loaded time-depth curves, the maps of speed for such horizons, the surfaces obtained in time and depth and the isopach maps of source rock in the aforementioned three basins. The project also includes the well records used and correlations made for identifying the thickness of the areas having potential organic material content using the methodology proposed by Passey et al., (1990).

9.2.1 International database

The digital file in Appendix 9-2, forming an integral part of this document, gives data extracted from a report entitled, "Review of Emerging Resources: U.S. Shale Gas and Shale Oil Play" (US Department of Energy, 2011) and from "Shale gas data release" (Beaton et al., 2009, 2010) published by the US energy and Canadian geological information services.

Langmuir volume and TOC data extracted from the Canadian reports were used for inferring a possible function regarding the concentration of absorbed gas for Colombia, as well as gas shale density values. The net-to-gross ratio was incorporated from the US publication for calculating the shale gas potential in Colombia in a second scenario.

9.2.2 National (Colombian) database

The digital file in Appendix 9-3, also forming an integral part of this document, gives the source rock volume values for the three basins interpreted, as well as the values extrapolated for the remaining basins, the thickness of the areas having potential organic material content, the thickness of the isopachs in the wells evaluated, the net-to-gross values calculated and TOC and S_1 information extracted from the Geochemical Atlas of Colombia (Agencia Nacional de Hidrocarburos, 2010) for calculating absorbed and free gas concentration.

The statistical distribution for the last three variables is given for each basin and all goodness-of-fit test parameters supporting the selected probability functions are included.

9.2.3 Hypotheses

9.2.3.1 Hypothesis 1

The source rock belt lying between Pre-Cretaceous non-conformity and Turonian maximum flooding surface seismic horizon is the most prospective regarding the presence of continuous hydrocarbon accumulations.

Note. Due to limitations regarding access to data when developing this work, a systematic approach to defining shale packets in other basins could not be adopted. Basins such as the Eastern Llanos and that of Caguán - Putumayo, which have traditionally been discarded as attractive prospects for hydrocarbons in shale (mainly shale gas) could form part of another scenario which should be carefully evaluated in future work. The Apiay-4 well in the Eastern Llanos and SA-11 and SM-4 wells in Caguán - Putumayo , all relatively close to the Macarena range which divides both basins, have advantages regarding gas (Ro% > 1.3). There is little geochemical information, but something similar happens in the Marañon basin, specifically in the Devonian units (Cabanillas Fm). Gas occurrences near this border for the basins may reflect the Palaeozoic play's upthrust (wells were relatively superficial < 3,000 m). If this is so, then such play could contain important resources due to its extension.

9.2.3.2 *Hypothesis 2*

The source rock belt continuity considered here would suppose a correlation between its volume and the extent of the basin bounding it. It would thus be possible to infer the volume of source rocks in as yet non-interpreted basins.

9.2.3.3 *Hypothesis 3*

The sonic record curve's intersection of the deep resistivity curve, when such curves have an appropriate scale and comparison unit, would lead to identifying areas having organic material content and the appropriate maturity for generating and storing hydrocarbons in shale within intervals having high gamma ray curve values, thereby making them deviate from the record's general tendency (Passey et al., 1990).

9.2.3.4 *Hypothesis 4*

The quotient between thickness with organic material content (net thickness), calculated for the whole interval recorded for a given well, and the thickness of the source rock package, obtained from seismic interpretation, is representative of the net-to-gross (NTG) ratio for such well's source rock belt (even when this cannot be counted in the numerator) regarding intervals in younger rocks than those defining the such belt's limits.

9.2.3.5 *Hypothesis 5*

The concentration of absorbed gas for rock samples in Colombia can be obtained from their TOC by applying the ratios found in Canadian samples for TOC and Langmuir volume.

9.2.3.6 *Hypothesis 6*

The free hydrocarbon values (S1) obtained in pyrolysis tests on source rock samples compiled from the Geochemical Atlas of Colombia (Agencia Nacional de Hidrocarburos, 2010) are a direct measurement of free gas concentration in such rocks.

9.2.3.7 *Hypothesis 7*

Net-to-gross (NTG) pattern in Colombia could be approached from the statistical distribution obtained for values extracted from a determined amount of wells.

9.2.3.8 *Hypothesis 8*

The statistical distributions obtained for free and absorbed gas concentrations, from the data available in the Geochemical Atlas of Colombia (Agencia Nacional de Hidrocarburos, 2010), are representative of such variables' pattern from basin to basin.

9.2.3.9 *Hypothesis 9*

A second scenario can be established for estimating resources for validating the results obtained in a first scenario by assigning the pattern given by such ratio in other areas of the world to the net-to-gross variable (Appendix 9-2).

9.2.3.10 *Hypothesis 10*

Taking the ratios for available shale gas and shale oil in other basins around the world, then it should be possible to estimate YTF shale oil resources in Colombia from available shale gas resources, and vice versa.

9.3 Methodology

The following equation was used for evaluating the shale gas potential in each Colombian basin:

$$\boldsymbol{OSGIP = 1 \cdot 10^{-6} * V_{gross} * NTG * \rho_{bulk} * \left(G_a + G_f\right)} \qquad \textbf{(9-1)}$$

OSGIP: original shale gas in place (in situ) (Tcf)

V_{gross}: source rock belt volume (109m^3)

NTG: net-to-gross thickness quotient with potential organic material content, net thickness and total source rock belt thickness (ft/ft)

ρ_{bulk}: total rock density (Kg/m^3)

G_f: free gas concentration (ft^3/ton)

G_a: absorbed gas concentration (ft^3/ton)

The procedure for estimating shale gas resources considered the following stages:

- A project was created in which all the seismic and well information supplied by ANH for the Middle Magdalena Valley, Cesar - Ranchería and Catatumbo basins was loaded.
  - ✓ Source rock volume in the 3 basins was calculated following the reflectors enclosing this rock package, involving the following steps:
    - Pre-Cretaceous non-conformity and Turonian maximum flooding surface seismic horizons were interpreted;
    - Surfaces for limit and base were produced;
    - Speed maps were calculated for limits and bases from the time depth curves available;
    - The surfaces so created were transformed into depths;

ANH AGENCIA NACIONAL DE HIDROCARBUROS

    - Isopach maps were obtained for the source rock belts; and
    - The belts' volume was calculated.
  - ✓ The methodology proposed by Passey et al., (1990) was used for determining shale thickness with organic material content, as follows:
    - The curves for the sonic (DT), deep resistivity (ILD) and gamma ray records (GR) were edited for those wells having the 3 curves;
    - The LogR curve was calculated from the deep resistivity logarithm;
    - A well by well Cartesian graph was drawn from the DT record points in the ordinate, the LogR curve in the abscissa and a colour scale regarding GR record value;
    - Areas having high GR, DT and LogR values were identified on the graphs;
    - A line was fitted separating the areas identified from the points' general tendency, taking into account that the methodology advanced by Passey et al., (1990) proposed a slope of 50 units from the DT record for each LogR record unit for such line (shale line);
    - A pseudo-sonic (DtR) curve was calculated from the equations for the lines obtained, well by well;
    - The calculated records were graphed in the way suggested by Passey et al.'s methodology (1990); GR record in track 1, ILD in track 2 and DT and DtR records in track 3 and inverse scale;
    - The intervals were shaded in which DT record values were higher than those for the DtR;
    - A cut-off point was defined in the GR for distinguishing between areas of sand and clay; and
    - The net thickness of areas having mature organic material content in shale intervals was calculated, well by well.
- A database was built from the most relevant features of shale gas prospects around the world; another included the geochemical characterisation of rock samples in Canadian prospects (Appendix 9-2):
  - ✓ Information was extracted from the "World shale gas resources: an initial assessment of 14 regions outside the United States" (US Department of Energy, 2011) report concerning age, extension, thickness organic material-rich, TOC, thermal maturity, total gas concentration and shale gas resources estimated for prospective areas around the world:
    - The net-to-gross ratio value was calculated from total maximum thickness and net thickness; and
    - Goodness-of-fit tests were run for determining the distribution best fitting the international Net-to-gross data, for applying this in the second scenario for estimating resources.
  - ✓ Information was extracted from the "Shale Gas Data Release" (Beaton et al., 2009, 2010) concerning TOC, S_1, S_2, S_3, Langmuir pressure, Langmuir volume and sample depth:
    - Langmuir volume values were transformed into absorbed gas concentration using Langmuir pressure and sample depth (for core data), supposing normally pressurised formations; and
    - Lineal regression was done between TOC and absorbed gas concentration values.

- A database was built using TOC, S_1, source rock belt volume in each basin, net-to-gross, free and absorbed gas concentrations and statistical analysis information for approaching the variables involved in the estimating resource equation (equation 9-1), and evaluation scenarios for Colombia (Appendix 9-3):
  - ✓ Information was extracted from the Geochemical Atlas of Colombia (Agencia Nacional de Hidrocarburos, 2010) regarding organic material content and S_1 for well samples, excluding that concerning outcrops:
    - Absorbed gas concentration was calculated by taking the regression obtained from the Canadian data and TOC from the samples in Colombia;
    - S_1 values were transformed to free gas concentration, assuming a gas just consisting of methane; and
    - Statistical analysis determined the distributions best fitting the free gas and absorbed gas concentrations data, basin by basin.
  - ✓ Representative net-to-gross (NTG) values in the respective wells were obtained from the net thickness values and thickness shown on the isopach maps:
    - The best statistical distribution was determined for NTG.
  - ✓ The distributions found were associated with those found regarding the pattern of the respective variables.
  - ✓ Lineal regression was made between the interpreted basins' area and the calculated belts' volume:
    - The regression equation led to determining source rock volume in the non-interpreted basins.
- Monte Carlo simulations were run using OSGIP formulation (equation 9-1) and assuming NTG, rock density, free gas and absorbed gas concentrations as random variables, and source rock volume as fixed parameter.
- The simulation was repeated using a fresh NTG distribution inferred from international data (Appendix 9-2).
- A shale gas/shale oil ratio was established from data regarding other basins around the world where volumetric information is available regarding the resource, aimed at inferring an average participation for both resources in the shale belts evaluated.

The way in which this methodology for making estimates was used led to establishing two scenarios:

9.3.1 Scenario 1

The net-to-gross ratio obtained from interpreted seismic and well data in Colombia was taken in this scenario.

9.3.2 Scenario 2

The distribution of net-to-gross ratio was substituted in this scenario for a new one obtained for the total and net thicknesses of different prospects around the world (Appendix 9-2).

9.4 Results

Evaluating of the shale gas potential required interpreting seismic horizons and some well records; 1,001 seismic lines were thus compiled, of which 387 were used for interpreting the reflectors of interest. The electronic records for 119 wells were also reviewed, editing and analysing those for 37 wells in 3 basins which were chosen for their content, quality, integrity and spatial distribution. Figure 9-10 shows the map with the location of the lines and wells so reviewed.

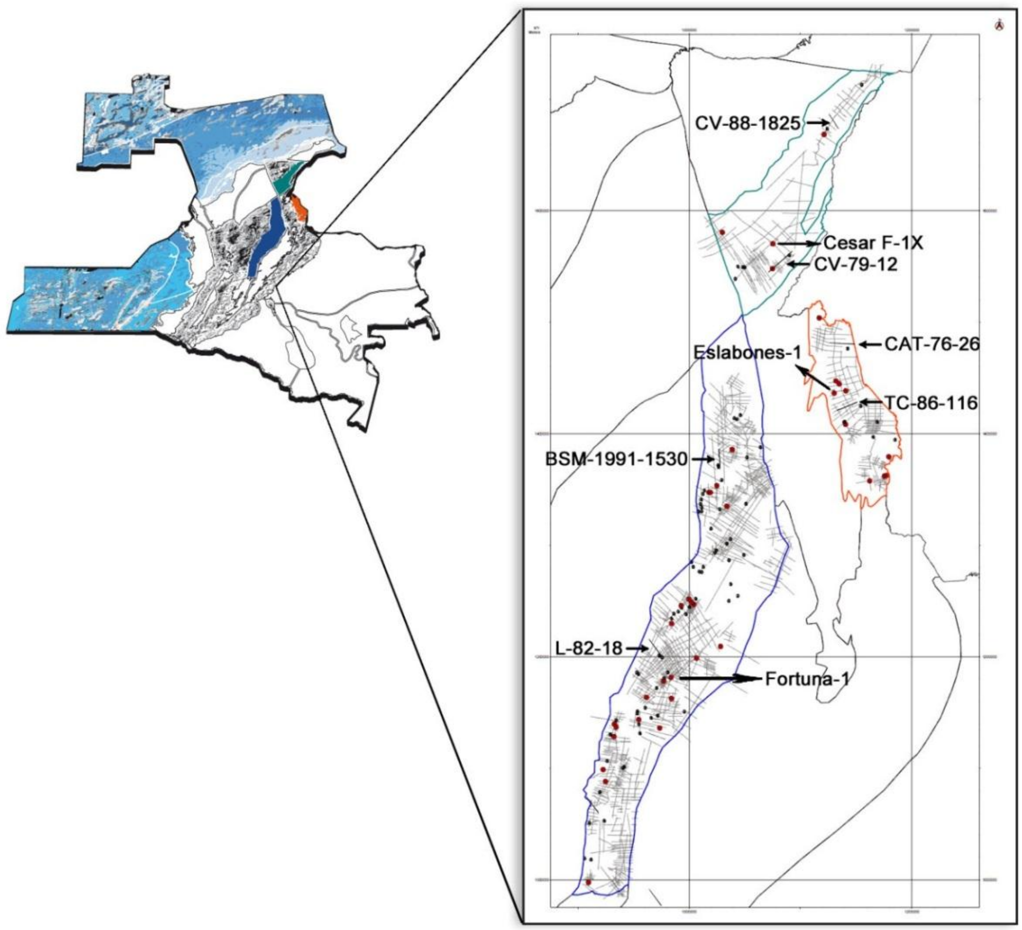

Figure 9-10. Seismic lines and wells reviewed. The wells selected for edition and analysis are shown in red. The labels show refer to some of the seismic lines and wells interpreted.

Goodness-of-fit tests were run for most variables included in equation 9-1 to ascertain their pattern. Random variables were fit to different distributions, first by estimating the parameters regarding such pattern from the data according to each distribution and then goodness-of-fit tests were run for identifying the best statistical value (least deviation regarding accumulated distribution). This report only gives the results of the best fits and estimates; the others are reported in the digital files mentioned in Appendixes 9-2 and 9-3.

9.4.1 Source rock volume

$$V_{sr} = 833.88 * A_b - 1933.1 \qquad \textbf{(9-2)}$$

V$_{sr}$: volume of source rock belt (109 m^3)

A$_b$: basin area (103 km^2)

Equation 9-2 (produced from the regression of source rock volume and basin area points) was applied for determining the volume of these belts in the other basins. Table 9-2 gives the values estimated.

Basin	Basin area (10^3 km^2)	Source rock volume (10^9 m^3)
The Middle Magdalena Valley	32.95	25,581
Catatumbo	7.72	4,709
Cesar - Ranchería	11.67	7,549
Amagá	2.82	**419**
Caguán - Putumayo	110.22	**89,976**
Cauca - Patía	12.80	**8,740**
Chocó	38.50	**30,170**
The Eastern Cordillera	71.75	**57,899**
La Guajira	13.79	**9,568**
The Eastern Llanos	224.94	**185,641**
Sinú - San Jacinto	39.59	**31,079**
Tumaco	23.67	**17,803**
Urabá	9.43	**5,930**
The Lower Magdalena Valley	37.98	**29,742**
The Upper Magdalena Valley	21.48	**15,981**
Vaupés - Amazonas	154.96	**127,287**

Table 9-2. Estimated volume for source rock belt considered per basin.

Equation 9-2 was obtained from calculating the points of source rock volume, in line with the proposed methodology; important intermediate results were obtained. A description of such results is given below.

9.4.1.1 Horizons

Identifying the horizons corresponding to Pre-Cretaceous non-conformity and Turonian maximum flooding surface, on some of the seismic lines supplied by ANH, led to their interpretation and follow-up throughout the Middle Magdalena Valley, Cesar - Ranchería, and Catatumbo basins. Figures 9-11 to 9-16 give examples of the interpretations so made.

9.4.1.1.1 The Middle Magdalena Valley

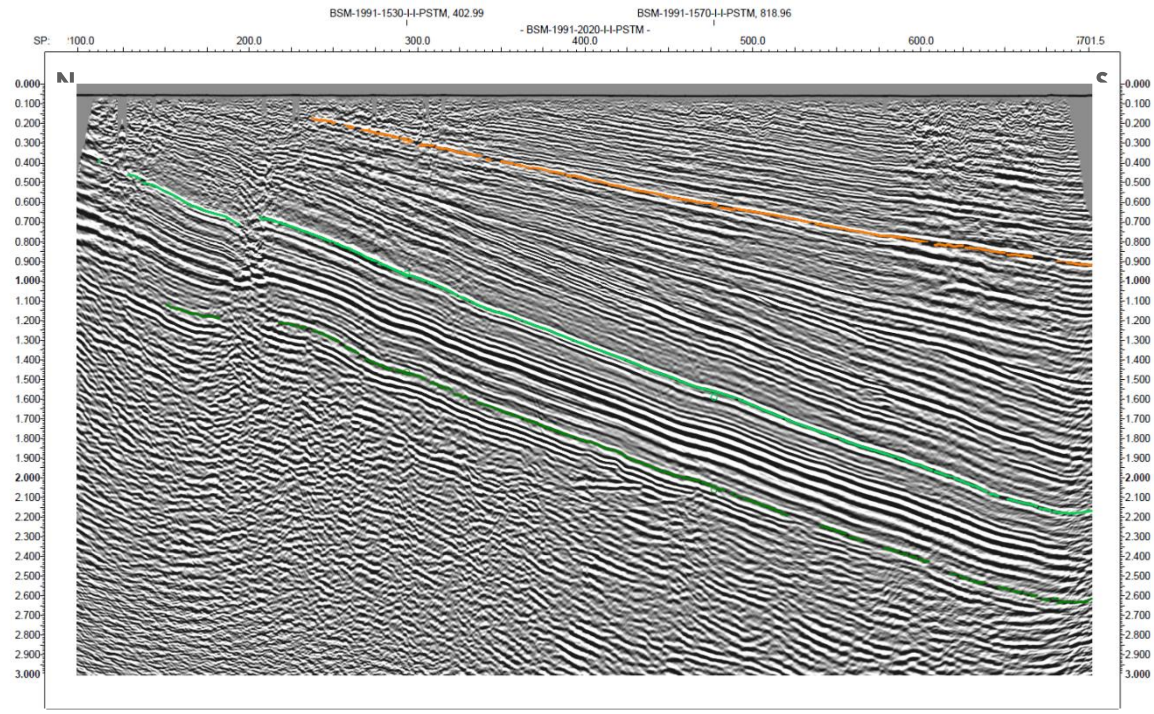

Figure 9-11. Seismic line L-82-18 located in the central part of the Middle Magdalena Valley basin. Reflector continuity for generated rock belt base and limit. Dark green shows the reflector for Pre-Cretaceous non-conformity and yellow the reflector for Miocene non-conformity. The location of the line is given on the map in Figure 9-10.

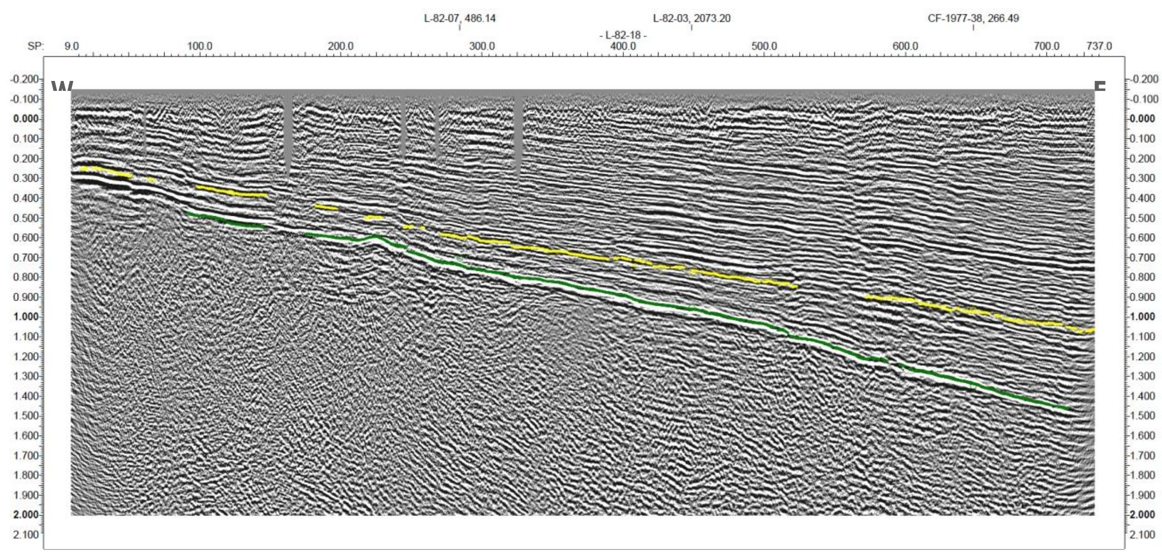

Figure 9-12. Seismic line L-82-18 located in the central part of the Middle Magdalena Valley basin. Reflector continuity for generated rock belt base and limit. Dark green shows the reflector for Pre-Cretaceous non-conformity and yellow the reflector for Miocene non-conformity. The location of the line is given on the map in Figure 9-10.

9.4.1.1.2 Cesar – Ranchería

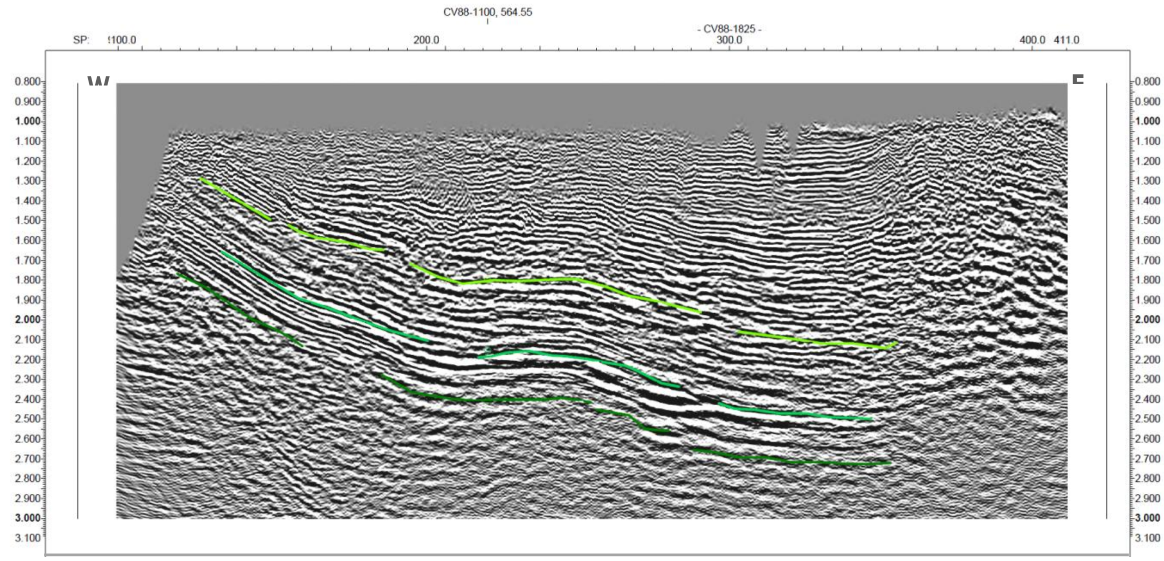

Figure 9-13. Seismic line CV-88-1825 located in the north of the Cesar - Ranchería basin. Reflector continuity for generated rock belt base and limit considered. Dark green shows the reflector for Pre-Cretaceous non-conformity, light green the reflector for the Turonian maximum flooding surface and lemon green the reflector for the Cretaceous limit. The location of the line is given on the map in Figure 9-10.

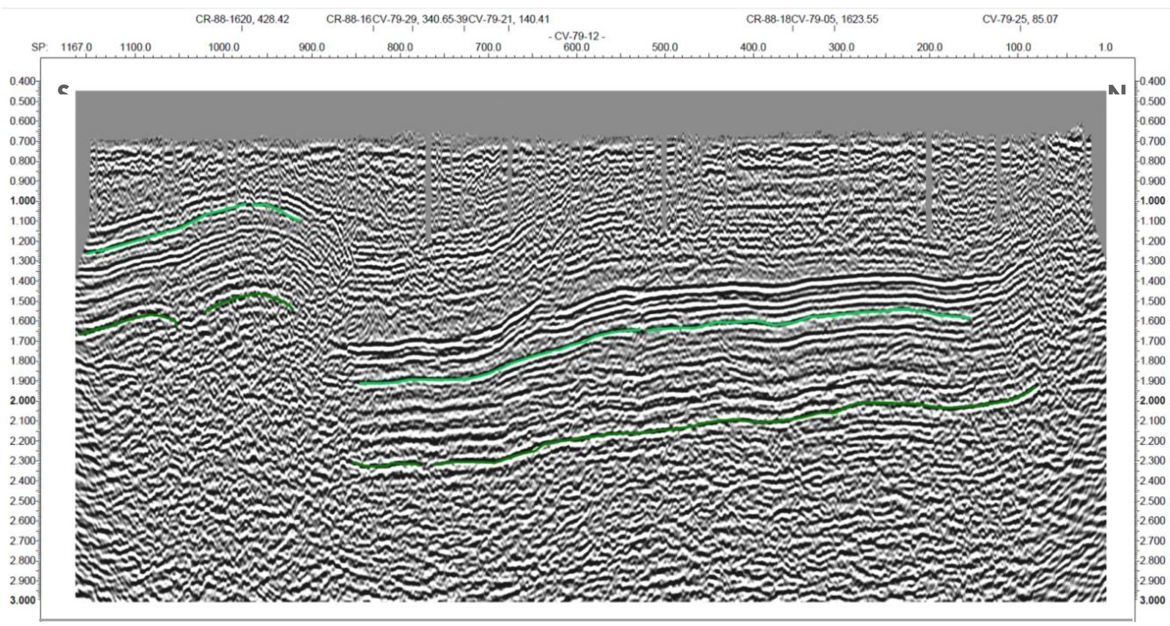

Figure 9-14. Seismic line CV-79-12 located to the south of the Cesar - Ranchería basin. Reflector continuity for generated rock belt base and limit considered. Dark green shows the reflector for Pre-Cretaceous non-conformity and Turonian maximum flooding surface reflector is shown in light green. The location of the line is given on the map in Figure 9-10.

9.4.1.1.3 Catatumbo

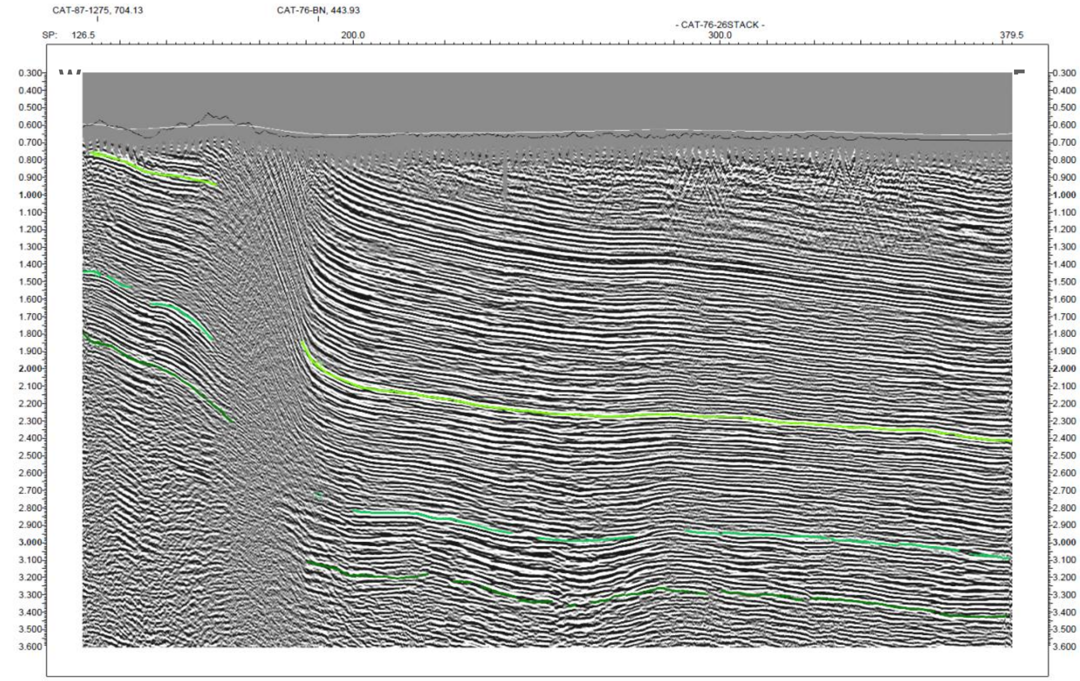

Figure 9-15. Seismic line CAT-76-26 located in the north of the Catatumbo basin. Reflector continuity for generated rock belt base and limit considered. Dark green shows the reflector for Pre-Cretaceous non-conformity, light green the reflector for the Turonian maximum flooding surface and lemon green the reflector for the Cretaceous limit. The location of the line is given on the map in Figure 9-10.

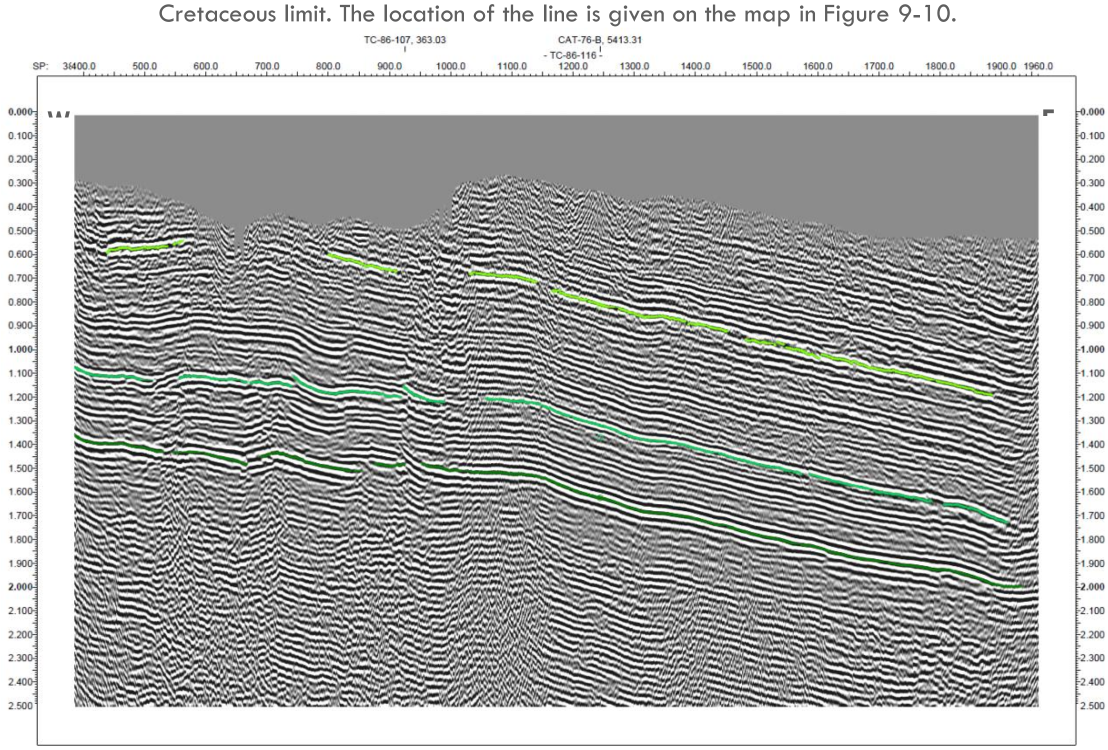

Figure 9-16. Seismic line TC-86-116 to the south of the Catatumbo basin. Reflector continuity for generated rock belt base and limit considered. Dark green shows the reflector for Pre-Cretaceous non-conformity, light green the reflector for the Turonian maximum flooding surface and lemon green the reflector for the Cretaceous limit. The location of the line is given on the map in Figure 9-10.

9.4.1.2 Surfaces in time

Figures 9-17, 9-18, and 9-19 give the surfaces in time for the limits and bases, generated from the interpolation "flex gridding" algorithm from the computational package used.

9.4.1.2.1 Middle Magdalena Valley

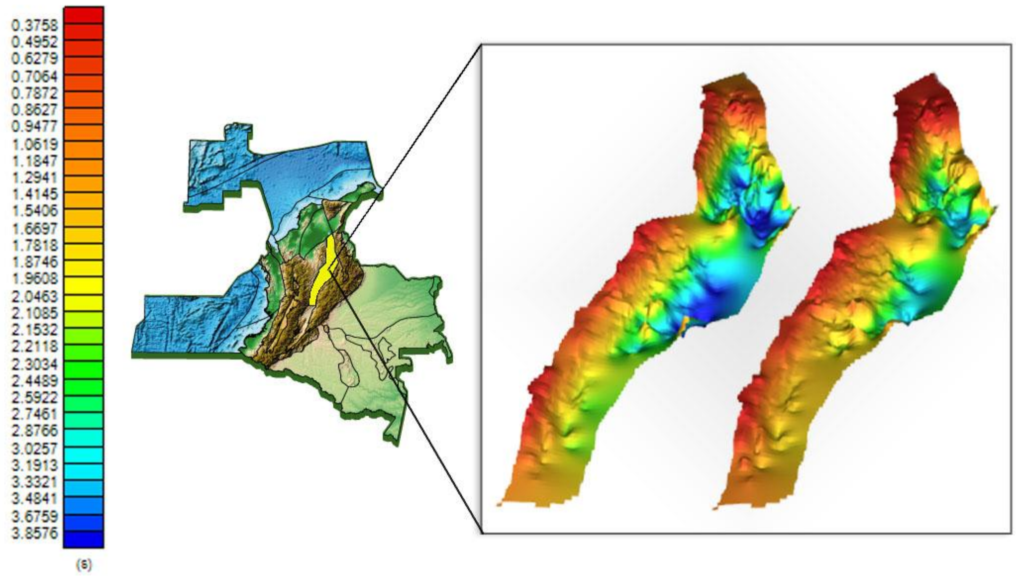

Figure 9-17. Source rock belt base and limit in time in the Middle Magdalena Valley basin. On the left-hand side, Pre-Cretaceous nonconformity between 0.09 s and 4.72 s and, on the right-hand side, Turonian maximum flooding surface between 0.0019 s and 4.39 s.

9.4.1.2.2 Cesar – Ranchería

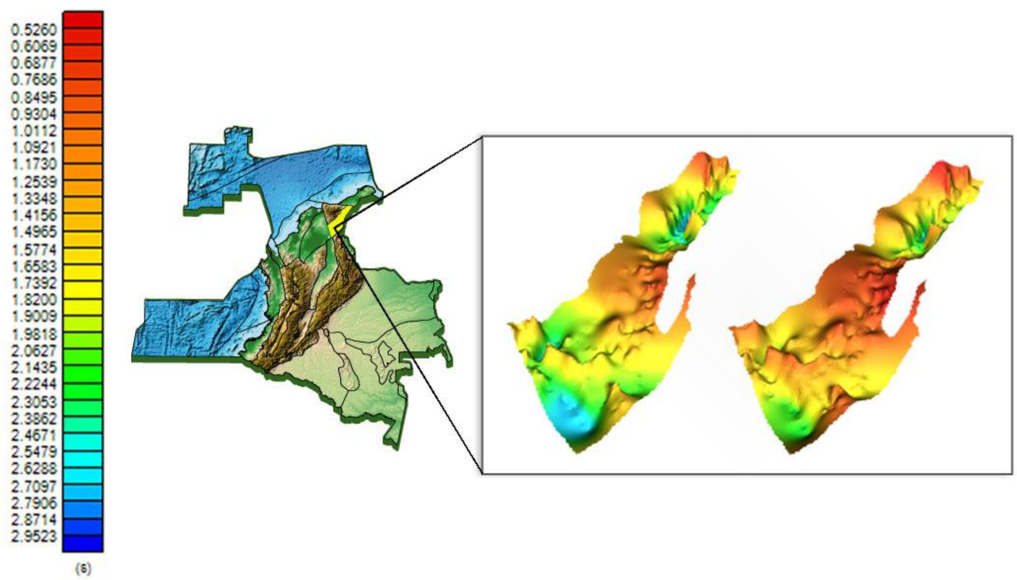

Figure 9-18. Source rock belt base and limit in time in the Cesar - Ranchería basin. On the left-hand side, Pre-Cretaceous nonconformity between 0.69 s and 3.03 s and, on the right-hand side, Turonian maximum flooding surface between 0.44 s and 2.83 s.

9.4.1.2.3 Catatumbo

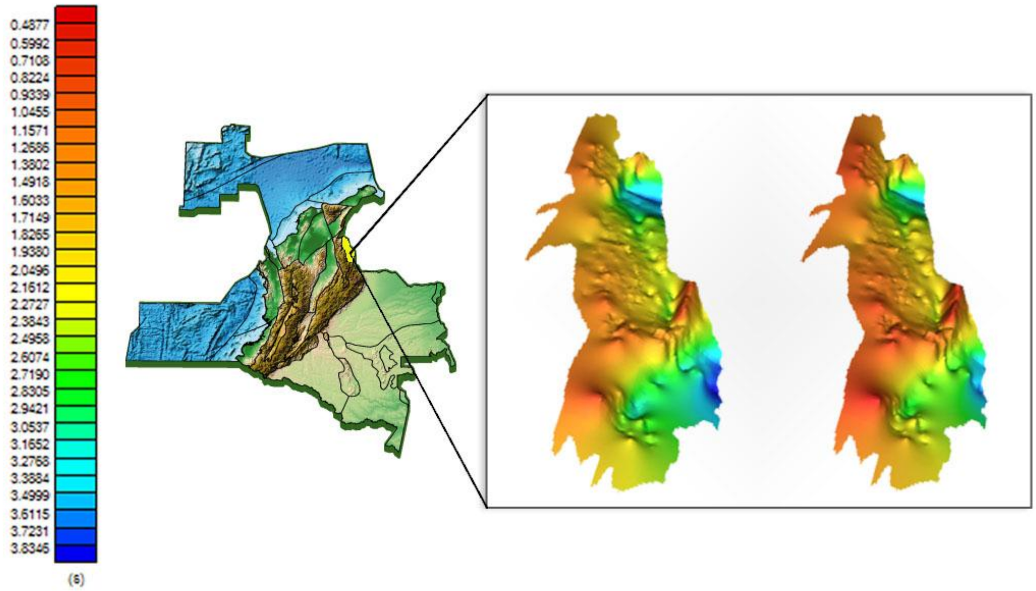

Figure 9-19. Source rock belt base and limit in time in the Catatumbo basin. On the left-hand side, Pre-Cretaceous nonconformity between 0.67 s and 3.94 s and, on the right-hand side, Turonian maximum flooding surface between 0.37 s and 3.69 s.

9.4.1.3 In depth surfaces

The time–depth curves from the 49 wells led to speed maps being drawn for source rock belt limit and base. Such maps are not given in this report, but may be consulted in the "ShaleGas.tks" project folder. Transforming surfaces in time using the speed maps obtained was direct. Figure 9-20 shows 3 of the time-depth curves used. Figures 9-21, 9-22 and 9-23 give the surfaces in depth calculated for the 3 basins in question.

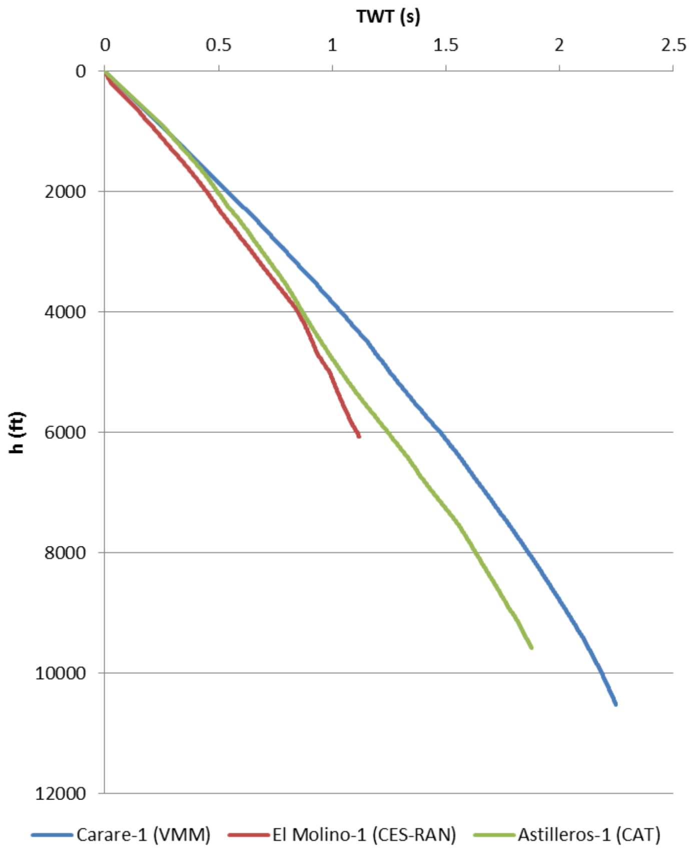

Figure 9-20. Time-depth curves. Blue shows the curve for the Carare-1 well in the Middle Magdalena Valley basin, green shows the Astilleros-1 well in the Catatumbo basin and red the El Molino-1 well in the Cesar - Ranchería basin.

9.4.1.3.1 Middle Magdalena Valley

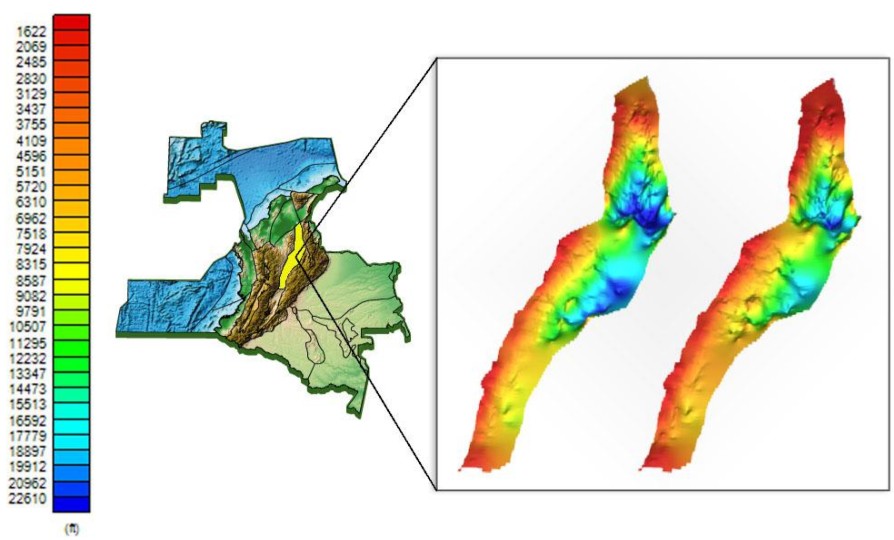

Figure 9-21. Source rock belt base and limit depth in the Middle Magdalena Valley basin. On the left-hand side, Pre-Cretaceous nonconformity between -343 ft and 30,183 ft (TVDSS) and, on the right-hand side, Turonian maximum flooding surface between -4 ft and 24,515 ft (TVDSS).

9.4.1.3.2 Cesar – Ranchería

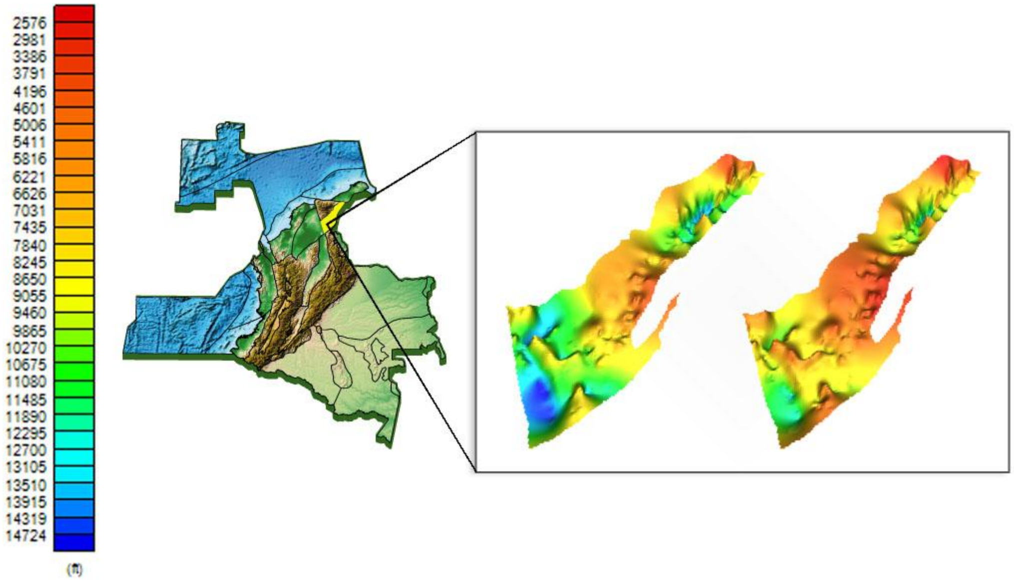

Figure 9-22. Source rock belt base and limit depth in the Cesar - Ranchería basin. On the left-hand side, Pre-Cretaceous nonconformity between 3,425 ft and 15,129 ft (TVDSS) and, on the right-hand side, Turonian maximum flooding surface between 2,171 ft and 13,655 ft (TVDSS).

9.4.1.3.3 Catatumbo

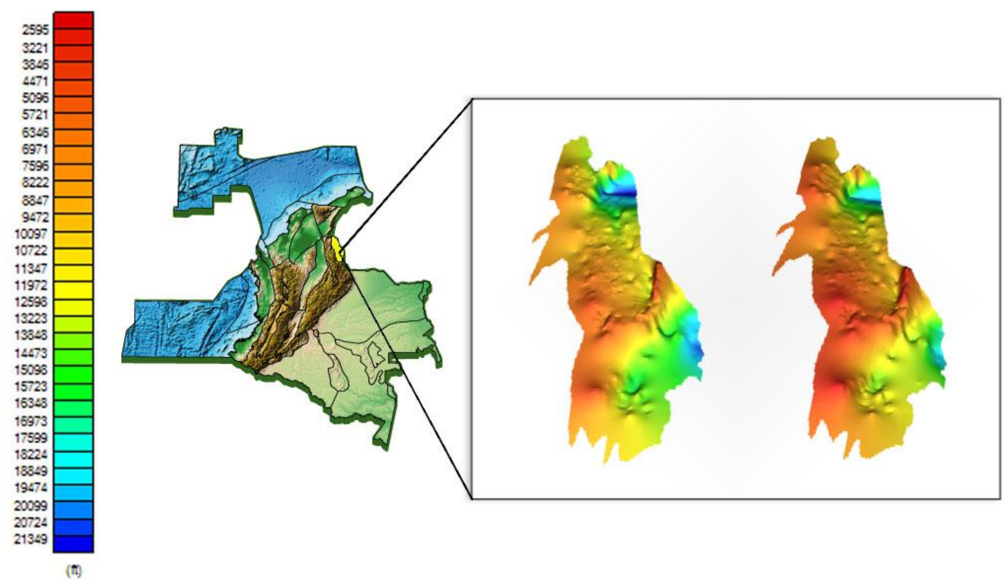

Figure 9-23. Source rock belt base and limit for the Catatumbo basin. On the left-hand side, Pre-Cretaceous nonconformity between 3,630 ft and 21,974 ft (TVDSS) and, on the right-hand side, Turonian maximum flooding surface between 1,970 ft and 20,021 ft (TVDSS).

9.4.1.4 Isopachs

The isopach maps produced from the limits and bases in depth in Figures 9-21, 9-22 and 8-23 are not given in this report, but can be consulted "ShaleGas.tks" project folder (Appendix 9-1). These isopach average values in the 3 basins analysed were 5,266 ft, 2,069 ft and 3,612 ft for the Middle Magdalena Valley, Cesar - Ranchería and Catatumbo basins, respectively.

9.4.2 Net-to-gross

Table 9-3 shows net and total thicknesses obtained by applying the methodology proposed by Passey et al., (1990) to the 37 wells highlighted in red in Figure 9-10.

The whole of the interval recorded for each well was used for calculating the NTG ratio numerator, since the available information did not allow an appropriate link to the Turonian and Pre-Cretaceous reflectors records used for determining the ratio's denominator. Intervals representing younger rocks than those in the source rock belt may thus have been counted within the NTG numerator, in spite of cut-off values having been defined for the GR record.

Well name	Basin	GR limit (API)	Net (ft)	Total (ft)	Name of well	Basin	GR limit (API)	Net (ft)	Total (ft)
Agata-1ST1	VMM	70	514	3,939	Perdiz-1	VMM	70	25	766
Andes-1	VMM	80	162	940	Purnio-1	VMM	80	4	1,168
Bambuco-1	VMM	60	166	870	Simiti-1A	VMM	60	79	3,444
Bronce-2	VMM	70	17	2,045	Simiti-2A	VMM	55	140	3,029
Cano Rico-1	VMM	80	14	547	Simiti-3	VMM	80	295	3,602
Cano Tablezo-1	VMM	90	477	831	Almendro-1	CAT	70	443	2,391
Cisne-1	VMM	70	145	725	Brubucanina-1	CAT	55	249	2,781
Cocodrilo-1	VMM	90	931	1,067	Chibagra-2	CAT	70	758	2,725
Corcovado-2	VMM	150	106	3,298	Cocodrilo-1	CAT	40	231	1,646
Dona Maria-2	VMM	90	891	2,664	Cucuta-2	CAT	110	1,543	2,186
Encanto-1	VMM	70	92	614	Eslabones-1	CAT	110	741	1,514
Escondido-1	VMM	80	42	445	Esperanza-3K	CAT	135	153	2,092
Fortuna-1	VMM	80	1264	3,862	Guasimales-1	CAT	90	458	1,299
Galeandra-1	VMM	60	26	1,718	Indio-1	CAT	80	668	1,579
Guayabito-1	VMM	70	944	5,455	Cesar A-1X	CES-RAN	60	121	2,511
Guayacan-1	VMM	45	845	5,325	Cesar F-1X	CES-RAN	120	565	2,957
Guineal-1	VMM	80	438	4,724	Cesar H-1X	CES-RAN	100	239	2,804
Las Lajas-1	VMM	100	225	4,282	El Molino-1	CES-RAN	70	297	1,557
Montoyas A-1	VMM	80	252	1,528					

Table 9-3. Data calculated for determining net-to-gross ratio. The GR limit column gives the gamma ray curve limit value, assigned to each well, for the distinguishing between sands in conventional deposits and source rocks in non-conventional deposits. VMM, CAT and CES-RAN refers to the Middle Magdalena Valley, Catatumbo and Ranchería (Cesar) basins, respectively.

The methodological approach adopted here meant that NTG was associated with a statistical distribution for describing its pattern. A gamma distribution thus had the best fit for the NTG values obtained by assigning form and scale parameters estimated from the same data. Table 9-4 summarises the results of such fit.

Estimated parameters						**Goodness-of-fit test**			
$\hat{x}$	Confidence interval		$\hat{y}$	Confidence interval		**Null hypothesis**	P	**Statistical value**	G.L
1.02	0.68	1.53	0.19	0.11	0.32	Was not rejected	0.55	0.36	1

Table 9-4. Goodness-of-fit parameters and test results applied to the net-to-gross data for determining statistical distribution associated with such data. Estimated parameters $\hat{x}$ **and** $\hat{y}$ are gamma distribution form and scale, respectively. Column P gives el value regarding the probability of the null hypothesis being accepted or rejected. G.L refers to goodness-of-fit test degrees of freedom.

Correlations were made for the wells analysed for determining net and total thickness values using the proposed methodology (pseudo-sonic curve). Figures 9-24 to 9-29 give examples of some of these correlations.

9.4.2.1 The Middle Magdalena Valley

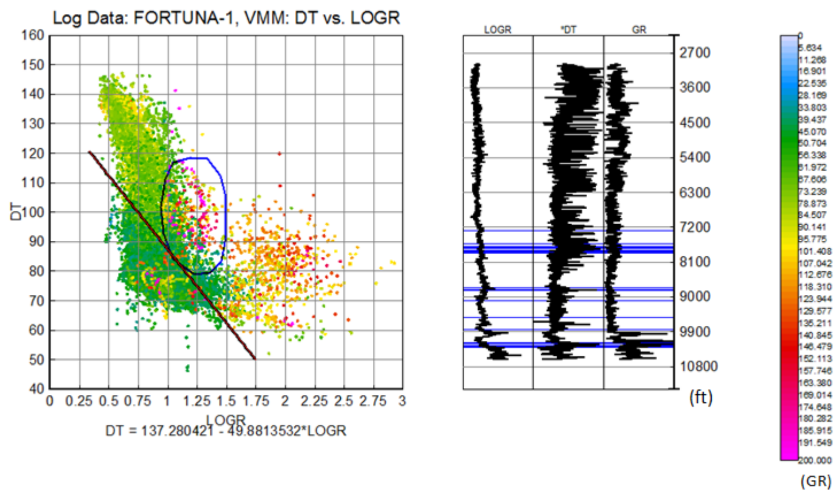

Figure 9-24. Linear regression for obtaining the pseudo-sonic curve in the Fortuna-1 well in the Middle Magdalena Valley basin. The points of the sonic curve (DT) on the ordinate on the graph and the logarithm of the resistive curve on the abscissa (LogR) are shown in the left-hand panel. The colour of the points reflects the gamma ray curve value. The points enclosed in the blue polygon show the in depth areas highlighted in the right-hand panel; these are prospective areas.

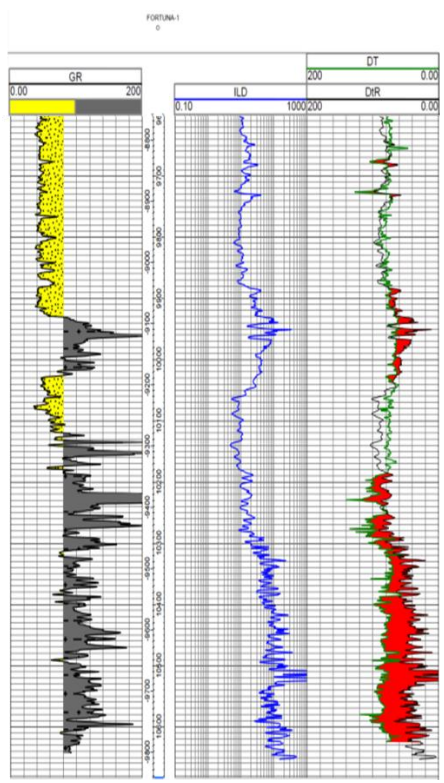

Figure 9-25. Associated organic material-rich hydrocarbon areas in the Fortuna-1 well in the Middle Magdalena Valley basin.

9.4.2.2 Cesar – Ranchería

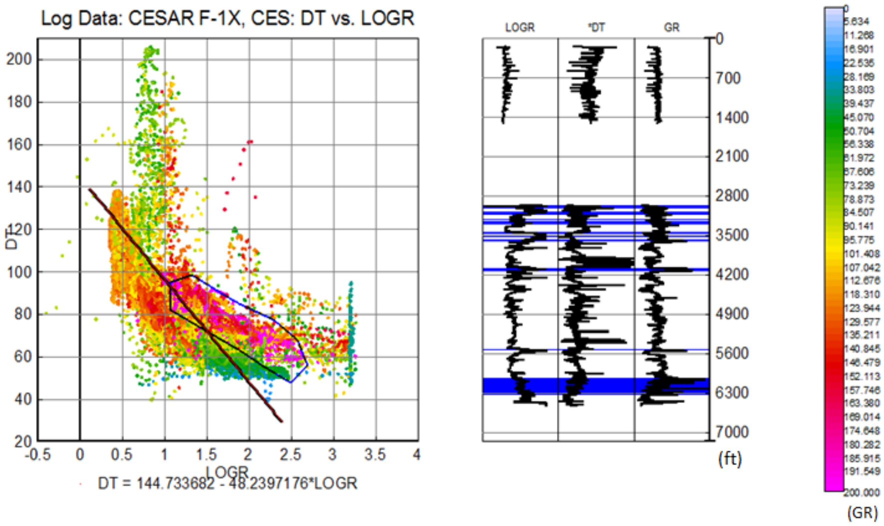

Figure 9-26. Linear regression for the obtaining the pseudo-sonic curve in the Cesar F-1X well in the Cesar - Ranchería basin.

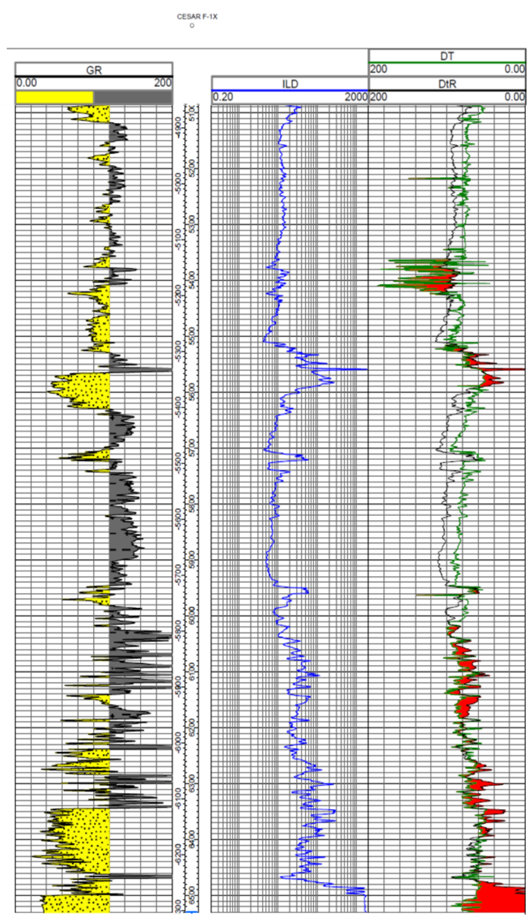

Figure 9-27. Associated organic material-rich hydrocarbon areas in the Cesar F-1X well in the Cesar - Ranchería basin.

9.4.2.3 Catatumbo

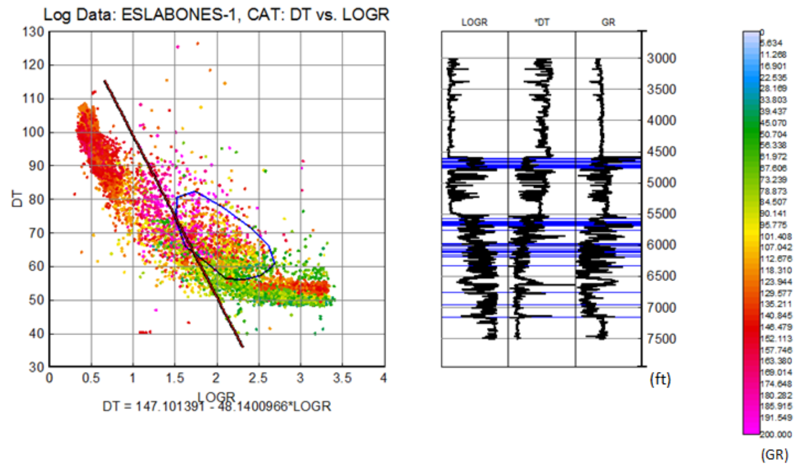

Figure 9-28. Linear regression for obtaining the pseudo-sonic curve in the Eslabones-1 well in the Catatumbo basin.

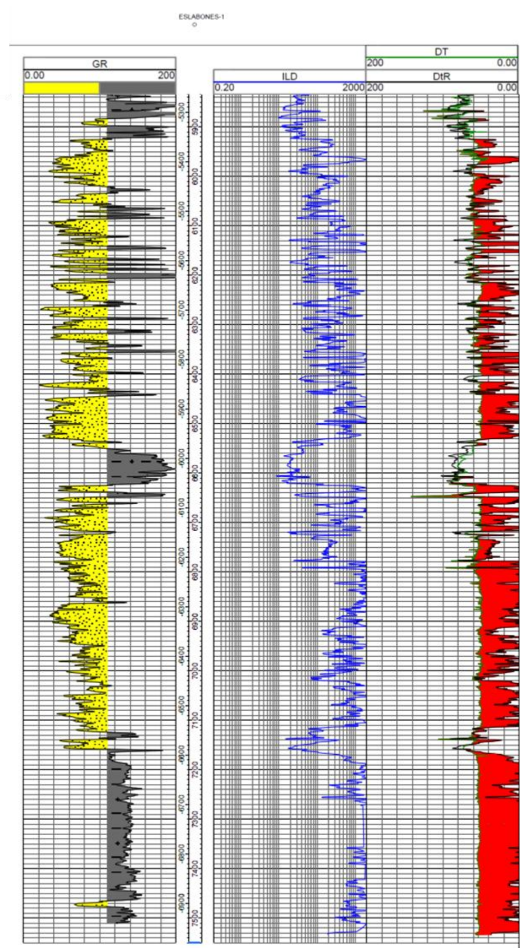

Figure 9-29. Associated organic material-rich hydrocarbon areas in the Eslabones-1 well in the Catatumbo basin.

9.4.3 Total rock density

Even though the wells reviewed and evaluated included density record (RHOB), the curves were found in sands in conventional deposits, not in source rock areas. Taking this into account, it was decided to take the density data from the already complied databases (Appendix 9-2).

The compiled density values' pattern was associated with a triangular distribution; this is reported in Table 9-5.

Parameter	Value (kg/m³)
Minimum	2120
Maximum	2800
Most probable	2540

Table 9-5. Estimated parameters for total rock density, assuming a triangular distribution.

9.4.4 Absorbed gas concentration

$$G_a = 5.6271 * TOC + 6.2945 \qquad \textbf{(9-3)}$$

Equation 9-3, obtained from the Canadian shale gas prospects information (Appendix 9-2.), was applied to the TOC data extracted from the Geochemical Atlas of Colombia to obtain absorbed gas concentration values (Appendix 9-3). Such values led to finding statistical regression distributions for the variable's pattern, basin by basin. Table 9-6 summarises the distributions, estimation parameters and goodness-of-fit test results for the best fits found.

Basin	Distribution	Estimated parameters						Goodness-of-fit test			
		$\hat{x}$	Confidence interval		$\hat{y}$	Confidence interval		Null hypothesis	P	**Statistical value**	G.L
VMM	Lognormal	2.71	2.67	2.75	0.38	0.35	0.41	Was rejected	0.04	4.21	1
CAT	Gamma	2.12	1.92	2.35	7.18	6.42	8.04	Was not rejected	M.B	0.44	0
CES-RAN	Gamma	6.02	4.98	7.28	2.06	1.69	2.50	Was not rejected	M.B	0.27	0
CAG-PUT	Weibull	15.77	15.27	16.29	1.47	1.43	1.51	Was not rejected	M.B	89.08	0
COR	Gamma	66.65	61.30	72.47	0.04	0.03	0.04	Was rejected	M.B	109.12	3
LLA	Gamma	2.74	2.56	2.93	4.76	4.41	5.12	Was not rejected	M.B	6.67	0
VSM	Lognormal	2.73	2.70	2.75	0.49	0.47	0.50	Was rejected	0.01	9.76	2
SIN-SJA	Gamma	4.63	4.01	5.35	2.96	2.54	3.44	Was not rejected	M.B	47.04	0
VIM	Lognormal	2.42	2.40	2.44	0.31	0.30	0.33	Was not rejected	M.B	0.75	0
TUM	Lognormal	2.56	2.48	2.65	0.40	0.35	0.47	Was not rejected	M.B	15.04	0
CHO	Exponential	40.18	30.94	54.32	N/A	N/A	N/A	Was not rejected	M.B	0.17	2

Table 9-6. Goodness-of-fit test distributions, fit parameters and results applied to the absorbed gas concentration data. Estimated parameters $\hat{x}$ and $\hat{y}$ are the mean and standard deviation for a lognormal distribution, form and scale for a gamma distribution and "a" and "b" for the Weibull distribution. Estimated $\hat{x}$ represents the mean for an exponential distribution. CAG-PUT, COR, LLA, VSM, SIN-SJA, VIM, TUM, CHO refer to the Caguán - Putumayo , The Eastern Cordillera, the Eastern Llanos, the Upper Magdalena Valley, Sinú - San Jacinto, the Lower Magdalena Valley, Tumaco and Chocó basins, respectively. The data used for the Chocó basin referred to outcrops, as no well data was available. N/A refers to parameters which did not apply to the type of distribution being considered. M.B refers to a very low probability of the null hypothesis being accepted or rejected.

Goodness-of-fit test response for the Middle Magdalena Valley, the Eastern Cordillera and Upper Magdalena Valley basins suggested that all distributions tested would be rejected, even though with very low probability of being rejected. Bearing this in mind, the distribution giving the lowest value was chosen for such basins (Appendix 9-3).

The only data reported for the Chocó basin concerned outcrops, so this was taken as no well data was available. No TOC data or well or outcrop data had been reported for the Guajira, Vaupés - Amazonas, Cauca – Patía, Urabá or Amagá basins, so no gas concentration values were calculated;

instead, they were associated with the same pattern given for this variable in analogous basin as follows: the Cauca - Patía and Amagá basins were associated with the Tumaco distribution, Guajira with that for Cesar - Ranchería, Vaupés - Amazonas with that for Caguán - Putumayo and Urabá with the Sinú - San Jacinto distribution.

9.4.5 Free gas concentration

Free gas concentration values, inferred from S_1 data (Appendix 9-3), were analysed for determining the distribution best fitting their pattern, in the same way as was done with absorbed gas concentration values. Likewise, analogous basins' distribution was used for basins lacking information. Table 9-7 gives the estimation parameters' values and the statistical tests made for the best fit found.

Basin	Distribution	Estimated parameters						Goodness-of-fit test			
		$\hat{x}$	Confidence interval		$\hat{y}$	Confidence interval		Null hypothesis	P	Statistical value	G.L
VMM	Lognormal	2.49	2.37	2.62	1.21	1.12	1.30	Was not rejected	0.10	2.82	1
CAT	Gamma	0.64	0.59	0.71	31.33	27.48	35.72	Was not rejected	M.B	4.41	0
CES-RAN	Exponential	20.59	18.03	23.74	N/A	N/A	N/A	Was rejected	0.04	13.33	0
CAG-PUT	Gamma	0.20	135.4	N/R	N/R	N/R	N/R	Was not rejected	0.08	6.87	3
COR	Exponential	18.72	17.64	19.90	N/A	N/A	N/A	Was not rejected	M.B	0.10	0
LLA	Gamma	0.15	140.1	N/R	N/R	N/R	N/R	Was not rejected	0.06	7.57	3
VSM	Exponential	46.62	44.73	48.63	N/A	N/A	N/A	Was rejected	0.01	7.51	1
SIN-SJA	Exponential	13.56	12.23	15.12	N/A	N/A	N/A	Was not rejected	M.B	1.20	0
VIM	Lognormal	1.24	1.16	1.32	1.15	1.10	1.21	Was rejected	M.B	17.22	2
TUM	Weibull	3.95	2.33	6.71	0.41	0.36	0.47	Was not rejected	M.B	0.16	0
CHO	Weibull	32.41	20.82	50.43	0.68	0.55	0.84	Was not rejected	M.B	0.65	0

Table 9-7. Goodness-of-fit test distributions, fit parameters and results applied to the free gas concentration data. N/R refers to parameters which, as they went beyond the algorithm's range of calculations which were not reported when making the statistical estimation.

9.4.6 Net-to-gross international databases

An extreme value distribution gave the best fit for the net-to-gross data calculated from international sources (Appendix 9-2). Table 9-8 shows the results of such fit.

Estimated parameters						Goodness-of-fit test			
$\hat{x}$	Confidence interval		$\hat{y}$	Confidence interval		Null hypothesis	P	Statistical value	G.L
-0.3	-0.52	-0.09	0.3	0.22	0.42	Was not rejected	0.27	3.94	3

Table 9-8. Goodness-of-fit parameters and test results applied to the NTG data in Appendix 8-2. Estimated parameters $\hat{x}$ **and** $\hat{y}$ are extreme value distribution location and scale.

9.4.7 Hydrocarbons in shale

The result of Monte Carlo simulation for calculating the hydrocarbons in shale is shown below, with the variables defined in equation 9-1, and their associated distributions. The percentage of evaluated resources which could be lying within environmental conservation areas, forestry reserves and natural parks was subtracted; Tables 9-9 and 9-10 give the final results.

Basin	P_{10}	P_{10}	P_{50}	P_{50}	P_{90}	P_{90}
	(Tcf)	(10^3MMBOE)	(Tcf)	(10^3MMBOE)	(Tcf)	(10^3MMBOE)
Amagá	1.37	0.24	0.41	0.07	0.06	0.01
Caguán - Putumayo	2,687.60	463.38	127.56	21.99	13.81	2.38
Catatumbo	185.43	31.97	38.98	6.72	4.89	0.84
Cauca - Patía	28.57	4.93	8.55	1.47	1.34	0.23
Cesar - Ranchería	107.13	18.47	28.46	4.91	4.18	0.72
Chocó	22.73	3.92	6.89	1.19	1.08	0.19
The Eastern Cordillera	729.26	125.73	206.65	35.63	31.61	5.45
Guajira	132.77	22.89	35.34	6.09	5.22	0.90
The Eastern Llanos	6,619.59	1,141.31	1,042.44	179.73	125.40	21.62
Sinú - San Jacinto	441.33	76.09	113.24	19.52	16.37	2.82
Tumaco	56.72	9.78	16.97	2.93	2.66	0.46
Urabá	91.22	15.73	23.37	4.03	3.36	0.58
The Lower Magdalena Valley	121.31	20.92	35.05	6.04	5.39	0.93
The Middle Magdalena Valley	148.80	25.65	43.50	7.50	6.71	1.16
The Upper Magdalena Valley	45.38	7.82	13.47	2.32	2.09	0.36
Vaupés, Amazonas	3,228.09	556.57	154.55	26.65	16.61	12.86
TOTAL	14,647.29	2,525.39	1,895.44	326.80	240.78	41.51

Table 9-9. Hydrocarbons in shale in Scenario 1 after subtracting resources possibly present in environmental conservation areas.

Basin	P_{10}	P_{10}	P_{50}	P_{50}	P_{90}	P_{90}
	(Tcf)	(10^3MMBOE)	(Tcf)	(10^3MMBOE)	(Tcf)	(10^3MMBOE)
Amagá	1.98	0.34	0.68	0.12	0.11	0.02
Caguán - Putumayo	4,177.70	720.29	200.22	34.52	23.71	4.09
Catatumbo	272.43	46.97	63.51	10.95	8.30	1.43
Cauca - Patía	41.27	7.12	14.22	2.45	2.28	0.39
Cesar - Ranchería	155.19	26.76	47.04	8.11	7.18	1.24
Chocó	32.82	5.66	11.44	1.97	1.85	0.32
The Eastern Cordillera	1,046.89	180.50	340.56	58.72	53.81	9.28
Guajira	191.78	33.07	58.18	10.03	8.89	1.53
The Eastern Llanos	9,736.40	1,678.69	1,703.01	293.62	215.61	37.17
Sinú - San Jacinto	643.41	110.93	186.87	32.22	27.67	4.77
Tumaco	81.95	14.13	28.16	4.86	4.52	0.78
Urabá	132.29	122.81	38.52	6.64	5.76	0.99
The Lower Magdalena Valley	173.81	29.97	57.83	9.97	9.23	1.59
The Middle Magdalena Valley	213.78	36.86	71.85	12.39	11.48	1.98
The Upper Magdalena Valley	65.50	11.29	22.35	3.85	3.59	0.62
Vaupés, Amazonas	5,075.44	875.08	240.21	41.42	28.29	4.88
TOTAL	22,042.67	3,800.46	3,084.66	531.84	412.29	71.08

Table 9-10. Hydrocarbons in shale in Scenario 2, after subtracting resources possibly present in environmental conservation areas.

9.4.8 Potential of shale oil and shale gas

The scarce information available about geological, geochemical and geometric characteristics and hydrocarbon resources available in shale belts has hindered a reliable shale oil/shale gas ratio being established. The degree of thermal maturity in a shale belt is not homogeneous and such ratio must thus be a little subjective. In spite of this, the data available in the "Review of Emerging Resources: US Shale Gas and Shale Oil Play" (US Department of Energy, 2011) has been used for consolidating an average for such ratio in basins having crude and gas windows. Table 9-11 shows gas and crude resources in three basins in the USA and a 0.11 to 0.48 range regarding shale oil/[total hydrocarbon]. Even though the scarce data observed did not enable understanding the above as being representative, it was evident that giving an idea about the order of magnitude could lead to understanding the problem. Assuming a 0.3 value and 20% favourable geological risk, suggested by the "World shale gas resources: An initial assessment of 14 regions outside the United States" (US Department of Energy, 2011), shale oil resources for the scenarios analysed reached the figures presented in Tables 9-12 and 9-13. Similarly, net shale gas resources are shown in Tables 9-14 and 9-15.

Play	Gas		Crude	Fraction
	Tcf	MMBOE	MMbbl	Oil/(Oil+Gas)
Barnett	75.5	13 017.2	1 580.0	0.11
Rocky Mountain Region	43.0	7 413.8	3 590.0	0.33
Eagle Ford	20.8	3 587.9	3 350.0	0.48

Table 9-11. Oil/[hydrocarbon] ratio for three US shale belts, taken from US Department of Energy (2011).

Graphs 9-30 to 9-33 compare shale gas and oil resources between basins extracted from Table 9-9, and Colombia's total potential within the international framework (Figure 9-34) taken from Table 9-1.

Basin	P_{10}	P_{50}	P_{90}
		Tcf	
Amagá	0.2	0.1	0.0
Caguán - Putumayo	376.3	17.9	1.9
Catatumbo	26.0	5.5	0.7
Cauca - Patía	4.0	1.2	0.2
Cesar - Ranchería	15.0	4.0	0.6
Chocó	3.2	1.0	0.2
The Eastern Cordillera	102.1	28.9	4.4
The Guajira	18.6	4.9	0.7
The Eastern Llanos	926.7	145.9	17.6
Sinú - San Jacinto	61.8	15.9	2.3
Tumaco	7.9	2.4	0.4
Urabá	12.8	3.3	0.5
The Lower Magdalena Valley	17.0	4.9	0.8
The Middle Magdalena Valley	20.8	6.1	0.9
The Upper Magdalena Valley	6.4	1.9	0.3
Vaupés, Amazonas	451.9	21.6	2.3
TOTAL	2,050.6	265.4	33.7

Table 9-12. Gas fraction present in shale from Colombian basins. Scenario 1.

Basin	P_{10}	P_{50}	P_{90}
		MMbbl	
Amagá	14.4	4.2	0.6
Caguán - Putumayo	27,802.8	1,319.4	142.8
Catatumbo	1,918.2	403.2	50.4
Cauca - Patía	295.8	88.2	13.8
Cesar - Ranchería	1,108.2	294.6	43.2
Chocó	235.2	71.4	11.4
The Eastern Cordillera	7,543.8	2,137.8	327.0
The Guajira	1,373.4	365.4	54.0
The Eastern Llanos	68,478.6	10,783.8	1,297.2
Sinú - San Jacinto	4,565.4	1,171.2	169.2
Tumaco	586.8	175.8	27.6
Urabá	943.8	241.8	34.8
The Lower Magdalena Valley	1,255.2	362.4	55.8
The Middle Magdalena Valley	1,539.0	450.0	69.6
The Upper Magdalena Valley	469.2	139.2	21.6
Vaupés - Amazonas	33,394.2	1,599.0	771.6
TOTAL	151,523.4	19,608.0	3,090.6

Table 9-13. The crude fraction present in shale from several Colombian basins. Scenario 1.

Basin	P10	P50	P90
		Tcf	
Amagá	0.3	0.1	0.0
Caguán - Putumayo	584.9	28.0	3.3
Catatumbo	38.1	8.9	1.2
Cauca - Patía	5.8	2.0	0.3
Cesar - Ranchería	21.7	6.6	1.0
Chocó	4.6	1.6	0.3
The Eastern Cordillera	146.6	47.7	7.5
The Guajira	26.8	8.1	1.2
The Eastern Llanos	1,363.1	238.4	30.2
Sinú - San Jacinto	90.1	26.2	3.9
Tumaco	11.5	3.9	0.6
Urabá	18.5	5.4	0.8
The Lower Magdalena Valley	24.3	8.1	1.3
The Middle Magdalena Valley	29.9	10.1	1.6
The Upper Magdalena Valley	9.2	3.1	0.5
Vaupés, Amazonas	710.6	33.6	4.0
TOTAL	3,086.0	431.9	57.7

Table 9-14. Gas fraction present in shale from several Colombian basins. Scenario 2.

Basin	P10	P50	P90
		MMBOE	
Amagá	20.4	7.2	1.2
Caguán - Putumayo	43,217.4	2,071.2	245.4
Catatumbo	2,818.2	657.0	85.8
Cauca - Patía	427.2	147.0	23.4
Cesar - Ranchería	1,605.6	486.6	74.4
The Chocó	339.6	118.2	19.2
The Eastern Cordillera	10,830.0	3,523.2	556.8
The Guajira	1,984.2	601.8	91.8
The Eastern Llanos	100,721.4	17,617.2	2,230.2
Sinú - San Jacinto	6,655.8	1,933.2	286.2
Tumaco	847.8	291.6	46.8
Urabá	7,368.6	398.4	59.4
The Lower Magdalena Valley	1,798.2	598.2	95.4
The Middle Magdalena Valley	2,211.6	743.4	118.8
The Upper Magdalena Valley	677.4	231.0	37.2
Vaupés, Amazonas	52,504.8	2,485.2	292.8
TOTAL	234,028.2	31,910.4	4,264.8

Table 9-15. Crude fraction present in shale from several Colombian basins. Scenario 2.

Figure 9-30. Map of Shale Gas potential in Scenario 1.

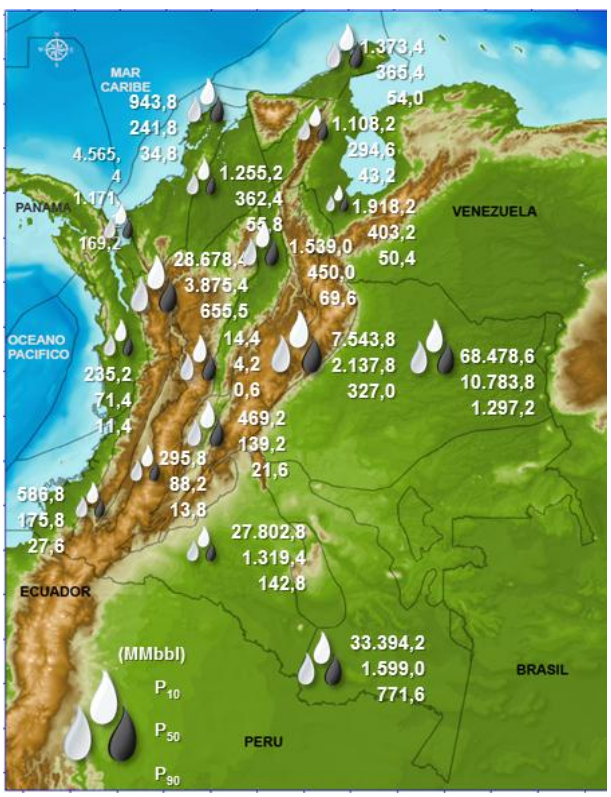

Figure 9-31. Map of Shale Oil potential in Scenario 1.

Evaluating total Yet-to-Find hydrocarbon volume in Colombia

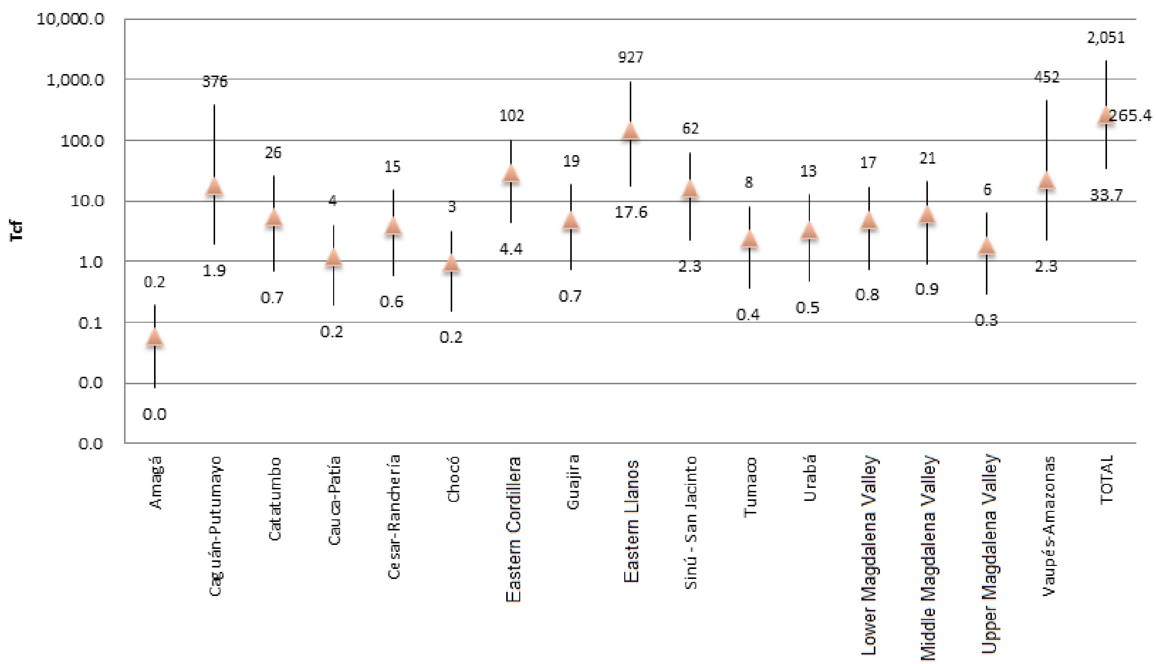

Figure 9-32. Shale gas potential in Scenario 1.

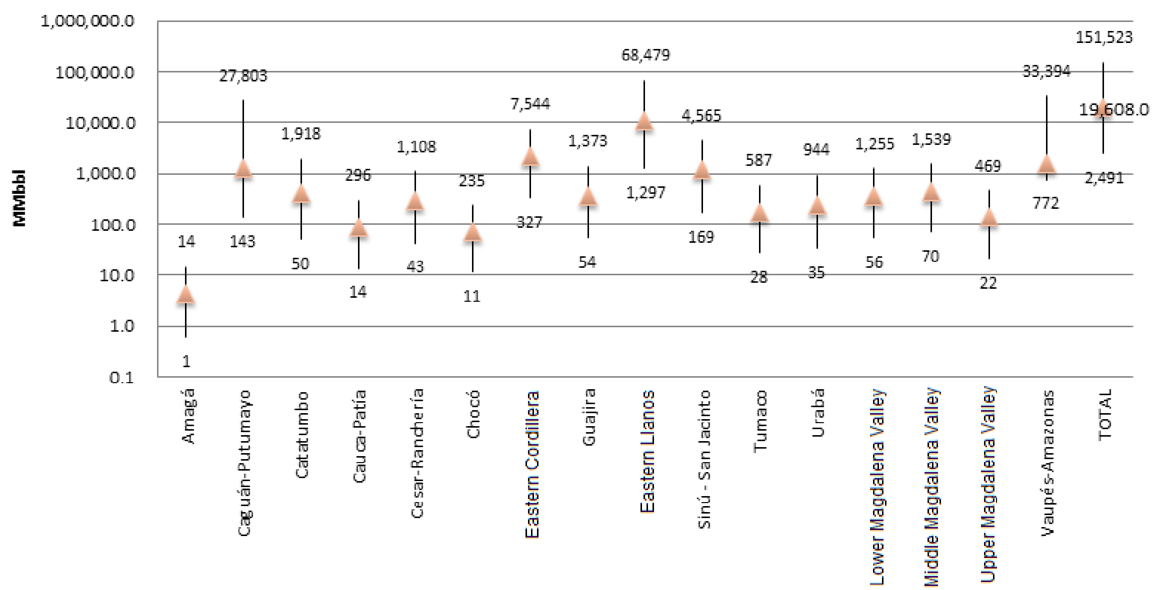

Figure 9-33. Shale Oil potential in Scenario 1.

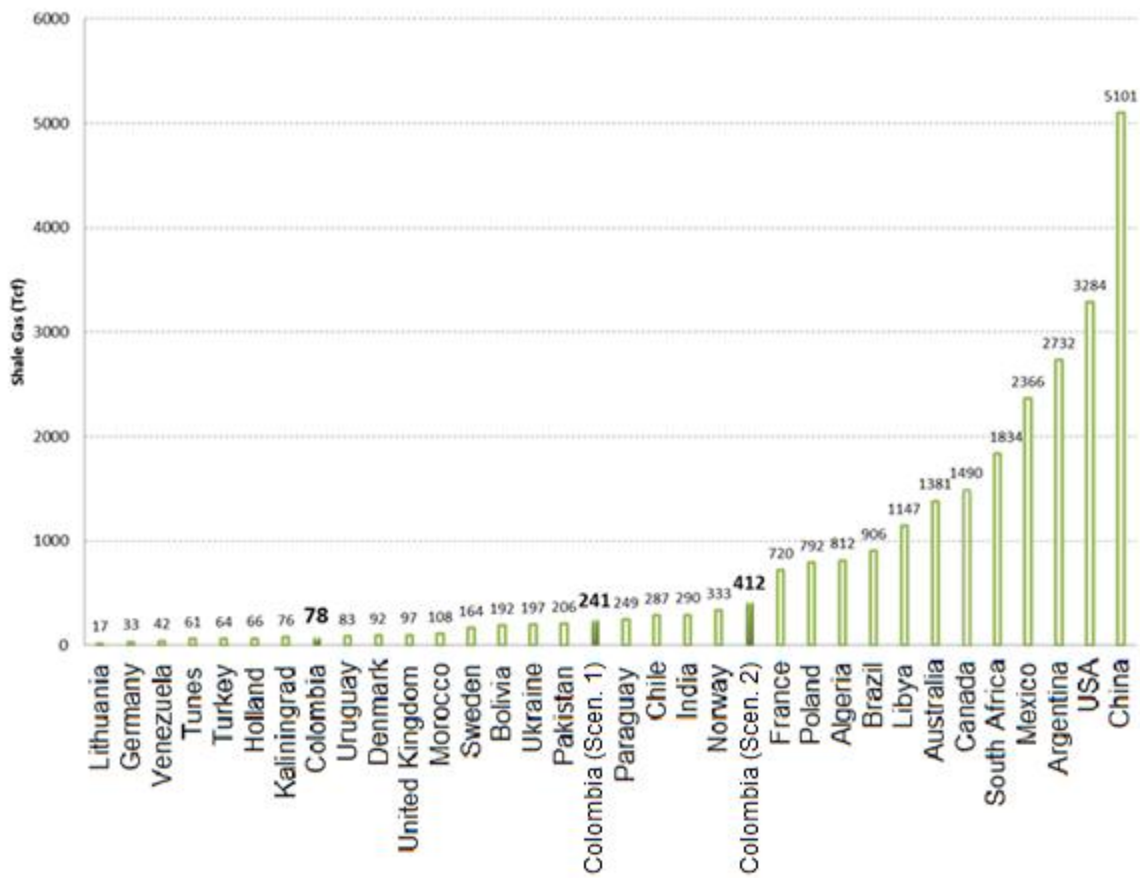

Figure 9-34. Shale gas resources in Colombia compared to those reported for other countries.

9.4.9 Sensitivity analysis

NTG usually most influenced estimates for all basins in both scenarios evaluated here, nearly always followed by G_a. Figure 9-35 shows the results from a sensitivity analysis.

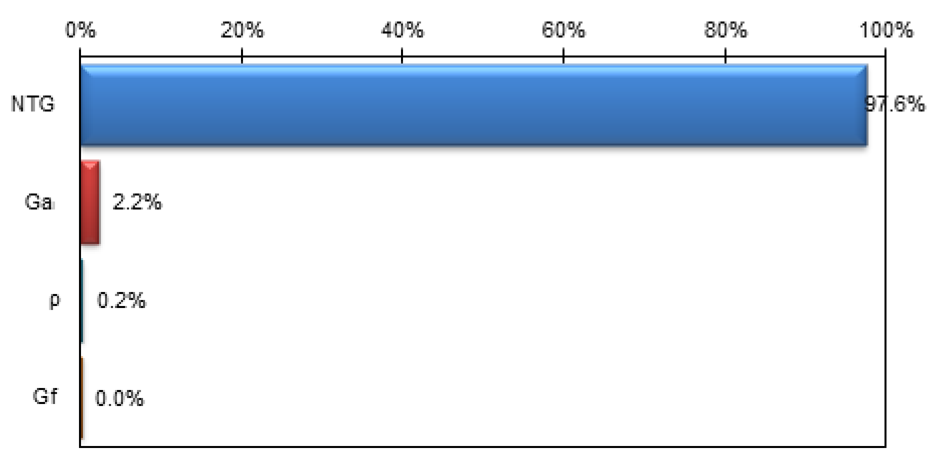

Figure 9-35. Average sensitivity for all basins in which hydrocarbons in shale was estimated.

9.5 Conclusions

- Estimated of the hydrocarbons shale potential is controlled by basin area, showing that basins covering a greater area were the most prospective ones;
- The Eastern Llanos basin had the greatest prospectivity in P_{90}, regarding the presence of hydrocarbons in shale, followed by the Eastern Cordillera and Vaupés - Amazonas;
- The order of the 3 basins having most estimated resources was maintained in P_{50};
- Estimated shale gas resources in P_{90} for the Middle Magdalena Valley basin (6.71 Tcf) and Ranchería basin in Cesar (4.18 Tcf) were lower than the values estimated by D. Little in 2008 (289 Tcf and 7.72 Tcf, respectively). Resources were greater for the Eastern Cordillera (31.61 Tcf compared to 19.3 Tcf); and
- The Lower Magdalena Valley, Caguán - Putumayo and Sinú - San Jacinto basins' prospectivity was high, even though control in their areas must be taken into account regarding the estimated results. Shale from the Palaeozoic age in the Eastern Llanos and Caguán - Putumayo, could have a positive impact on their hydrocarbon potential.

9.6 Bibliography

Agencia Nacional de Hidrocarburos. (2007). Colombian sedimentary basins: nomenclature, boundaries and petroleum geology, a new proposal. Bogota: B & M Exploration Ltda.

Agencia Nacional de Hidrocarburos. (2010). Atlas Geoquímico de Colombia. (UN.Colombia, Ed.) Bogota.

Arthur, M. A., Schlanger, S. O., & Jenkyns, H. C. (1987). The Cenomanian–Turonian Oceanic Anoxic Event, II. Palaeoceanographic controls on organic-matter production and preservation. London Geological Society Special Publications, 26, 401-420.

Beaton, A. P., Pawlowicz, J. G., Anderson, S. D., & Rokosh, C. D. (2009). Rock Eval, total organic carbon, adsorption isotherms and organic petrography of the Banff and Exshaw formations: shale data release. Alberta Geological Survey. Alberta: Energy Resources Conservation Board.

Beaton, A. P., Pawlowicz, J. G., Anderson, S. D., & Rokosh, C. D. (2009). Rock Eval, Total organic carbon, adsorption isotherms and organic petrography of the Colorado Group: shale data release. Alberta Geological Survey. Alberta: Energy Resources Conservation Board.

Beaton, A. P., Pawlowicz, J. G., Anderson, S. D., & Rokosh, C. D. (2010). Rock Eval, total organic carbon, adsorption isotherms and organic petrography of the duverny and muskwa formations in alberta: shale data release. Alberta Geological Survey. Alberta: Energy Resources Conservation Board.

Beaton, A. P., Pawlowicz, J. G., Anderson, S. D., & Rokosh, C. D. (2010). Rock Eval, total organic carbon, adsorption isotherms and organic petrography of the Montney Formation in Alberta: shale data release. Alberta Geological Survey. Alberta: Energy Resources Conservation Board.

Boyer, C., Kieschnick, J., Suarez, R., Lewis, R. E., & Waters, G. (2006). Producing gas from its source. Oilfield Review, Autumn, 36-49.

D. Little, A. (2008). Evaluation of Potential of Unconventional Energy Resources in Colombia. Agencia Nacional de Hidrocarburos. Houston: Arthur D. Little Inc.

Erbacher, J., Hubert, B. T., Norris, R. D., & Markey, M. (2001). Intensified thermohaline stratification as a possible cause for an ocean anoxic event in the Cretaceous Period. Nature, 409, 325-327.

Loucks, R. G., Reed, R. M., Ruppel, S. C., & Jarvie, D. M. (Junio de 2009). Morphology, genesis, and distribution of nanometer-scale pores in siliceous mudstones of the Mississippian Barnett Shale. Journal of Sedimentary Research, 79, 848-861.

Meyer, B. L., & Nederlof, M. H. (Febrero de 1984). Identification of source rocks on wireline logs by density / resistivity and sonic transit time / resistivity crossplots. The American Association of Petroleum Geologist Bulletin, 68(2), 121-129.

Mojica, J., Arévalos, O. J., & Castillo, H. (Diciembre de 2009). Agencia Nacional de Hidrocarburos. Consulted on June xx 2011, de Informacion Geológica and Geofisica - Givesciones and Poster Técnicos: www.anh.gov.co

Passey, Q. R., Creaney, S., Kulla, J. B., Moretti, F. J., & Stroud, J. D. (December 1990). A practical model for organic richness from porosity and resistivity logs. The American Association of Petroleum Geologist Bulletin, 74(12), 1777-1794.

Rios , A. (2010). Gas no convencional: Hacia un nuevo paradigma. (Americas Business News, Ed.) Energy Intelligence Series, 1-19.

Ryan, W. B., & Cita, M. B. (1977). Ignorance Concerning Episodes of Ocean Wide Stagnation. Marine Geology, 23, 197-215.

Schmoker, J. W. (2005). U.S. Geological Survey Assessment Concepts for Continuous Petroleum Accumulations. In U.S. Geological Survey, Petroleum Systems and Geologic Assessment of Oil and Gas in the Southwestern Wyoming Province, Wyoming, Colorado, and Utah. Denver: U.S. Department of the Interior.

Thiede, J., & Van Andel, T. H. (1977). The Paleoenvironment of Anaerobic Sediments in the Late Mesozoic South Atlantic. Earth and Planetary Science Letters, 33, 301-309.

U.S. Department of Energy. (2009). Modern shale gas development in the United States: A Premier. Oklahoma City: Ground Water Protection Council.

U.S. Department of Energy. (2011). World shale gas resources: an initial assessment of 14 regions outside de United States. Washington: Advanced Resources International.

Utah Geological Survey. (2005). Shale Gas Reservoirs of Utah: survey of an unexploited potential energy resource. Utah Geological Survey. Salt Lake city: GeoX Consulting Inc.

West, J. (1996). International Petroleum Encyclopedia. Tulsa: Pennwell Publishing Co.

Zhao, H., Givens, N. B., & Curtis, B. (Abril de 2007). Thermal Maturity of the Barnett Shale determined form well-log analysis. The American Association of Petroleum Geologist Bulletin, 91(4), 535-549.

9.7 Appendixes

Digital files in the ANH'S Document Center:

- ✓ Appendix 8-1: "Shale Gas"
- ✓ Appendix 8-2: "Base de Datos Internacional Shale Gas.xlsx"
- ✓ Appendix 8-3: "Base de Datos Shale Gas Colombia.xlsx"
- ✓ Kindom Suit project

10 GAS RESOURCES IN TIGHT SANDS

10.1 General comments

Gas in tight sands (unconventional natural gas which is difficult to access because of the nature of the rock and sand surrounding the deposit) is the term used for referring to low permeability deposits mainly producing dry natural gas. Low permeability is considered to be less than 0.1 milidarcies (mD) (Holditch, 2006). Figure 10-1 shows a cross-section of a tight area.

Tight gas sands is defined as being a belt of sands or carbonates (which may contain natural fractures) exhibiting less than 0.1 mD in-situ gas permeability (Figure 1); many "extra tight " reservoirs may have less than 0.001 mD in-situ permeability, meaning that gas usually flows through these rocks at low rates and special methods are needed for its production (Naik, 2003).

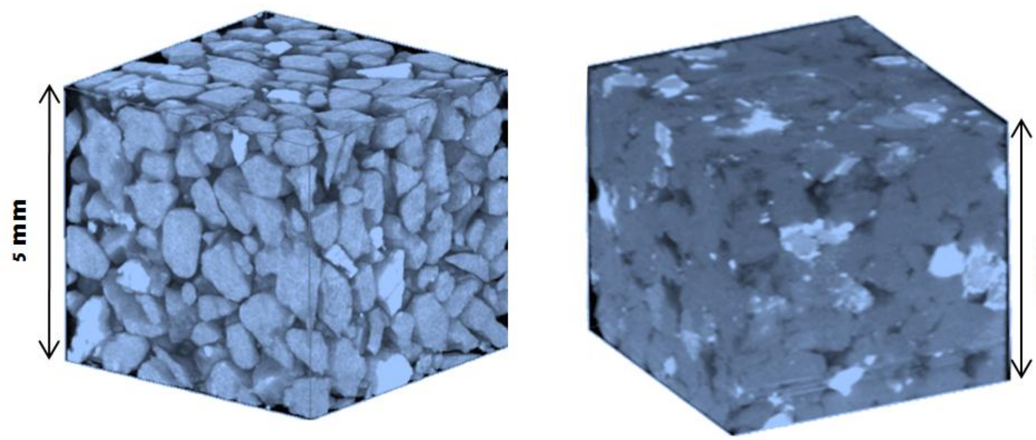

Figure 10-1. Comparison between conventional sand and tight sand. On left-hand-side: high porosity (39%) and permeability sand; right-hand-side: tight sand. the dark grey areas are the pores whilst the clearer grey ones are quartz and heavy minerals, modified from (INGRAIN Digital Rock Physics Lab s.f.).

10.1.1 Origin and formation

Effective porosity, viscosity, fluid saturation and capillary pressure are some of the parameters affecting a deposit's effective permeability (Naik 2003). These are controlled by the setting in which a deposit occurs and later processes which such deposits undergo. Even though fine grain sand and limolite deposits saturated with gas are particularly prone to forming tight gas sands, post-depositional compaction and cementation can reduce permeability in thick grain sediments, leading to the formation of tight rocks.

A reservoir's architecture is another important factor regarding permeability. Different settings regarding deposits lead to different architectures, thereby resulting in completely different reservoir properties. Permeability within individual sediment layers could thus be much lower than total reservoir permeability determined per well (Muntendam-Bos et al., 2009).

The deposit settings most associated with forming tight gas plays are deep basins, delta-fronts and the banks of dikes on food plains or river systems (Muntendam-Bos et al., 2009).

10.1.2 Exploration of and production from tight gas deposits

Considerable data regarding nuclei, geophysical records, drilling records and well tests must be complied for the correct tight gas play evaluation and development; this is often more the case for evaluating a tight gas sand play than for evaluating a conventional gas reservoir (Holditch, 2006).

Natural fractures play a determinant role in tight rock permeability. Hydraulic fracturing (fracking) could produce new fractures in a particular deposit or open up existing natural fractures. Their properties and the regime regarding formation efforts must thus be ascertained for planning wells and hydraulic fracturing for optimising production. It should be stressed that even though tight gas reservoirs (differently to conventional gas reservoirs) often have a very poor response to fracking, resulting in low production rates and high economic risk. Figure 10-2 gives a diagram showing the permeability and porosity associated with tight rocks.

Tight gas sands reservoirs require advanced techniques for reducing the migration distance of fluids from a formation towards a particular well. Horizontal and multilateral well drilling are the most modern technologies for tight gas reservoir production, as well as low-balance drilling and stimulation and cementation technologies (Naik, 2003).

Data from different sources is needed for the effective characterisation of tight gas sands deposits, i.e. seismic (multi-component, 3D seismic imaging), specialised records, cementation and stimulation methodologies/designs, drilling and conventional subsoil data, reservoir engineering data. All the foregoing is used for defining the lithological and geometrical combination regarding the faults and fractures associated with a particular reservoir.

10.1.3 Tight gas sands distribution around the world

Tight rock deposit technology has been developed in the USA for more than 40 years (Holditch, 2006); different technologies have been developed during this time for improving economic success rates. Much of this technology is currently being used around the world to contribute towards both tight gas sands and conventional reservoir development. The most studied reservoirs have been in North America due to the high level of activity and the volume of available data for analysing them; however, it is expected that activity levels will become increased regarding tight gas or unconventional gas exploration in Latin-American, Russia, the Middle East, Asia and other major gas production areas

Tight gas sand resources are distributed throughout the whole world; even though the greatest accumulations have been found in North America, Russia and China, many unexplored reservoirs are outside the USA (TOTAL, 2007).

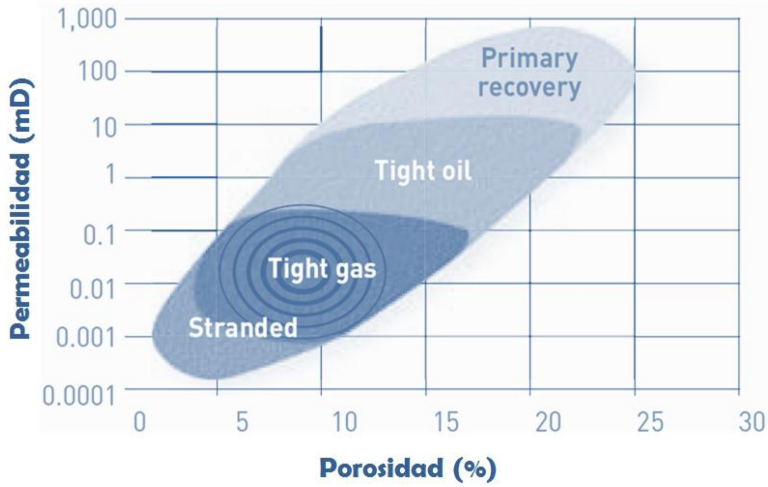

Figure 10-2. Ranges of porosity and permeability for tight gas sands reservoirs, modified from TOTAL (2007).

There has been little development in the field of tight gas sands deposits due to scarce knowledge about their geology and pertinent information in addition to natural gas policy and market conditions not having been favourable for their development in several countries. Rogner (1996) has estimated tight gas sands around the world to be about 7,400 Tcf (Table 10-1).

Region	Tight gas sands volume (Tcf)
North America	1,371
Latin-America	1,293
Western Europe	353
Central and Eastern Europe	78
The Soviet Union	901
North Africa and the Middle East	823
Sub-Saharan Africa	784
The central plain of Asia and China	353
Pacific (Organisation for Economic Cooperation and Development)	705
Pacific Asia	549
Southern Asia	196
Total around the world	7,406

Table 10-1. Estimating tight gas sands around the world, taken from Rogner (1996).

10.2 Data and hypotheses

10.2.1 International data

Tight gas sands' reservoir databases in the USA were consulted for estimating yet-to-find tight gas sands resources, as well as studies aimed at estimating such resources around the world.

10.2.2 National (Colombian) data

ANH petroleum exploitation records concerning wells in continental basins in Colombia was used; such information involved records for 435 wells located in the Guajira, Sinú - San Jacinto, Urabá, Cesar - Ranchería, Catatumbo, the Lower and Upper Middle Magdalena Valley, the Eastern Cordillera, Eastern Llanos and Caguán - Putumayo basins (Figure 10-3). Data was also taken from ANH reports.

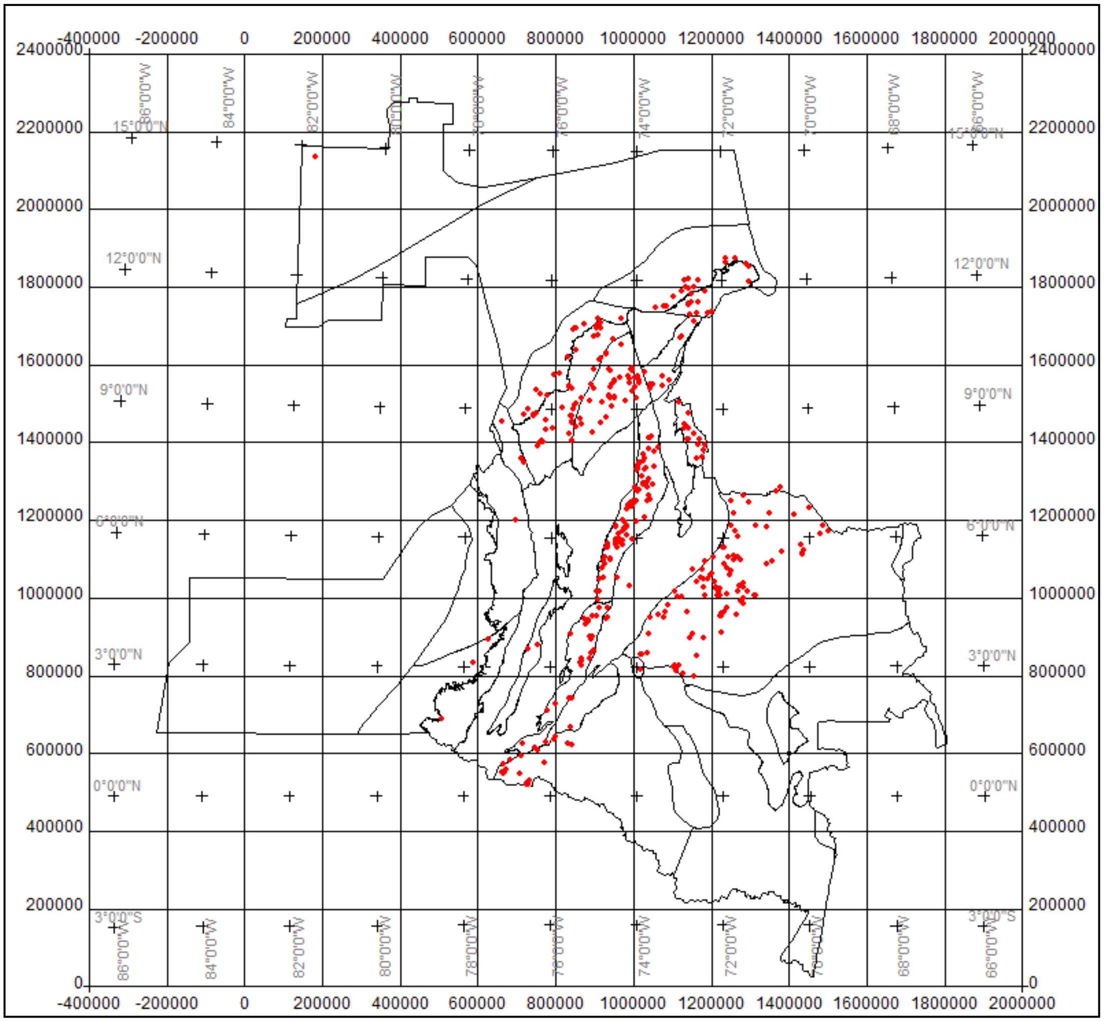

Figure 10-3. Map showing the location of wells having information from records, i.e. 435 wells (red points) from which records were loaded.

10.2.3 Hypotheses

Tight gas sands volume for Colombia's continental basins was estimated in line with the following hypotheses:

10.2.3.1 Hypothesis 1

Depending on a particular basin's genesis, there is an almost constant ratio between total tight gas sands-containing plays' area and the pertinent basin's total area. Such ratio can be expressed as:

$$\%\ basin\ area_{yet-to-find\_tight\_gas} = 100 \times \frac{Area_{Tight\_gas\_plays}}{Area_{Total\ basin}}$$

10.2.3.2 Hypothesis 2

Areas having tight gas sands may be discriminated by gamma ray, neutron porosity, density and permeability records. Such areas fulfil the following conditions:

- Gamma ray < tight-sand cut-off value
- Permeability < 0.1 mD
- Neutron porosity < porosity per density

10.2.3.3 Hypothesis 3

There is a ratio between resources and the area of a basin containing tight gas sands reservoirs (Figure 10-4); such ratio leads to estimating tigh gas resources in basins for which no well information is available.

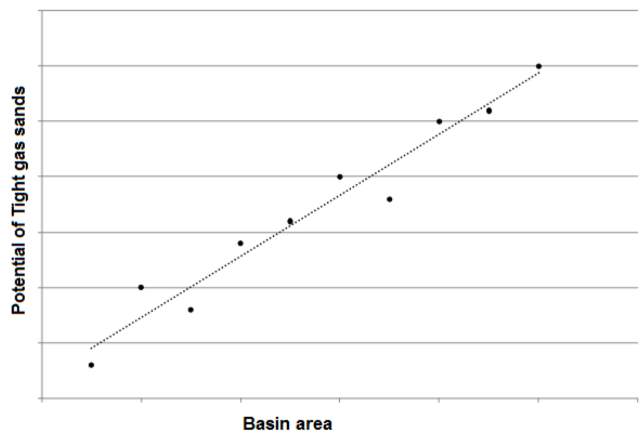

Figure 10-4. The graph shows the ratio between gas and the area of a basin containing tight gas sands reservoirs.

10.2.3.4 Hypothesis 4

Tight gas sands' volume for Colombian continental basins can be estimated in line with the following scenarios:

Scenario 1

The values obtained regarding thickness, effective porosity and water saturation could be grouped for basins having similar characteristics. Considering all the formations found having tight gas sands, distributions could be estimated for each variable thereby leading to resources being assessed.

Scenario 2

Only tight rocks saturated with gas, having thickness greater than 23 feet thick, could validate using techniques for exploiting the resources and only these should be taken into account for the estimating tigh gas sands' potential.

10.3 Methodology

The following equation was used for calculating tight gas sand volume in Colombian continental basins:

$$G = 0.035315 * A * h * \varphi * (1 - S_w) * E_g \qquad (10\text{-}1)$$

$\boldsymbol{G}$: in situ gas (Tcf)

$\boldsymbol{A}$: tight gas sands occurrence area (km^2)

$\boldsymbol{h}$: thickness of areas containing tight gas sands (km)

$\boldsymbol{\varphi}$: total rock density (v/v)

$\boldsymbol{s_w}$: water saturation (v/v).

$\boldsymbol{E_g}$: gas expansion factor, is equal to $\frac{1}{\mathrm{B_g}}$ where Bg is the volumetric factor of gas (ft$^3_{\text{normal}}$ / ft$^3_{\text{deposit}}$).

The methodology used for estimating resources included the following activities:

- Available well and record data was loaded into a Kingdom Suite project;
- The data regarding the loaded well records was reviewed and edited to determine which wells had the necessary records for making the petro-physical calculations and discriminating tight gas-bearing areas; and
- Effective porosity, water saturation and permeability were calculated for the selected wells. The Kingdom Suite's petro-physics module was used for making the calculations. The parameters used for the calculations were:

  - ✓ A density/neutron gas porosity model was used for estimating effective porosity:

$$\emptyset_{DHG_e} = \sqrt{\frac{(\emptyset_{De}^2 + \emptyset_{NE}^2)}{2}}$$

$\emptyset_{DHGe}$: effective porosity per density-neutron area of gas (v/v)

$\emptyset_{De}^2$: effective porosity per density (v/v)

$\emptyset_{NE}^2$: effective neutron porosity (v/v)

  - ✓ Stieber's gamma ray model was used for estimating clay volume

$$V_{sh} = \frac{0.5 \times GRI}{1.5 \times GRI}$$

V_{sh}: clay volume in the formation (v/v)

GRI: gamma ray index (API)

$$GRI = \left(\frac{Gr_{log} - Gr_{clean}}{Gr_{shale} - G_{clean}}\right)$$

Gr_{log}: gamma ray from the records (API)

Gr_{clean}: gamma ray in clean formations (API)

Gr_{shale}: gamma ray in 100% clay areas (API)

The Gr_{clean} and Gr_{shale} values used can be verified in the file cited in the Appendixes.

✓ The Simandoaux model was used for calculating water saturation.

$$S_w = \left(\frac{0.45 \times R_w}{\emptyset_e^m}\right) \times \left(\left[\left(\frac{5.0 \times \emptyset_e^m}{R_w \times R_t}\right) + \left(\frac{V_{sh}}{R_{sh}}\right)^2 \right]^{\frac{1}{n}} - \frac{V_{sh}}{R_{sh}} \right)$$

m: cementation exponent

n: saturation exponent

S_w: water saturation (v/v)
R_w: water resistivity (ohm-m)
R_t: area resistivity (ohm-m)
R_{sh}: shale resistivity (ohm-m)
V_{sh}: volume of clay in the formation (v/v)

Water and shale resistivity values can be found in the file cited in the Appendixes.

✓ Permeability was estimated using the Wylie-Rose ratio:

$$k = \frac{62{,}500 \times \emptyset_e^6}{S_{wi}^2}$$

k: permeability (mD)
$\emptyset_e$: effective porosity (v/v)
S_{wi}: irreducible water saturation (v/v)

- Porosity per density was estimated using a sand matrix:

$$DPHI = \frac{RHOM - RHOB}{RHOM - RHOF}$$

DPHI: porosity per density
RHOM: matrix density: 2.65 g/cm^3
RHOB: bulk density (g/cm^3)
RHOF: fluid density: 1 g/cm^3

- A record was produced indicating areas of gas having neutron porosity and porosity per density records, using the following condition:

$$Si\ DPHI > PHI \quad \rightarrow \quad Area_{Gas} = 1$$
$$If\ not\ \rightarrow \mathrm{Area}_{Gas} = 0$$

DPHI: porosity per density
PHI: neutron porosity

- A gamma ray cut-off was established leading to differentiating the areas of sands in each well (Figure 10-5).
- The thickness of areas having the presence of tight gas sands was calculated per well fulfilling the necessary conditions (Figure 10-5); average effective porosity and water saturation values were estimated for these areas.

$$Gamma\ ray < Corte_{gamma\ ray\ sand} \rightarrow Determine\ whether\ an\ area\ is\ sand$$

$$Permeability < 0.1\ mD \rightarrow Determine\ whether\ an\ area\ is\ tight$$

$$Permeability < 0.1\ mD \rightarrow Determine\ whether\ an\ area\ is\ tight$$

Adding the areas complying with the foregoing conditions led to establishing effective thickness for tight gas sands per well.

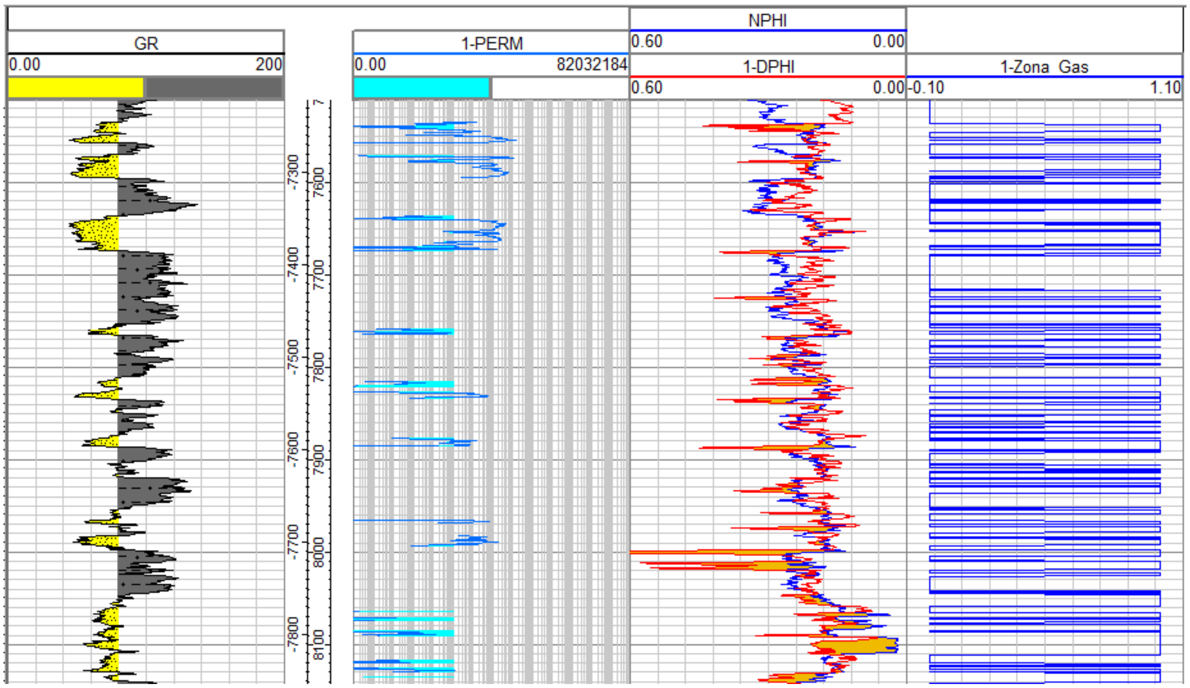

Figure 10-5. Montoya A-1 well record. Track 1 shows the gamma ray; the yellow areas represent sands (80 API sand cut-off); track 2 shows the permeability record, light blue highlighting tight areas (permeability < 0.1 mD); track 3 shows neutron porosity records (blue) and porosity per density (red) and areas having gas (orange); the last track shows records indicative of gas, 1 standing for areas having gas and 0 where there is no gas. The light green rectangle shows areas of tight gas sands.

- A ratio between a particular basin's total area and the area of plays containing tight gas sands was calculated for 13 basins in the USA (Figure 10-6) for estimating the percentage area of a basin which could contain tight gas sands (hypothesis 1). This factor was applied to Colombia's continental basins.

The values used for obtaining the ratio used here can be found in the file cited in this report's Appendixes.

- Monte Carlo simulation was used for calculating tight gas sands' potential with equation 10-1. This was only done for basins having the necessary data available; and
- Potential for basins lacking the necessary information was calculated by using the ratio between estimated in-situ gas volume and basin area, according to hypothesis 3.

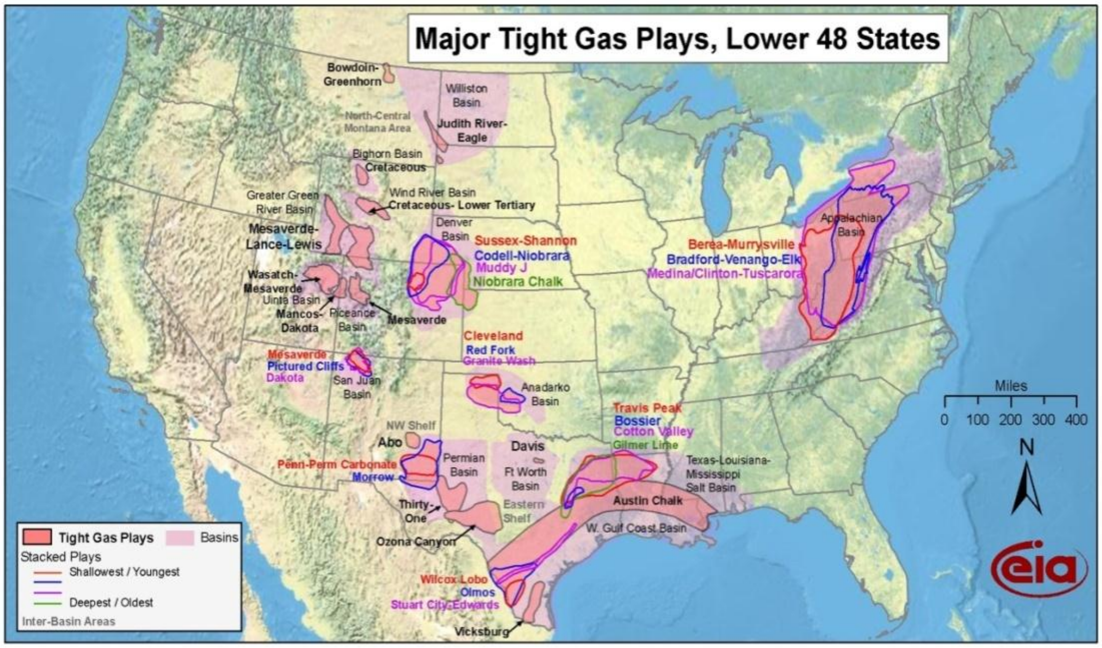

Figure 10-6. Map of the main tight gas plays in 13 basins in the USA (US Energy information Administration).

10.4 Results

When estimating resources using equation 10-1, the area was determined according to Hypotheses 1 and taken as being constant. The others variables used were defined by distributions of probability obtained from analysing the petro-physical records for the 62 wells showing evidence of tight gas sands (Figure 10-7). The data used, as well as the distributions, are contained in the aforementioned file "Colombian tight gas sands" which is attached to this report.

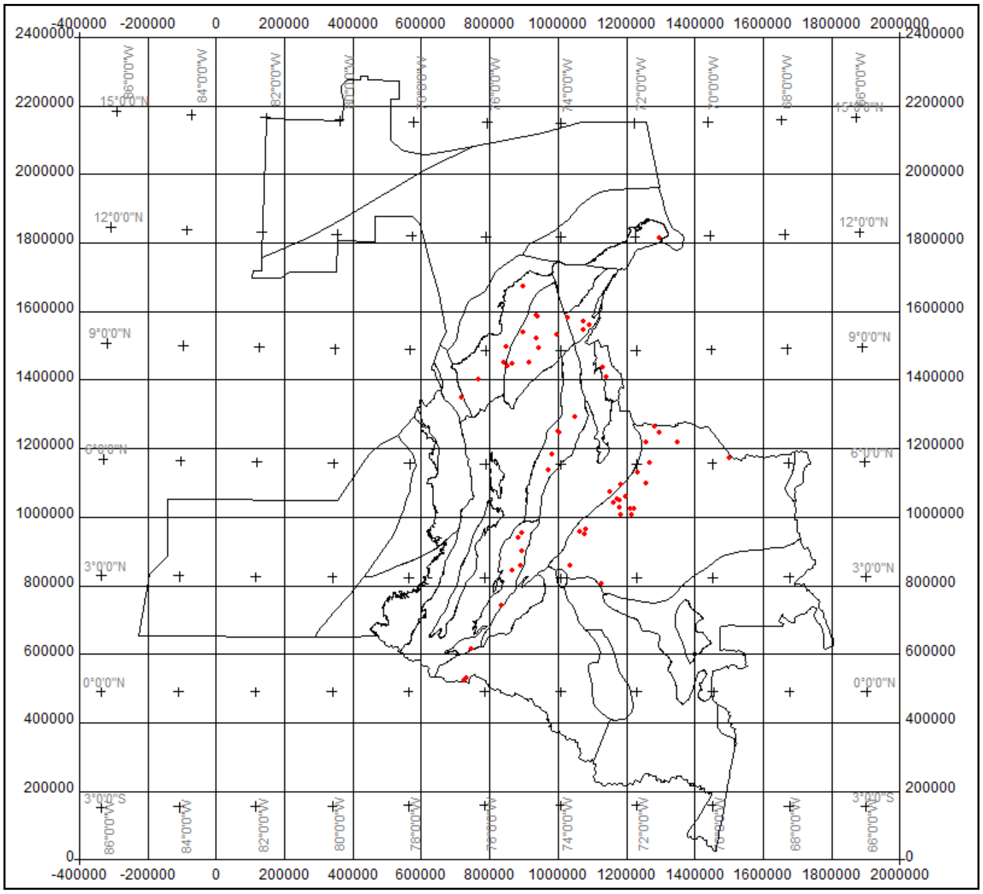

Figure 10-7. Map showing the location of the 63 wells used for estimating the gas potential in tight sands.

10.4.1 Area of tight gas sands occurrence

Analysing the data regarding basins in the USA led to identifying that 34.8% of a basin's area could contain tight gas sands. This factor was applied to the total area of continental basins in Colombia for obtaining the basins' effective area for this resource.

Basin	Area (km²)	Effective areas (km²)
Amagá	2,824.9	983.1
Caguán - Putumayo	110,304.1	38,385.8
Catatumbo	7,715.0	2,684.8
Cauca - Patía	12,823.3	4,462.5
Cesar - Ranchería	11,668.7	4,060.7
Chocó	38,582.0	13,426.5
The Eastern Cordillera	71,766.2	24,974.6
Guajira	13,778.9	4,795.1
The Eastern Llanos	225,603.3	78,509.9
Sinú - San Jacinto	39,644.6	13,796.3
Tumaco	23,732.4	8,258.9
Urabá	9,448.9	3,288.2
The Lower Magdalena Valley	38,017.4	13,230.1
The Middle Magdalena Valley	32,949.4	11,466.4
The Upper Magdalena Valley	21,512.8	7,486.5
Vaupés - Amazonas	154,867.3	53,893.8

Table 10-2. Effective area of a particular basin having gas potential in tight sands.

10.4.2 The thickness of tight gas sands areas

The gamma ray, permeability, neutron porosity and density records led to summing areas per well which complied with the conditions established for containing tight gas sands.

Two scenarios were established for the calculations. In the first, the data obtained (63 wells having tight gas sands) were analysed by groups of basin, 3 different areas being defined. A distribution was thus estimated for each group from all the values so obtained (Table 10-3). The distributions obtained were used for each basin contained in the respective areas.

The second scenario only considered the results for wells reported to have thicknesses greater than 23 ft for tight gas sands, thereby reducing the number of wells to 15; a single distribution of probability was thus found for all the data for calculating all of Colombia's continental basins (Table 10-4). Porosity and water saturation were dealt with in the same way.

10.4.3 Sediment porosity

The distribution parameters obtained for the 3 areas defined in Scenario 1 are gives in Table 10-5. Table 10-6 gives the results for Scenario 2.

10.4.4 Water saturation

Table 10-7 gives probability functions and goodness-of-fit tests used for the areas produced in Scenario 1. Table 10-8 gives the results for Scenario 2.

Basin	Distribution	Estimated parameters						Goodness-of-fit test			
		$\hat{x}$	Confidence interval		$\hat{y}$	Confidence interval		Null hypothesis	P	Statistical value	G.L
Area 1	Gamma	0.47	0.30	0.72	0.02	0.01	0.04	Was not rejected	M.B	0.89	0
Area 2	Lognormal	-5.81	-6.73	-4.89	1.96	1.49	2.86	Was not rejected	M.B	0.05	0
Area 3	Lognormal	-7.13	-7.71	-6.55	1.05	0.77	1.65	Was not rejected	M.B	0.02	0

Table 10-3. Goodness-of-fit test distributions, fit parameters and results applied to the thickness data used in estimating the gas potential in tight sands in Scenario 1. Area 1 groups the Caguán - Putumayo, the Eastern Cordillera and the Eastern Llanos basins. Area 2 groups Catatumbo, Cesar - Ranchería, the Middle Magdalena Valley and Upper Magdalena Valley basins. Area 3 groups the Sinú - San Jacinto, Urabá and the Lower Magdalena Valley basins. Estimated parameters $\hat{x}$ and $\hat{y}$ are gamma distribution form and scale and the mean and standard deviation for lognormal distribution. M.B refers to a very low probability of the null hypothesis being accepted or rejected.

Estimated parameters						Goodness-of-fit test			
$\hat{x}$	Confidence interval		$\hat{y}$	Confidence interval		Null hypothesis	P	Statistical value	G.L
0.22	-0.43	0.86	0.03	0.01	0.07	Was not rejected	M.B	0.42	0

Table 10-4. Pareto distribution goodness-of-fit test results and parameters applied to the thickness data used in estimating tight gas sands in Scenario 2. Estimated parameters $\hat{x}$ **and** $\hat{y}$ are Pareto distribution form and scale.

ANH AGENCIA NACIONAL DE HIDROCARBUROS

Basin	Distribution	Estimated parameters						Goodness-of-fit test			
		$\hat{x}$	Confidence interval		$\hat{y}$	Confidence interval		Null hypothesis	P	Statistical value	G.L
Area 1	Extreme Minimum	0.07	0.06	0.07	0.02	0.01	0.02	Was not rejected	M.B	0.02	0
Area 2	Triangular	0.07	0.02	0.09	N/A	N/A	N/A	N/R	N/R	N/R	N/R
Area 3	Extreme Minimum	0.06	0.05	0.07	0.02	0.01	0.02	Was not rejected	M.B	0.29	0

Table 10-5. Goodness-of-fit test distributions, fit parameters and results applied to porosity data used in estimating the gas potential in tight gas sands in Scenario 1. Estimated parameters $\hat{x}$ and $\hat{y}$ are extreme value distribution location and scale. Estimated $\hat{x}$ for triangular distribution is the most probable value, and their confidence interval gives minimum and maximum values as extremes. N/A refers to parameters which did not apply to the type of distribution being considered. "N/R" refers to parameters which, as they went beyond the algorithm's range of calculations, were not reported when making the statistical estimation.

Estimated parameters						Goodness-of-fit test			
$\hat{x}$	Confidence interval		$\hat{y}$	Confidence interval		Null hypothesis	P	Statistical value	G.L
12.23	4.72	31.68	226.07	84.23	606.79	Was not rejected	M.B	0.08	0

Table 10-6. Beta distribution and goodness-of-fit parameters and test results applied to porosity data used in estimating tight gas sands in Scenario 2. Estimated parameters $\hat{x}$ and $\hat{y}$ are Beta distribution parameters "a" and "b".

Basin	Distribution	Estimated parameters						Goodness-of-fit test			
		$\hat{x}$	Confidence interval		$\hat{y}$	Confidence interval		Null hypothesis	P	Statistical value	G.L
Area 1	Beta	0.66	0.15	3.04	0.15	0.12	0.18	Was not rejected	M.B	16.15	0
Area 2	Weibull	0.83	0.73	0.95	3.61	2.47	5.26	Was not rejected	M.B	0.44	0
Area 3	Beta	0.29	0.001	165.7	0.02	0.01	0.05	Was not rejected	M.B	14.22	0

Table 10-7. Goodness-of-fit test distributions, fit parameters and results applied to the water saturation data used in estimating tight gas sands in Scenario 1. Estimated parameters $\hat{x}$ and $\hat{y}$ are Weibull distribution parameters "a" and "b", respectively.

Estimated parameters						Goodness-of-fit test			
$\hat{x}$	Confidence interval		$\hat{y}$	Confidence interval		Null hypothesis	P	Statistical value	G.L
0.33	N/A	N/A	0.99	N/A	N/A	N/R	N/R	N/R	N/R

Table 10-8. Uniform distribution goodness-of-fit parameters and test results applied to the water saturation data used in estimating tight gas sands in Scenario 2. Estimated parameters $\hat{x}$ and $\hat{y}$ are uniform distribution maximum and minimum, respectively.

10.4.5 Gas expansión

A series of values obtained from ANH reports for different gas fields in Colombian basins was used for obtaining a probabilistic distribution for gas expansion. Distribution functions associated with such data and their goodness-of-fit parameters are listed in Table 10-9.

Estimated parameters						Goodness-of-fit test			
$\hat{x}$	Confidence interval		$\hat{y}$	Confidence interval		Null hypothesis	P	Statistical value	G.L
5.26	5.18	5.34	0.30	0.26	0.37	Was not rejected	0.11	6.10	3

Table 10-9. Lognormal distribution goodness-of-fit parameters and test results applied to the gas expansion factor data used in estimating tight gas sands in both Scenarios.

10.4.6 Sensitivity analysis

The distribution functions established for random variables (thickness, porosity, water saturation, gas expansion) resulted from analysing the distribution of known data regarding the area. Consequently, sensitivity analysis of the basins in question suggested that tight gas sands exploration studies for Colombian continental basins must reduce uncertainty, mainly regarding thickness and water saturation, according to sensitivity analysis results in both scenarios.

The greatest uncertainty in this scenario was presented regarding gas layer thickness (69.99%) and water saturation (24.45%); the variables having least uncertainty were gas expansion and porosity (Figure 10-8).

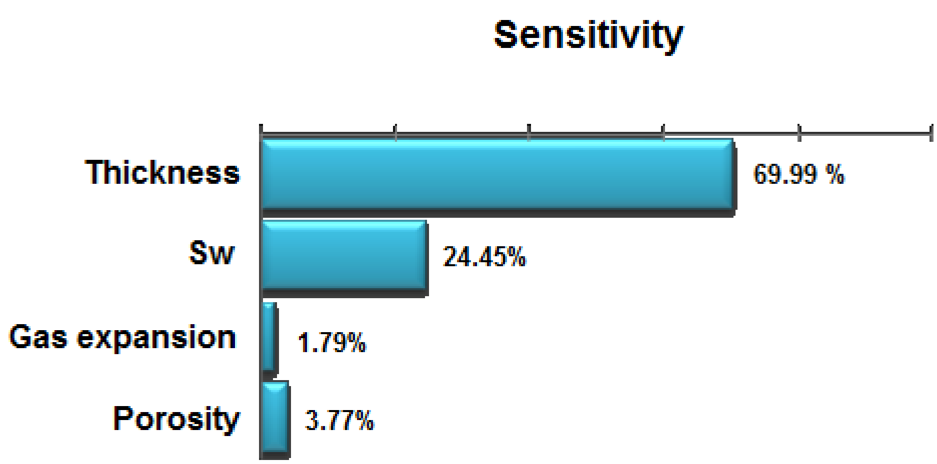

Figure 10-8. Percentage analysis of the sensitivity of the variables used for estimating tight gas sands.

10.4.7 Sensitivity analysis – Scenario 2

Likewise, the greatest uncertainty was presented regarding gas layer thickness (53%) and water saturation (36.4%); the variables having least uncertainty were gas expansion and porosity (Figure 10-9).

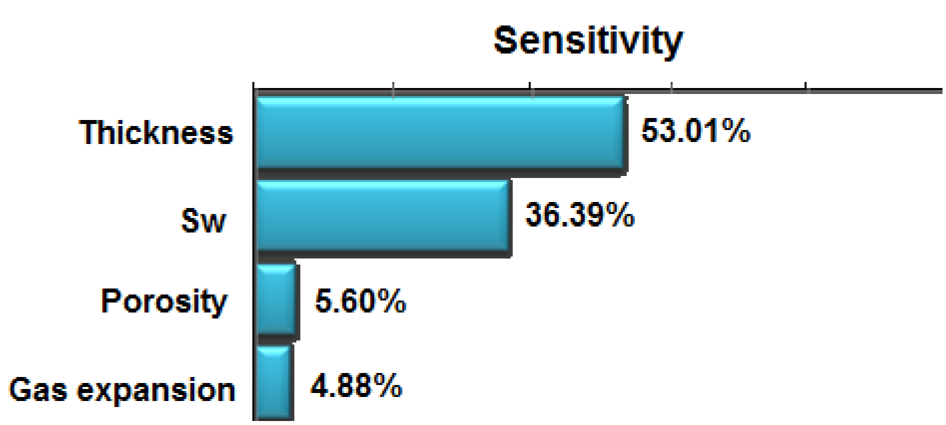

Figure 10-9. Percentage analysis regarding the sensitivity of the variables used for estimating gas in tight sands.

10.4.8 Estimating resources for those basins lacking information

There was no well information or production field data regarding some of Colombia's continental basins to enable determining the necessary distributions for using equation 10-1; a ratio was thus identified in such cases associating basin area and the volume of tight gas sands contained by such basin (Figures 10-10 and 10-11). A linear fit for such ratios led to identifying tendencies for P_{90}, P_{50} and P_{10}. The equations derived from the linear fit led to estimating gas values for basins lacking pertinent information.

The basins to which these ratios were applied due to a lack of data are listed in Table 10-10.

Basin	Total area km²	Effective area km²
Amagá	2,824.929129	983.0753367
Patía - Cauca	12,823.30684	4462.510782
Chocó	38,581.98137	13,426.52952
Tumaco	23,732.41861	8,258.881678
Vaupes - Amazonas	154,867.3143	53,893.82539

Table 10-10. Basins lacking data for estimating tight gas sands.

10.4.8.1 Basin area cf gas volume ratio - Scenario 1

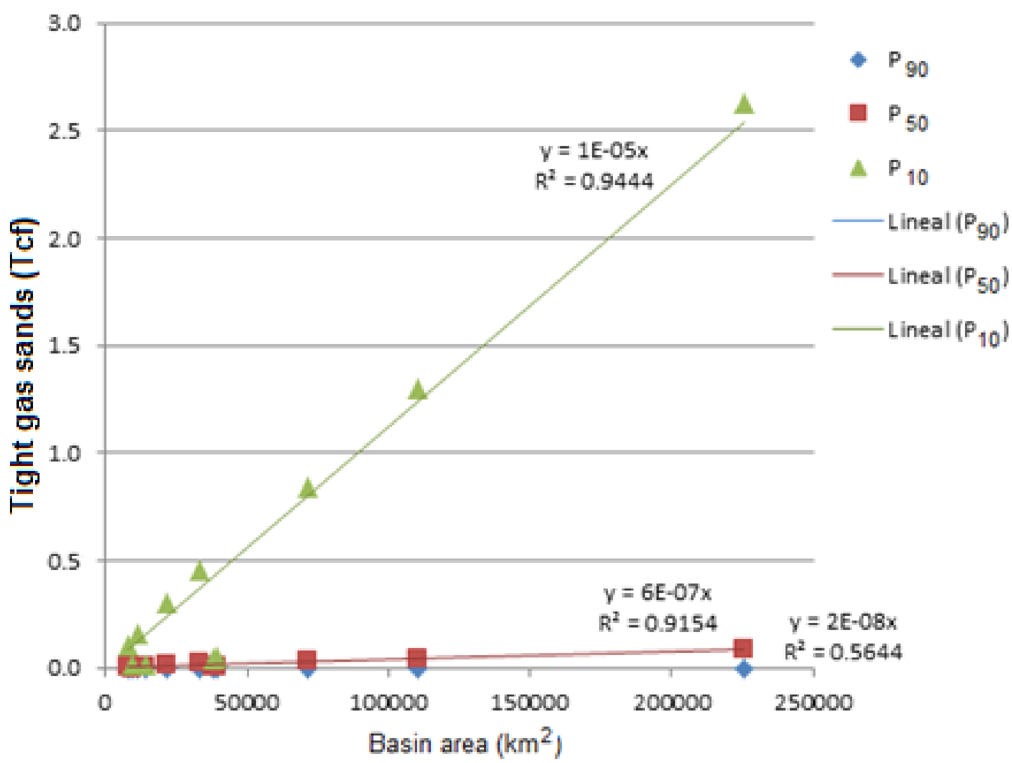

Figure 10-10. A graph of basin area compared to gas volume and the ratios obtained for P_{90}, P_{50} and P_{10} in Scenario 1.

10.4.9 Basin area cf gas volume ratio - Scenario 2

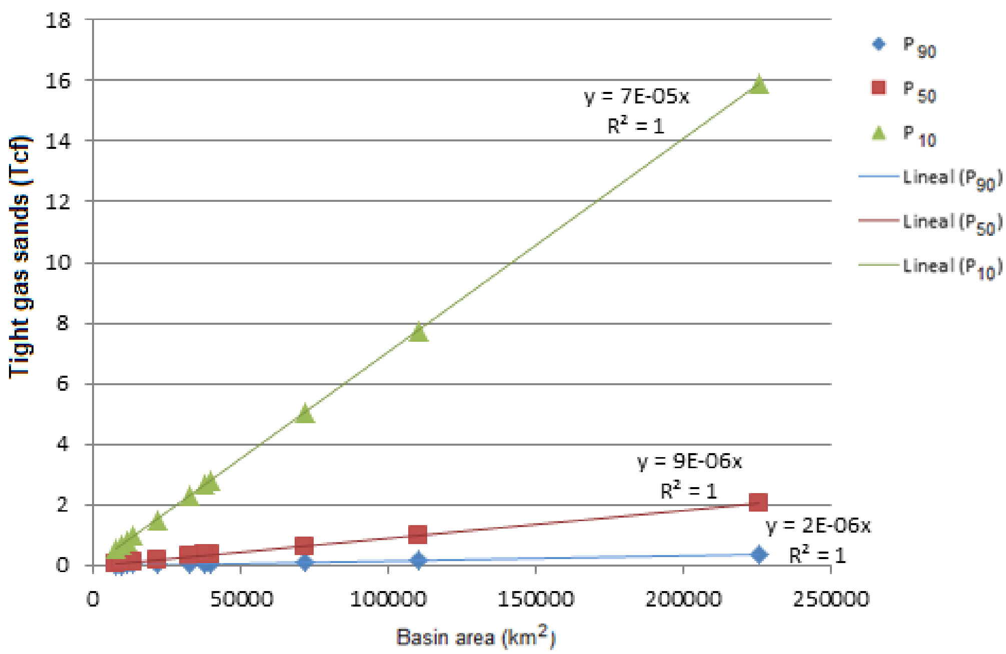

Figure 10-11. Graph of basin area compared to gas volume and the ratios obtained for P_{90}, P_{50} and P_{10} in Scenario 2.

10.4.10 Tight gas sands in Colombia

Based on the aforementioned hypotheses and the definition of the random variables expressed in equation 10-1, gas resources in tight sands were calculated for basins having available data and linear ratios were applied for basins lacking the necessary information for P_{90}, P_{50} and P_{10} from the Monte Carlo simulation results. Gas was thus estimated for Colombia's continental basins in the aforementioned two scenarios. Tables 10-11 and 10-12 shows the results obtained after discounting resources found in areas where environmental considerations applied.

Basin	Tight gas sands - Scenario 1					
	P_{90} (Tcf)	P_{90} (MMBOE)	P_{50} (Tcf)	P_{50} (MMBOE)	P_{10} (Tcf)	P_{10} (MMBOE)
Amagá	0.0000	0.0026	0.0009	0.0884	0.0087	1.4696
Caguán - Putumayo	0.0001	0.0102	0.0415	7.0815	1.2001	206.9095
Catatumbo	0.0002	0.0358	0.0047	0.8368	0.1018	17.5149
Patía - Cauca	0.0001	0.0150	0.0030	0.4618	0.0450	7.6911
Ranchería - Cesar	0.0003	0.0570	0.0080	1.3450	0.1620	27.9970
Chocó	0.0003	0.0450	0.0078	1.3597	0.1312	22.6611
The Eastern Cordillera	0.0000	0.0062	0.0258	4.4087	0.7513	129.5166
Guajira	0.0002	0.0274	0.0020	0.3331	0.0156	2.7540
The Eastern Llanos	0.0001	0.0205	0.0870	15.0096	2.5674	442.5870
Sinú - San Jacinto	0.0004	0.0709	0.0054	0.8756	0.0422	7.2294
Tumaco	0.0002	0.0273	0.0049	0.8328	0.0809	13.8847
Urabá	0.0001	0.0184	0.0010	0.2249	0.0107	1.8572
The Lower Magdalena Valley	0.0004	0.0760	0.0050	0.9340	0.0450	7.7230
The Middle Magdalena Valley	0.0009	0.1620	0.0220	3.7990	0.4560	78.6260
The Upper Magdalena Valley	0.0006	0.0975	0.0130	2.2910	0.2785	48.0563
Vaupes - Amazonas	0.0009	0.1458	0.0251	4.3703	0.4225	72.8408
TOTAL	0.005	0.818	0.257	44.252	6.319	1089.318

Table 10-11. Tight gas sands in Scenario 1, discounting resources in natural parks.

Basin	Tight gas sands - Scenario 1					
	P_{90} (Tcf)	P_{90} (MMBOE)	P_{50} (Tcf)	P_{50} (MMBOE)	P_{10} (Tcf)	P_{10} (MMBOE)
Caguán - Putumayo	0.147	25.725	0.858	147.597	6.720	1158.744
Catatumbo	0.009	1.909	0.065	10.968	0.498	86.376
Ranchería - Cesar	0.019	2.959	0.094	16.953	0.773	133.703
The Eastern Cordillera	0.110	19.273	0.640	110.528	5.028	867.051
Guajira	0.020	3.720	0.120	21.290	0.970	167.020
The Eastern Llanos	0.343	59.264	1.977	341.302	15.555	2682.450
Sinú - San Jacinto	0.053	9.491	0.312	54.532	2.504	431.407
Urabá	0.010	2.472	0.078	14.254	0.655	112.389
The Lower Magdalena Valley	0.059	9.965	0.332	57.170	2.608	449.818
The Middle Magdalena Valley	0.045	7.913	0.260	45.531	2.081	359.386
The Upper Magdalena Valley	0.029	5.656	0.185	32.306	1.463	252.428
Amagá	0.002	0.330	0.010	1.483	0.068	11.496
Patía - Cauca	0.010	1.540	0.040	6.920	0.310	53.860
Chocó	0.030	4.630	0.120	20.830	0.940	162.040
Tumaco	0.019	2.646	0.065	11.901	0.538	92.533
Vaupes - Amazonas	0.086	14.565	0.384	65.558	2.955	509.886
TOTAL	0.991	172.058	5.540	959.123	43.666	7530.587

Table 10-12. Tight gas sands in Scenario 2, discounting yet-to-find tight gas sands in natural park areas.

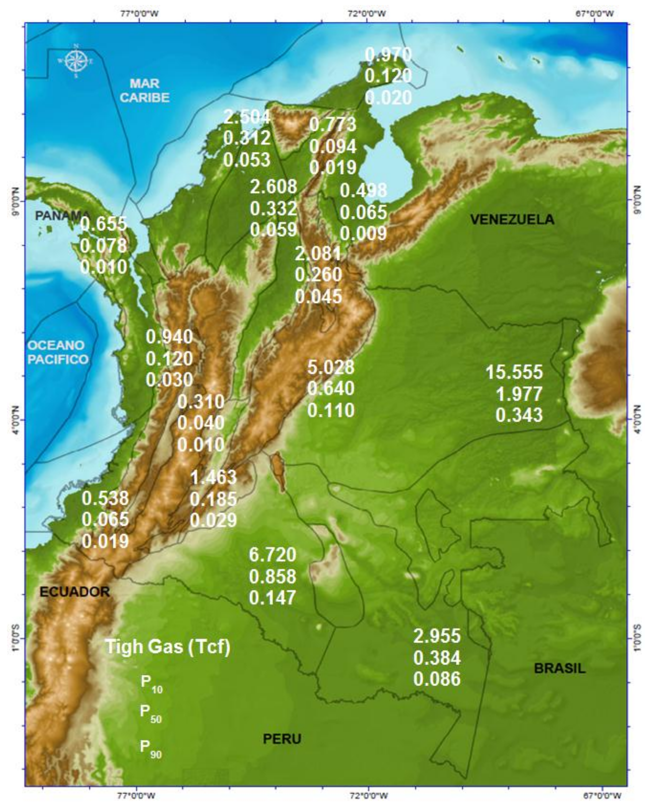

Figure 10-12. Map of tight gas sands estimated for Colombia's continental basins- Scenario 2.

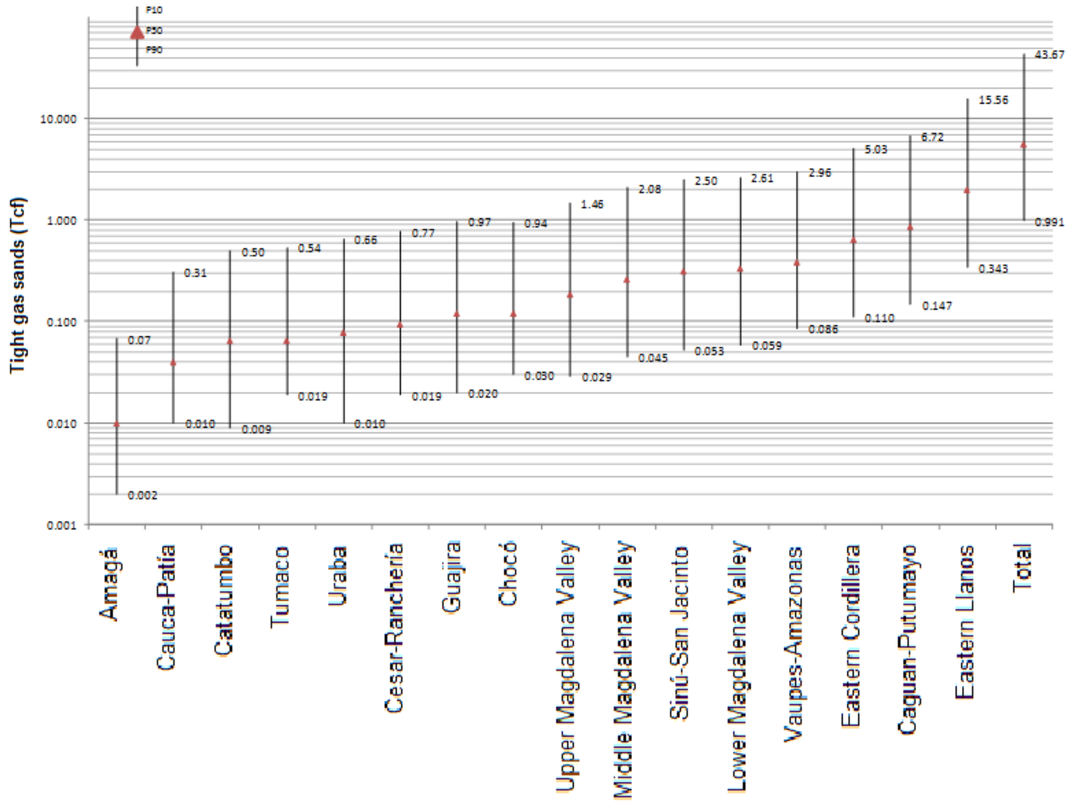

Figure 10-13. Tight gas sands estimated for Colombia's continental basins - Scenario 2.

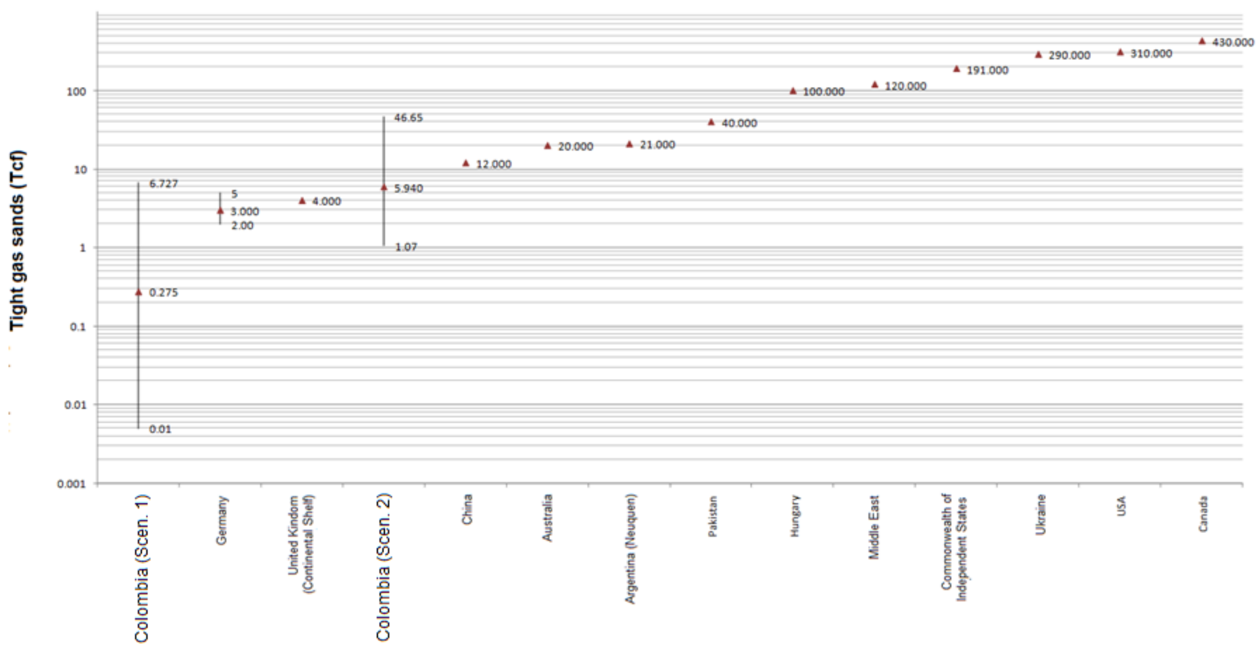

Figure 10-14. Tight gas sands around the world.

ANH AGENCIA NACIONAL DE HIDROCARBUROS

10.5 Conclusions

- The information about wells led to identifying that the basins having the greatest tight gas sands in P_{10} were the Middle Magdalena Valley, the Upper Magdalena Valley and Sinú - San Jacinto, for Scenario 1 and the Eastern Llanos, Caguán - Putumayo and the Eastern Cordillera for Scenario 2;
- Analysing the results obtained in P_{50} and P_{10} from well information showed that the most prospective basins were the Eastern Llanos, Caguán in Putumayo and the Eastern Cordillera in both scenarios;
- The results obtained regarding tight gas sands in Colombia regarding those reported by ADL (1.2 Tcf) were considerably greater in Scenario 2 (1.07–46.66 Tcf) and ranged from 0.01–6.73 Tcf in Scenario 1; and
- Part of the tight gas sands potential was found to lie in natural park areas (Scenario 1: P_{10} 0.408 Tcf - P_{50} 0.018 Tcf - P_{90} 0 / Scenario 2: P_{10} 2.99 Tcf - P_{50} 0.40 Tcf - P_{90} 0.08 Tcf).

10.6 Bibliography

Aziz Jabr, Abdel. Unconventional Reservoirs Episode 1: Tight Gas Reservoir. SPE Suez Canal University Student Chapter. 2010. http://www.spesuez.org/spe/virtualcampus/unconventionalreservoir.html (Last consulted: 2nd November, 2011).

Chakhmakhchev, Alex, and Kris McKnight. Searching for Tight Gas Reservoir. http://a1024.g.akamai.net/f/1024/13859/1d/ihsgroup.download.akamai.com/13859/energy/searchingfortightgasreservoirs.pdf (Last consulted: 2nd November, 2011).

China National Petroleum Corporation. Status and Development Prospects of China´s Unconventiona Natural Gas Exploration and Exploitation. http://uschinaogf.org/Forum9/pdfs/Xinhua_English.PDF (Last consulted: 2nd November, 2011).

Department of Resources, Energy and Tourism. Australian Energy Resource Assessment 2010. 2010. http://adl.brs.gov.au/data/warehouse/pe_aera_d9aae_002/aeraCh_04.pdf (Last consulted: 2nd November, 2011).

Energy, Centrica. Unconventional Gas in Europe Response to DECC Consultation. 2010. http://www.decc.gov.uk/assets/decc/what%20we%20do/global%20climate%20change%20and%20energy/international%20energy/policy/1290-unconventional-gas-centrica-response.pdf (Last consulted: 2nd November, 2011).

Gas, unconventional gas subgroup of the technology task group of the NPC committee on global oil and unconventional gas reservoirs - tight gas, col seams, and shales. The National Petroleum Conuncil (NPC), 2007.

Holditch, Stephen A. Tight Gas Sands. Society of Petroleum Engineers, 2006: 86-94.

Muntendam-Bos, A. G., B.B. T. Wassing, J. H. Heege, and F. Bergen. TNO report Inventory non-conventional gas. Utrecht: TNO Built Enviroment and Geosciences, 2009.

Naik, G C. Tight gas reservoirs: An unconventional natural energy source for the future. 2003.

Rogner, Hans-Holger. An Assessment of World Hydrockrbon Resources. IIASA, 1996: 96-26.

Shahab, Alam. Potential of Tight Gas in Pakistan: Productive, Economic and Policy Aspects. Search and Discovery Article #80149 , 2011.

TOTAL. The Know - How series // Tight Gas Reservoirs Technology - Intensive Resources. Paris: Exploration & Production, 2007.

U. S. Energy Information Administration - Energy Mineral Division. http://emd.aapg.org/technical_areas/tightGas.cfm (Last consulted: 2nd November, 2011).

U.S.A. Energy information Administration. http://205.254.135.24/pub/oil_gas/natural_gas/analysis_publications/maps/maps.htm (Last consulted: 31st October 2011).

Vidas, Harry, and Bob Hugman. Availability, economics, and production potential of north american unconventional natural gas supplies. INGAA Foundation, Inc. 2008. http://www.ingaa.org/File.aspx?id=7878 (Last consulted: 2nd November, 2011).

10.7 Appendixes

Digital files in the ANH'S Document Center:

- ✓ "Gas Arenas Apretadas Colombia.xlsx"
- ✓ Kindom Suit project

11 HEAVY CRUDES

11.1 General comments

One of liquid hydrocarbons' characteristics is its fluidity or viscosity, indirectly reflecting its density (or specific gravity). This property is slightly conditioned by temperature, thereby leading to defining the type of crude in terms of specific gravity and degrees API (American Petroleum Institute) being used as measurement unit.

When petroleum has greater viscosity and density it will be heaviest; the denser the crude, the lower are its API degrees (Table 11-1).

Hydrocarbon	API
Condensed	> 40.0
Light crude	30.0<API≤40.0
Medium crude	22,0<API≤29,9
Heavy crude	10,0<API≤21,9
Extraheavy crude	<10.0
Bitumen	crude, asphalt, sand

Table 11-1. Types of hydrocarbons regarding API.

Classification regarding heavy crudes' physical properties is ambiguous. Viscosity is variable in each type of compound; the H/C ratio becomes reduced when gas and conventional oil change from being natural to becoming heavy, asphalts and then kerogen, even though this not a weighty parameter for differentiating them. The environmental factors which determined the way in which degradation (e.g. oxidation, bacteria, being washed by water, etc) or maturation lead to resolving such ambiguity.

11.1.1 Origin and characteristics

- Petroleum becomes heavy due to the degradation which could occur during migration and entrapment. Degradation could result from various processes, such as:
- A biological, chemical or physical process, by bacteria transported by surface water metabolising the hydrocarbons in the heaviest molecules;
- By means of formation water removing the lightest components by solution, due to these being most soluble in water;
- Due to crude's volatility when a seal is not efficient, allowing the lightest molecules to pass through its interconnected pores; and
- Another characteristic of these crudes is that they have high sulphur content. Likewise, they could have an appreciable salt content and also contain metals (i.e. nickel, vanadium). They may sometimes contain a certain amount of hydrogen sulphide.

The terms heavy and extra-heavy attempt to group hydrocarbons having specific properties, essentially having density values higher than those for water (>920 kg/m^3), in deposits in sedimentary rocks (whether consolidated or not) containing highly viscous bitumen, solid or semisolid hydrocarbons.

The accumulation of heavy crudes is associated with young formations and/or shallow deposits having low efficiency rocks seals. During many phases of hydrocarbons being generated in and expelled from the basins during the Cretaceous and Palaeogene periods large volumes migrated towards their margins, originating accumulations of heavy crudes at relatively shallow depths according to a particular petroleum system's conditions allowing this.

There is usually a high probability of heavy crudes being found in any onshore sedimentary basin. The basins having the greatest presence of heavy crudes in Colombia or having proven evidence are the Eastern Llanos, Caguán in Putumayo, the Eastern Cordillera, the Upper and Middle Magdalena Valley and Chocó (Table 11-2, Figure 11-1).

Basin	Rock source	Migration	Rock reservoir	Seal	Trap
Caguán, Putumayo	Caballos and Villeta Fm	Migration from west to east throughout the sandstone in the Caballos and Villeta Fm. vertical migration throughout the fractures and fault areas. Expulsion during the late Miocene after the formation of larger structures	Caballos. Villeta and Pepino Fm	Villeta, Rumiyaco and Orteguaza Fm	Structural traps associated with thrusting and sub-thrust in the west of the basin and upthrusts in the foreland. Pinching out and carbonates
Chocó	Iró Fm	Lateral migration. Vertical migration associated with the fault systems	Iró and La Mojarra Fm Naturally fractured deposits	La Siena and Itsmina Fm	Structural highs, anticlines having a mud nucleus on diapir flanks, anticlinal thrusts, normal faults, carbonated rocks and fractured cherts in fault areas
The Eastern Cordillera	La Luna Fm Middle Albian - and Turonian condensed sections	The first generation pulse occurred during the late Cretaceous. The second pulse occurred from the Miocene up to the present	Albian and Cenomanian and Palaeogene siliciclasts	Esmeralda, Mugrosa. and Socha Fm	Inverse faults involving plinths, inversion of normal faults, faults related to folding and duplex structures
The Eastern Llanos	Gacheta and Villeta Fm	Eocene - Upper Oligocene, Miocene and continuing up to the present	Une, Gacheta, Carbonera (C3, C5 and C7) and Mirador	Gacheta, Carbonera (C2, C8)	Faulted anticlines, antithetic faults, stratigraphic traps
The Middle Magdalena Valley	La Luna v Simití-Tablezo Fm	Direct vertical migration due to Eocene nonconformity or through faults and lateral migration throughout the sands of the Eocene period	Lisama. Esmeraldas-La Paz, and Colorado-Mugrosa, la Luna, Umir, Barco Fm	Esmeraldas, Colorado Fm Potentially the shales of the Simiti and Umir Fm	1) Faults related to folding below thrust surfaces, 2) duplex structures having faults with independent closure, 3) structural strikes where the deposits' strata dip against the faults, 4) traps in the hanging wall fault-block
The Upper Magdalena Valley			Caballos. Monserrate. Honda Fm		

Table 11-2. General comments regarding potential basins' petroleum system. Fm refers to formation.

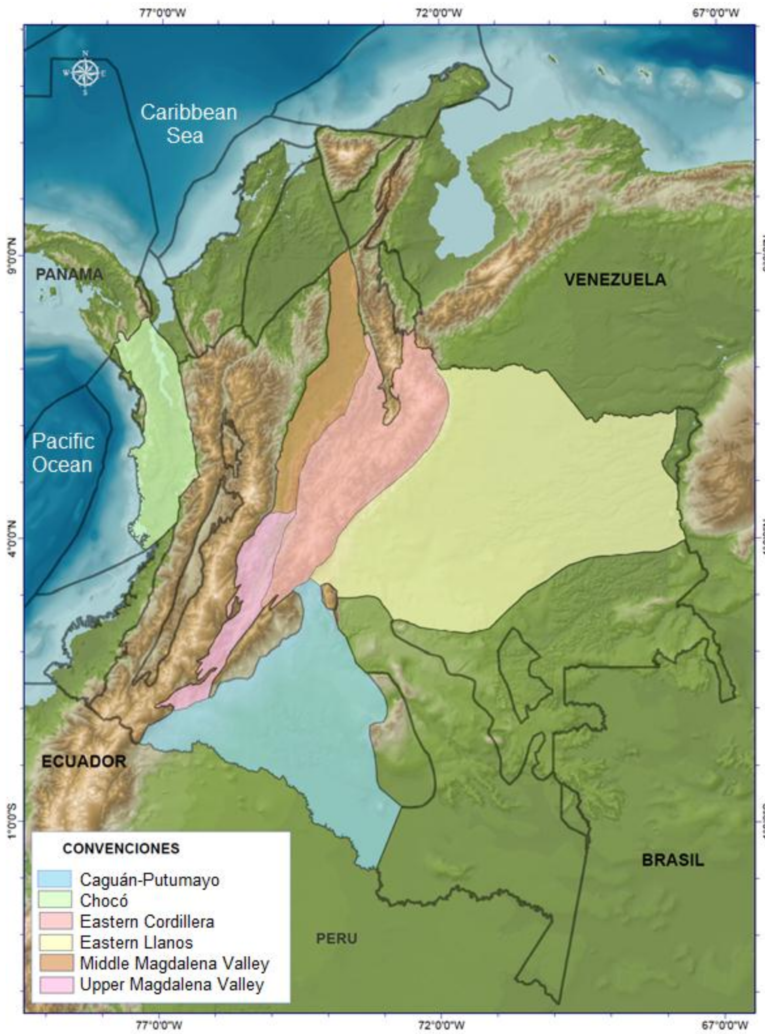

Figure 11-1. Basins having heavy crudes in Colombia.

11.2 Data and hypotheses

The set of compiled data attached as part of this document in the Appendix 1, contains information from heavy crudes studies for Colombia. The data contains information regarding wells, formation limits and bases, thicknesses, lithological analysis, stratigraphs and recovery factors. Such information/data was used for calculating weighting factors per scenario and resource category, estimating porosity, thickness and water saturation distribution functions from the results of each goodness-of-fit test and correlations made.

The information about heavy crudes occurrences in Colombia was obtained from the following sources:

- Seismic and well information supplied by ANH referring to areas having heavy crudes;
- An integral study carried out between ANH and Halliburton in 2007 estimating sustainable proven and probable reserves for crudes having gravity less than or equal to (<) 20 API in the Eastern Llanos basin;

- A reserves and resources report containing data from heavy crude-producing fields in Colombian basins (Resolution 494/2009, issued by ANH);
- Publications by ANH forming part of an agreement with the EAFIT, UIS and UPTC universities associated with evaluating potential of various sedimentary basins; and
- Other publications regarding heavy crudes in Colombia.

11.2.1 Hypotheses

The compiled information was scrutinised to identify plays having the presence of heavy crudes in Colombian basins. A weighting factor was then applied to such recorded areas to reduce uncertainty regarding the effective presence of heavy crudes in line with the following hypotheses:

11.2.1.1 Hypothesis 1

The maximum value for an area containing hydrocarbons having lower than (<) 22 API density in a mature sedimentary basin is defined by the ratio between existing fields' total area and a particular basin's total extension;

11.2.1.2 Hypothesis 2

Total production thickness is derived from reported well and field production data, seismic information and field studies about a formation of interest;

11.2.1.3 Hypothesis 3

Thickness is derived from well data and/or that reported in plays, establishing net thickness having greater than 10% effective porosity, lower than 30% clay volume and plays having less than 50% water saturation;

11.2.1.4 Hypothesis 4

Porosity and water saturation values will be derived from well data and production information from assessing net and play thickness;

11.2.1.5 Hypothesis 5

The distribution for basins having scarce field information regarding heavy crudes will be considered triangular, assuming maximum and minimum values as limits and the average as the value having the greatest probability; and

11.2.1.6 Hypothesis 6

Basins having potential interest arise from areas reported as having heavy crudes.

11.3 Methodology

The following equations were used for evaluating heavy crudes in Colombian basins, as follows:

$$\mathrm{OOIP} = 7758.367 * A_{Cuenca} * \boldsymbol{k} * h_{Pay} * \boldsymbol{\Phi} * (1 - Sw) * \frac{1}{Bo} \quad \textbf{(11-1)}$$

$OOIP_{Heavy\ Oil}$: (original oil in place): volume of deposit's original petroleum (MMBbl)

7758.367: conversion factor acre/foot to barrels of oil

A: basin area (acres)

h: play area total thickness (ft)

Ntg: net-to-gross ratio (net/h)

h_{Pay}: play thickness, where Sw > 50%

Φ: porosity (%)

Sw: water saturation (%)

Bo: play formation volumetric factor, expressed as barrel in deposit/barrel on the surface

The procedure for estimating resources considered the following stages:

- Existing information regarding heavy crude deposits dealing with plays, well data, lithology, thickness and saturation was reviewed:
  - ✓ A database was built from well information relating formation and play thickness, porosity and saturation. The compiled information contained the name of the well, its location, net thickness, porosity and saturation having heavy crudes of interest (Appendix 11-1);
  - ✓ Greater than 10% effective porosity, lower than 30% clay volume and play thickness having less than 50% water saturation were considered for estimating net thickness from well information (Halliburton, 2006);
  - ✓ Play thickness was established for the different fields from the reported information, also considering porosity, thickness, saturation and real crude recovery values;
  - ✓ The porosity (< 10%) described in production reports was assumed for the Eastern Cordillera basin;
  - ✓ Three scenarios were considered for the Llanos basin, as follows:
    - Scenario 1: heavy crudes were calculated from the net-to-gross (Ntg) ratio derived from well data relating net thickness to total thickness (Halliburton, 2006);
    - Scenario 2: heavy crudes were calculated from play thickness derived from well data (Halliburton, 2006); and
    - Scenario 3: heavy crudes were calculated from reported play thickness (ANH, 2010);
- Distribution functions were established for thickness, porosity and saturation in yet-to-find areas:
  - ✓ Goodness-of-fit tests were applied, considering the best distribution for each variable and distribution parameters and their pertinent confidence intervals were estimated;
- An aerial ratio was established allowing maximum extension for heavy hydrocarbon occurrence per basin to be considered. According to Vargas (2009), each sedimentary basin gives a fraction of area which could reflect the whole of its hydrocarbon potential in actual technological exploration and production conditions. Such area may be projected from the

ratio regarding total production area in a mature basin to such basin's total area. Annual production data per hydrocarbon field having < 22° API density and those reported to the ANH were used for such modelling; and

- Monte Carlo simulations used the SOOIP equations for calculating heavy crudes, taking thickness, porosity, water saturation and volumetric factor as distribution functions.

11.4 Results

The random variables used in equation 11-2 were used for iterative Monte Carlo simulation.

Only the results of the best fits and estimates following 500,000 iterations are given in this report; the others results may be consulted in digital files in Appendix 11-2.

Except for the area involved, statistical analysis of the variables analysed in the different basins has been expressed in line with the following parameters (Table 11-4):

Net and Play	Distribution	Extreme max	Log normal	Beta	Exponential	Extreme max	Log normal	Triangular	Triangular
	Average	93	74	23	80	89	31	27	430
	Mean	78	32	20	55	80	18	28	387
	Standard deviation	88	156	15	80	53	40	10	256
	Minimum	1	0.5	2	4	3	3	1	32
	Maximum	1259	426	86	180	271	152	55	1,154
Porosity	Distribution	Beta	Beta	Extreme min	Extreme max	Beta	Logistical	Triangular	Triangular
	Average	22%	22%	21%	20%	21%	14%	12%	12%
	Mean	22%	22%	22%	19%	21%	14%	12%	12%
	Mode	20%	20%	24%	17%	22%	14%	12%	12%
	Standard deviation	7%	7%	7%	5%	4%	3%	2%	2%
	Minimum	10%	10%	10%	15%	**6%**	7%	8%	8%
	Maximum	48%	48%	33%	26%	30%	25%	15%	15%
Sw	Distribution	Extreme min	Extreme min	Extreme min	Log normal	Logistical	Beta	Triangular	Triangular
	Average	36%	36%	29%	34%	38%	25%	33%	86%
	Mean	37%	37%	30%	29%	38%	24%	35%	85%
	Mode	40%	40%	33%	23%	38%	21%	45%	81%
	Standard deviation	10%	10%	10%	16%	11%	11%	10%	5%
	Minimum	3%	3%	10%	18%	16%	6%	5%	78%
	Maximum	50%	50%	42%	49%	50%	45%	50%	99%
Bo	Distribution	Log normal	Log normal	Log normal	Extreme min	Extreme max	Beta	Triangular	Triangular
	Average	1.06	1.06	1.06	1.03	1.08	1.13	1.09	1.07
	Mean	1.05	1.05	1.05	1.04	1.07	1.11	1.08	1.07
	Mode	1.03	1.03	1.03	1.07	1.05	1.04	1.05	1.05
	Standard deviation	0.05	0.05	0.05	0.09	0.06	0.09	0.02	0.03
	Minimum	1.01	1.01	1.01	1.01	1	1.03	1.05	1.01
	Maximum	1.19	1.19	1.19	1.1	1.2	1.4	1.16	1.16

Table 11-3. Estimated statistical parameters regarding calculation variables, corresponding to net thickness (hNet), play thickness (hPay), porosity (Φ), water saturation (Sw) and volumetric factor per basin (Bo).

Variable		**Estimated parameters**						**Goodness-of-fit test**			
Statistical value	Distribution	ẋ	Confidence interval		ȳ	Confidence interval		Null hypothesis	P	Statistical value	G.L
Llanos Scenario 1	Extreme maximum	181.06	166.10	196.02	233.90	226.47	241.57	1%	0.00	175%	0%
Llanos Scenario 2	Lognormal	2.49	2.30	2.69	1.59	1.46	1.74	0%	29%	2.5%	2%
Llanos Scenario 3	Beta	-0.48	-0.67	-0.28	34.78	25.81	46.86	0%	1%	1.7%	3%
Upper Magdalena Valley	Exponential	80.22	53.05	NaN	NaN	135.35	NaN	0%	NaN	0.9%	0%
Middle Magdalena Valley	extreme max	120.63	95.94	145.31	69.90	56.25	86.87	0%	NaN	0.3%	0%
Caguán – Putumayo	Lognormal	2.97	2.75	3.19	0.93	0.80	1.12	1%	3%	5%	0%
Eastern Cordillera	Triangular	27	1	55	NaN	NaN	NaN	NaN	NaN	NaN	NaN
Chocó	Triangular	430.67	32	1154	NaN	NaN	NaN	NaN	NaN	NaN	NaN

Table 11-4. Goodness-of-fit distribution parameters and test results applied to net (hNet) and play thickness data used in estimating heavy crudes.

Variable		Estimated parameters						Goodness-of-fit test			
Statistical value	Distribution	**ẋ**	Confidence interval		**ȳ**	Confidence interval		**Null hypothesis**	P	**Statistical value**	G.L
Llanos Scenario 1	Beta	7.85	5.05	10.65	27.92	17.56	38.27	0%	0.5%	5.5%	6%
Llanos Scenario 2	Beta	7.85	5.05	10.65	27.92	17.56	38.27	0%	0.5%	5.5%	6%
Llanos Scenario 3	Extreme min	0.24	0.23	0.25	0.04	0.03	0.05	0%	0%	4%	3%
Upper Magdalena Valley	Extreme max	0.21	0.19	0.23	0.04	0.02	0.05	0%	NaN	6%	0%
Middle Magdalena Valley	BetaPERT	16.7	8.16	25.35	63.62	27.79	99.44	0%	NaN	0%	0%
Caguán – Putumayo	Logistical	0.13	0.13	0.14	0.014	0.012	0.01	NaN	NaN	NaN	NaN
Eastern Cordillera	Triangular	0.12	0.08	0.15	NaN	NaN	NaN	NaN	NaN	NaN	NaN
Chocó	Triangular	0.12	0.07	0.15	NaN	NaN	NaN	NaN	NaN	NaN	NaN

Table 11-5. Goodness-of-fit parameters' distribution and test results applied to the porosity data, used in estimating heavy crudes.

Variable		**Estimated parameters**						**Goodness-of-fit test**			
Statistical value	Distribution	**ẋ**	Confidence interval		**ȳ**	Confidence interval		**Null hypothesis**	P	**Statistical value**	G.L
Llanos Scenario 1	Extreme min	0.40	0.38	0.41	0.07	0.06	0.08	0%	0%	8%	5%
Llanos Scenario 2	Extreme min	0.40	0.38	0.41	0.07	0.06	0.08	0%	0%	8%	5%
Llanos Scenario 3	Extreme min	0.33	0.31	0.35	0.07	0.06	0.09	0%	0%	7%	3%
Upper Magdalena Valley	Lognormal	-1.17	-1.34	-1.00	0.36	0.28	0.52	0%	NaN	1%	0%
Middle Magdalena Valley	Logistic	0.38	0.34	0.41	0.05	0.04	0.07	NaN	NaN	NaN	NaN
Caguán – Putumayo	Beta	3.8	2.33	5.34	11.24	6.43	16.05	0%	0%	9%	5%
Eastern Cordillera	Triangular	0.33	0.05	0.50	NaN	NaN	NaN	NaN	NaN	NaN	NaN
Chocó	Triangular	0.89	0.77	0.99	NaN	NaN	NaN	NaN	NaN	NaN	NaN

Table 11-6. Goodness-of-fit distribution parameters and test results applied to the water saturation data used in estimating heavy crudes.

Variable		Estimated parameters						Goodness-of-fit test			
Statistical value	Distribution	ẋ	Confidence interval		ȳ	Confidence interval		**Null hypothesis**	P	**Statistical value**	G.L
Llanos Scenario 1	Lognormal	0.06	0.03	0.08	0.04	0.03	0.07	0%	NaN	6%	0%
Llanos Scenario 2	Lognormal	0.06	0.03	0.08	0.04	0.03	0.07	0%	NaN	6%	0%
Llanos Scenario 3	Lognormal	0.06	0.03	0.08	0.04	0.03	0.07	0%	NaN	6%	0%
Upper Magdalena Valley	Extreme min	1.07	1.06	1.08	0.02	0.02	0.03	0%	NaN	0%	0%
Middle Magdalena Valley	Extreme max	1.10	1.08	1.12	0.05	0.04	0.06	0%	NaN	2%	0%
Caguán – Putumayo	Beta	1.12	0.91			1.43	0	NaN	41%	0%	
Eastern Cordillera	Triangular	1.09	1.05	1.16	NaN	NaN	NaN	NaN	NaN	NaN	NaN
Chocó	Triangular	1.07	1.01	1.16	NaN	NaN	NaN	NaN	NaN	NaN	NaN

Table 11-7. Goodness-of-fit distribution parameters and test results applied to volumetric factor data used in estimating heavy crudes.

11.4.1 Area

Areas were calculated using the approach proposed by Vargas (2009); heavy crude production information in several sedimentary basins was taken into account. Figure 11-2 shows that maximum production per basin in current technological conditions and reported 1 MMBOE per hectare maximum condition would be 1.7%. Following this approach, the effective areas have been estimated for each basin's having heavy crudes (Table 11-7).

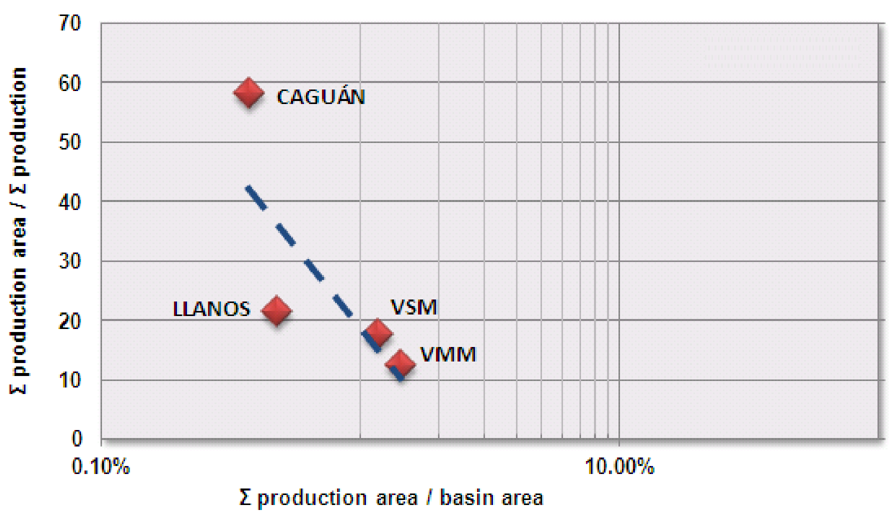

Figure 11-2. Approach adopted for deducing basins' maturity and efficiency based on production areas regarding total basin area.

Basin	Maximum area for heavy hydrocarbons (acres)
Llanos	395,896
The Upper Magdalena Valley	37,810
The Middle Magdalena Valley	57,960
The Eastern Cordillera	126,283
Caguán - Putumayo	193,984
Chocó	27,480

Table 11-8. Areas having maximum occurrence of heavy hydrocarbons per basin.

11.4.2 Heavy crudes in Colombia

Table 11-8 gives Monte Carlo simulation results for the calculations regarding the potential of crudes having <22° API density. The scenarios for the Eastern Llanos basin illustrate the results' variability regarding the thickness used. Figures 11-3 and 11-4 give a synthesis of the estimates made in this work.

Basin	Potential (MMbbl)		
	P_{90}	P_{50}	P_{10}
Llanos Scenario 1	6,806	46,735	319,455
Llanos Scenario 2	4,879	29,700	168,610
Llanos Scenario 3	5,178	20,082	51,529
The Middle Magdalena Valley	3,526	10,216	22,459
Caguán - Putumayo	1,628	5,794	21,500
The Upper Magdalena Valley	582	4,444	16,318
The Eastern Cordillera	1,369	3,052	5,467
Chocó	313	1,145	3,454
TOTAL	14,224	71,384	388,654

Table 11-9. Heavy crudes for Colombia, excluding areas in natural parks and environmental reserve areas for the basins. Total resource for all the basins has been estimated from Scenario 1 for the Eastern Llanos basin.

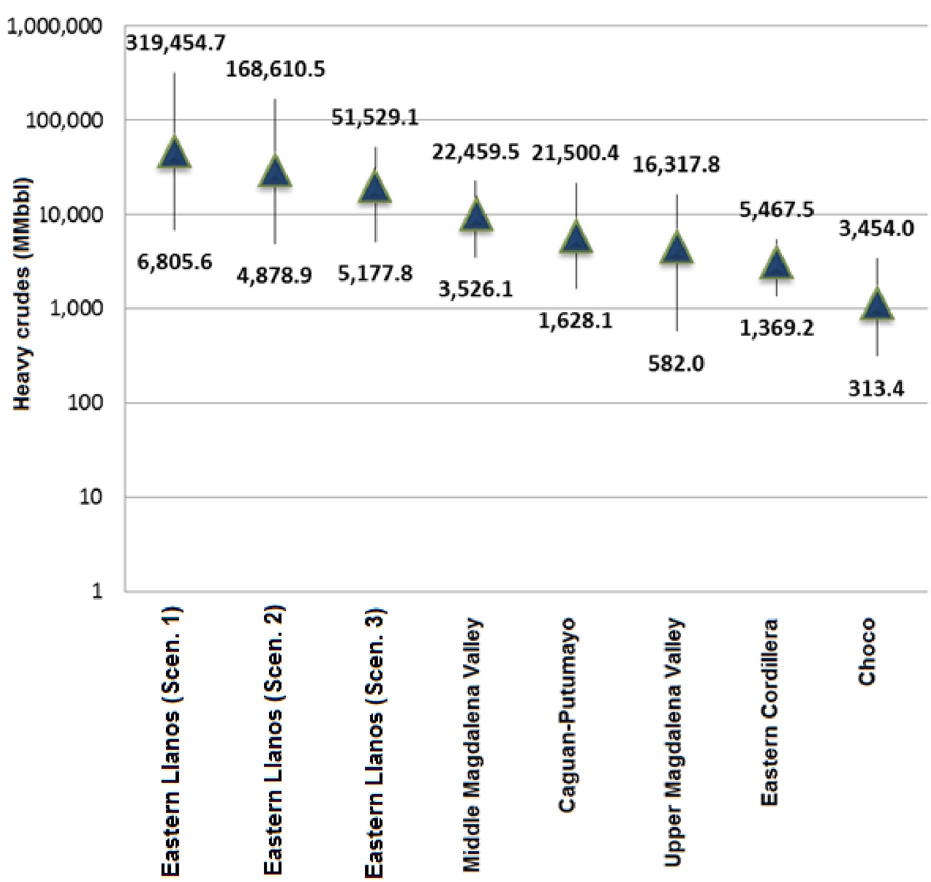

Figure 11-3. Heavy crudes for basins of interest.

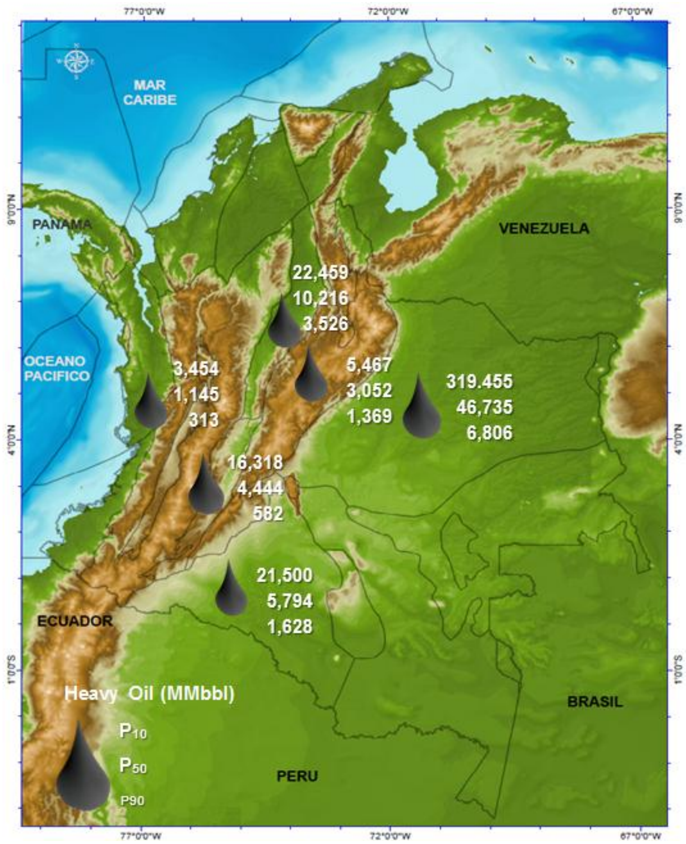

Figure 11-4. Resumen del Potencial de Crudos pesados para Colombia.

11.4.3 Sensitivity analysis

A sensitivity analysis regarding the distribution functions used in estimating heavy crude (thickness, porosity, saturation and recovery factor), suggesting that target formation thickness was the random variable having the greatest uncertainty (Figure 11-5), consequently exploratory exercises should make greater efforts at defining it (porosity was next in order followed by saturation). The areas' reflectivity must also be validated due to the nature of the hypotheses used in this work.

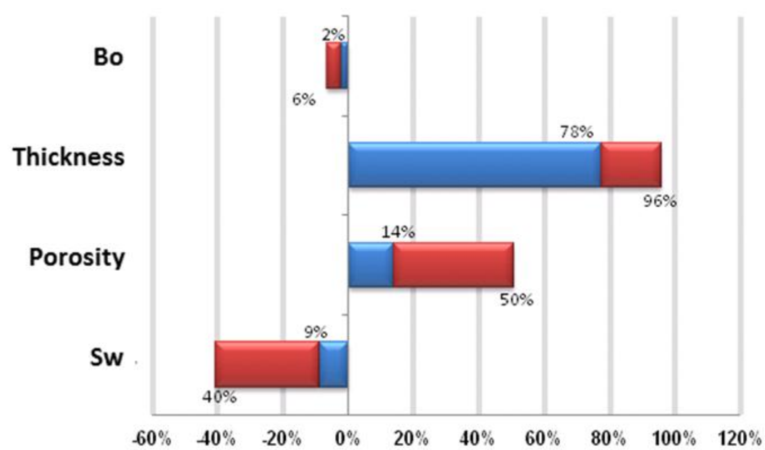

Figure 11-5. Analysis of the sensitivity of the variables used in calculating heavy crudes for potential basins.

11.5 Conclusions

- The sensitivity analysis suggested that thickness was the most sensitive variable in calculating potential, followed by porosity and saturation;
- The basins having the greatest heavy crude prospectivity were the Eastern Llanos and Middle Magdalena Valley; and
- Heavy crudes in the five Colombian basins analysed came within the P_{90} 14,224 MMbbl and P_{10} 388,654 MMbbl range.

11.6 Bibliography

ANH. (2010). Orgaic Geochemistry Atlas of Colombia, scale 1:2,800,000. Bogotá.

ANH. (s.f.). Perforación del primer pozo de reconocimiento del subsuelo en la cuenca Chocó, Subcuenca San Juan, como parte de la visión de la Agencia Nacional de Hidrocarburos de Colombia. Consulted on the March 2011, de Agencia Nacional de Hidrocarburos: www.anh.gov.co

Curtis Carl, D. E. (2003). Yacimientos de petróleo pesado. Oilfield Review 14 , 3, 32-55.

E&P. (2011). Exploration and Production. Obtained from http://www.epmag.com

ECPA. (2011). Energy and Climate Partnership of the Americas . Obtained from http://www.ecpamericas.org: http://www.ecpamericas.org/data/files/Initiatives/heavy_oil_wkg/2nd_heavy_oil_working_group_report_esp.pdf

FONADE-UIS-ANH. (2009). Informe ejecutivo evaluacion del potencial hidrocarburífero de las cuencxas Colombianas. Bogotá.

GEMS Ltda, ANH. (2007). Caracterización geoquímica de rocas y crudos en las cuencas de Cesar - Ranchería, Sinú - San Jacinto , Chocó y area de Soápaga (cuenca Cordillera Oriental). Bogotá.

Halliburton. (2006). Estudio integral que permita calculas the reserves provadas and probables sustentables para crudos con gravityes menores o iguales a 20 API en la Basin de the The Eastern Llanos. Bogotá,.

http://ercb.ca/portal/server.pt/gateway/PTARGS_0_0_303_263_0_43/http;/ercbContent/publishedcontent/publish/ercb_home/public_zone/ercb_process/enerfaqs/enerfaqs12.aspx.

http://www.eia.doe.gov.

Stach, E. (1982). Stach's textbook of coal petrology. Berlin: Grebruder .

U.S. Geological Survey . (1990). Bulletin No. 1944.

UPTC-ANH. (2009). Cartografía geológica de 51267.45 km2 en la cuenca Caguán – Putumayo a partir de sensores remotos a escala 1:100.000 y 739 km2 con control de campo a escala 1:50.000 en las planchas ICAG 413 y 414 departamentos de Meta, Caquetá, Putumayo. Bogotá.

USGS. (2010). "An estimate of recoverable heavy oil resources of the Orinoco Oil Belt, Venezuela.

Vargas Jiménez, C. A. (2009). Nuevos aportes a la estimacion del potencial de hidrocarburos en Colombia. Revista Colombiana de Ciencias , 33, 17-34.

YEN, G. C. (1978). Bitumens, Asphalt and Tar Sands. Amsterdam, The Netherlands: Elsevier Scientific Publishing Company.

Yen, T. (1984). Characterization of heavy oil, in Meyer, R.F., Wynn, J.C., and Olson, J.C., eds., The Future of Heavy Crude and Tar Sands. 2nd International Conference, Caracas (pages. p. 412-423.). New York: McGraw-Hill.

11.7 Appendixes

Digital files in the ANH'S Document Center:

- ✓ "Anexo 1 - Base de Datos Crudos pesadosColombia.xlsx"

12 PRODUCTION PROJECTIONS

12.1 General comments

Production projections form part of development schemes where variables such as reserves, infrastructure, technical aspects regarding the process and the market are sufficiently well-known within the framework of conceptual models predicting future scenarios.

The uncertainty of predictions or forecasts is linked to the sustainability of actual production conditions and models in the case of developing oil and conventional gas fields. In turn, permanent changes in production are coming regarding reserves of non-conventional resources due to the nature of the resource and ongoing refinement of extraction. However, the ranges of uncertainty change drastically when trying to forecast production scenarios regarding any type of resources from estimates of yet-to-find hydrocarbons. The dramatic change in the magnitude of uncertainty intervening in calculating potential impedes developing realistic schemes regarding production projections.

A lack of historical records regarding conventional production in Colombia and scarce reports around the world means that environmental debate has been related to shale exploitation (oil and gas), hydrates and tar sands, regulatory problems regarding coalbed methane (CBM) and costly investment in developing heavy and extraheavy crudes and tight sands. All this creates a restrictive framework imposing limitations on reliable scenarios being established.

So, production projections can only be made for conventional oil and gas. However, even though there are historical records regarding conventional production in Colombia, the availability of resources is only part of the problem. Other macroeconomic variables intervene in production such as the price of crude, national capacity for exporting the resource and its derivatives, production and worldwide reserves, etc. a production forecast is given in this work by analysing a time series regarding national production and other macroeconomic variables in line with hypotheses concerning cointegral relationships.

12.1.1 Cointegral time series

These deal with non-stationary time series whose linear combination becomes stationary, thereby reflecting long-term equilibrium conditions. Engle and Granger (1987) have given a broad and formal mathematical description of them. Their development has been linked to a description of econometric series of different kinds.

They have been used in the present work as an approach for forecasting oil and gas production in Colombia, based on annual average evolution of reserves and production in Colombia and around the world, hydrocarbon price and the amount of oil exports and its derivatives from Colombia.

12.2 Data and hypotheses

12.2.1 Data

Data regarding Colombian production, reserves and exports was taken from different institutions:

- Average annual evolution of reserves and production in Colombia (ANH, 2011);
- Reserves and production around the world, hydrocarbon price (BP, 2011); and
- The amount of oil exports and its derivatives from Colombia (BANREPUBLICA, 2011).

Most series were comparable from 1980 (Table 12-1).

Historical record	Period having complete data
Oil production in Colombia	1980-2010
Oil production around the world	1980-2010
Oil price (USD/barrel)	1980-2010
Gas production in Colombia	1980-2010
Gas production around the world	1980-2010
Gas price (U$/Btu)	1980-2010
Colombian exports of oil and its derivatives	1980-2010

Table 12-1. Time series taken into account for forecasting oil and gas production in Colombia in line with cointegral variables.

12.2.2 Hypotheses

Only analysing production projections from resources can guarantee historical production information in Colombia, i.e. conventional oil and gas. The time series were thus used and took the following hypotheses into account:

12.2.2.1 Hypothesis 1

Territorial prospectivity (resources and reserves' volume) is no more important than Colombia's political situation and/or that around the world. Depending on these parameters' tuning, production will be increased or reduced.

12.2.2.2 Hypothesis 2

Hydrocarbon prices, reserves, production and demand around the world and Colombian exporting capacity will reflect the political situation; and

12.2.2.3 Hypothesis 3

The time series regarding reserves in Colombia and amounts of exports regarding oil-derived products, the same as annual historical figures regarding the price of worldwide crude or gas production and reserves may be approached using cointegral series.

12.3 Methodology

The work consisted of collecting the longest, most coincident time series, and those which were reflective of processes promoting hydrocarbon production in Colombia and which could guarantee estimating a cointegral series, thereby inferring oil and gas production pattern during the next 20 years. A cointegral series guarantees long-term equilibrium, i.e., leads to inferring a linear ratio between a set of variables which has been maintained for a long period of time. The production pattern has been forecast in the present work in the following way:

- The time series shown in Table 12-1 were homogenised in annual steps;
- The time series seasonal patterns hypothesis was accepted and the Engle-Granger numerical approach adopted (Engle and Granger, 1987);
- Four scenarios were estimated which combined oil or gas production with the remaining five time series shown in Table 1. The most stable triplets were chosen; and
- Scenarios having annual steps were projected until year 25 (frontier), but only the results for 5, 10, 15 and 20 years were evaluated.

12.4 Results

Given that this was an exercise involving a mobile analysis of historical records, its forecasts were not asymptotic. The projections rather maintained a certain pattern derived from the records being evaluated. Figures 12-1 and 12-2 give the results of the analysis from treatment as cointegral variables.

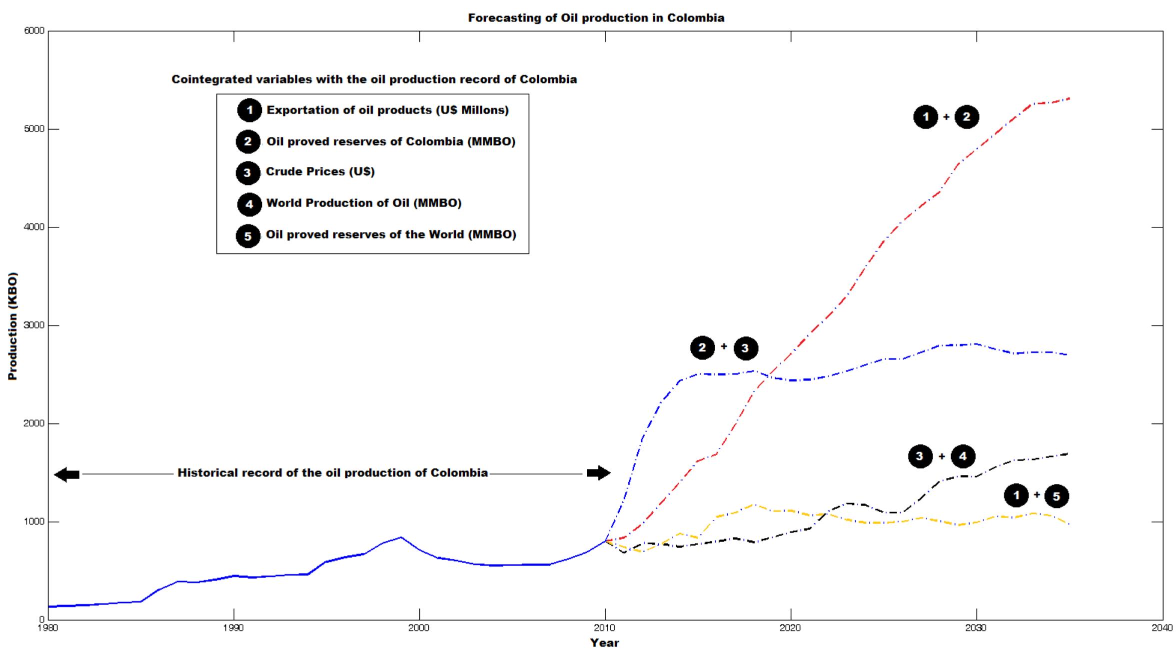

Figure 12-1. Forecast of oil production in Colombia from analysing time series from a cointegral variables' approach. The continuous blue line shows the historical record of oil production in Colombia. The dashed lines indicate projected oil production intervals (20 years), taking the other two cointegral variables (numbed within black squares) into account.

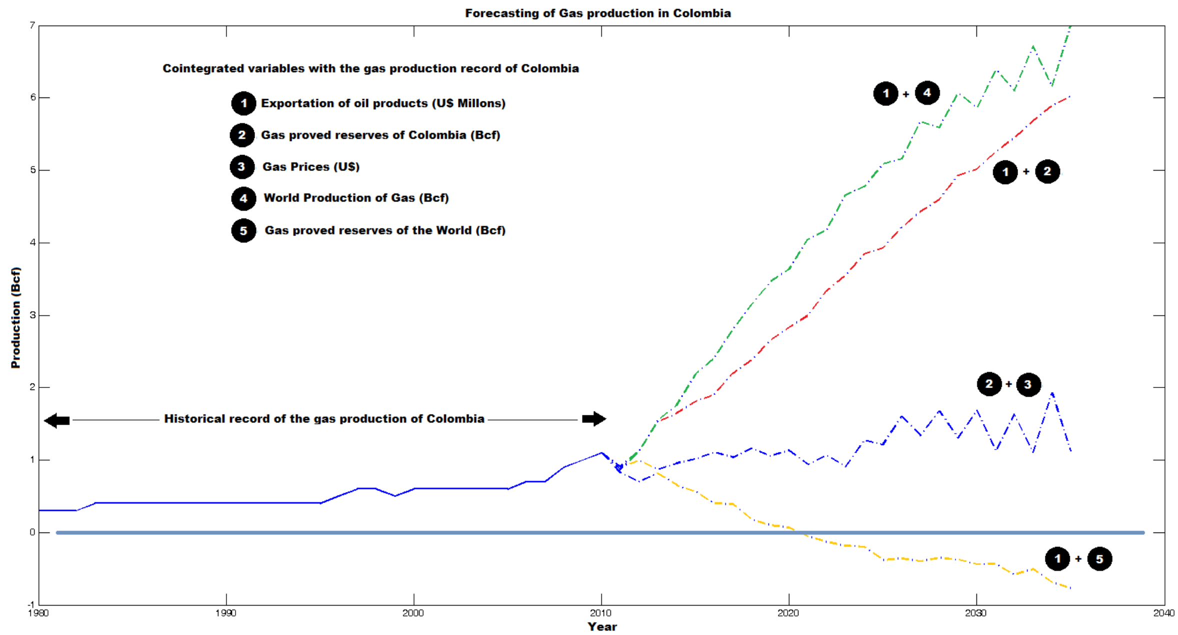

Figure 12-2. Forecast for gas production in Colombia from analysing time series from a cointegral variables' approach. The continuous blue line shows the historical record of gas production in Colombia. The dashed lines indicate projected gas production intervals (20 years), taking the other two cointegral variables (numbed within black squares) into account.

12.5 Bibliography

ANH. Figures and Statistics 2011. 2011. http://www.anh.gov.co/es/index.php?id=8 (last accessed: 30th November 2011)

BANREPUBLICA. Exportaciones totales (FOB) - Principales exportaciones y resto de exportaciones. http://www.banrep.gov.co/estad/dsbb/sec_ext_009.xls (latest access: 30th November 2011)

BP. Statistical Review of World Energy 2011. http://www.bp.com/sectionbodycopy.do?categoryId=7500&contentId=7068481 (latest access: 30th November 2011)

Engle, R F, and C W J Granger. Cointegration and error correction: representation, estimation and testing. Econometrica 55, 1987: 25 1-276.

12.6 Appendixes

Digital files in the ANH'S Document Center:

- ✓ "Aceite_Gas_Col_Pronostico_Producción.xlsx"

13 EXECUTIVE REPORT

13.1 General comments

The in situ potential of conventional and non-conventional hydrocarbons has been estimated, as well as that of resources in Colombia. The results have been based on geoscientific information acquired to date and supplied by ANH and open-access national and international sources

The methodologies used and the hypotheses supporting the estimates have been described throughout the chapters of this work. It is worth stating that such estimates have been based on the assumption that all Colombian basins may have conventional or non-conventional hydrocarbon potential, even when no occurrences have been evidenced in some of them, or exploratory studies have not been carried out to show this. Likewise, the calculations (Monte Carlo simulations) have been intimately linked to the hypothesis directly relating aerial extension to in situ potential.

13.2 Estimated potential of conventional hydrocarbons in Colombia

Three approaches have been adopted for estimating hydrocarbon resources in Colombia. The first concerned conventional resources generated and trapped in Colombian sedimentary basins and the second adopted a volumetric in situ (or in place) approach which could be inferred from current exploration information (OOIP and GIIP). The third was based on a fractal geometric approach in line with a hypothesis concerning the sustainability of economic, socio-environmental and political conditions allowing findings and production in past years.

Table 13-1 gives a summary of such overall estimates where conventional resource's share can be appreciated. Good consistency was usually observed between volumetric results (P90) and the fractal approach (weak scenario). It seemed evident that there was a significant availability of gas which has not been detected in both cases. Greater exploratory efforts must be made in the next few years aimed at adding new reserves.

Estimate	Oil (MMbbl)			Gas (Tcf)		
	P_{10}	P_{50}	P_{90}	P_{10}	P_{50}	P_{90}
Generated and trapped	1,918,000	335,000	56,000	2,558	447	75.0
In place (OOIP and IGIP)	430,361	117,963	20,000	234	28	3.5
% of resource generated/trapped	**~22.4%**	**~35.2%**	**~35.7%**	**~9.1%**	**~6.3%**	**~4.7%**
Yet-to-find (YTF) resources	High 33,146	Medium 26,072	Low 22,798	High 348.9	Medium 49.9	Low 6.6
% of resource being produced (P_{90})	**~1.7%**	**~7.8%**	**~40.7%**	**~13.6%**	**~11.1%**	**~8.8%**

Table 13-1. Synthesis of conventional hydrocarbon generated in Colombia, as well as volumetric (OOIP and IGIP) and fractal estimates (YTF).

Figure 13-1 gives the results obtained for conventional oil in Colombia in the present work and compares them with results found by other authors regarding Colombia. The results were comparable and allude to recoverable resources. Two types of OOIP calculations were used in this work: a 20% average recovery factor (RF) and 30% geological risk (GR) factor.

Basins with significant potential for conventional hydrocarbons were usually:

- OOIP: Vaupes in the Amazonas, Colombia and Deep Pacific basins
- IGIP: The Eastern Llanos, Colombia and Deep Pacific basins

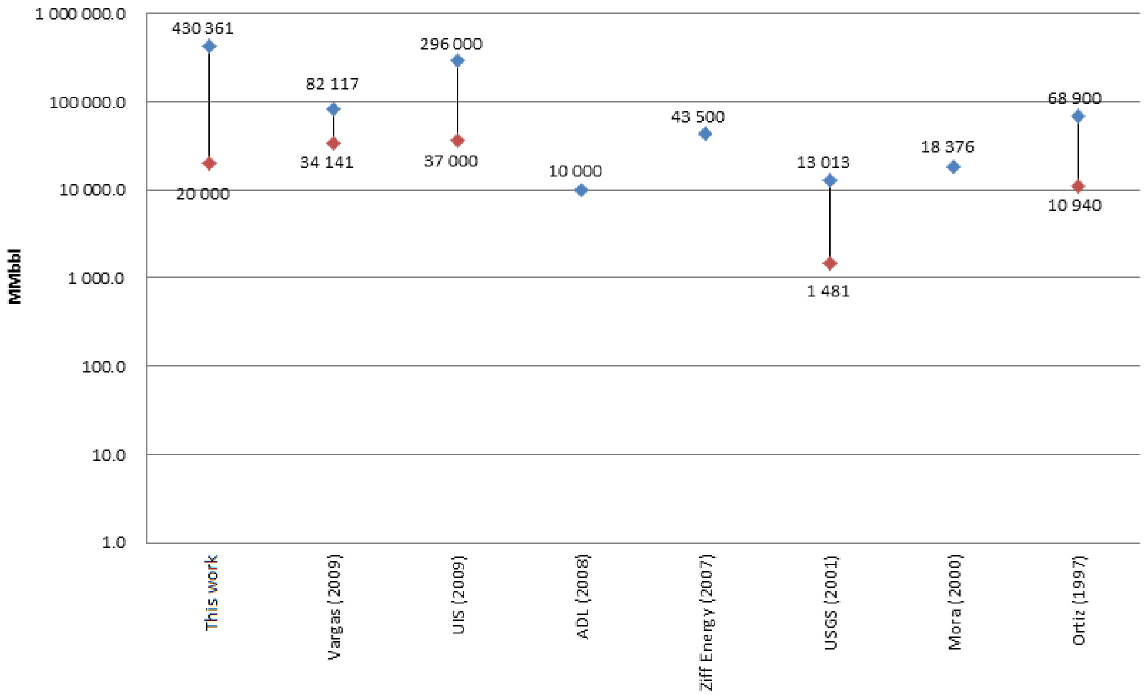

Figure 13-1. Conventional crude potential for Colombia, estimated by different authors. UIS (Universidad Industrial de Santander), USGS (United States Geological Survey), ADL (Arthur De Little). The OOIP range is the value estimated in this study, modified from Vargas (2009).

13.3 Estimated potential of non-conventional hydrocarbons in Colombia

Table 13-2 shows non-conventional resources in Colombia. The range of recoverable resources and the basins having the greatest prospectivity have been suggested. A sensitivity analysis associated with the most critical variables has been included; such analysis will allow prioritising and planning exploratory work in terms of each resource

Figure 13-2 compares the results obtained in the present study with those obtained by Arthur De Little (ADL, 2008), discriminating each non-conventional resource.

The results presented in this work were comparable with the estimates made by ADL (2008) concerning most estimated resources. The only case where ADL results did not come within this report's range of values concerned gas hydrates; ADL results gave 400 Tcf (74,862 MMBOE) by contrast with 4.89 - 75.63 Tcf (843 - 13,040 MMBOE) in this work (Figure 13-2).

Resource	Results (maximum-minimum)	Most prospective basins (P_{50})	Sensitivity analysis (variable having the greatest uncertainty)
Gas hydrates	4.89 – 75.63 Tcf	Marine Chocó Marine Guajira Marine Sinú Marine Tumaco	Hydrate saturation Los Cayos, Colombia and Deep Pacific basins were not analysed regarding their complete extension due to a lack of information
Coalbed methane	Scenario 1: 0.75 - 77.5 Tcf Scenario 2: 14.7 – 21.9 Tcf	Sinú - San Jacinto Cesar - Ranchería The Upper Magdalena Valley The Middle Magdalena Valley	G_c (average *in situ* gas content Scf/ton)
Tar sands	Scenario 1: 22.6 - 990.4 MMbbl measured resources Scenario 2: 155.7 – 6,812.6 MMbbl indicated resources Scenario 3: 1,056.9 - 46,244.8 MMbbl inferred resources Scenario 4: 3,455.1 - 151,173.8 MMbbl hypothetical resources	The Eastern Cordillera The Eastern Llanos The Middle Magdalena Valley The Upper Magdalena Valley Caguán - Putumayo	Thickness of the layers
Oil shale	Scenario 1: 60.5 - 91,078.0 MMbbl indicated resources Scenario 2: 511.7 - 677,745.2 MMbbl hypothetical resources	The Eastern Cordillera Chocó The Upper Magdalena Valley The Middle Magdalena Valley	The uncertainty of all the variables used in the calculations was considerable, due to a lack of information
Shale gas	Scenario 1: 33.7 – 2,050.6 Tcf Scenario 2: 57.7 – 3,086.0 Tcf	The Eastern Llanos The Eastern Cordillera Caguán - Putumayo	Net-to-gross The original resource has been risked
Shale oil	Scenario 1 3,090.6 – 157,523.4 MMbbl Scenario 2 4,264.8 – 234,028.2 MMbbl	The Eastern Llanos The Eastern Cordillera Caguán - Putumayo	Net-to-gross The original resource has been risked (30%)
Tight gas sands	Scenario 1: 0.005 – 6.3 Tcf Scenario 2: 0.9 – 43.7 Tcf	The Eastern Llanos Caguán - Putumayo The Eastern Cordillera	Thickness of the gas and water saturation layers
Heavy crude	14,224 – 388,654 MMbbl	The Eastern Llanos The Middle Magdalena Valley Caguán - Putumayo	Formation thickness

Table 13-2. Results obtained in estimates of non-conventional resources for Colombia.

ANH AGENCIA NACIONAL DE HIDROCARBUROS

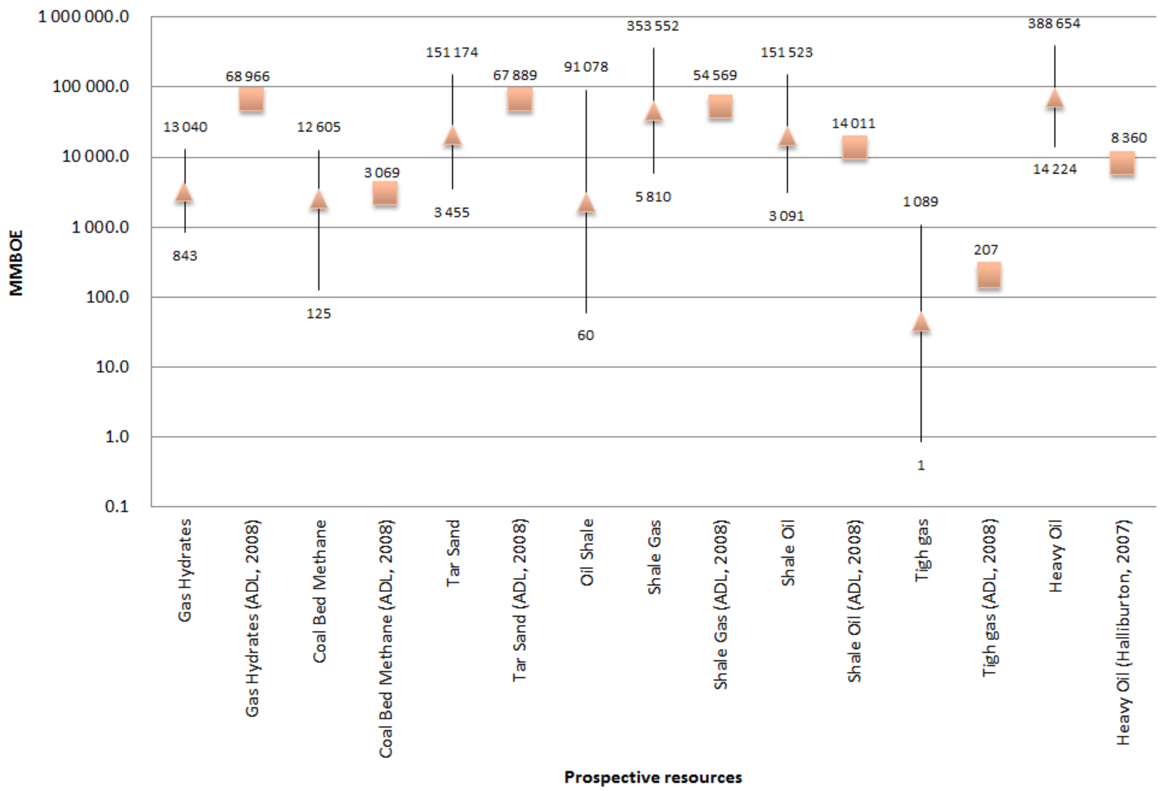

Figure 13-2. Non-conventional resources for Colombia estimated in this work and compared to ADL's estimates (2008).

13.4 Hydrocarbon resources matrix

A summary of the basins having the greatest probability for the presence of conventional and non-conventional resources is given below. The matrix synthesises the estimates derived from the available geological information or from data from exploratory or production projects. The most optimistic scenario was considered for estimated resources (Table 13-3).

Basin / resources (MMbbl / Tcf)	Conventional crude (MMbbl)			Associated and free gas (Tcf)			Heavy crude (MMbbl)		
	P_{10}	P_{50}	P_{90}	P_{10}	P_{50}	P_{90}	P_{10}	P_{50}	P_{90}
Offshore	276,413.0	75,815.0	12,570.0	205.8	20.6	1.9			
Los Cayos	43,050.0	11,774.0	1,950.0	21.8	2.6	0.3			
Chocó offshore	12,589.0	3,453.0	575.0	58.9	4.4	0.1			
Colombia	90,992.0	24,923.0	4,138.0	39.9	4.9	0.6			
Guajira offshore	18,721.0	5,131.0	855.0	10.0	1.1	0.1			
Colombian Deep Pacific	92,961.0	25,566.0	4,224.0	39.4	4.7	0.6			
Sinú offshore	8,182.0	2,248.0	377.0	10.4	1.0	0.1			
Tumaco offshore	9,918.0	2,720.0	451.0	25.3	2.0	0.1			
Onshore	153,952.0	42,148.0	7,436.0	289.4	25.6	1.8	388,653.0	71,386.0	14,224.0
Amagá	804.0	233.0	75.0	3.3	0.3	0.0			
Chocó	13,444.0	3,682.0	607.0	14.2	1.3	0.1	3,454.0	1,145.0	313.0
Caguán - Putumayo	419.0	137.0	34.0	15.8	1.9	0.2	21,500.0	5,794.0	1,628.0
Catatumbo	213.0	59.0	17.0	8.8	0.7	0.0			
Cauca - Patía	4,553.0	1,247.0	208.0	60.5	4.3	0.1			
Cesar - Ranchería	4,137.0	1,135.0	189.0	9.7	0.8	0.0			
The Eastern Cordillera	22,653.0	6,221.0	1,030.0	44.9	3.6	0.2	5,467.0	3,052.0	1,369.0
Guajira	4,777.0	1,307.0	218.0	17.4	1.3	0.0			
The Eastern Llanos	3,250.0	892.0	148.0	40.2	4.4	0.5	319,455.0	46,735.0	6,806.0
San Jacinto, Sinú	13,469.0	3,697.0	614.0	15.5	1.3	0.1			
Tumaco	4,486.0	1,651.0	611.0	6.6	0.6	0.0			
Urabá	4,413.0	710.0	159.0	3.9	0.3	0.0			
The Lower Magdalena Valley	13,177.0	3,609.0	602.0	12.3	1.1	0.1			
The Middle Magdalena Valley	11,885.0	3,252.0	539.0	7.2	0.6	0.1	22,459.0	10,216.0	3,526.0
The Upper Magdalena Valley	999.0	274.0	45.0	10.5	0.9	0.0	16,318.0	4,444.0	582.0
Vaupés, Amazonas	51,273.0	14,042.0	2,340.0	18.6	2.2	0.3			
Non-prospective areas or lying adjacent to the basin									
Total	430,365.0	117,963.0	20,006.0	495.1	46.3	3.8	388,653.0	71,386.0	14,224.0

Table 13-3. Most probable conventional and non-conventional resources in Colombian basins, indicating estimated resources. These results take environmental considerations into account.

Continuation of Table 12-3

Basin / resources (MMbbl / Tcf)	Gas hydrates (Tcf)			Coalbed methane (Bcf)[1]			Tar sands		
	P_{10}	P_{50}	P_{90}	P_{10}	P_{50}	P_{90}	P_{10}	P_{50}	P_{90}
Offshore	75.6	19.1	4.9						
Los Cayos									
Chocó offshore	46.9	11.8	3.0						
Colombia	1.9	0.5	0.1						
Guajira offshore	12.2	3.1	0.8						
Colombian Deep Pacific	3.7	0.9	0.2						
Sinú offshore	5.8	1.5	0.4						
Tumaco offshore	5.2	1.3	0.3						
Onshore				77,510.7	14,612.0	725.4	151,173.8	20,428.8	3,455.2
Amagá				516.0	96.0	4.0	318.6	43.1	7.3
Chocó							2,187.7	295.6	50.0
Caguán - Putumayo				167.0	31.4	1.8	14,203.0	1,919.3	324.6
Catatumbo				682.3	128.2	6.6	816.9	110.4	18.7
Cauca - Patía				720.7	134.9	7.0	711.9	96.2	16.3
Cesar - Ranchería				17,713.0	3,296.0	161.0	756.1	102.2	17.3
The Eastern Cordillera				4,585.2	867.1	43.7	22,109.1	2,987.7	505.3
Guajira				832.4	156.3	7.8	1,035.9	140.0	23.7
The Eastern Llanos				573.0	107.3	5.3	16,526.0	2,233.2	377.7
Sinú - San Jacinto				33,286.6	6,338.5	313.1	9,067.2	1,225.3	207.2
Tumaco							753.9	101.9	17.2
Urabá							1,027.7	138.9	23.5
The Lower Magdalena Valley				252.0	47.0	2.0	4,174.3	564.1	95.4
The Middle Magdalena Valley				4,448.0	830.0	42.0	18,650.3	2,520.3	426.3
The Upper Magdalena Valley				11,177.7	2,099.8	106.8	25,404.0	3,432.9	580.6
Vaupés - Amazonas							4,752.8	642.3	108.6
Non-prospective areas or lying adjacent to the basin				2,556.9	479.5	24.3	28,678.4	3,875.4	655.5
Total	75.6	19.1	4.9	77,510.7	14,612.0	725.4	151,173.8	20,428.8	3,455.2

Continuation of Table 12-3

Basin / resources (MMbbl / Tcf)	Oil shale [3] (MMbbl)			Shale oil [4] (MMbbl)			Shale gas [4] (Tcf)		
	P_{10}	P_{50}	P_{90}	P_{10}	P_{50}	P_{90}	P_{10}	P_{50}	P_{90}
Offshore									
Los Cayos									
Chocó offshore									
Colombia									
Guajira offshore									
Colombian Deep Pacific									
Sinú offshore									
Tumaco offshore									
Onshore	91,078.0	2,220.1	60.5	151,524.0	19,607.4	3,090.6	2,050.7	265.5	33.8
Amagá	3.5	0.1	0.0	14.4	4.2	0.6	0.2	0.1	-
Chocó	412.2	10.9	0.3	235.2	71.4	11.4	3.2	1.0	0.2
Caguán - Putumayo	259.1	5.0	0.0	27,802.8	1,319.4	142.8	376.3	17.9	1.9
Catatumbo	85.0	3.6	0.1	1,918.2	403.2	50.4	26.0	5.5	0.7
Cauca - Patía	240.2	7.8	0.2	295.8	88.2	13.8	4.0	1.2	0.2
Cesar - Ranchería	622.9	13.9	0.3	1,108.2	294.6	43.2	15.0	4.0	0.6
The Eastern Cordillera	294.6	9.5	0.3	7,543.8	2,137.8	327.0	102.1	28.9	4.4
Guajira	10,443.3	198.7	1.2	1,373.4	365.4	54.0	18.6	4.9	0.7
The Eastern Llanos	798.9	33.3	1.2	68,478.6	10,783.8	1,297.2	926.7	145.9	17.6
San Jacinto, Sinú	1,135.1	47.5	1.9	4,565.4	1,171.2	169.2	61.8	15.9	2.3
Tumaco	2,678.0	99.3	3.0	586.8	175.8	27.6	7.9	2.4	0.4
Urabá	1,950.3	97.1	4.1	943.8	241.8	34.8	12.8	3.3	0.5
The Lower Magdalena Valley	12,166.0	220.4	3.8	1,255.2	362.4	55.8	17.0	4.9	0.8
The Middle Magdalena Valley	39,432.2	549.6	7.3	1,539.0	450.0	69.6	20.8	6.1	0.9
The Upper Magdalena Valley	5,986.4	240.9	8.5	469.2	139.2	21.6	6.4	1.9	0.3
Vaupés, Amazonas	14,564.9	682.2	28.3	33,394.2	1,599.0	771.6	451.9	21.6	2.3
Non-prospective areas or lying adjacent to the basin	5.5	0.3	0.0						
Total	91,078.0	2,220.1	60.5	151,524.0	19,607.4	3,090.6	2,050.7	265.5	33.8

ANH AGENCIA NACIONAL DE HIDROCARBUROS

Continuation of Table 12-3

Basin / resources (MMbbl / Tcf)	Gas in tight sands [5] (Tcf)		
	P_{10}	P_{50}	P_{90}
Offshore			
Los Cayos			
Chocó offshore			
Colombia			
Guajira offshore			
Colombian Deep Pacific			
Sinú offshore			
Tumaco offshore			
Onshore	43.7	5.5	1.0
Amagá	0.1	0.0	0.0
Chocó	0.9	0.1	0.0
Caguán - Putumayo	6.7	0.9	0.1
Catatumbo	0.5	0.1	0.0
Cauca - Patía	0.3	0.0	0.0
Cesar - Ranchería	0.8	0.1	0.0
The Eastern Cordillera	5.0	0.6	0.1
Guajira	1.0	0.1	0.0
The Eastern Llanos	15.6	2.0	0.3
San Jacinto, Sinú	2.5	0.3	0.1
Tumaco	0.5	0.1	0.0
Urabá	0.7	0.1	0.0
The Lower Magdalena Valley	2.6	0.3	0.1
The Middle Magdalena Valley	2.1	0.3	0.0
The Upper Magdalena Valley	1.5	0.2	0.0
Vaupés, Amazonas	3.0	0.4	0.1
Non-prospective areas or lying adjacent to the basin			
Total	43.7	5.5	1.0

[1] Llanos, Scenary 1
[2] Scenary 1
[3] Scenary 2
[4] Indicated resources

Resources
High probability
Moderate probability
Low probability